INNOVATIVE TECHNOLOGY APPLICATIONS IN ENGINEERING SCIENCES

EDITORS

Prof. Dr. Rakesh JAIN

Prof. Dr. Abdulkadir GÜLLÜ

Assist.Prof. Senai YALÇINKAYA

INNOVATIVE TECHNOLOGY APPLICATIONS IN ENGINEERING SCIENCES

EDITORS
Prof. Dr. Rakesh JAIN
Prof. Dr. Abdülkadir GÜLLÜ
Assist. Prof. Senai YALÇINKAYA

INNOVATIVE TECHNOLOGY APPLICATIONS IN ENGINEERING SCIENCES

EDITORS
Prof. Dr. Rakesh JAIN
Prof. Dr. Abdulkadir GÜLLÜ
Assist. Prof. Senai YALÇINKAYA

Güven Plus Group Inc. Publications: 23/2022
20 DECEMBER 2021

Publisher Certificate No: 52866
E-ISBN: 978-625-7367-57-8
Güven Plus Group Inc. Publications

Text and Language Editors
Assoc. Prof. Gökşen ARAS (Turkish – English)
Assist. Prof. L. Santhosh KUMAR (English)

Cover and Graphic Design
Lec. Ozan KARABAŞ
Ozan DÜZ

Page Layout
Burhan MADEN

Print-Binding
GÜVEN PLUS GROUP CONSULTANCY INC. PUBLICATIONS®
Kayaşehir Neighborhood Evliya Çelebi Street Emlakkonut Başakşehir Houses 1/A D Block Floor 4 Number 29 Başakşehir İstanbul - Turkey Phone: +902128014061- 62 Fax: +902128014063 Mobile: +9053331447861

BOOK LICENSEE
GÜVEN PLUS GROUP CONSULTANCY INC. PUBLICATIONS ®
Kayaşehir Neighborhood Evliya Çelebi Street Emlakkonut Başakşehir Houses 1/A D Block Floor 4 Number 29 Başakşehir İstanbul - Turkey Phone: +902128014061- 62 Fax: +902128014063 info@guvenplus.com.tr, www.guvenplus.com.tr

CONTENTS

PREFACE

In our world, while there are many negativities in the areas of nature, health, social, etc.; technological developments are becoming a necessity in the industry in general for the solution of these and other problems. Technological developments, triggered by quality competition, desire for comfort, fear and anxiety, emerge as a fact that we face in many and difficult to follow. Academic studies conducted in this context; It is brought together with its interlocutors, sometimes in the form of open-access sites, and sometimes in the form of congresses, panels, periodicals and scientific books.

We wanted to have a finger in the pie with this academic book study called **"Innovative Technology Applications in Engineering Sciences"** which consists of ten different chapters and covers the researches of valuable academicians. This book; we pre-sent it to you, valuable scientists and industry employees through "Güven Plus Grup Inc. Publications" which a major part of its publications consisting of academic books, has gained a great reputation with its qualified activities in the national and international arena.

This book consists of many engineering subjects and experimental studies and applied academic subjects. In the book;

You will find valuable research and experimental studies on many important subjects.

We believe that the book, which includes chapters dealing with many inter-esting topics of engineering technologies, will shed light on the academic studies of many researchers, and will find a valuable place in the catalogs of the Higher Education Institution, public libraries and personal archives.

We would like to express our gratitude to our esteemed editors, writers, ref-erees and you, our dear readers, who have contributed to the realization of this important work, which emerged as a result of the long-lasting and meticulous work. **December 2022**

Prof. Dr. Rakesh JAIN
Prof. Dr. Abdulkadir GÜLLÜ
Assist. Prof. Senai YALÇINKAYA

ÖNSÖZ

Dünyamızda doğa, sağlık, sosyal vb. alanlarda birçok olumsuzluk yaşanırken; bunların ve diğer problemlerin çözümüne yönelik olarak genel anlamda endüstride, teknolojik gelişmeler zorunluluk halini almaktadır. Kalite rekabeti, konfor arzusu, korku ve endişenin de tetiklediği teknolojik gelişmeler, takipte zorlanılacak derecede ve çok sayıda yüzleştiğimiz bir gerçek olarak karşımıza çıkmaktadır. Bu bağlamda yapılan akademik çalışmalar; kimi zaman açık erişimli siteler, kimi zaman da kongre, panel, süreli yayınlar ve bilimsel kitaplar şeklinde muhataplarıyla buluşturulmaktadır.

Biz de birbirinden kıymetli akademisyenlerin araştırmalarını kapsayan, on farklı bölümden oluşan **""Innovative Technology Applications in Engineering Sciences"** adını verdiğimiz bu akademik kitap çalışması ile çorbada tuzumuz olsun istedik. Bu kitabı; yayınlarının önemli bir bölümünü akademik kitaplardan oluşan, Ulusal ve Uluslararası alanda nitelikli faaliyetleriyle oldukça saygınlık kazanmış olan "Güven Plus Grup A.Ş. Yayınları" aracılığı ile siz değerli bilim insanları ve endüstri çalışanlarının hizmetine sunuyoruz.

Bu kitap, birçok mühendislik konuları ve deneysel çalışmalar ile uygulama yapılmış akademik konulardan meydana gelmiştir. Kitapta;

Birçok problemlerin çözümüne yönelik birçok önemli konuda değerli araştırma ve deneysel çalışmaları bulacaksınız.

Mühendislik teknolojilerinin birçok ilgi çekici konularına değinilen bölümlerin yer aldığı kitabın, çok sayıda araştırmacının akademik çalışmalarına ışık tutacağına, Yükseköğretim Kurumu kataloglarında, kamu kütüphanelerinde ve kişisel arşivlerde oldukça değerli bir yer bulacağına inanıyoruz.

Uzun zaman alan ve büyük bir titizlikle yapılan çalışmaların sonucu olarak ortaya çıkan bu önemli eserin gerçekleşmesinde emeği geçen saygıdeğer editörlerimize, yazarlarımıza, hakemlerimize ve kitabımızı edinen siz sevgili okurlarımıza teşekkürlerimizi sunarız. **Aralık 2022**

Prof. Dr. Rakesh JAIN
Prof. Dr. Abdulkadir GÜLLÜ
Dr. Öğr. Üyesi Senai YALÇINKAYA

PLANT-BASED FIBER-REINFORCED GEOPOLYMER COMPOSITES

Kübra Ekiz BARIŞ[1]

Abstract: The excessive production of Portland cement is becoming unsustainable because of an enormous requirement for raw materials, energy use, greenhouse gas emissions, and environmental damage. Because of the aforementioned negative effects, it is essential to develop and utilize alternative binders that have lower carbon footprints. Recent research on geopolymer binders indicates that this novel binder has the potential to replace cement. There is a reduced effect on the environment from these binders because they use less calcium-based raw materials. They are also more energy-efficient because there is no calcination during the production stages and the production temperature is lower. However, the usage of geopolymers in various applications may be adversely impacted by their low tensile strength, brittle nature, and limited crack resistance. The geopolymer matrix can be reinforced with either short or continuous fibers to enhance the mechanical properties of the material, decrease brittle fracture, and enhance ductility. Natural fibers are now preferred over other fibers in the reinforcing of geopolymers due to the recent trend toward the production of environmentally friendly and energy-efficient materials. In contrast to the quantity of studies concentrating on inorganic and synthetic fiber reinforcement, it is, nevertheless, comparatively insufficient. The goal of the current chapter is to compile the most recent scientific data on the impact of plant-based fiber reinforcement on the enhancement of the mechanical and physical characteristics of geopolymer composites. The Scopus and SCI databases were checked for recently published articles on plant-based fiber-reinforced geo-

1 Kocaeli University, Faculty of Architecture and Design, Kocaeli / Turkey, e-mail: kubra.ekizbaris@kocaeli.edu.tr, Orcid No: 0000-0002-3830-7185

polymer composites. The characteristics (chemical structure, physical, and mechanical properties) of plant-based fibers, mixture ratios, production stages, and curing conditions of plant-based fiber-reinforced geopolymer composites are also within the scope. Various plant-based fibers, including sisal, coir, jute, cotton, hemp, lignin, raffia, pineapple, bamboo, musa basjoo, sorghum, and sugarcane bagasse, can be incorporated as reinforcement in geopolymer matrices, according to study results. In order to produce plant-based fiber-reinforced geopolymer composites with higher physical and mechanical characteristics, it is vital to consider the type, chemical structure, and characteristics of the fibers as well as their content, manufacturing process, and curing conditions. The uniform dispersion of the fibers and matrix must be maintained throughout production since balling and fiber coalescence weaken the necessary properties. Depending on the characteristics of the fiber and the aluminosilicate source, the appropriate curing conditions should be applied. The workability of fiber-reinforced geopolymers was worse than that of the unreinforced geopolymer matrix, regardless of the type of fiber utilized. More water is added to the matrix to decrease the viscosity of the geopolymer. During temperature curing, this free water evaporates, leaving a significant number of pores in the microstructure. As a result, adding fibers causes composites' porosity and water absorption ratio to increase while their density and ultrasound pulse velocity decrease. Flexural, compressive, and impact strengths of unreinforced geopolymers increase with increasing fiber content until they reach their optimum amount. However, inclusion of additional fibers over the optimum level results in the fibers balling and coalescing, and also leaves voids in the matrix, which weakens the interfacial adhesion between the fiber and the matrix and, in turn, lowers the mechanical properties.
Keywords: Geopolymer Composite, Plant-Based Fiber, Fiber Content, Strength

INTRODUCTION

Climate change, one of the most important environmental problems facing our planet, is caused by CO_2 emissions. The atmospheric CO_2 ratio in the 18th century was 280 ppm per million, while today it is 450 ppm. If progress continues at this rate, it is predicted that the CO_2 ratio will be 731 ppm in 2130 (Pacheco-Torgal, 2015). The very large-scale production of Portland cement is becoming unsustainable due to an unprecedented

need for raw materials, energy consumption, greenhouse gas emissions, and environmental pollution (Farhan et al., 2021). Cement production is responsible for 5% of global CO_2 emissions, which is quite a high rate (IPCC, 2001). Significant consumption of traditional non-renewable raw materials such as limestone, calcination of clinker at 1400 1450 °C, energy consumption for the grinding process, and high greenhouse gas emissions (0.9 tons of CO_2 emissions per 1 ton of clinker production) are adverse effects of cement-based materials (Hendriks et al., 1999). Therefore, the aforementioned adverse effects make it necessary to develop and use alternative binders with lower carbon footprints (Ganesan et al., 2013).

Recent studies on geopolymer binders show that this new binder can be an alternative to Portland cement. Geopolymer binders are obtained as a result of the reaction of an amorphous or glassy aluminosilicate source with various alkali activators (Garcia-Lodeiro et al., 2015). Various natural materials, including agricultural, industrial, and urban waste materials, containing mostly silica (SiO_2) and alumina (Al_2O_3), can be used as an aluminosilicate source. Alkali hydroxides, weak and strong acid salts, and silica salts are various chemical solutions used as alkali activators (Robayo-Salazar and de Gutiérrez, 2018). Because less calcium-based raw materials are used in these binders, the environmental impact is lower. In addition, they are more energy-efficient due to the absence of a calcination stage in the production process, the lower production temperature, and the need for less fuel (Bondar et al., 2011). CO_2 emissions from geopolymer production are approximately 60-80% lower than those from conventional cement production (Zhang et al., 2014).

The reaction mechanism of geopolymers is an exothermic process and consists of successive dissolution, oligomerization, and polycondensation reactions. The first reaction begins with the dissolution of covalently bonded Si–O–Si and Al–O–Si compounds from the aluminosilicate source by means of an alkali solution, and silicate and aluminate monomers are formed. These silicate and aluminate monomers form an oligomer during the oligomerization stage. Then, the oligomers condense and cross-linking occurs between various polymeric chains to

form a three-dimensional geopolymer network (NASH gel) (Ferone et al., 2011).

Geopolymer binders have the following advantages, depending on the properties of the aluminosilicate source, the alkali activator type, the mixing ratio, and the production and curing conditions (Davidovits, 2011; Provis and Bernal, 2014; RILEM TC 224-AAM, 2014):

- *High compressive strength (compressive strength that can increase up to 90 MPa for 28 days)*
- *Rapid hardening, reaching 70% of its ultimate compressive strength within 4 hours (Comrie et al., 1989). This value is approximately 24 hours for Portland cement.*
- *Thermal stability up to 1200 °C (Zheng et al., 2009; Abdul Aleem and Arumairaj, 2012)*
- *Exhibiting excellent adhesion with other materials,*
- *Reduced permeability and dimensional stability (low shrinkage),*
- *Durability against acid and chemical effects.*

Despite the advantages mentioned above, geopolymers' low tensile strength, brittle behavior, and low resistance to cracks can negatively affect their use in many applications. There are two approaches applied in order to improve the mechanical properties of the material (such as its tensile, flexural, and impact strengths), and to suppress brittle behavior and to provide ductility. In the first approach, the geopolymer matrix is reinforced with nanoparticles, and in the second approach, the matrix is reinforced with either short or continuous fibers. Considering factors such as practicality and production cost during production, reinforcement of the geopolymer matrix with short fibers is more preferred in civil engineering applications (Abbas et al., 2022).

In the literature, there are studies on the reinforcement of geopolymers with steel, inorganic, synthetic, and natural fibers. However, recently, the trend towards producing ecologically friendly and energy-saving materials has brought about the preference of natural fibers over other fibers in the reinforcement of geopolymers (Silva et al., 2020). However, it is relatively insufficient in comparison to the number of the works focuses on the reinforcement with inorganic and synthetic fibers.

Natural fibers are classified into three groups: mineral-based, animal-based, and plant-based fibers. The use of mineral-based fibers in geopolymers leads to high environmental impact because their production requires melting and spinning the mineral at high temperatures, and several processing steps are required before usage (Alzeer and MacKenzie, 2021). In addition, some mineral-based fibers, such as asbestos, are carcinogenic materials. On the other hand, animal-based fibers are not convenient for producing a large-scale geopolymers due to the difficulty in collecting them from animals (Silva et al., 2020). Since plant-based fibers are more cost-effective and easier to apply, they are the most suitable natural fiber type in terms of being used in the production of geopolymer materials.

The aim of the current chapter is to synthesize the latest research findings regarding the influence of plant-based fiber reinforcement on the improvement of the physical and mechanical properties of geopolymer composites. Recently published articles on plant-based fiber-reinforced geopolymer composites in the Scopus and SCI databases are reviewed. Only the effectiveness of "randomly oriented short fibers" on the properties is included in the study because they don't need specialized production methods and conventional production techniques can be used (Silva et al., 2020). The effectiveness of continuous fibers (fabrics) is excluded. The characteristics of plant-based fibers, mixture ratios, production process, and curing conditions of plant-based fiber-reinforced geopolymer composites are also within the scope of the current section.

THE COMPONENTS of PLANT-BASED FIBER-REINFORCED GEOPOLYMER COMPOSITES

A geopolymer composite reinforced with plant-based fiber consists of three basic components: (i) an aluminosilicate source, (ii) an alkali activator, and (iii) plant-based fiber (Figure 1). The aluminosilicate sources are various natural or artificial raw materials having high silica and alumina contents. The widely used alkali activators are sodium silicate (SS), sodium hydroxide (NaOH), and potassium hydroxide (KOH), and their combinations in various proportions (NaOH +SS and KOH+SS), which react with the aluminosilicate source to form geopolymer binders. In the

literature, geopolymer binders and mortars are reinforced with different types of plant-based fibers, such as sisal, jute, coir, cotton, hemp, lignin, raffia, pineapple, bamboo, musa basjoo, sorghum, and sugarcane bagasse, as shown in Figure 1.

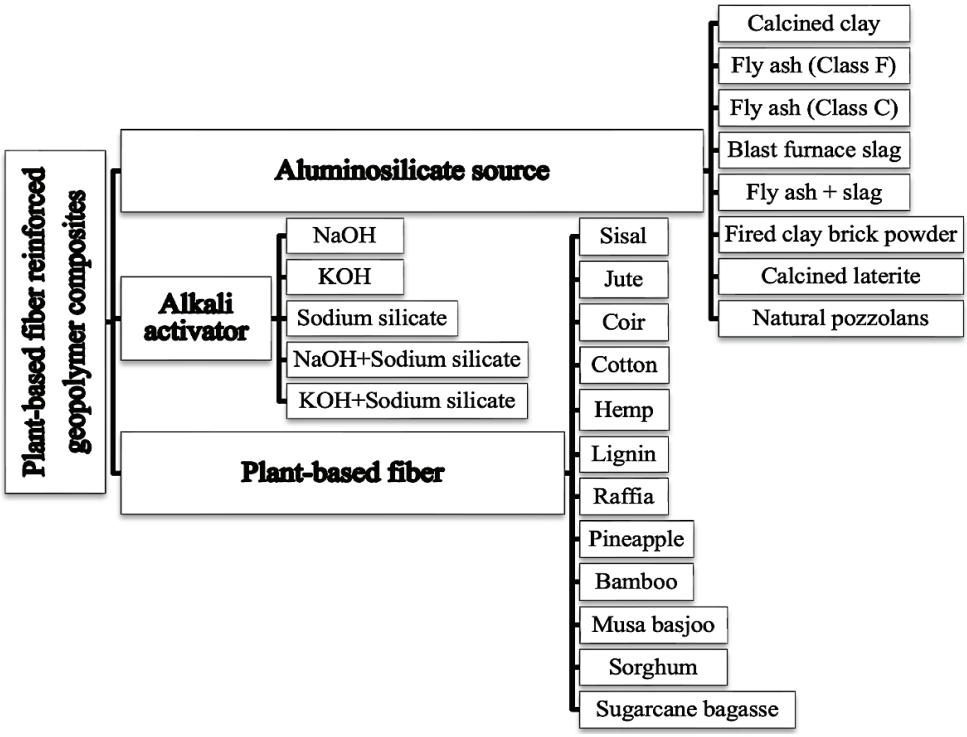

Figure 1. The Components of Plant-Based Fiber-Reinforced Geopolymer Composites

Chemical Structure of Plant-Based Fibers

Wood and non-wood fibers are the two subcategories of plant-based fibers. These latter materials are known as lignocellulose fibers, and they can be further separated into stem or bast fibers (such as hemp, jute, and flax), seed fibers (such as cotton), leaf fibers (such as banana, pineapple, and sisal), coir fibers (such as coconut), grass fibers (such as bamboo), and straw fibers (such as rice) (Alzeer and MacKenzie, 2021).

Cellulose, hemicellulose, and lignin are the main components of all plant-based fibers. Their chemical composition differs according to the

type of plant, location, climate, technique of harvesting, and plant maturity (Santana et al., 2021). Table 1 presents the chemical compositions of plant-based fibers frequently preferred as reinforcements in geopolymer matrices. Cellulose is a hydrophilic glucan polymer made from a straight chain of glucose compounds connected by β(1→4) bonding. The mechanical strength of the plant-based fibers is influenced by the orientation of the cellulose microfibrils (Alzeer and MacKenzie, 2021) and by the degree of cellulose polymerization, which varies according to the type of plant (Silva et al., 2020). Therefore, plant-based fibers with a high cellulose content (such as cotton, hemp, flax, and pineapple) are the most preferred ones to be used as a reinforcement in geopolymer matrices.

Table 1. Chemical Compositions of Plant-Based Fibers

		Chemical composition (wt %)			
Reference	Fiber type	Cellulose (%)	Hemicellulose (%)	Lignin (%)	Others (%)
(Pacheco-Torgal and Jalali, 2011)	Coir	31	19.2	29.7	20.1
(Jawaid and Abdul Khalil, 2011)	Flax	64.1	16.7	12	7.2
(Silva et al., 2020)	Jute	58–63	58–63	12– 15	-
	Sisal	43–56	21–24	7–9	-
(Mishra et al., 2004)	Pineapple	70-82	-	5-12	6-25
(Gassan and Bledzki, 1996)	Cotton	82.7	5.7	-	11.6
(Yan et al., 2016)	Bamboo	34.5	20.5	26	19
	Abaca	62.5	21	12	4.5
(Poletanovic et al., 2020)	Hemp	74.4	17.9	3.7	1.7
(Pacheco-Torgal and Jalali, 2011)	Banana	31.5	15.0	15.0	38.5

Hemicellulose is an amorphous, cross-linked polymer consisting of complex saccharide monomers (Alzeer and MacKenzie, 2021). Hemicel-

luloses connect and stabilize the cellulosic micro-fibers to increase the stability of the fibers rather than acting as load-bearing components. In contrast to the crystalline structure of cellulose, the structure of hemicellulose is entirely amorphous, which makes it more susceptible to an alkaline environment (Santana et al., 2021).

Lignin is an amorphous, complex aromatic hydrocarbon polymer and gives plants their structural support (Alzeer and MacKenzie, 2021). Lignin works as an adhesive, keeping the cellulosic units connected to one another. However, as with hemicellulose, the amorphous structure of lignin makes it vulnerable to deterioration (Santana et al., 2021). Pectin, a heteropolysaccharide that gives plants flexibility, is frequently present in the fibers of bast and fruits (Alzeer and MacKenzie, 2021).

Physical and Mechanical Properties of Plant-Based Fibers

Plant fibers provide a number of desirable benefits over synthetic fibers, including low cost, low weight, wide availability, biodegradability, recyclable resources, the desired aspect ratio, and strong tensile strength (Silva et al., 2020). The density of plant-based fibers varies between 1.2 and 1.5 g/cm^3, their tensile strength is between 120 and 900 MPa, their modulus of elasticity is between 4.8 and 90 GPa, and their ultimate elongation is between 0.59 and 25%, depending on the fiber type, length, chemical structure, and maturity level. They absorb moisture and water easily, and they are weakly dimensionally stable. When these fibers are incorporated in mortars, the hydrophobic and hydrophilic properties of the fibers and their interactions with the matrix can have an impact on how well they adhere to the matrix. The lower mechanical properties of the material can be caused by the existence of pendant hydroxyl and polar groups, which can result in significant moisture absorption and poor fiber-matrix adhesion (Yan et al., 2016).

According to the literature (Biagiotti et al., 2004), there are nearly 2.5 billion hydrogen bonds in cellulosic fibers. Even though hydrogen bonds only have about 1/10 the strength of covalent bonds, the high tensile strength of these fibers is due to the predominance of 2.5 billion hydrogen bonds. So, compared with synthetic fibers, plant-based fibers exhibit similar specific mechanical properties (Santana et al., 2021). The

tensile strength of cellulose fibers declines as fiber length increases because long fibers may have more imperfections and break rapidly compared to short fibers (Silva et al., 2020).

Plant-Based Fiber Content in Geopolymer Composites

Fiber content is often represented as a weight percentage (wt%) or volume fraction (vol%), as shown by Table 2. Some researchers selected to describe the inclusion of fiber in terms of the weight/volume of the aluminosilicate source (0.2-10%), whereas other researchers selected to describe the addition of fiber in terms of the weight/volume of the total of the raw materials (1-5%). A fiber with a smaller shape generates more fibers compared to a fiber with a larger shape for the same volume fraction.

MANUFACTURING PROCESS, CURING CONDITIONS and APPLIED TESTS of PLANT-BASED FIBER-REINFORCED GEOPOLYMER COMPOSITES

Throughout time, many methods, including extrusion, 3D printing, cold and hot pressing, have been used to mix and place geopolymer composites. However, the order in which the fibers are added must be carefully considered because it has a significant impact on the dispersion of the fibers and the uniformity of the matrix. Fiber surface deposition, fiber balling, and agglomeration should be avoided (Farhan et al., 2021) during mixture process.

Generally, the randomly oriented short fibers are blended with the aluminosilicate source in dry conditions for a short period of time. Afterwards, an alkali activator is gradually added, and the mixture process is continued until homogeneity is achieved (Alomayri et al., 2013). However, in some investigations, the fibers are finally incorporated into the geopolymer matrix after the mortar completely prepared (Ribeiro et al., 2016). The mixing period is extended for longer fibers with a high aspect ratio until uniform distribution is attained.

The curing conditions (curing temperature, duration, and humidity) have such an influence on how the geopolymer structure develops

as well as the final product's properties that it is essential to select the most effective curing conditions. The performance of the produced material may be deteriorated by improper curing, which can increase porosity and permeability and decrease mechanical properties. The curing temperature is the most important factor. Although heat curing takes more energy, it is frequently applied because the aluminosilicate precursor needs energy to start the geopolymerization reactions (Athira et al., 2021). Because the beginning of setting is delayed and the rate of the chemical reaction is incredibly slow, geopolymers cannot be successfully cured at temperatures below room temperature (7–20 °C) (Jiang et al., 2022; Nath and Sarker, 2015; Wang et al., 2004; Hardjito et al., 2004; Heah et al., 2011). The increase in curing temperature to 90 °C enhances the dissolution of an aluminosilicate source (Heah et al., 2011), increases cross-linking in an amorphous structure (Ferone et al., 2011), and finally increases the compressive strength of the material (Wang et al., 2004; Chindaprasirt et al., 2007).

Curing conditions for plant-based fiber-reinforced geopolymer composites are presented in Table 2. Depending on the type of aluminosilicate source, a variety of thermal curing conditions are used, ranging from ambient temperature to 90°C for 1 to 24 hours. Some studies have increased the curing temperature and period to over 90°C (Alomayri and Low, 2013) and 24 hours (Silva et al., 2020; Wongsa et al., 2020).

According to the Table 2, the physical properties of plant-based fiber-reinforced geopolymer composites are investigated in terms of workability, density, porosity, water absorption ratio, thermal conductivity, and ultrasound pulse velocity (UPV), while the mechanical properties are investigated in terms of flexural strength, compressive strength, impact strength, and hardness. In addition, the effects of fiber addition on the toughness of the unreinforced geopolymers are also determined in the experimental studies.

Table 2. Aluminosilicate, Activator and Fiber Types, Fiber Contents, Curing Conditions, and Applied Tests of Plant-Based Fiber-Reinforced Geopolymer Composites

Ref	Aluminosilicate precursor	Activator type	Fiber type	Fiber length (mm)	Fiber Content (wt% of precursor)	Curing	Workability	Density	Porosity	Water abs.	Thermal cond.	UPV	Flexural strength	Compressive Strength	Impact strength	Hardnes
(Wongsa et al., 2020)	High calcium fly ash	10 M NaOH+ SS*	Sisal	35–40	0	60 ° C for 48 h	•	•	•	•	•	•	•	•		
					0.5**		•	•	•	•	•	•	•	•		
					0.75**		•	•	•	•	•	•	•	•		
					1**		•	•	•	•	•	•	•	•		
			Coir	35–40	0		•	•	•	•	•	•	•	•		
					0.5**		•	•	•	•	•	•	•	•		
					0.75**		•	•	•	•	•	•	•	•		
					1**		•	•	•	•	•	•	•	•		
(Su et al., 2019)	Fly ash (70%) + slag (30%)	10 M NaOH+ SS	Lig-nin	-	0*	60 ° C for 24 h	•						•	•		
					0.25*		•						•	•		
					0.5*		•						•	•		
					0.75*		•						•	•		
					1*		•						•	•		
					1.25*		•						•	•		
(Silva et al., 2020)	Fired clay brick powder	8 M NaOH+ SS	Sisal	10	0	65 ° C for 72 h	•	•					•	•		
					0.5		•	•					•	•		
					1		•	•					•	•		
					1.5		•	•					•	•		
					2		•	•					•	•		
					2.5		•	•					•	•		
					3		•	•					•	•		
			Jute	10	0		•	•					•	•		
					0.5		•	•					•	•		
					1		•	•					•	•		
					1.5		•	•					•	•		
					0		•	•					•	•		

(Reddy et al., 2022)	Fly ash	6, 8, 10, and 12 M NaOH	Musa basjoo	20	0	-	•			•			•	•		
					0.25		•			•			•	•		
					0.5		•			•			•	•		
					0.75		•			•			•	•		
					1		•			•			•	•		
					1.25		•			•			•	•		
					1.5		•			•			•	•		
(Alomayri and Low, 2013)	Fly ash	8 M NaOH+ SS	Cotton	10	0	105 C for 3 h		•	•				•	•	•	•
					0.3			•	•				•	•	•	•
					0.5			•	•				•	•	•	•
					0.7			•	•				•	•	•	•
					1.0			•	•				•	•	•	•
(Yanou et al., 2021)	Calcined laterite	10 M NaOH+ SS	Sugarcane bagasse	-	0	at room temperature for 28 days		•	•	•				•		
					1.5			•	•	•				•		
					3			•	•	•				•		
					4.5			•	•	•				•		
					6			•	•	•				•		
					7.5			•	•	•				•		
(Nkwaju et al., 2019)	Calcined laterite	10 M NaOH+ SS	sugarcane bagasse	20	0	at room temperature for 28 days					•		•			
					1.5						•		•			
					3						•		•			
					4.5						•		•			
					6						•		•			
					7.5						•		•			
(Poletanovic et al., 2020)	fly ash and fly ash/slag	SS	Hemp	10	0**	20C, 60C, and 80C for 24 h		•		•			•	•		
					0.5**			•		•			•	•		
					1**			•		•			•	•		

SS=Sodium Silicate
*= the addition of fiber in terms of the mass of total dry materials
**= the addition of fiber in terms of the volume of total dry materials

PHYSICAL PROPERTIES of PLANT-BASED FIBER-REINFORCED GEOPOLYMER COMPOSITES

Workability

The higher qualities during the fresh condition are crucial to obtain higher mechanical properties after hardening (Abbas et al., 2022). The influence of fiber content on the workability of geopolymer composites is given in Figure 2.

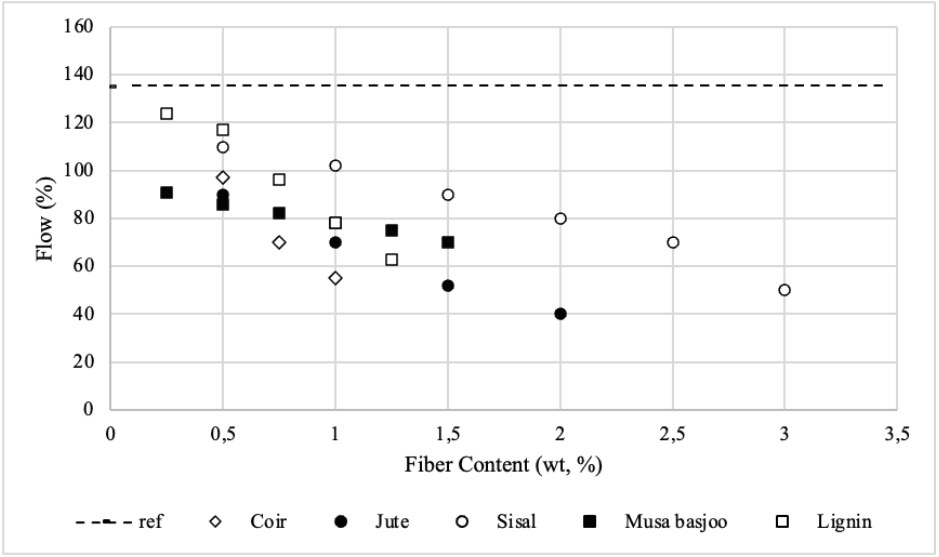

Figure 2. Influence of Plant-Based Fiber Content on the Workability of Geopolymer Composites, Adopted from Refs. (Silva et al., 2020; Wongsa et al., 2020; Su et al., 2019; Reddy et al., 2022)

The flow value of geopolymer matrices without fiber is in the range of about 130-135%. The workability of geopolymers containing various types of fibers was lower than that of the unreinforced geopolymer matrix, and this effect is independent of the type of fiber used. This is a result of the hydrophilic plant-based fiber's high moisture absorption. A significant shear force in between the matrix and fibers, which hinders fluidity and leads to a less workable matrix, is another factor contributing to this behavior (de Azevedo et al., 2021).

The content of fibers present in the geopolymer matrix affects the degree of workability reduction. With the inclusion of more fiber, the flow of all geopolymer mortars decrease. As seen in Figure 2, the flow fluctuates between 40 and 125% depending on the fiber ratio. Low fiber dispersion is observed at higher fiber contents (Su et al., 2019). The possibility of adding more water to compensate for this loss of workability should not be taken into account because it will reduce the mechanical properties of the material (Silva et al., 2020). Therefore, the fiber con-

tent should have a saturation limit in order to prevent challenges during molding and vibration of the fresh mixture (Silva et al., 2020). The maximum contents of coir, jute, sisal, musa basjoo, and lignin fibers are 1, 2, 3, 1.5, and 1.25, respectively. Since the casting process becomes incredibly difficult, a higher fiber content is not feasible.

The level of workability reduction in geopolymers is influenced by the aspect ratio of the fibers. As seen in Figure 2, for the same fiber content (for instance, 2 wt%), geopolymer composites reinforced with sisal fibers demonstrates a flow capacity that is 50% higher than that of jute fibers. This is explained by the lower aspect ratio that sisal fibers provide. As the aspect ratio increases, fiber-reinforced geopolymers become less workable (Silva et al., 2020).

Porosity and Density

Porosity is a key factor that greatly impacts the other mechanical and physical properties of geopolymer materials. The influence of fiber content on the porosity of geopolymer composites is given in Figure 3.

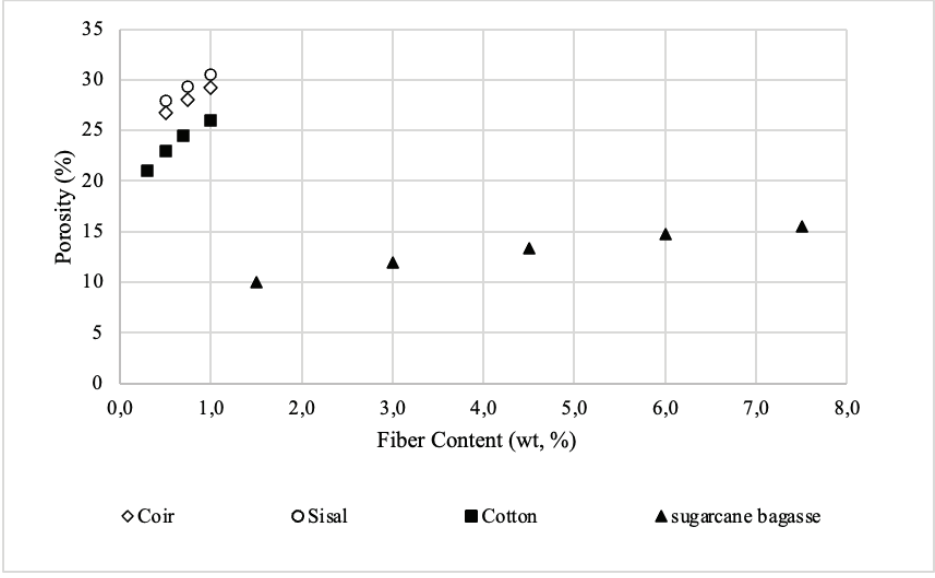

Figure 3. Influence of Plant-Based Fiber Content on the Porosity of Geopolymer Composites, Adopted from Refs. (Wongsa et al., 2020; Alomayri and Low, 2013; Yanou et al., 2021)

Generally, with the inclusion of plant-based fibers, the porosity of composites increases. While the porosity of the unreinforced geopolymer matrix is 27%, when the matrix is reinforced with 0.5, 0.75, and 1% sisal fiber, the porosity increases by 1.02, 1.10, and 1.15 times, respectively. When the same matrix is reinforced with the same proportion of coir fiber, the porosity increases 1.03, 1.05, and 1.09 times, respectively. The porosity of the geopolymer matrix is also increased by 1.05, 1.15, 1.22, and 1.30 times, respectively, by the incorporation of cotton fiber at concentrations of 0.3, 0.5, 0.7, and 1.0%. Higher contents of sugarcane bagasse fibers (1.5, 3.0, 4.5, 6.0, and 7.5%) increase the porosity of the matrix (10%), which is lower in the first case compared to other studies by 1.05, 1.09, 1.22, 1.34, and 1.40 times, respectively. The fact that fibers absorb water because of their porous structure may also help to explain why porosity increases as fiber concentration increases (Alomayri et al., 2013). A higher water ratio is necessary to lower the viscosity of fiber-reinforced geopolymers, and this leads to an increase in porosity. The higher amounts of water incorporation leads to more free water that is trapped inside inter-granular space and large pores after geopolymerization. During curing, this water evaporates, leaving a large number of inter-granular pores in the microstructure. In order to have a homogeneous microstructure, fiber clumping, which may be increased by a higher fiber content, is undesirable (Alomayri et al., 2013).

The influence of fiber content on the density of geopolymer is given in Figure 4.

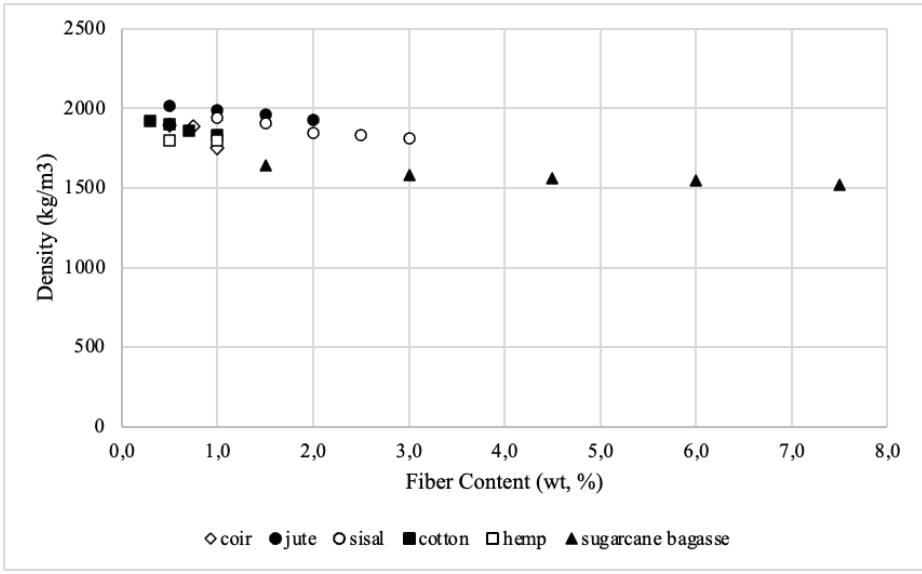

Figure 4. Influence of Plant-Based Fiber Content on the Density of Geopolymer Composites, Adopted from Refs. (Silva et al., 2020; Poletanovic et al., 2020; Wongsa et al., 2020; Alomayri and Low, 2013; Yanou et al., 2021)

Sisal fibers (up to 1% by weight) reduce the density of the reference geopolymer mortar by 0.97 times, while coir fibers decrease by 0.92 times. Incorporating cotton fibers (0.30, 0.50, 0.70, and 1.00 %) gradually decrease the density of the mortar by 0.96, 0.95, 0.93, and 0.91 times, respectively. Hemp fibers added at the content of 0.50% and 1.00% provide 0.96 and 0.95 times decrease in the density of the geopolymer composite, respectively. In addition, the density of sugarcane bagasse fiber-based geopolymer composites with higher contents (from 0% to 1.5%, 3%, 4.5, 6, and 7.5) decrease 0.98, 0.97, 0.96, 0.95, and 0.94 times, respectively. Generally, the decrease in density of fiber-reinforced mortars is the result of their higher porosity. In addition, regardless of the type of composite, density decreases as fiber content increases. Due to an increase in fiber content, the fibers clustered during mixing (Alomayri et al., 2013), and an uneven dispersion of fibers inside the matrix encourages the formation of fiber coalescence and voids confined between them. These spaces are filled with water when the matrix is in a fresh state, but as it

hardens, the evaporation of the water causes the composite to become porous and less dense (de Azevedo et al., 2021). Additionally, the final density of the composites is lower due to the reduced density of plant-based fibers themselves (Poletanovic et al., 2020). Contrary to other studies, the bulk density is maximized at a specific fiber content (1% for both sisal and jute fiber-reinforced geopolymers). The increase in density in comparison to the unreinforced matrix is explained by the greater compaction energy used throughout production because of workability loss and the increased viscosity due to fiber addition. However, when the fiber content is higher than 1%, the density decreases. Even though more compaction energy is used during production (at 1% fiber content), this loss in bulk density may be due to fiber agglomeration during mixing at high fiber content (Silva et al., 2020).

Water Absorption Ratio

Macropores and wider capillary pores, both of which are larger than 1 μm, are able to permit water to penetrate (Poletanovic et al., 2020). The influence of fiber content on the water absorption ratio of geopolymer composites is given in Figure 5. Plant-based fiber-reinforced geopolymer composites absorb more water as their porosity and density increase. While the water absorption ratio of the unreinforced geopolymer matrix is 5%, the water absorption values increase approximately 1.20, 1.22, and 1.26 times when the material is reinforced with 0.5, 0.75, and 1% sisal fiber, respectively. When the same matrix is reinforced with the same amount of coir fiber, the effect of fiber content on water absorption is not significant. The addition of 1.5, 3.0, 4.5, 6, and 7.5% sugarcane bagasse fibers leads to an increase in the water absorption ratio of the unreinforced matrix (18%) by approximately 1.06, 1.11, 1.17, 1.22, and 1.33 times, respectively. In comparison to the unreinforced specimen, the increasing level of the water absorption ratio of hemp fiber-reinforced geopolymers (with 0.5 and 1% fiber content) is the highest, approximately 1.48 and 1.57 times, respectively.

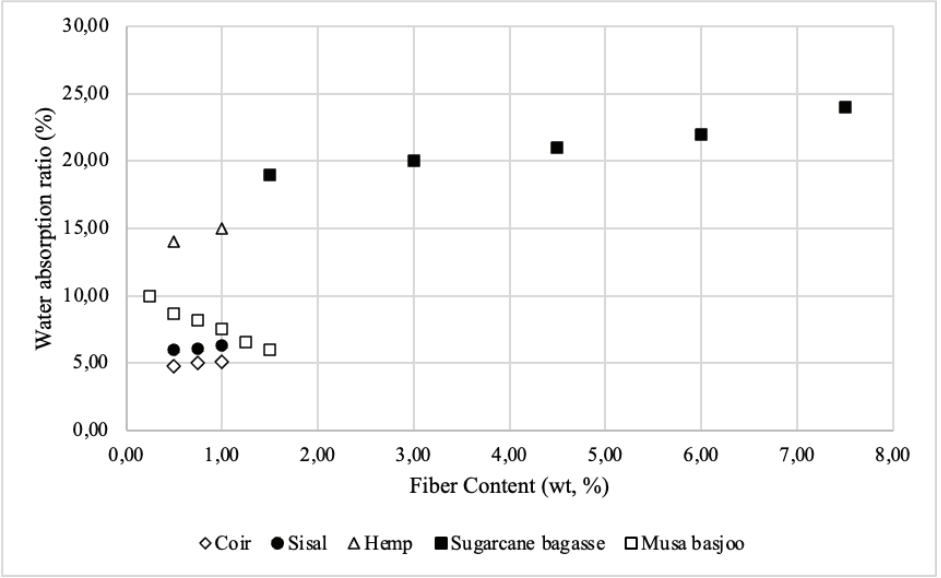

Figure 5. Influence of Plant-Based Fiber Content on the Water Absorption Ratio of Geopolymer Composites, Adopted from Refs. (Poletanovic et al., 2020; Wongsa et al., 2020; Reddy et al., 2022; Yanou et al., 2021)

The hydrophilic characteristics of natural fibers and the inclusion of air voids into the geopolymers as a result of the fiber's addition are considered to be responsible for the increase in water absorption ratio (Yanou et al., 2021). Water molecules enter a natural fiber-reinforced composite in a moist environment via microcracks and the hydrophilic properties of the fiber allow the fiber to absorb this water (Alomayri et al., 2014). Water molecules absorbed onto the hydrophilic groups on plant fibers form a significant number of hydrogen bonds, which form a physical barrier between the matrix and the fiber and result in decreasing the adhesion at the interface (Camargo et al., 2020). As a result, the fibers swell, which may cause microcracks in the material and lead to debonding between the matrix and the fiber. Furthermore, the high cellulose content of plant-based fibers absorbs additional water that enters the interface through these microcracks, causing swelling pressures that induce composite failure (Alomayri et al., 2014). However, unlike other studies, the addition of musa basjoo fibers leads to a decrease in water

absorption ratio from 12.67% to 5.1%. This may be a result of fiber addition creating a dense microstructure (Reddy et al., 2022).

Ultrasonic Pulse Velocity (UPV)

The sound vibrations that can be heard are between 16 and 16,000 Hz. Sound waves with a frequency above 16,000 Hz are called "ultrasound," and these waves are not audible to the human ear. In order for these waves to propagate, the object must be in a solid, liquid, or gaseous state. Otherwise, ultrasound waves cannot propagate through a vacuum. If there is a gap in their orbit, sound waves cannot pass this gap and go around it. This leads to a prolongation of the sound transition time in the material and, thus, a decrease in the sound transmission velocity (Postacıoğlu, 1981).

The porosity-UPV relationship of geopolymer composites is shown in Figure 6.

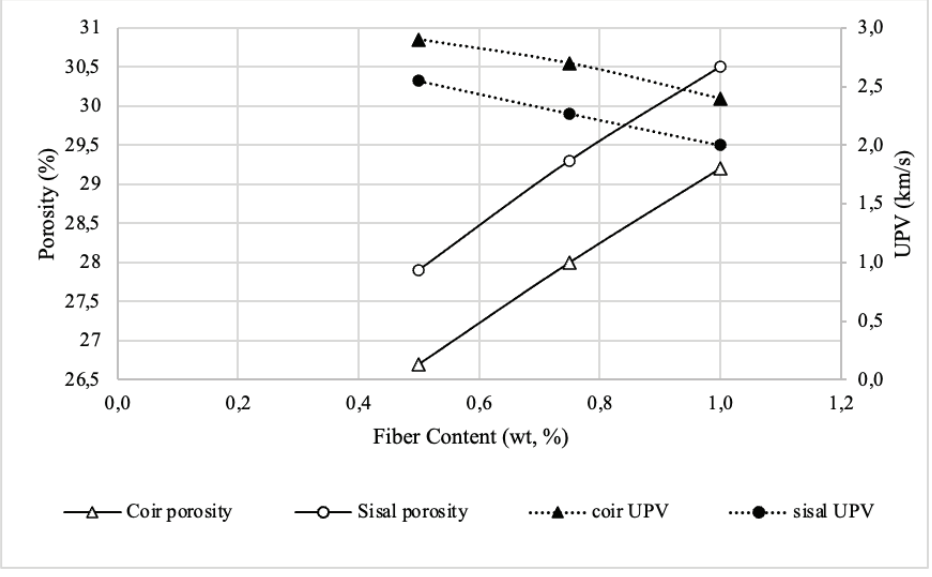

Figure 6. The Porosity-UPV Relationship of Geopolymer Composites Reinforced with Plant-Based Fibers, Adopted from Ref. (Wongsa et al., 2020)

The sisal and coir fiber incorporation increases the porosity compared to the reference sample, and accordingly, the UPV decreases. The

increase in porosity due to the higher fiber contents in sisal fiber samples causes a decrease in UPV until 2.55, 2.27, and 2.00 km/s, respectively. In addition, reinforcing the same geopolymer mortar with the same contents of coir fiber causes the UPV to decrease until 2.90, 2.70, and 2.40 km/h, respectively. As a result, the matrix's porosity really does have a significant impact on the UPV, and air void discontinuities in the matrix can restrict and impede the UPV (Muñoz-Sánchez et al., 2016; Mohammed and Rahman, 2016).

Thermal Conductivity

The thermal conductivity of a material (λ); It is the sum of (i) conduction by solid (λ conduction, solid) and air (λ conduction, air), (ii) convection by air (λ convection), and (iii) radiation between adjacent faces of pores perpendicular to the direction of heat flow (λ radiation) (Ghazi Wakili et al., 2015):

$$\lambda = \lambda_{conduction,solid} + \lambda_{conduction,air} + \lambda_{convection} + \lambda_{radiation}$$

Heat conduction is the primary form of heat energy transfer in solid bodies. Energy spreads by being transferred from one molecule to another as a result of the vibration of the molecules. For a porous material, conduction is the main type of heat transfer (Prud'homme et al., 2015) and $\lambda_{conduction,solid}$ is responsible for the majority of the heat conduction at ambient temperature (Ghazi Wakili et al., 2015). Hence, the thermal conductivity of materials is a function of the ratio between the solid and air amounts of the material (i.e., the total porosity) (Dhasindrakrishna et al., 2021). Generally, porous materials with high porosity or low density have a lower λ value (Liu et al., 2014; Huang et al., 2018; Cui et al., 2018; Bai et al., 2019). Because the thermal conductivity of inert air (0.026 W/mK) is lower than that of the surrounding solid geopolymer matrix (usually 1.0-1.2 W/mK) and the higher porosity of the material means it has more voids that can serve as thermal insulation (Prud'homme et al., 2015). Since low thermal conductivity is equivalent to high insulation capacity (Azimi et al., 2016), the resistance to heat transfer increases as the thermal conductivity coefficient of the material decreases (Davraz et al., 2020).

The influence of plant-based fiber content on the thermal conductivity of geopolymer composites is shown in Figure 7. The thermal conductivity of sugarcane bagasse fiber-reinforced geopolymer (with 7.5 wt% fiber content) decreases to 0.55 W/mK compared to that of the unreinforced matrix (0.77 W/mK) (Nkwaju et al., 2019). The low thermal conductivity of bagasse fibers (0.08 W/mK.), the existence of pores in the geopolymer matrix, which reduce the heat transmission rate due to the lowest thermal conductivity of the air contained in these pores, and the existence of further pores at the fiber-matrix interface all contribute to decreasing thermal conductivity. (Nkwaju et al., 2019). The thermal conductivity of sisal (0.984–1.025 W/mK) and coir (0.949–0.976 W/mK) fiber-reinforced mortars also decreases with increasing fiber contents (Wongsa et al., 2020). The decreasing trend of thermal conductivity of all specimens is also consistent with the increasing trend of porosity and density, as shown in Figures 3 and 4.

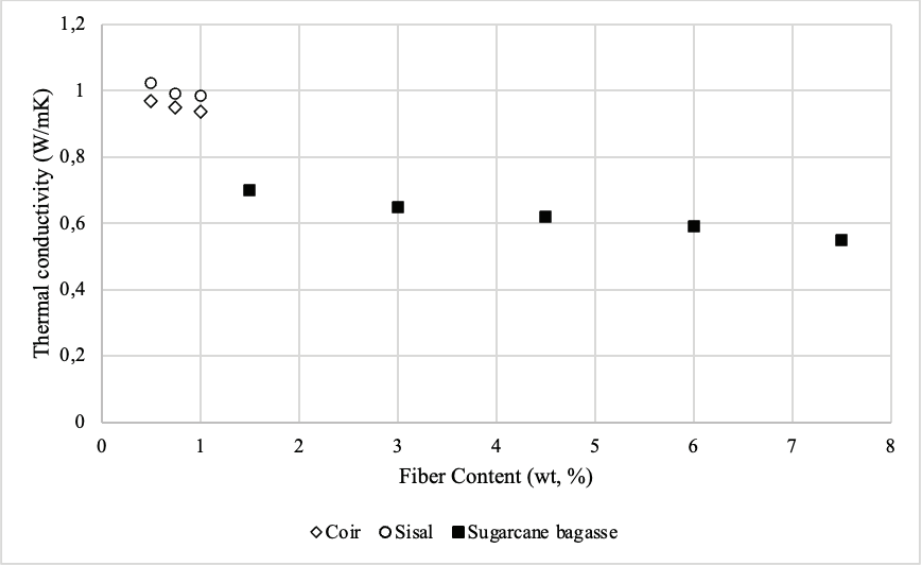

Figure 7. Influence of Plant-Based Fiber Content on the Thermal Conductivity of Geopolymer Composites Adopted from Refs. (Wongsa et al., 2020; Nkwaju et al., 2019)

MECHANICAL PROPERTIES of PLANT-BASED FIBER-REINFORCED GEOPOLYMER COMPOSITES

Flexural Strength

The flexural test is an indirect tensile test that evaluates the geopolymer's resistance to failure under bending. Usually, three- and four-point loading is applied during flexural tests (Abbas et al., 2022). The mechanical resistance of a geopolymer matrix to bending loads and the energy absorption capacity are generally improved by the incorporation of fibers (de Azevedo et al., 2021). For the development of the flexural strength, the fibers' capacity to act as bridges between the cracks and restrict the growth of those cracks is very crucial. Once a crack occurs, the strength of the composite decreases, and the fibers receive bending stresses from the matrix. When a crack contacts a fiber, a specific quantity of energy is required in order to separate the fiber from the matrix, overcome adhesion, and cause crack propagation throughout the matrix. The fiber may be destroyed or separated (pulled) from the matrix during this procedure. Because of the further energy required to break the friction between the fiber and the matrix, the maximum improvement in flexural strength happens only when fiber is pulled from the matrix (de Azevedo et al., 2021). The "bridge effect" distributes the stress to different parts of the composite, preventing it from breaking suddenly. New cracks develop when the material's capacity has been again surpassed by stresses in other regions, and the process repeated. Despite the presence of many additional secondary cracks, there is an active crack that continues to grow and leads the sample to fracture (de Azevedo et al., 2021).

The influence of plant-based fiber content on the flexural strength of geopolymer composites is shown in Figure 8.

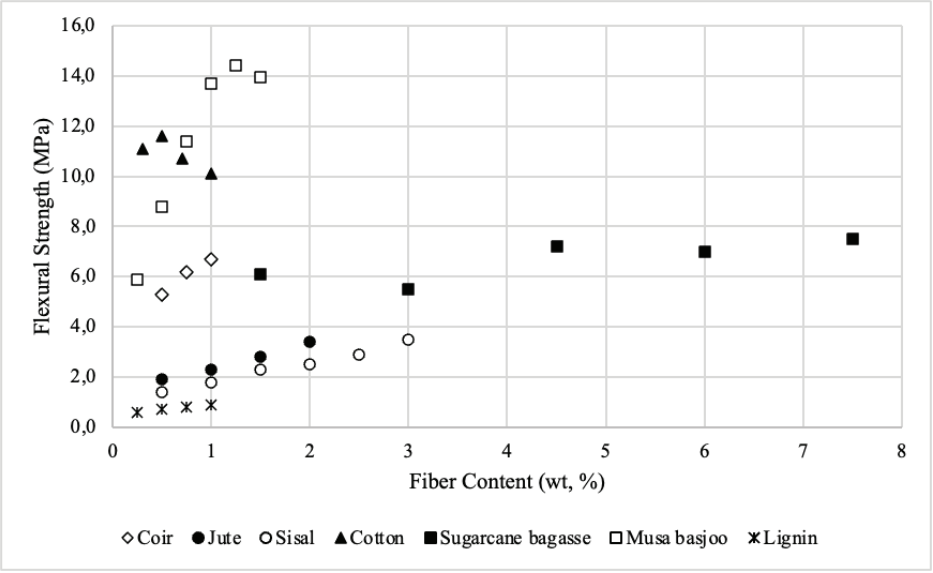

Figure 8. Influence of Plant-Based Fiber Content on the Flexural Strength of Geopolymer Composites, Adopted from Refs. (Silva et al., 2020; Poletanovic et al., 2020; Wongsa et al., 2020; Su et al., 2019; Reddy et al., 2022; Alomayri and Low, 2013; Nkwaju et al., 2019)

The flexural strength of fly ash and slag-based unreinforced geopolymer mortar (0.5 MPa) increases with increasing lignin fiber content (from 0% to 0.25, 0.50, 0.75, and 1.0 %) up to 1.0 MPa (Su et al., 2019). In a different study, the flexural strengths of the unreinforced specimens (5.55 MPa) and those reinforced with the addition of (1 wt%) of coir (5.25 MPa), cotton (5.85 MPa), or sisal fibers (5.90 MPa) are essentially comparable. However, due to the absence of cohesion between the raffia fibers and the matrix, the addition of the raffia fibers results in a 0.55 times lower flexural strength than that of the unreinforced geopolymer (Korniejenko et al., 2016).

In comparison to the unreinforced specimen, geopolymers reinforced with jute and sisal fibers demonstrate better flexural strength. With 2% of jute fibers as the fiber content, the greatest flexural strength of 3.3 MPa is attained; this is an increase of 4.1 times over the unreinforced geopolymer matrix. On the other hand, the geopolymer matrix's

flexural strength increases by 4.3 times with the inclusion of 3% sisal fibers, reaching 3.5 MPa (Silva et al., 2020). In a different investigation, the increasing of fiber content increases the flexural strength of the Musa basjoo fiber-reinforced ash-based geopolymers. The samples with 1.25% fiber content provide a maximum flexural strength of 14.39 MPa. When the plant-based fibers sustain additional stress, they are good at resisting both initial cracks and their development. Over 1.25% fiber content, a 0.95-times reduction in flexural strength is detected. When there are too many fibers in the matrix, the gap between the fibers narrows and agglomerates are formed. As a result of the production of agglomerates, the bond between the fiber and the matrix becomes weaker. This could be the cause of the reduced flexural strength in the specimens with fiber contents greater than 1.25% (Reddy et al., 2022). A similar result is obtained in another study. The flexural strength of cotton fiber-reinforced geopolymer first increases until the fiber content reaches 0.5 %. The efficient distribution of the fibers inside the matrix, which promotes increased adhesion at the matrix-fiber interface, may be responsible for the improvement in flexural strength. As a result, the stress transmission from the matrix to the fibers may function at its optimum, which enhances the strength. However, when cotton fiber concentration exceeds 0.5 wt%, the homogeneity of the composite is prevented, causing agglomerations that weaken the interfacial adhesion between the fiber and the matrix. As a result, the flexural strength decreases (Alomayri et al., 2013). In another research, the incorporation of sisal and coir fibers (0.5%, 0.75%, and 1.0%) into high-calcium fly ash-based geopolymers results in increased flexural strength. This is caused by the fiber's high tensile strength and elasticity modulus, as well as the fact that the fiber's interaction with the matrix allowed for the transfer of stress from the matrix to the fiber. The maximum fiber content is set at 1% volume fraction because fiber contents higher than that have poor workability and made mixtures difficult to cast and compress (Wongsa et al., 2020). Only one study's results differ from those of the others. Flexural strength in laterite-based geopolymers does not appear to be significantly correlated with sugarcane bagasse fiber contents (1.5%, 3%, 4.5%, 6%, and 7.5% wt). The fibers' irregular orientation is probably the reason. According

to research, fibers with a particular orientation (horizontal or vertical) may absorb and evenly distribute the stress all across the matrix (Nkwaju et al., 2019).

Compressive Strength

Compressive loads lead to inelastic volumetric dilatancy in the brittle materials and cause the development of axially splitting microcracks that run parallel to the direction of the applied load. The formation of transversal tensile stress at the crack tips of these microcracks aids in its propagation in the load direction, causing local cracks. Around "weak areas," such as large voids or pores, these local fracture points occur significantly more readily. The compressive stress response of brittle materials is controlled by their density, pore structure, brittleness, and microcrack distribution (Farhan et al., 2021).

Conflicting findings on the compressive strength of fiber-reinforced geopolymer composites have been reported in the literature. Studies show that fibers do not always result in a reduction in the compressive strength and frequently enhance the compressive strength of geopolymers, despite the fact that using fibers is intended to induce an increment in ductility and prevent crack propagation instead of improving the compressive strength (de Azevedo et al., 2021).

The influence of plant-based fiber content on the compressive strength of geopolymer composites is shown in Figure 9.

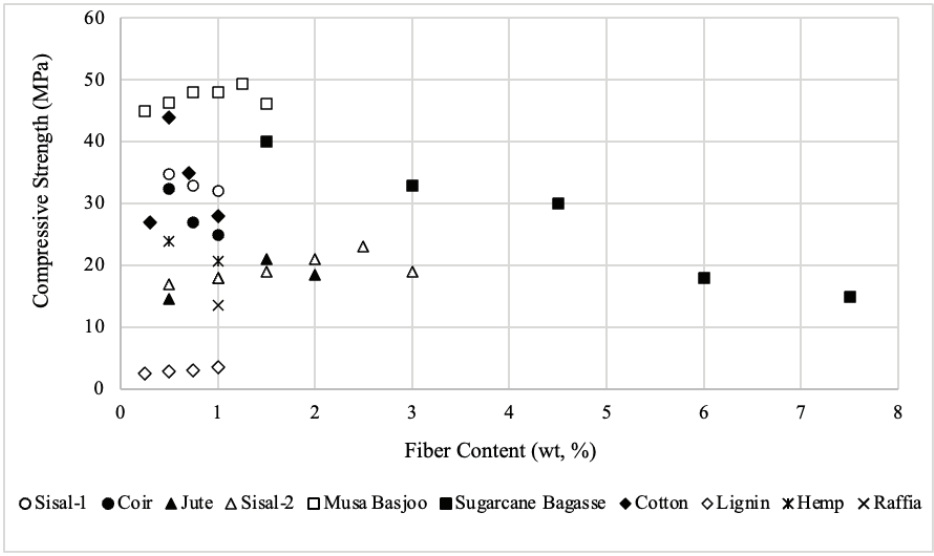

Figure 9. Influence of Plant-Based Fiber Content on the Compressive Strength of Geopolymer Composites, Adopted from Refs. (Silva et al., 2020; Poletanovic et al., 2020; Wongsa et al., 2020; Su et al., 2019; Reddy et al., 2022; Alomayri and Low, 2013; Yanou et al., 2021)

Fly ash and slag-based unreinforced geopolymer mortar's compressive strength (2.4 MPa) improves with higher lignin fiber content (from 0% to 0.25, 0.50, 0.75, and 1.0%), up to a maximum of 3.5 MPa (Su et al., 2019). The results of the compressive strength tests reveal that adding cotton, sisal, and coir fibers (1 wt%) increase the compressive strength of the unreinforced fly ash-based geopolymer by 1.15, 1.05, and 1.26 times, respectively. The absence of adhesion between the raffia fibers and the matrix, however, results in the reinforced matrix's compressive strength being 0.55 times lower than that of the unreinforced matrix (Korniejenko et al., 2016). When compared to the unreinforced geopolymer, specimens reinforced with jute and sisal fibers show improved compressive strength. When the fiber content in jute fiber is 1.5% by weight, the maximum compressive strength is 20.6 MPa, which is an increase of 1.75 times above the reference specimen. When the fiber content is 2.5% by weight, sisal fiber-reinforced geopolymers achieve a maximum compressive strength of 22.1 MPa, an increase of 1.84 times over the reference spec-

imen. Higher fiber contents cause a decrease in compressive strength for both types of fiber-reinforced specimens (Silva et al., 2020). Similar results are also obtained in another study. The compressive strength of the Musa basjoo fiber-reinforced ash-based geopolymer increases with the higher fiber content. Because fibers increase the cohesive force and strengthen the interlocking between aggregates, respectively. Hence, providing a stronger bridging effect and preventing crack development may subsequently result in increased strength (Reddy et al., 2022).

The compressive strength, however, decreases by 0.93 times over 1.25% fiber content. When there are too many fibers, the distance between each fiber decreases, and the bond between the fibers and matrix weakens. Additionally, too many fibers cause the balling effect, which reduces the fiber bridging action (Reddy et al., 2022). The trend in the results is consistent with another study. Following the introduction of 0.5 wt% cotton fibers, the geopolymer's compressive strength improves from 19.1 to 46.0 MPa. This is explained by the probability that more loads are transmitted from the matrix to the fibers, increasing the load carried by the fibers. Good fiber dispersion inside the matrix, which enhances the bonding strength between the fiber and the matrix, may also be a factor in this positive behavior. The compressive strength, however, decreases with the higher contents of cotton fibers (0.7 and 1.0 wt%). The loss in compressive strength may be caused by a greater tendency for these fibers to ball up and form pores in the matrix (Alomayri and Low, 2013). Sisal and coir fibers result in an increment in the compressive strength until 0.5% fiber content in high calcium fly ash geopolymer mortars. However, as the fiber concentration is increased beyond 0.5%, the composite's density decreases, lowering its compressive strength. High fiber content makes the matrix difficult to pack and causes the sample's porosities to increase, which reduces its compressive strength (Wongsa et al., 2020). On the other hand, in some studies where geopolymer mortars are reinforced with various plant-based fibers, the compressive strength may tend to decrease. For instance, it is examined how the inclusion of fibers from alkali-treated sweet sorghum affected the mechanical performance of geopolymers made from fly ash. When the fiber contents are 1, 2, and 3%, the compressive strength decline by

9, 17, and 26%, respectively (Chen et al., 2014). In the other research, the addition of sugarcane bagasse fibers decreases the compressive strength of the laterite-based geopolymers. When the geopolymers are reinforced with 1.5, 3, 4.5, 6, and 7.5% fiber contents, respectively, the compressive strength decreases by 18.3, 31.8, 431, 65.9, and 71.8% in comparison to the unreinforced geopolymer. Higher void content in the composites, which results in weaker zones within the matrix, is responsible for decreasing compressive strength (Yanou et al., 2021). The loss in strength may also be brought on by the orientation of the fibers. Because the fibers are distributed randomly, this may lead to low-stress transmission in the matrix, which will reduce its strength (Nkwaju et al., 2019).

Impact Strength

Impact strength is the quantity of energy that a material may endure when the load is abruptly applied on the material. It can also be described as the amount of force per unit area that must be applied before a material fracture. The bonds at the matrix and fiber interface and the characteristics of the matrix and the fibers control the impact strength of a fiber-reinforced material. As the composites experience an abrupt load, the combination of fiber pull-out, fiber rupture, and matrix deformation dissipates the impact energy (Wambua et al., 2003). Whereas there are a lot of findings on the compressive and flexural strengths of plant-based fiber-reinforced geopolymers, there are comparatively few findings regarding this material's impact behavior.

Figure 10 illustrates how cotton fiber content affects the geopolymer matrix's ability to withstand impact loads. The impact strength of the geopolymer paste is increased after 0.5 weight percent cotton fibers are added. The uniform distribution of the fibers within the matrix, which increases adhesion at the matrix-fiber interface, may be responsible for the improvement in impact strength. The impact strength tends to increase with increasing fiber content due to increased fiber pullout and fiber breakage. Better stress transfer from the matrix to the fibers is made possible by this, and consequently the strength increases. Conversely, as the fiber content increases beyond 0.5 wt%, the impact strength decreases. This decrease at higher fiber content is brought about by the

production of voids and fiber coalescence owing to the higher viscosity, which in turn decreases the adhesion of the fiber and matrix (Alomayri and Low, 2013).

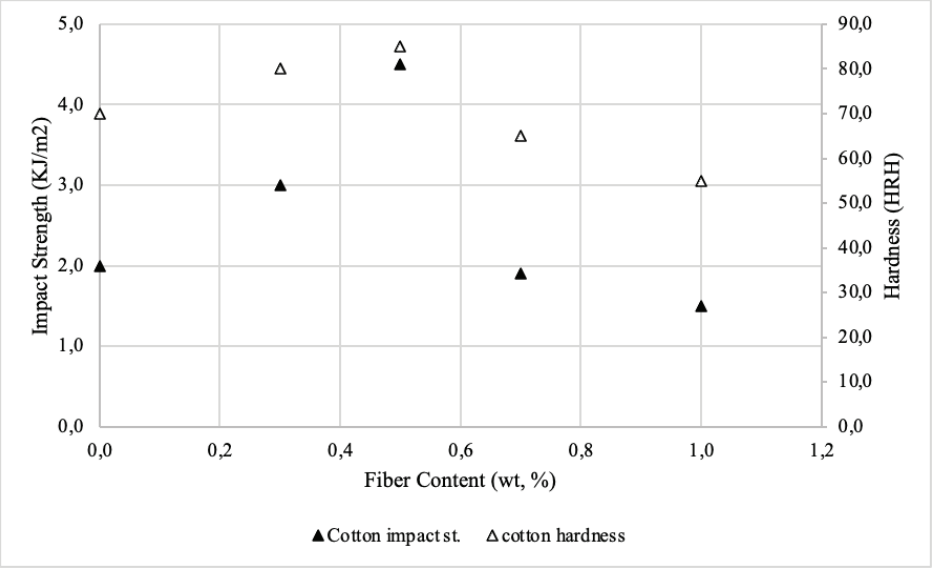

Figure 10. Influence of Plant-Based Fiber Content on the Impact Strength and Hardness of Geopolymer Composites, Adopted from Ref. (Alomayri and Low, 2013)

Hardness

The hardness test is one of the most general mechanical tests performed on the material because it is simple to apply and does not damage the material. In addition, there is a parallel relationship between the hardness of a material and its other mechanical properties, so that an idea can be obtained about the strength values of that material. Hardness is a relative measure and is defined as the resistance of materials to friction, cutting, scratching, and plastic deformation. In scientific terms, it is defined as the resistance of materials to dislocation motion.[2]

Figure 10 shows the impact of cotton fiber content on the hardness of geopolymer composites. The geopolymer with 0.5 wt.% fiber incorpora-

2 Bursa Teknik Üniversitesi Mühendislik ve Doğa Bilimleri Fakültesi Makine Mühendisliği Bölümü, Makine Mühendisliği Laboratuvarı Sertlik Ölçme Deneyi Deney Föyü

tion increases the Rockwell hardness from 70 to 93 in comparison to the unreinforced geopolymer. The considerable increase in hardness is the result of the test load being distributed over the fibers, which decreases the test ball's capacity to penetrate the composite material's surface. However, as the fiber content increases, the hardness decreases because the fibers are poorly dispersed. The incorporation of 0.7 and 1.0 wt.% fibers lead to a decrease in the consistency of the matrix and a low wettability between the fibers and the matrix, so the fibers are easily separated from the matrix. A higher water content in the geopolymer mixture is required to make up for this. In order to solve that problem, increasing water content may result in low hardness (Alomayri and Low, 2013).

Toughness

The amount of energy that a material absorbs during plastic deformation is expressed by its toughness (de Azevedo et al., 2021). Almost all studies on plant-based fiber-reinforced geopolymer composites (Silva et al., 2020; Poletanovic et al., 2020; Alomayri et al., 2013; Ribeiro et al., 2016) show that unreinforced materials with low toughness exhibit abrupt and fragile fracture. However, geopolymers reinforced with plant fiber do not deteriorate after the formation of just a single crack. Usually, fibers carry all of the tensile force in the area where a crack first forms. When the load is increased without rupturing or pulling out the fibers near the existing crack, new cracks will form and the force will be transferred to the fibers at this location. Multiple cracks form as a result of this process, which persists until the fibers break or pull out of the matrix. This mechanism is termed "deflection hardening behavior" and is identified in the load–deflection curve by the strength increases over deflection when the first cracking load is greater compared to the peak load. After the initial crack formation, the composites that show deflection hardening behavior have an increased load-carrying capability and also a higher energy absorption capacity (toughness) (Abbas et al., 2022). Contrary to unreinforced matrix, composites with a higher toughness ensure prolonged ruptures that exhibit signs of emergence, trying to alert to the collapse of the material (de Azevedo et al., 2021). In addition, the higher the plant-based fiber content, the higher the energy absorp-

tion capacity of the plant-based fiber-reinforced geopolymer composites (Poletanovic et al., 2020).

CONCLUSION

This study focuses on a review of the published articles on plant-based fiber-reinforced geopolymer composites. The physical and mechanical properties of randomly oriented short fibers included in geopolymer composites are thoroughly discussed. The conclusions that can be reached are as follows:

- *Various types of plant-based fibers, such as sisal, coir, jute, cotton, hemp, lignin, raffia, pineapple, bamboo, musa basjoo, sorghum, and sugarcane bagasse, can be effectively used as a reinforcement in geopolymer binders, mortars, and concrete. However, the effectiveness of more fiber types, such as banana and palm fibers, on geopolymer composites should also be investigated.*
- *The physical and mechanical properties of geopolymer composites consisting of either artificial (such as fly ash, boiler ash, slag, calcined clay, and fired clay brick powder) or natural (such as natural earth, volcanic earth, and volcanic ash) aluminosilicate sources are significantly impacted by these plant-based fibers.*
- *The type, chemical structure, and properties of the fibers, their content (as a weight percentage (wt%) or volume fraction (vol%)), the manufacturing process, and the curing conditions are important key parameters in order to produce plant-based fiber-reinforced geopolymer composites with higher physical and mechanical properties.*
- *It is crucial to maintain homogeneous dispersion of the fibers and the matrix throughout production since balling and fiber coalescence reduce the required properties.*
- *Plant-based fiber-reinforced geopolymer composites are usually produced with thermal curing between ambient temperature and 90°C for 1 to 24 hours. The optimum curing conditions (curing temperature, duration, and humidity) should be applied, depending on the properties of both the fiber and the aluminosilicate source.*

- *No matter what kind of fiber is used, the workability of fiber-reinforced geopolymers is less than that of the unreinforced geopolymer matrix. The workability of the matrix imposes a limit on the fiber content in order to prevent negative casting conditions brought on by difficulties in molding, vibration, and compacting.*
- *To reduce the viscosity of the geopolymer, more water is added to the matrix. This free water evaporates during temperature curing, leaving a large number of pores in the microstructure. Thus, with the inclusion of fibers, the porosity and the water absorption ratio of composites increase, whereas the density and the ultrasound pulse velocity (UPV) decrease. The porosity has a significant impact on the density and UPV results.*
- *The thermal conductivity of the unreinforced geopolymer matrix decreases after fiber inclusion because of the higher porosity of the composite, the presence of additional pores at the fiber-matrix interface, and also because of the lower thermal conductivity of the plant-based fibers. Therefore, it may be stated that incorporating plant-based fibers may enhance a material's insulating properties.*
- *In general, the flexural, compressive, and impact strengths of unreinforced geopolymers increase with increasing fiber content up to the optimum level. At the optimum fiber content, the fibers are uniformly distributed in the matrix, adhesion at the matrix-fiber interface is good, stress is transmitted from the matrix to the fibers, the fibers can resist both initial cracks and their development, and consequently the mechanical properties improve. However, more fiber incorporation beyond the optimum content causes balling and coalescence of the fibers and creates voids in the matrix that weaken the interfacial adhesion between the fiber and the matrix and, finally, reduce the mechanical properties.*
- *Contrary to unreinforced matrix, plant-based reinforced geopolymer composites have a higher energy absorption capacity which ensure prolonged ruptures that exhibit signs of emergence, trying to alert to the collapse of the material.*

REFERENCES

Abbas, A. G. N., Abdul Aziz, F. N. A., Abdan, K., Nasir, N. A. M., and Huseien, G. F. (2022). A State-of-the-Art Review on Fibre-Reinforced Geopolymer Composites. *Construction and Building Materials,* 330, 127187. https://doi.org/10.1016/j.conbuildmat.2022.127187

Abdul Aleem, M. I., and Arumairaj, P. D. (2012). Geopolymer Concrete-A Review. *International Journal of Engineering Sciences & Emerging Technologies,* 1(2), 118–122. http://dx.doi.org/10.7323/ijeset/v1_i2_14

Alomayri, T., Assaedi, H., Shaikh, F. U. A., and Low, I. M. (2014). Effect of Water Absorption on the Mechanical Properties of Cotton Fabric-Reinforced Geopolymer Composites. *Journal of Asian Ceramic Societies,* 2(3), 223–230. https://doi.org/10.1016/j.jascer.2014.05.005

Alomayri, T., and Low, I. M. (2013). Synthesis and Characterization of Mechanical Properties in Cotton Fiber-Reinforced Geopolymer Composites. *Journal of Asian Ceramic Societies,* 1(1), 30–34. https://doi.org/10.1016/j.jascer.2013.01.002

Alomayri, T., Shaikh, F. U. A., and Low, I. M. (2013). Characterisation of Cotton Fibre-Reinforced Geopolymer Composites. *Composites Part B,* 50, 1–6. https://doi.org/10.1016/j.compositesb.2013.01.013

Alzeer, M. I. M., MacKenzie, K. J. D. (2021). Fiber Composites of Inorganic Polymers (Geopolymers) Reinforced with Natural Fibers. *Composite Materials,* 117–147. https://doi.org/10.1016/B978-0-12-820512-9.00016-2

Athira, V. S., Bahurudeen, A., Saljas, M., and Jayachandran, K. (2021). Influence of Different Curing Methods on Mechanical and Durability Properties of Alkali Activated Binders. *Construction and Building Materials,* 299, 123963. https://doi.org/10.1016/j.conbuildmat.2021.123963

Azimi, E. A., Al Bakri Abdullah, M. M., Ming, L. Y., Yong, H. C., Hussin, K., and Aziz, I. H. (2016). Processing and Properties of Geopolymers as Thermal Insulating Materials: A Review. *Reviews on Advanced Materials Science,* 44, 273–285.

Azevedo, A. R. G., Cruz, A. S. A., Marvila, M. T., de Oliveira, L. B., Monteiro, S. N., Vieira, C. M. F., Fediuk, R., Timokhin, R., Vatin, N., and Dailonas, M. (2021). Natural Fibers as an Alternative to Synthetic Fibers in Reinforcement of Geopolymer Matrices: A Comparative Review. *Polymers,* 13, 2493. https://doi.org/10.3390/polym13152493

Bai, C., Li, H., Bernardo, E., and Colombo, P. (2019). Waste-to-Resource Preparation of Glass-Containing Foams from Geopolymers. *Ceramics International,* 45(6), 7196–7202.

Biagiotti, J., Puglia, D., and Kenny, J. M. (2004). A Review on Natural Fibre-Based Composites- Part I: Structure, Processing and Properties of Veg-

etable Fibres, *Journal of Natural Fibers,* 1(2), 37–68. https://doi.org/10.1300/J395v01n02_04

Bondar, D., Lynsdale, C. J., Milestone, N. B., Hassani, N., and Ramezanianpour, A. A. (2011). Effect of Type, Form, and Dosage of Activators on Strength of Alkali-Activated Natural Pozzolans. *Cement and Concrete Composites,* 33, 251–260. https://doi.org/10.1016/j.cemconcomp.2010.10.021

Camargo, M. M., Adefrs Taye, E., Roether, J. A., Tilahun Redda, D., and Boccaccini, A. R. (2020). A Review on Natural Fiber-Reinforced Geopolymer and Cement-Based Composites. *Materials,* 13, 4603. https://doi.org/10.3390/ma13204603

Chen, R., Ahmari, S., and Zhang, L. (2014). Utilization of Sweet Sorghum Fiber to Reinforce Fly Ash-Based Geopolymer. *Journal of Material Science,* 46(6), 2548–2558. https://doi.org/10.1007/s10853-013-7950-0

Chindaprasirt, P., Chareerat, T., and Sirivivatnanon, V. (2007). Workability and Strength of Coarse High Calcium Fly Ash Geopolymer. *Cement and Concrete Composites,* 29(3), 224–229. https://doi.org/10.1016/j.cemconcomp.2006.11.002

Cui, Y., Wang, D., Zhao, J., Li, D., Ng, S., and Rui, Y. (2018). Effect of Calcium Stearate-Based Foam Stabilizer on Pore Characteristics and Thermal Conductivity of Geopolymer Foam Material. *Journal of Building Engineering,* 20, 21–29. https://doi.org/10.1016/j.jobe.2018.06.002

Davidovits, J. (2011). *Geopolymer Chemistry and Applications*. Saint-Quentin: Institut Géopolymère.

Davraz, M., Koru, M., Akdağ, A., Kılınçarslan, Ş., Delikanlı, Y., and Çabuk, M. (2020). Investigating the Use of Raw Perlite to Produce Monolithic Thermal Insulation Material. *Construction and Building Materials,* 263, 1–7. https://doi.org/10.1016/j.conbuildmat.2020.120674

Dhasindrakrishna, D. K., Pasupathy, K., Ramakrishnan, S., and Sanjayan, J. G. (2021). Progress, Current Thinking and Challenges in Geopolymer Foam Concrete Technology. *Cement and Concrete Composites,* 116, 103886. https://doi.org/10.1016/j.cemconcomp.2020.103886

Farhan, K. Z., Johari, M. A. M., and Demirboğa, R. (2020). Assessment of Important Parameters Involved in the Synthesis of Geopolymer Composites: A Review. *Construction and Building Materials,* 264, 120276. https://doi.org/10.1016/j.conbuildmat.2020.120276

Farhan, K. Z., Johari, M. A. M., and Demirboğa, R. (2021). Impact of Fiber Reinforcements on Properties of Geopolymer Composites: A Review. *Journal of Building Engineering,* 44, 102628. https://doi.org/10.1016/j.jobe.2021.102628

Ferone, C., Colangelo, F., Cioffi, R., Montagnaro, F., and Santoro, L. (2011). Mechanical Performances of Weathered Coal Fly Ash Based Geopoly-

mer Bricks. *Procedia Engineering,* 21, 745–752. https://doi.org/10.1016/j.proeng.2011.11.2073

Ganesan, N., Indira, P. V., and Santhakumar, A. (2013). Prediction of Ultimate Strength of Reinforced Geopolymer Concrete Wall Panels in One-Way Action. *Construction and Building Materials,* 48, 91–97. https://doi.org/10.1016/j.conbuildmat.2013.06.090

Garcia-Lodeiro, I., Palomo, A., and Fernández-Jiménez, A. (2015). An Overview of the Chemistry of Alkali-Activated Cement-Based Binders. *Handbook of Alkali-Activated Cements, Mortars and Concretes,* 2, 19–47. https://doi.org/10.1533/9781782422884.1.19

Gassan, J., Bledzki, A. K. (1996). Modification Methods on Nature Fibers and Their Influence on the Properties of the Composites. *Technical Papers of the Annual Technical Conference-Society of Plastics Engineers Incorporated,* Society of Plastics Engineers Inc, 2552–2557.

Hardjito, D., Wallah, S. E., Sumajouw, D. M. J., and Rangan, B.V. (2004). On the Development of Fly Ash-Based Geopolymer Concrete. *ACI Materials Journal,* 101, 467–472.

Heah, C. Y., Kamarudin, H., Mustafa Al Bakri, A. M., Binhussain, M., Luqman, M., Khairul Nizar, I., Ruzaidi, C. M., and Liew, Y. M. (2011). Effect of Curing Profile on Kaolin-based Geopolymers. *Physics Procedia,* 22, 305–311. https://doi.org/10.1016/j.phpro.2011.11.048

Hendriks, C. A., Worrell, E., Price, L., Martin, N., and Ozawa Meida, L. (1999). *The Reduction of Green House Gas Emissions from the Cement Industry.* IEA Greenhouse Gas R&D Programme Report PH3/7, Cheltenham: IEA.

Huang, Y., Gong, L., Shi, L., Cao, W., Pan, Y., and Cheng, X. (2018). Experimental Investigation on the Influencing Factors of Preparing Porous Fly Ash- Based Geopolymer for Insulation Material. *Energy and Buildings,* 168, 9–18. https://doi.org/10.1016/j.enbuild.2018.02.043

IPCC, Climate Change. (2001). *The Scientific Basis, Intergovernmental Panel on Climate Change.* Cambridge: Cambridge University Press.

Jawaid, M., and Abdul Khalil, H. P. S. (2011). Cellulosic/Synthetic Fibre Reinforced Polymer Hybrid Composites: A Review. *Carbohydrate Polymers,* 86(1), 1–18. https://doi.org/10.1016/j.carbpol.2011.04.043

Jiang, D., Shi, C., and Zhang, Z. (2022). Recent Progress in Understanding Setting and Hardening of Alkali-Activated Slag (AAS) Materials. *Cement and Concrete Composites,* 134, 104795. https://doi.org/10.1016/j.cemconcomp.2022.104795

Korniejenko, K., Frączek, E., Pytlak, E., and Adamski, M. (2016). Mechanical Properties of Geopolymer Composites Reinforced with Natural Fibers. *Procedia Engineering,* 151, 388–393. https://doi.org/10.1016/j.proeng.2016.07.395

Liu, M. Y. J., Alengaram, U. J., Jumaat, M. Z., and Mo, K. H. (2014). Evaluation of Thermal Conductivity, Mechanical and Transport Properties of Lightweight Aggregate Foamed Geopolymer Concrete. *Energy and Buildings,* 72, 238–245. https://doi.org/10.1016/j.enbuild.2013.12.029

Mishra, S., Mohanty, A. K., Drzal, L. T., Misra, M., and Hinrichsen G. (2004). A Review on Pineapple Leaf Fibers, Sisal Fibers and Their Biocomposites. *Macromolecular Materials and Engineering,* 289(11), 955–974. https://doi.org/10.1002/mame.200400132

Mohammed, T. U., and Rahman, M. N. (2016). Effect of Types of Aggregate and Sand-To- Aggregate Volume Ratio on UPV in Concrete. *Construction and Building Materials,* 125, 832–841. https://doi.org/10.1016/j.conbuildmat.2016.08.102

Muñoz-Sánchez, B., Arévalo-Caballero, M. J., and Pacheco-Menor, M. C. (2016). Influence of Acetic Acid and Calcium Hydroxide Treatments of Rubber Waste on the Properties of Rubberized Mortars. *Materials and Structures,* 50(75). https://doi.org/10.1617/s11527-016-0912-7

Nath, P., and Sarker, P. K. (2015). Use of OPC to Improve Setting and Early Strength Properties of Low Calcium Fly Ash Geopolymer Concrete Cured at Room Temperature. *Cement and Concrete Composites,* 55, 205–214. https://doi.org/10.1016/j.cemconcomp.2014.08.008

Nkwaju, R. Y., Djobo, J. N. Y., Nouping, J. N. F., Huisken, P. W. M., Deutou, J. G. N., and Courard, L. (2019). Iron-Rich Laterite-Bagasse Fibers Based Geopolymer Composite: Mechanical, Durability and Insulating Properties. *Applied Clay Science,* 183, 105333. https://doi.org/10.1016/j.clay.2019.105333

Pacheco-Torgal, F. (2015). Introduction to Handbook of Alkali-Activated Cements, Mortars and Concretes. *Handbook of Alkali- Activated Cements, Mortars and Concretes,* 1, 1-16. https://doi.org/10.1016/B978-1-78242-276-1.50029-0

Pacheco-Torgal, F., and Jalali, S. (2011). Cementitious Building Materials Reinforced with Vegetable Fibres: A Review. *Construction and Building Materials,* 25(2), 575–581. https://doi.org/10.1016/j.conbuildmat.2010.07.024

Poletanovic, B., Dragas, J., Ignjatovic, I., Komljenovic, M., and Merta, I. (2020). Physical and Mechanical Properties of Hemp Fibre Reinforced Alkali-Activated Fly Ash and Fly Ash/Slag Mortars. *Construction and Building Materials,* 259, 119677. https://doi.org/10.1016/j.conbuildmat.2020.119677

Postacıoğlu, B. (1981). *Cisimlerin Yapısı ve Özellikleri-İç Yapı ve Mekanik Özellikler.* İstanbul: İTÜ Matbaası.

Provis, J. L., and Bernal, S. A. (2014). Geopolymers and Related Alkali-Activated Materials. *Annual Review of Materials Research,* 44, 299–327. DOI: 10.1146/annurev-matsci-070813-113515

Prud'homme, E., Joussein, E., and Rossignol, S. (2015). Alkali-Activated Concrete Binders as Inorganic Thermal Insulator Materials. *Handbook of Alkali-Activated Cements, Mortars and Concretes,* 26, 687–728. https://doi.org/10.1533/9781782422884.5.687

Reddy, Y. B. S., Praburanganathan, S., and Mishra, M. (2022). Experimental Investigation on the Fiber Reinforced Ash-Based Geopolymer Concrete with Musa Basjoo Fibers. *Materials Today: Proceedings,* 65(8), 3700–3706. https://doi.org/10.1016/j.matpr.2022.06.297

Ribeiro, R. A. S., Ribeiro, M. G. S., Sankar, K., and Kriven, W. M. (2016). Geopolymer-Bamboo Composite-A Novel Sustainable Construction Material. *Construction and Building Materials,* 123, 501–507. https://doi.org/10.1016/j.conbuildmat.2016.07.037

RILEM TC 224-AAM. (2014). State-of-the-Art Report. *Alkali Activated Materials*. DOI 10.1007/978-94-007-7672-2_6

Robayo-Salazar, R. A., and de Gutiérrez, R. M. (2018). Natural Volcanic Pozzolans as an Available Raw Material for Alkali-Activated Materials in the Foreseeable Future: A Review. *Construction and Building Materials,* 189, 109–118. https://doi.org/10.1016/j.conbuildmat.2018.08.174

Santana, H. A., Júnior, N. S. A., Ribeiro, D. V., Cilla, M. S., and Dias, C. M. R. (2021). Vegetable Fibers Behavior in Geopolymers and Alkali-Activated Cement Based Matrices: A Review. *Journal of Building Engineering,* 44, 103291. https://doi.org/10.1016/j.jobe.2021.103291

Silva, G., Kim, S., Aguilar, R., and Nakamatsu, J. (2020). Natural Fibers as Reinforcement Additives for Geopolymers – A Review of Potential Eco-Friendly Applications to the Construction Industry. *Sustainable Materials and Technologies,* 23, e00132. https://doi.org/10.1016/j.susmat.2019.e00132

Silva, G., Kim, S., Bertolotti, B., Nakamatsu, J., and Aguilar, R. (2020). Optimization of A Reinforced Geopolymer Composite Using Natural Fibers and Construction Wastes. *Construction and Building Materials,* 258, 119697. https://doi.org/10.1016/j.conbuildmat.2020.119697

Su, Z., Guo, L., Zhang, Z., and Duan, P. (2019). Influence of Different Fibers on Properties of Thermal İnsulation Composites based on Geopolymer Blended with Glazed Hollow Bead. *Construction and Building Materials,* 203, 525–540. https://doi.org/10.1016/j.conbuildmat.2019.01.121

Wakili, K. G., Hugi, E., Karvonen, L., Schnewlin, P., and Winnefeld, F. (2015). Thermal Behaviour of Autoclaved Aerated Concrete Exposed to Fire. *Cement and Concrete Composites,* 62, 52–58. https://doi.org/10.1016/j.cemconcomp.2015.04.018

Wambua, P., Ivens, J., and Verpoest, I. (2003). Natural Fibres: Can They Replace Glass in Fibre Reinforced Plastics?. *Composites Science and Technology,* 63(9), 1259–1264. https://doi.org/10.1016/S0266-3538(03)00096-4

Wang, K., Shah, S. P., and Mishulovich, A. (2004). Effects of Curing Temperature and NaOH Addition on Hydration and Strength Development of Clinker-Free CKD-Fly Ash Binders. *Cement and Concrete Research,* 34(2), 299–309. https://doi.org/10.1016/j.cemconres.2003.08.003

Wongsa, A., Kunthawatwong, R., Naenudon, S., Sata, V., and Chindaprasirt, P. (2020). Natural Fiber Reinforced High Calcium Fly Ash Geopolymer Mortar. *Construction and Building Materials,* 241, 118143. https://doi.org/10.1016/j.conbuildmat.2020.118143

Yan, L., Kasal, B., and Huang, L. (2016). A Review of Recent Research on the Use of Cellulosic Fibres, Their Fibre Fabric Reinforced Cementitious, Geo-Polymer and Polymer Composites in Civil Engineering. *Composites Part B: Engineering,* 92, 94–132. https://doi.org/10.1016/j.compositesb.2016.02.002

Yanou, R. N., Kaze, R. C., Adesina, A., Nemaleu, J. G. D., Jiofack, S. B. K., and Djobo, J. N. Y. (2021). Performance of Laterite-Based Geopolymers Reinforced with Sugarcane Bagasse Fibers. *Case Studies in Construction Materials,* 15, e00762. https://doi.org/10.1016/j.cscm.2021.e00762

Zhang, Z., Provis, J. L., Reid, A., and Wang, H. (2014). Geopolymer Foam Concrete: An Emerging Material for Sustainable Construction. *Construction and Building Materials,* 56, 113–127. https://doi.org/10.1016/j.conbuildmat.2014.01.081

Zheng, G., Cui, X., Zhang, W., and Tong, Z. (2009). Preparation of Geopolymer Precursors by Sol–Gel Method and Their Characterization. *Journal of Material Science,* 44, 3991–3996. https://doi.org/10.1007/s10853-009-3549-x

INDUSTRIAL VIEW TO FRICTION DRILLING TECHNOLOGY

Mustafa ER[1], Bahattin YILMAZ[2], Abdulkadir GÜLLÜ[3]

Abstract: Screws, pins, rivets, etc. are used in the assembly process with mechanical fastening. machine elements are used. In the screw mounting of thin-walled materials, it is a problem that a sufficient length of screw thread cannot be created. For the solution of this problem, alternative methods such as welding the elements like nut etc. to the hole output have been developed. However, these methods have brought additional operational costs, long processing times and new problems such as axial misalignment. Friction drilling method has been developed to generate the screw connection of thin-walled materials. In this method, with the help of the high heat released as a result of the contact of the tool and the workpiece, the workpiece is drilled and a bushing is formed at the hole exit in the form of a natural extension of the material. This bushing makes it possible to open the connection needed for the screw connection. This process, which is carried out by plastering the part without removing chips, allows lower costs and faster assembly processes. In this study, drilling with friction is introduced. Academic studies conducted with the friction drilling process have been compiled and the output information about the operation is presented in the conclusion section. It has been observed that the friction drilling process reduces the operation times,

1 Gazi Üniversitesi, Teknoloji Fakültesi, Ankara / Türkiye, e-mail: mustafa.er2@gazi.edu.tr, Orcid No: 0000-0001-6335-8438

2 Gazi Üniversitesi, Teknoloji Fakültesi, Ankara / Türkiye, e-mail: bahattinyilmaz@gazi.edu.tr, Orcid No: 0000-0002-0457-7291

3 Gazi Üniversitesi, Teknoloji Fakültesi, Ankara / Türkiye, e-mail: agullu@gazi.edu.tr, Orcid No: 0000-0003-1088-4105

creates a screw connection with high strength, and provides a more environmentally friendly process.

Keywords: Friction Drilling, Drilling Process, Screwing, Assembly Process

INTRODUCTION

The process of producing a product consists of two stages namely the manufacturing processes of the parts that make up the product and the assembly processes of these parts (Sözügüzel, 2007). Producing a product with high efficiency is possible by performing these two stages at low costs and with high quality. It is of great importance in terms of efficiency that the manufacturing processes are carried out with low energy costs and tool consumption. Again, in the manufacturing process, the production of the products within the appropriate tolerance ranges helps both the high quality of the product and the easier assembly phase. A quick and easy assembly process is required for a successful manufacturing process.

The assembly process is carried out with three different methods: mechanical joining, welded joining and bonding (Brinksmeier, 1990). The most preferred of these methods is the mechanical joining process. Standard machine elements are utilized in this process. The most important element of assembly processes is possible with the use of right machine elements (Cantero, et al., 2005). Machine elements like screws, rivets, pins, etc. are often used in assembly lines. The effective use of these parts is possible by drilling holes with high accuracy. This has led to the widespread use of hole drilling. Drilling with a drill constitutes 40% of all machining operations (Brinksmeier, 1990). In addition to drilling with helical drills within the scope of machining, secondary hole operations such as hole enlargement, reaming, tapping etc. are also frequently utilized (Yılmaz et al., 2020). In addition to machining operations, drilling operations are also carried out by using cutting molds and laser cutting, especially in thin-walled parts. In the drilling process with a drill, the evacuation of the sawdust by contacting the tool and the workpiece, and the frictions disrupt the hole surface and distort the hole dimensions. Furthermore, thermal and mechanical loads that occur during drilling

cause stresses on the part (Cantero, et al., 2005). In addition, secondary operations are required to obtain adequate thread lengths for threaded connections in thin-walled materials with conventional drilling methods. Such adverse situations necessitated the development of alternative methods to hole drilling.

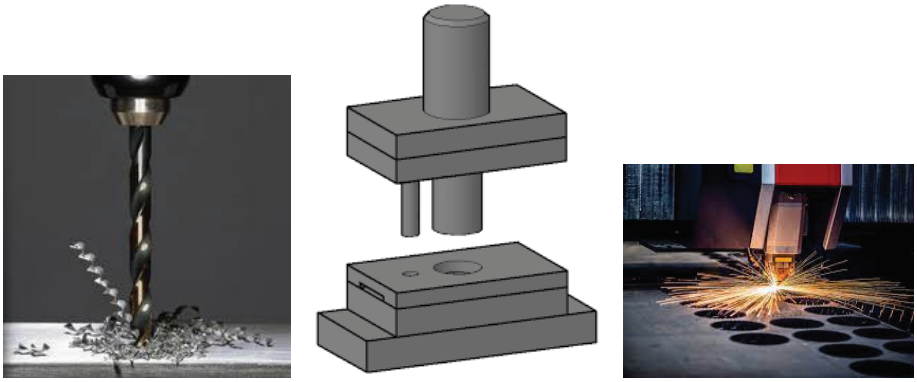

a) b) c)

Figure 1. Different Drilling Methods
a) with a helical drill b) with a cutting template c) drilling with a laser cut

Lightening of products is one of the most important R&D studies in many of the industries that have a large share in the development of today's technology such as the automotive industry, aerospace and aviation industry. Developing material technology has enabled the production of materials with high strength at low wall thicknesses. This has also contributed greatly to the production of lighter products. Thin-walled materials are widely used in many fields such as automotive, plumbing, steel construction, medical, aerospace and aviation (Chow et al., 2008). These materials are mounted as welded, screwed, pinned or riveted according to part function. In order to use the screw connection, it is necessary to thread the thin-walled material. However, the low part thickness causes the necessary thread height for the screw to not be formed, and thus the assembly process cannot be performed. Particularly in bolts with a high pitch, the thickness of the piece does not allow even a single screw thread to occur. For the solution of this problem, nut welding is performed at the hole outlet[1] (Hang-Ming et al., 2007). This additional

operation increases processing times and costs. Moreover, concentricity problems may occur between the hole and the nut. As a result of the welding process, there may be changes in the mechanical structure of the workpiece due to heating and cooling. Boiling the nut also creates a disadvantage in terms of product weights (Kumar and Jesudoss Hynes, 2019).

Figure 2. Nut Welding Application to the Hole Outlet (Özkan and Ünlü 2016)

These mentioned problems have led to the development of a different perspective to the drilling operation. In this newly developed drilling process, it is aimed to accumulate/stack the material thrown as sawdust in the traditional drilling method to the hole exit as a bushing. This new drilling strategy is defined as friction drilling operation (Shalamov et al., 2016, Özler, 2019). In this process, a conical tool makes rotational motion and contacts to the workpiece. Due to the friction that occurs as a result of the contact and the high heat released due to this friction, the strength of the material decreases. This facilitates the shaping of the workpiece. Tool drilling process is performed the with the contribution of the plastic deformation caused by the progress movement of the tool. During the drilling process, excess material accumulates at the hole exit and forms a bushing. No sawdust formation is observed in this process. The material discarded as sawdust in traditional methods accumulates

as a bushing at the exit of the hole in this method. The bushing height can be several times the material thickness and provides the necessary height for threading (Raju and Swamy, 2012).

The simultaneous creation of the hole and the bushing with the same tool ensures concentricity. It prevents additional processing costs such as welding the nut. Drilling and threading can be performed if used with the right tools and operating parameters. Friction drilling provides significant time savings compared to conventional drilling methods. Friction drilling is also known by different names such as thermal drilling, flow drilling, and form drilling (Miller et al., 2006).

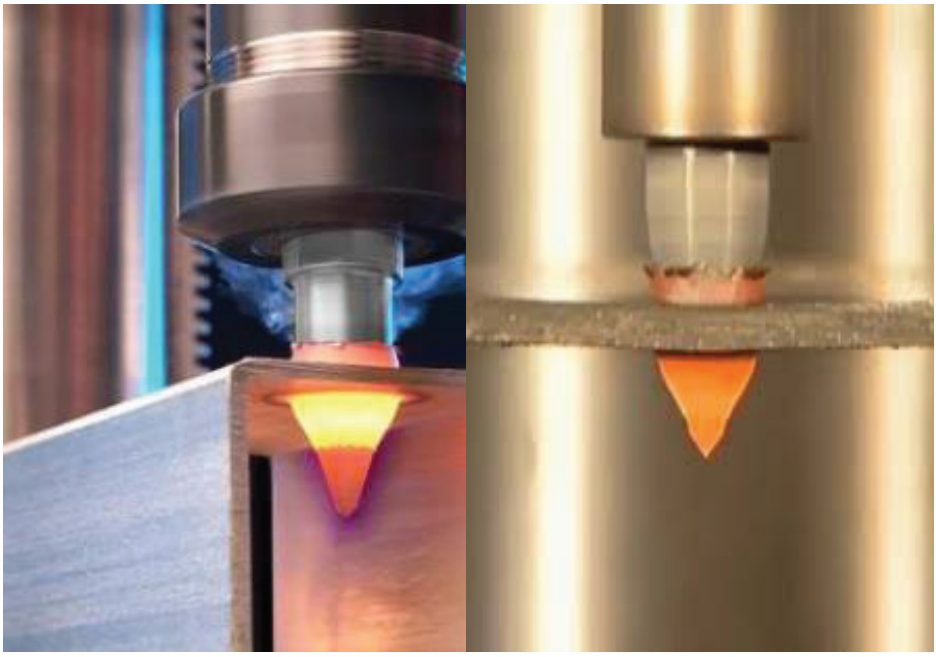

Figure 3. Friction Drilling Process

FRICTION DRILLING STRATEGY

Friction drilling was first introduced in 1923 by the French Jean Claude de Valiere as an alternative to the traditional drilling operation. However, the lack of suitable tool material and the inability to develop the required tool geometry in the early years hindered the development of friction drilling. By the end of the 20th century, arrangements made in

developing material technology and tool geometries increased the use of friction drilling operation (France, 1990).

The friction drilling process starts with the contact of the formed special cutting tool to the workpiece. As a result of this contact and cutting motion (rotational motion), friction and high heat due to friction are generated between the tool and the workpiece. This heat increases the tool's forming ability by decreasing the workpiece strength. With the tool moving into the workpiece, the drilling and bushing process is completed. With this process, a bushing height that is 2-3 times of the wall thickness is created so that the required thread height for the screw is provided (Rao et al., 2017, Miller et al., 2007). Friction drilling is a method that is performed without removing chips and unconventional (Demir, 2013).

Figure 4. Friction Drilling Application to Welded Square (Doğru, 2010)

The friction drilling process is carried out using different processing steps. The formation of the bushing shape depends on the operating

conditions, drill diameter, drill geometry (conical length, tip angle, etc.) (Dekkers, 1993). The drilling process takes place in three stages (Doğru, 2010).

Initial Phase

Friction with drilling process requires high deformation energies. High frictional energies are needed for the formation of high heat. For this reason, high cutting and feed rates of the tool are required. Due to the high feed rate, high feed forces occur with tool and workpiece contact. At the initial stage, the advance forces are at their highest. With the high temperature caused by friction, the strength of the material and the feed forces decrease. At this stage, the shaping of the material becomes easier with the decreasing strength (Doğru, 2010).

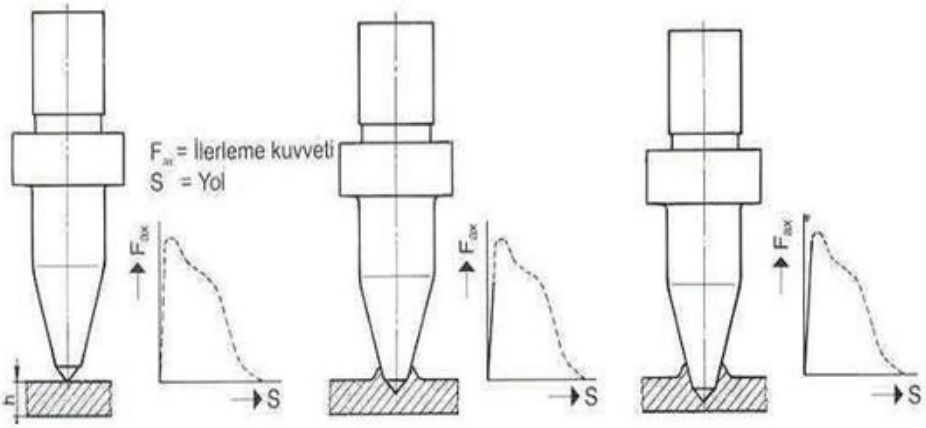

Figure 5. Initiation Phase of Friction Drilling and Force Generation (Wu et al., 2016)

Flow Phase

With the effect of high temperature, the workpiece whose yield strength decreases, begins to take shape. As the tool starts to sink into the workpiece, the material starts to pile up towards the hole entrance. As the tool advances into the part, the stacking moves towards the hole exit and taper begins to form. With the increase in temperature and the onset of deformation, the feed forces tend to decrease (Dekkers, 1993).

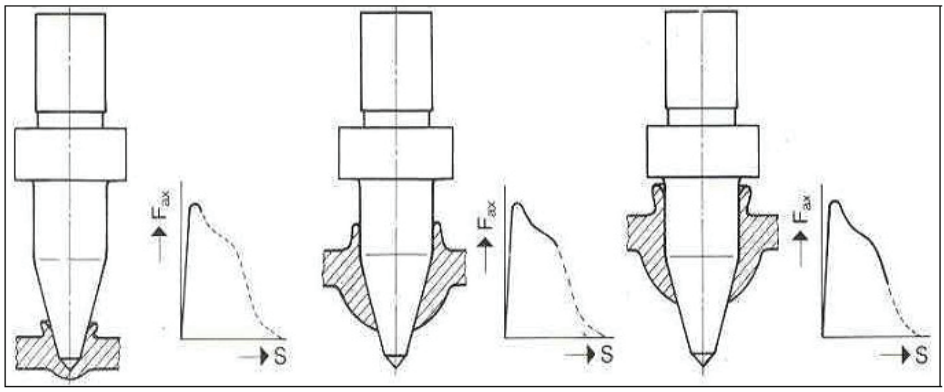

Figure 6. Flow Phase and Force Generation in Friction Drilling Process (Wu et al., 2016)

Shaping Phase

In the last stage, the conical and cylindrical area of the tool drills the workpiece and a taper is formed at the hole exit. The wide cylindrical part of the tool forms by applying pressure to the material piled up at the hole entrance and creates a sealing washer at the hole entrance. With the completion of the drilling process and the formation of the bushing at the hole exit, the feed forces decrease to zero. After the end of the drilling process, the tool is withdrawn and the operation is completed (Dekkers, 1993, Doğru, 2010).

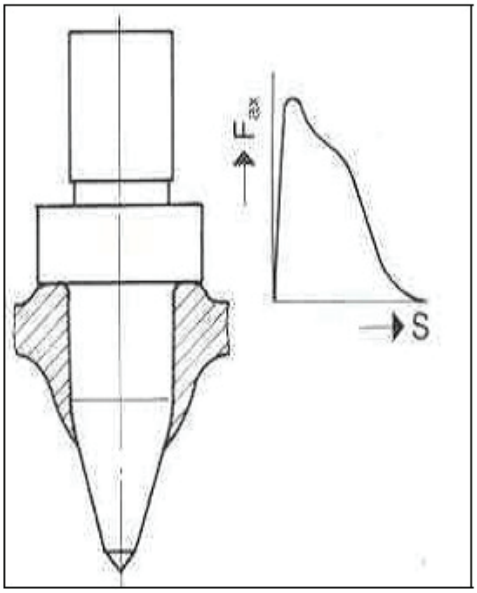

Figure 7. Shaping Phase in Friction Drilling and Force Generation (Wu et al., 2016)

TOOLS USED in FRICTION DRILLING OPERATIONS

The tools utilized in friction drilling operations are required to be resistant to heat. These tools should be able to work comfortably at high temperatures at least 0.7 times higher than the melting temperature of the workpiece. It is desired that the tapered tip, which is the first area of the tool to come into contact with the workpiece, has the necessary mechanical and thermal strength. In this framework, tungsten carbide (WC) and high speed steel (HSS) are used as tool materials in drilling applications with friction. TiAlN and AlCrN coatings are frequently utilized with these tools to increase adhesion and thermal resistance. The tools used in the drilling process with friction consist of five parts: the conical tip, the conical part, the cylindrical part, the neck, and the clamping handle (Sara et al., 2018, Demir, 2016).

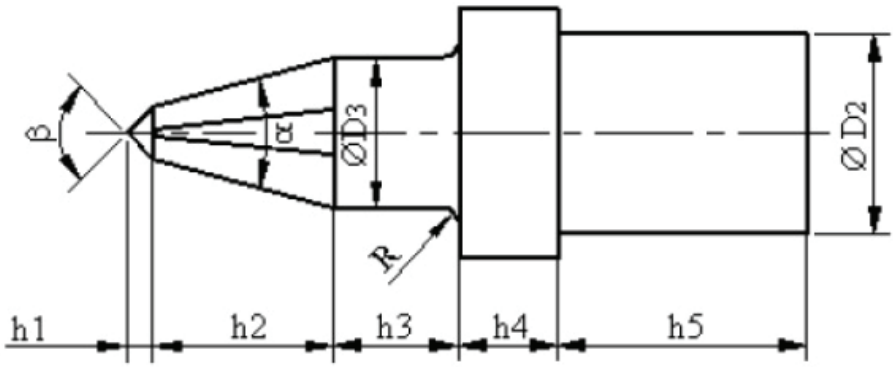

Figure 8. Tool Sections of Drilling with Friction (Doğru, 2010)

Conical tip (h1): This is the tool area that first comes into contact with the workpiece in friction drilling operation. This area guides the entire drilling process. It is the area that is exposed the most to thermal and mechanical loads. The tip angle (β) ensures penetration into the workpiece and determines the magnitude of the feed forces that occur during the process (Tunalıoğlu, 2019, Bal, 2020).

Conical part (h2): The second region of the tool is the conical area, this region gradually enlarges the hole. The conical part angle (α) is smaller (α<β) than the tip angle (β). As the taper angle changes, the tool and workpiece contact surface changes. This contact provides friction and heat generation due to friction. This region generates the formation of the bushing by proceeding the inner region of the workpiece (Tunalıoğlu, 2019, Honey, 2020).

Cylindrical part (h3): This region of the tool is the region that allows the desired hole to be formed in the workpiece, the final hole size is created with this region. The diameter of the cylindrical region must be the same as the hole diameter. The length of this area must be longer than the sum of the workpiece thickness and the bushing height. For this reason, the length of the cylindrical region should be chosen as 3-4 times the material thickness. Otherwise, the drilled hole will be conical. This situation negatively affects the threading process to be made after drilling (Tunalıoğlu, 2019, Bal, 2020).

Neck (h4): During the friction drilling process, some of the material is piled up at the hole entrance. This material accumulated at the hole entrance is pressed with the neck of the tool, forming a washer for sealing at the hole entrance. The neck region diameter is the region with the largest diameter in the tool. The thickness of this region is selected according to the strength that can meet the loads during the formation of flakes at the hole entrance (Tunalıoğlu, 2019, Bal, 2020).

Binding handle (h5): This is the area required for the tool to be attached to the workbench. The diameter of this area is determined according to the binding method. The length of this zone should be designed to create the necessary bonding strength.

The tools used in friction drilling operations vary depending on the desired hole characteristics and workpiece thicknesses. Different tool types were created by adding a cutter to the neck of the tool, depending on the demand for flake formation at the hole entrance. Also, tapping and friction drilling tools are combined to perform all operations at once. According to the desired properties, friction drilling tools are evaluated in four different types (Wu et al., 2016).

- Long Type Friction Drilling Tools
- Short Type Friction Drilling Tools
- Cutter Neck Friction Drilling Tools
- Cutting Edge Friction Drilling Tools.

Tool Life in Friction Drilling Process

There are many variables that affect tool performance in friction drilling. Different principles of operation cause this situation.

During the shaping of hard metals in friction drilling, high feed rates can cause tool deformation. The high moments that occur when the tool sinks into the workpiece also cause breakage at the tool tip. Exposure of the tool to high temperatures during the operation and the sudden discharge of the tool at the end of the operation cause thermal and mechanical loads on the tool. Furthermore, rapid temperature changes can cause dimensional changes and deformation in the tool (Sözügüzel, 2007).

Considering all these situations, the tool material should be selected from materials that have high impact resistance, can maintain its hardness at high temperatures, and are resistant to thermal and mechanical fatigue.

The feed rate and cutting speeds should be chosen carefully by taking into account the operating conditions. Axial misalignment, gaps in the machine spindle and vibration during the bonding of the tool cause errors. Moreover, removing the impurities on the tool is of great importance in terms of the efficiency of the operation (Doğru, 2010).

FRICTION DRILLING AREA of USAGE AND its ADVANTAGES

The friction drilling operation has made a significant contribution to the production process by allowing effective threading of thin-walled materials. This is the biggest advantage of friction drilling process. Friction drilling is widely preferred in the industry due to this and many other advantages (Doğru, 2010). The advantages of friction drilling can be listed as follows;

- Thanks to the bushing formation, no additional processing is required like nut welding to the hole exit, centering etc., thus reducing production costs,
- The current process provides safety and tightness in installation applications, and also allows for mass production (Brinksmeier, 1990, Cantero, et al., 2005),
- It allows automation and tool performance is higher than traditional drilling methods (Sözügüzel, 2007),
- Friction drilling provides an important alternative in operations that are difficult to perform with traditional drilling methods. Reducing the strength of the workpiece with the effect of high heat is effective in this.
- Not using coolants in this drilling method both reduces cooling costs and causes a more environmentally friendly and healthy manufacturing process.

Friction drilling is preferred in all applications where thin-walled materials are used. It is a processing method that can be used in all materials with the use of correct operating parameters. It can be applied to many materials, especially structural steel, stainless steel, brass, copper, aluminum and special alloys. Friction drilling processes are preferred in many industries (Bal, 2020). These usage areas;

- Space and aerospace industry
- Automotive industry
- At the connection points of steel construction furniture
- In pressure tanks and liquid tanks where sealing is required
- In the installation of pipes and profiles in the assembly of plumbing systems
- Connecting bearings and plain bearings to thin-walled systems
- In the production of mechanisms with low wall thickness
- In medical applications
- In screw connections of materials with low wall thickness with high peel strength

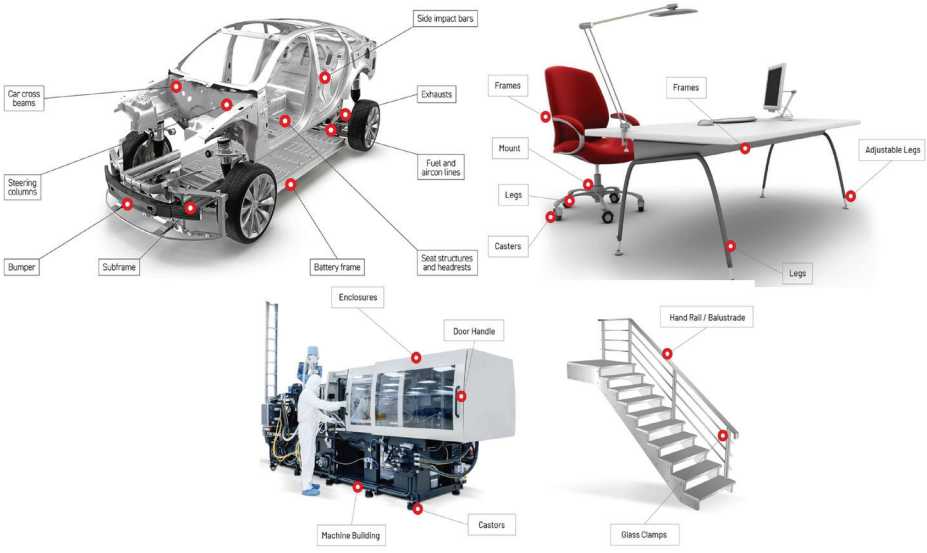

Figure 9. Friction Drilling Application Regions in Different Industry Areas[4]

4 https://flowdrill.com/blogs/sectors/hvac

STUDIES on FRICTION DRILLING

In the study conducted by Gemalmayan and Tunalıoğlu, the results of the drilling of St37-2, CM22NBK and S460MC materials with friction drilling were evaluated. The researchers threaded the test specimens after drilling and tested the specimens for cracks. Then, the hardness of the samples was examined and all test samples were evaluated in terms of strength values by performing a tensile test. In the experiments, it was determined that the materials did not undergo any cracking after the friction drilling process. It was understood that the hardness values of the materials increased with the effect of friction and heat generated as a result of drilling. This situation showed that there was an increase in strength in the materials as a result of thread cutting operations by friction drilling and cold forming. In addition, it has been determined that the the breaking forces are at acceptable values according to the place of use of the materials (Gemalmayan and Tunalıoğlu 2009).

Özek and Demir investigated the most appropriate rotational speed and feed rate parameters according to criteria such as surface roughness, bushing height, bushing shape, and shell wall thickness by drilling the St37 sheet material with a tungsten carbide tool by friction drilling method. As the amount of material that provides the bushing formation increases with the ratio of the material thickness to the hole diameter (t/d) increases, it has been stated that this ratio is an important parameter in terms of the bushing shape and bushing height formed as a result of the process. Also, it was observed that increasing the feed rate and rotational speed increased the deformation in the bushing formation, the bushing height decreased due to the spreading of the flowing material around the hole in the radial direction, and the bushing wall thickness increased (Özek and Demir 2012).

Miller et al. examined the advantages of friction drilling in thin-walled materials. In their study, they investigated the friction drilling process (Figure 10) and tool wear (Figure 11) using AISI 1015 carbon steel with a wall thickness of 1.5 mm. It took an average of 2 to 3 seconds for each hole to be drilled in the study, and a 10-second wait was made between drilling operations in order for the tool to cool. During the study, thrust force, torque, tool weight were examined and a total

of 11,000 holes were drilled, and it was seen that the tool still performs without problems (Miller et al., 2007).

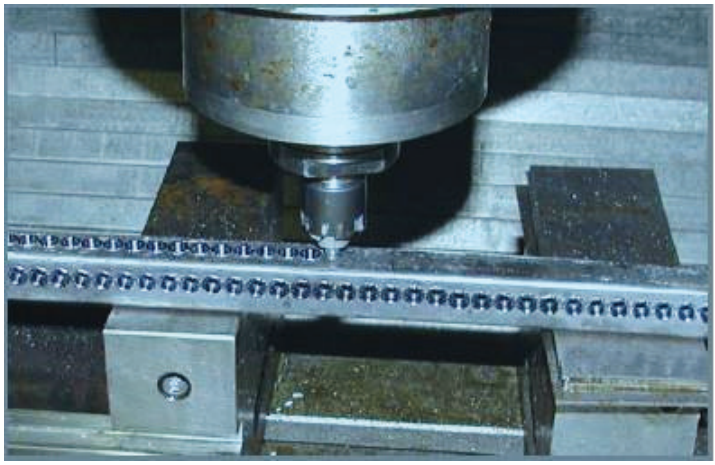

Figure 10. Friction Drilling Process View (Miller et al., 2007)

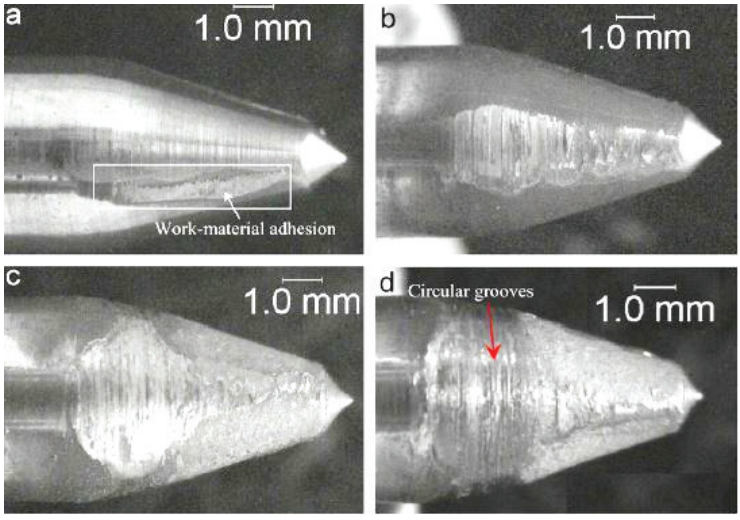

Figure 11. Tool Views by Number of Drills:
(a) 2 holes; (b) 1000 holes; (c) 5000 holes; (d) 11,000 holes (Miller et al., 2007)

Kaya et al., investigated the effects of the material on the surface temperature, thrust force, and torque value in friction drilling of St12 sheet material on process parameters such as tool friction angle, friction

contact area ratio (FCAR), feedrate, and rotational speed. According to the results of the study, it was observed that the thrust force and torque values increased gradually with the increase of friction angle, feed rate, and FCAR values, on the other hand, the thrust force and torque values decreased with increasing drilling speed value. It has been observed that the surface temperature of the workpiece increases in direct proportion with the increase of drilling speed. It has been determined that the friction angle and FCAR have no effect on the surface temperature of workpiece (Kaya et al., 2014).

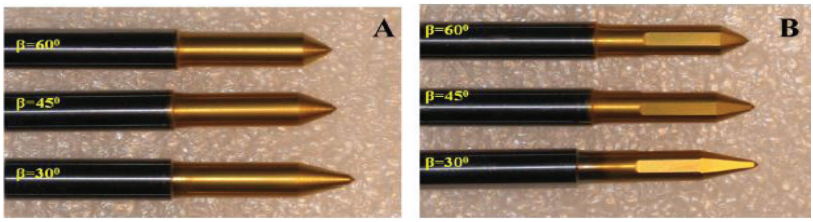

Figure 12. Appearances of Tools with Different FCARs

(a) FCAR 100% and (b) FCAR 50% (Kaya et al., 2014)

Pantawane et al. applied friction drilling to thin-walled AISI 1015 box section workpiece material. The material thickness was chosen as 1 mm. Input parameters such as speed and feed of the process were examined, and ideal drilling conditions were found with the multiple response method using an objective function called the attractiveness function of the results of the machining conditions (Pantawane and Ahuja 2015).

Figure 13. AISI 1015 Section Drilled with Friction Tool Perspective View b) Sectional View (Pantawane and Ahuja 2015)

In the study of Özler and Doğru, a 2 mm thick AISI 1010 box section was drilled with tungsten carbide in different diameters and the effects of machining parameters on force and temperature were investigated. In addition, bushing height, geometry, and leaf geometry formed at the bushing mouth were also investigated in terms of drilling conditions such as friction cone angle, feed rate, and drilling speed. As a result of the study, it was determined that the temperature increased with increasing drilling speed and decreasing feed rate (Figure 14). Additionally, it has been observed that high feed rate causes defects in the geometry of the bushing (Özler and Doğru 2013).

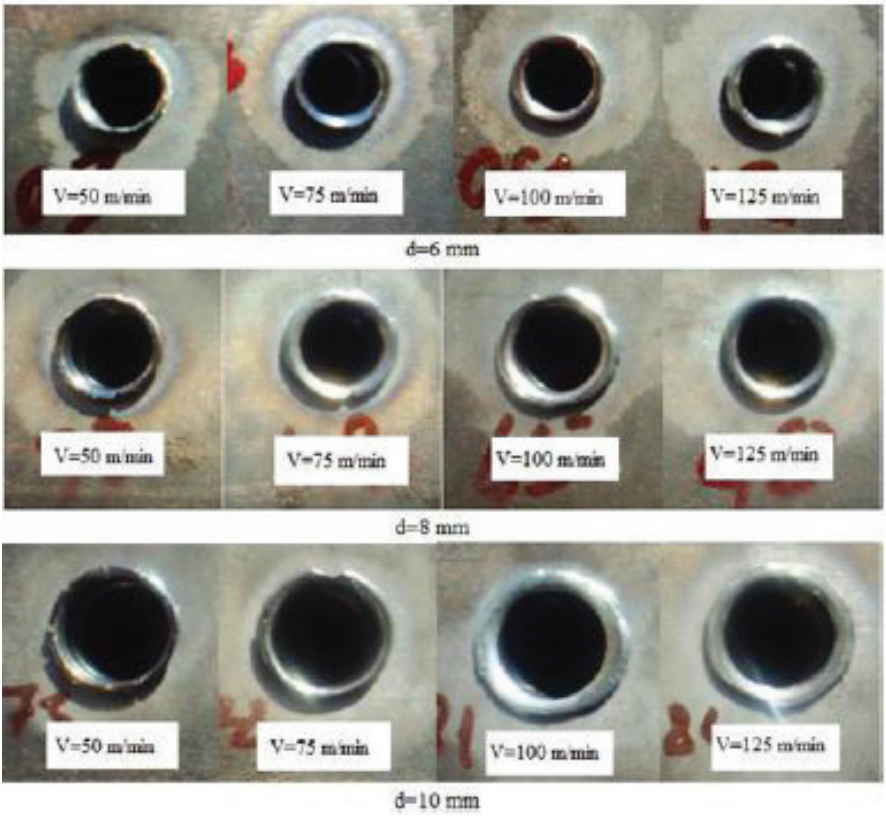

Figure 14. Effects of Different Drilling Speeds on Bushing Geometries at α=30° Tip Angle and f=225 mm/min Feed Speed (Özler and Doğru 2013)

Lee et al. drilled 2 mm thick AISI 304 sheet material with three different friction drilling tools including uncoated, TiAlN, and AlCrN coated at different speeds. Axial forces, tool surface temperature, and tool wear were investigated in this study. As a result of the experiments, it was observed that the tool surface temperatures increased in direct proportion with the increase in the rotation speed. The highest surface temperature was measured in the AlCrN coated drill. It has been determined that AISI 304 stainless steel material increases the tool surface roughness by sticking to the tool during drilling, which increases the tool friction coefficient in subsequent drillings. It has been observed that the tools that have drilled at a constant speed and the same number of drills and the coated tools wear less than the uncoated tool and the least tool wear occurs in the AlCrN coated tool. While TiAIN and AlCrN coated tools caused less change in axial thrust force and tool surface temperature, it was observed that AlCrN coated tool showed the least change (Lee et al., 2009).

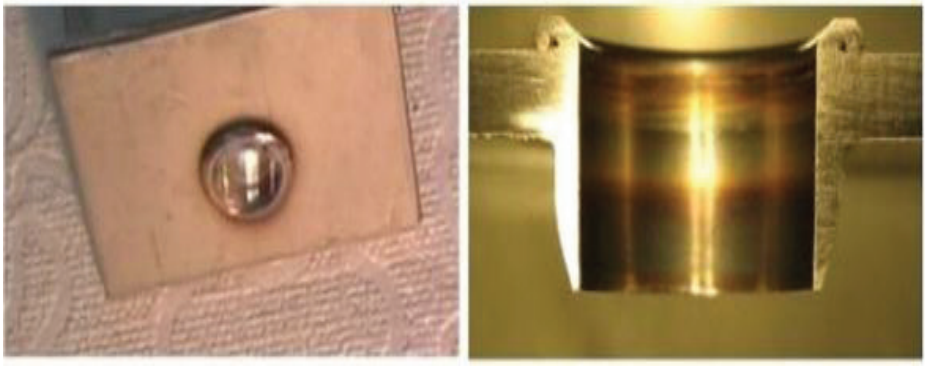

Figure 15. Friction Drilling Application in AISI 304 Sheet Material a) General View b) Section View (Lee et al., 2009)

In their study, Özek and Demir (2013) drilled a hole in A7075-T651 aluminum alloy with friction drilling method. In the research, the bushing height was examined depending on the material thickness and hole diameter. The workpiece with material thicknesses of 2, 4, 6, 8, and 10 mm and tools with tool taper angles of 24°, 36°, and 48° were used. The number of rotation was determined as 2400, 3600, and 4800 rev/min and

the feed rate is 50, 75, and 100 mm/min. In the experiments, 8, 10 mm diameter holes were drilled on the material using a high speed steel (HSS) tool. According to the results of the study, it has been reported that the bushing length is inversely proportional to the tool taper angle and rotational speed. It has been observed that the bushing length increases with the increase of the workpiece thickness, hole diameter, and feed rate (Özek and Demir 2013).

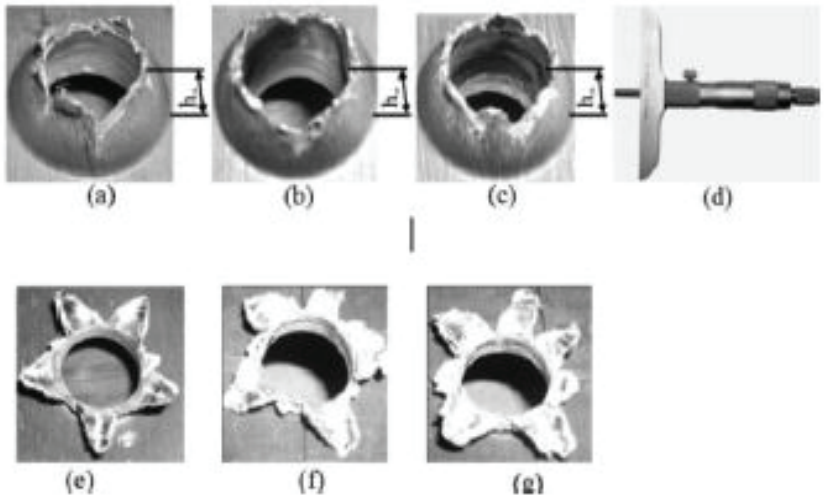

Figure 16. Types of Measuring Bushing Height (a, b, and c) Micrometer of Depth Measuring (d) and Petal Shaped Bushings (e, f, and g) (Özek and Demir 2013)

In the study of Özek and Bak, the effects of material thickness and tool diameter on bushing height, bushing outer diameter, and bushing shapes, and changes in microhardness were investigated. In the experimental study, tungsten carbide (WC) tools with a taper angle of 36° and diameters of 5, 10, 15, and 20 mm were used. As the workpiece material, St37 steel with thicknesses of 2, 4, 6, 8, and 10 mm was chosen. The experimental parameters were determined as constant cutting speed (1120 rev/min) and feed rate (25 mm/min). As a result of the research, it was observed that the bushing wall thickness and bushing height increased as the material thickness and tool diameter increased. It has been deter-

mined that the microhardness decreases as the distance increased from the hole center towards the periphery (Özek and Bak 2020).

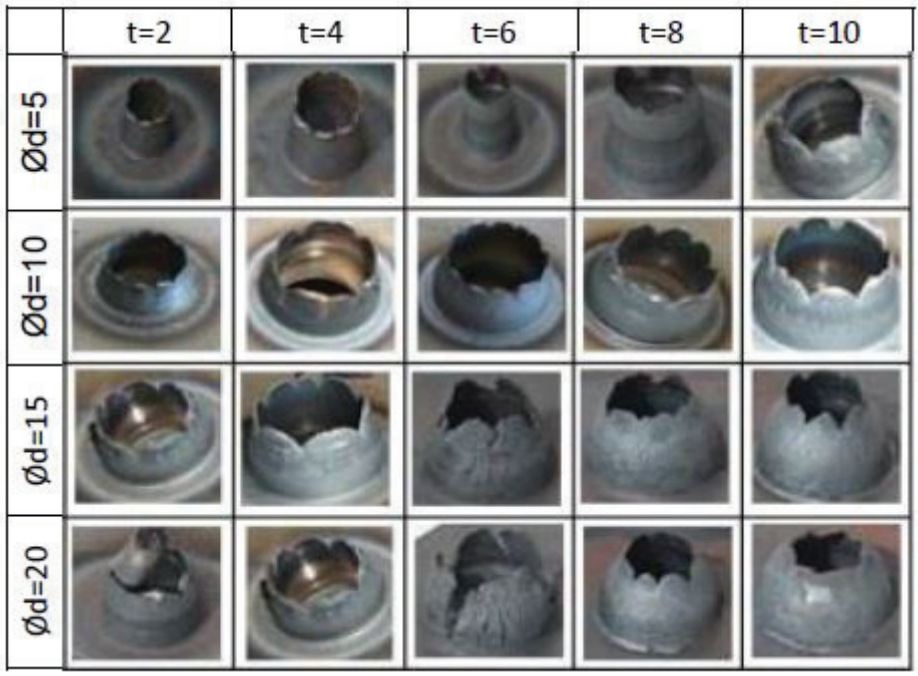

Figure 17. Obtained Bushing Pictures Based on Material Thickness and Tool Diameter (Özek and Bak 2020)

In their study, Bilgin, Gök and Gök statistically and experimentally investigated the friction perforation of AISI 1020 carbon steel material with a thickness of 2.7 mm. The temperature, torque, and axial force results obtained from the experimental and statistical analysis were compared. A tungsten carbide tool with a diameter of 5.4 mm was used as the cutting tool. As the experimental parameters, the cutting speed was determined as 2400-4800 rev/min, the feed rate as 150 mm/min. They used deform-3D software based on the finite element method (FEM) for the statistical data. They observed that the temperature value in the center of the workpiece increased while the moment and axial force values decreased with the increase in cutting speed (Bilgin et al., 2015).

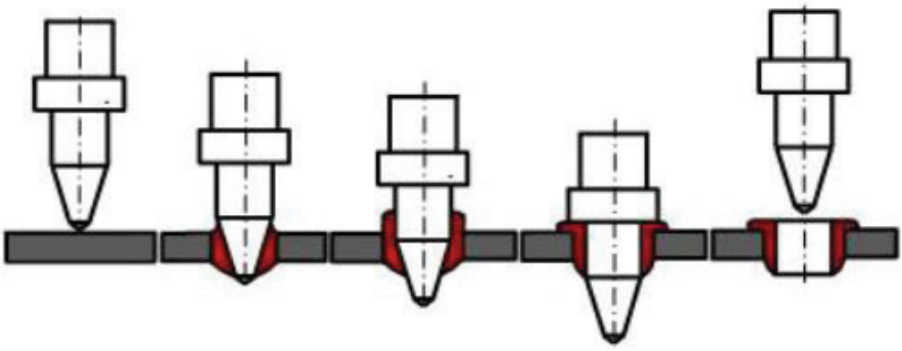

Figure 18. Stages of Friction Drilling Method (Bilgin et al., 2015)

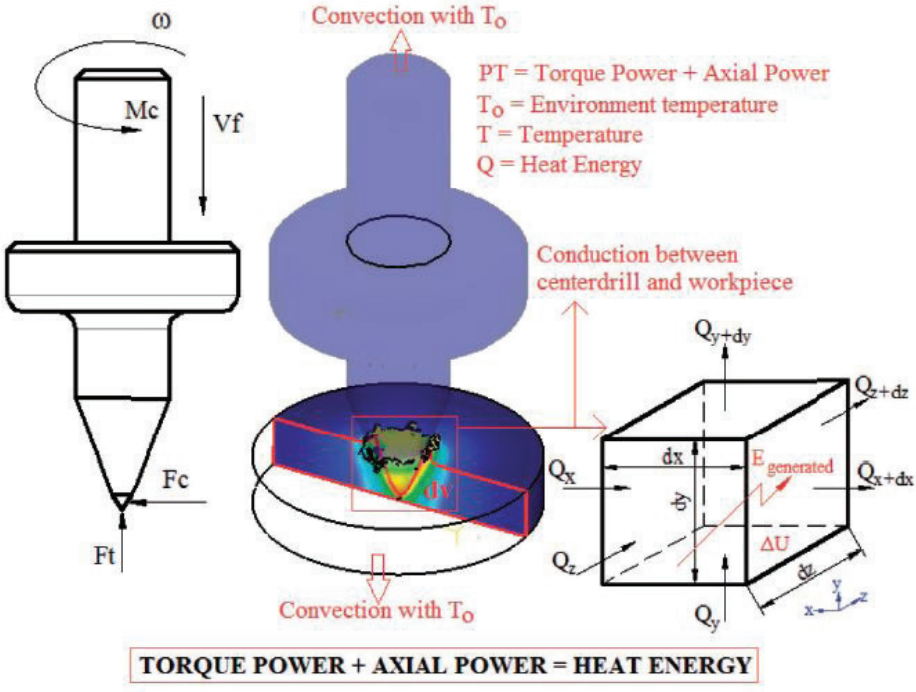

Figure 19. Friction Drilling Process Prepared with Deform 3D Software (Bilgin et al., 2015)

Friction drilling directly affected the bushing formation in brittle materials. Since petals and cracks were formed in the bushing formation, the bushing length was negatively affected. (Demirel and Karaağaç

2017). In a different study, this problem was addressed. In the friction drilling of AA7075-T651 aluminum alloy, which is known as a brittle material, the effects on bushing shape, deformation, and frictional heat of the front hole depth and diameter were investigated. The results showed that the pre-hole effect was dependent on the geometric dimensions of the tool tip. In cases where the diameter of the front hole is close to the tip diameter of the tool and the depth of the front hole is greater than the length of the tool, the initial deformation is reduced, the friction heat is regulated, and fewer cracks and petals are formed in the cylindrical shape of the bushing (Demir, 2016).

Lee et al. investigated the nickel-based super alloy IN-713LC, which is frequently used in the defense industry, automotive, nuclear, and other engineering fields, by drilling with friction drilling method. Experiments were carried out under different rotations and feed rates. In their study, they examined hardness, roundness tolerance, and surface roughness. It has been observed that the hardness value is higher near the hole wall and decreases as it moves away from the hole edge. Surface roughness and roundness tolerance were found to be better at high speed and feed (Lee et al., 2007).

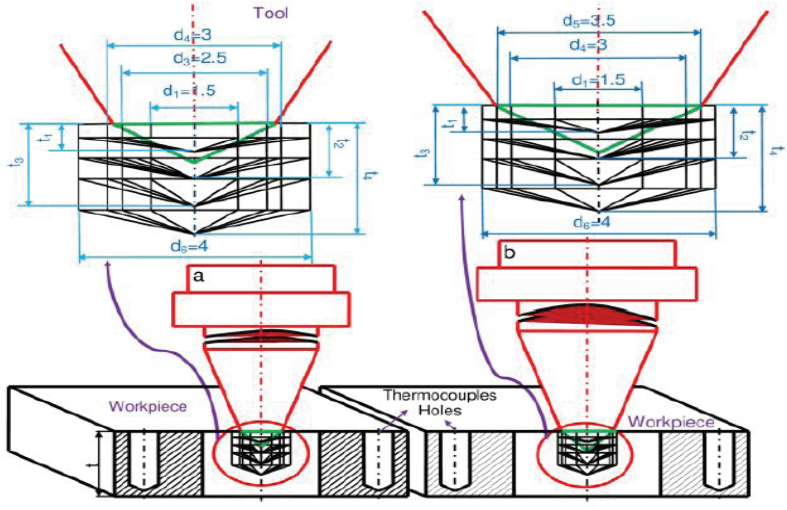

Figure 20. Front Drilling Depths and Diameters for Friction Drilled Holes of a) 8 mm Diameter and b) 10 mm Diameter (Demir, 2016)

Miller et al. performed friction drilling on cast metals, which are frequently used in the automotive industry. They investigated cracks that cause bushing failure in cast metals. In their work, 4 mm thick aluminum-silicon-copper alloy A1380 and magnesium-aluminum-zinc alloy MgAZ91D work piece were used. Before drilling, both preheating and friction drilling were performed and compared. The bushing views as a result of the experiments are given in Figure 21.

Figure 21. Friction Drilling Holes Applications a) A1382 b) AISI 1020 (Miller et al., 2006)

As a result of the study, they proved that preheating the workpiece and high spindle speed reduce the thrust force, torque, energy and power values required for friction drilling in brittle cast metals. They observed that the bushing geometry of the Al380 workpiece, which was preheated at 100°C, 200°C, and 300°C, was smoother. Besides, it was determined that less cracks and petals were formed on the bushings (Miller et al., 2006).

Sobotava et al. drilled AlMgSi, aluminum alloy, copper, and S2356JR workpieces by friction drilling method and tapped the drilled holes. In their study, they examined the geometry of the bushing and the strength of the extracted threads. It has been observed that the bushing geometry of the copper material is not very smooth, but the strength values of the threads are acceptable (Sobotova et al., 2011).

In their research, Boopathi et al. applied friction drilling to brass, aluminum, and stainless steel used in manufacturing. In the experiments, tungsten tools were preferred. After the procedure, micro-images of the tool were examined. As a result of the research, it was observed that the brass material adhered to the tool less than the aluminum material. A smoother process was observed in drilling stainless steel in respect to drilling aluminum and brass materials. Comparing the measured thrust forces, a low thrust of 1512 N was sufficient for aluminum, while a thrust of 1798 N was required for brass material. It has been observed that a thrust force of 2745 N is required to drill stainless steel with friction (Boopathi et al., 2013).

RESULTS

In the industry, screw connection of thin sheet materials with friction drilling process is frequently used since it has advantages in terms of cost and time. In this study, the development of the friction drilling process, used tools, applied materials, and the studies in this field were examined. The advantages of friction drilling are briefly outlined below.

- Thanks to the bushing formation, no additional processing like nut welding to the hole exit and centering etc. is required, thus production costs reduces.
- It is suitable for mass production and the tool is not easily deformed.
- It does not pollute the environment during the process as it is produced without chips.
- The process can be performed successfully on aluminum, steel, copper, brass, magnesium alloys, stainless steel, and many materials.
- It is carried out with drills and CNC benches, without requiring any other machine equipment.
- Friction drilling provides an important alternative for the operations that are difficult to perform with traditional drilling methods. Reducing the strength of the workpiece with the effect of high heat is effective in this.

Friction drilling method has some disadvantages as well as its advantages. The disadvantages of the method are also given below.

- In brittle materials, the bushing geometry is formed in the form of petals due to crack formation.
- In soft materials, it has been observed that the material is plastered on the tool.

ACKNOWLEDGMENTS

This study was supported by Gazi University Scientific Research Projects (Project no: FYL-2021-7061).

REFERENCES

Bal M., (2020). Termal Sürtünmeli Delme İşleminde Kovanın Geometrik ve Fiziksel Özelliklerinin Araştırılması. Doktora Tezi, Fırat Üniversitesi Fen Bilimleri Enstitüsü, Elazığ, Türkiye.

Bilgin M. B., Gök K., and Gök A. (2015). Three-dimensional finite element model of friction drilling process in hot forming processes. Journal of Process Mechanical Engineering 1-7. DOI: 10.1177/0954408915614300

Boopathi M., Shankar S., Manikandakumar S., Ramesh R. (2013). Experimental investigation of friction drilling on brass, aluminium and stainless steel. Procedia Engineering, 64, 1219-1226.

Brinksmeier, E. (1990). Prediction of Tool Fracture in Drilling. Ann CIRP 39,97-100.

Cantero, J. L., Tard'ıo, M. M., Canteli, J. A., Marcos, M., and Migu' elez, M. H. (2005). Dry Drilling of Ti – 6Al – 4V Alloy. International Journal of Machine Tools & Manufacture, 45, 1246–1255.

Chow, H. M., Lee, S. M., and Yang, L. D. (2008). Machining Characteristics Study of Friction Drilling on AISI 304 Stainless Steel. Journal of Materials Processing Technology, 207, 180–186.

Dekkers, G. (1993). Flowdrill prosesi firma katologları. Copyright by Flowdrill, B. V.Holland, 1-30.

Demir Z. (2013). Sürtünmeli delmede mikro yapı ve mikro sertliğin araştırılması. New World Sciences Academy Technological Applied Sciences. 8(1), 54-66.

Demir Z. (2016). An experimental investigation of the effect of depth and diameter of pre-drilling on friction drilling of A7075-T651 alloy. Journal of Sustainable Construction Materials and Technologies, 1(2), 46-56.

Demirel M. Y., Karaağaç İ. (2017). Sürtünmeli Delik Delme Prosesi ve Prosesin Başlıca Uygulamaları. El-Cezerî Fen ve Mühendislik Dergisi, 4(2), 234-248.

Doğru, N. (2010). AISI 1010 Çelik Malzemenin Sürtünmeli Delme Yöntemiyle Delinmesinde İşleme Karakteristiklerinin Araştırılması. Yüksek Lisans Tezi, Fırat Üniversitesi Fen Bilimleri Enstitüsü, Elazığ, Türkiye.

France J.E., Davison J.B., Kirby P.A. (1990). Strength and rotational stiffness of simple connections to tubular columns using flowdrill connectors. Journal of Constructional Steel Research, 50, 15-34.

Gemalmayan N., Tunalıoğlu M.Ş. (2009, 8-9 Mayıs). Farklı tip ince cidarlı malzemeler için sıvayarak delik delme prosesi ile diş açma yöntemi, TMMOB Makina Mühendisleri Odası 11. Otomotiv Sempozyumu, Bursa, Türkiye.

Han-Ming C., Shin-Min L., Lieh-Dai Y. (2007). Machining characteristic study of friction drilling on AISI304 stainless steel. Journal of Materials Processing Technology, 207, 180–186.

Kaya M. T., Aktas A., Beylergil B., and Akyildiz H. (2014). An Experımental Study on Friction Drilling of St12 Steel. Transactions of the Canadian Society for Mechanical Engineering, 38 (3), 15-23.

Kumar R. and Jesudoss Hynes N. R. (2019). Thermal drilling processing on sheet metals: A review. Int. J. of Lightweight Mat. and Man., 2(3):193-205.

Lee S.M., Chow H.M., Huang F.Y., Yan B.H. (2009). Friction drilling of austenitic stainless steel by uncoated and PVD AlCrN and TiAlN-coated tungsten carbide tools. International Journal of Machine Tools & Manufacture, 49(1), 81-88.

Lee S.M., Chow H.M., Yan B.H. (2007). Friction drilling of IN-713LC cast superalloy. Materials and Manufacturing Processes, 22: 893-897.

Miller S. F., Tao J. and Shih A. J. (2006). Friction drilling of cast metals. Int. Journal of Mac. Tools and Man., 46(12–13), 1526–1535.

Miller, S. F., Blau, P. J., and Shih, A. J. (2007). Tool Wear in Friction Drilling. International of Machine Tool and Manufacture, 47, 1636–1645.

Özek C. ve Demir Z. (2012, 29-30 Kasım). St 37 Çeliğinin Sürtünmeli Delinmesinde Optimum Dönme Hızı ve İlerleme Oranının Araştırılması, 3. Ulusal Tasarım İmalat ve Analiz Kongresi, Balıkesir, Türkiye.

Özek C., Demir Z. (2013). A7075-T651 alaşımının sürtünmeli delinmesinde kovan yüksekliğinin malzeme kalınlığına göre araştırılması. Dicle Üniversitesi Mühendislik Fakültesi Mühendislik Dergisi, 4(2), 61-67.

Özek C. ve Bak M., (2020). Sürtünmeli Delme İşleminde Elde Edilen Kovanın ve Pulun Oluşmasına Etki Eden Parametrelerin Araştırılması. Pamukkale Univ Muh Bilim Derg, 26(4), 620-627. doi: 10.5505/pajes.2019.65148

Özkan D. Ç. ve Ünlü B. S., (2016). Kaynak Cıvata Ve Somunlarının Çeşitleri, Üretimi, Yöntemi Ve Kullanım Alanları. Mühendis ve Makine Dergisi, 57(678), 44-52.

Özler L. (2019). The influence of variable feed rate on bushing and surface roughness in friction drilling. Journal of the Brazilian Soc. of Mec. Sci. and Eng., 41(8), 308-316.

Özler L., Doğru N. (2013). An experimental investigation of hole geometry in friction drilling. Materials and Manufacturing Processes, 28(4), 470-475.

Pantawane P.D., Ahuja B.B. (2011). Experimental investigations and multi-objective optimization of friction drilling process on AISI 1015. International Journal of Applied Engineering Research, 2(2), 448-461.

Raju B.P., Swamy M.K. (2012). Finite element simulation of a friction drilling process using deform-3d. International Journal of Engineering Research and Applications, 2(6): 716-721.

Rao K. H., Gopichand A., Kumar N. P. and Jitendra K. (2017). Optimization of machining parameters in friction drilling process. Int. J. of Mec. Eng. and Technology, 8(4): 242–254.

Sara A. El-Bahloul , Hazem E. El-Shourbagy, Ahmed M. El-Bahloul, and Tawfik T. El-Midany. (2018). Experimental and Thermo-Mechanical Modeling Optimization of Thermal Friction Drilling for AISI 304 Stainless steel. CIRP Journal of Manufacturing Science and Technology, 20, 84-92.

Shalamov P. V., Kulygina I. A. and Yaroslavova E. N. (2016). ANSYS software-based study of thermal drilling process. Procedia Eng. 150, 746-752.

Sobotová L., Kmec J., Bıčejová Ľ. (2011). Thermal drıllıng – new progressıve technology. Annals of Faculty Engineering Hunedoara – International Journal Of Engineering, IX(3), 371-373.

Sözügüzel, D. (2007). İnce Cidarlı CM22NBK Malzemesi İçin Sıvayarak Delik Delme (Flowdrill) Prosesi ile Diş Açma ve Alternatif Malzeme Seçimi. Yüksek Lisans Tezi, Gazi Üniversitesi Fen Bilimleri Enstitüsü, Ankara, Türkiye.

Tunalıoğlu M. Ş. (2019). İnce Et Kalınlığına Sahip Kare Profil Borularda Sıvama ile Delik Delme ve Kılavuz Çekmenin Deneysel İncelenmesi. Yüksek Lisans Tezi, Hitit Üniversitesi Fen Bilimleri Enstitüsü, Çorum, Türkiye.

Wu J., Wen J. M and Wang Z.Y. (2016). Study on the Predicted Model and Experiment of Drilling Forces in Drilling Ti6Al4V. Journal of the Brazilian Society of Mechanical Sciences and Engineering, 38 (2), 1-8.

Yılmaz, B., Uzun, G., Güllü, A. (2020). Ti6Al4V Malzemeye Uygulanan Delme İşleminde Kesme Parametrelerinin İtme Kuvveti, Kesme Momenti Ve Kesme Sıcaklığına Etkileri. İmalat Teknolojileri ve Uygulamaları, 1-3, 1-8.

INTERNET RESOURCES

https://flowdrill.com/blogs/sectors/hvac, (E.T. 16.12.2022)

AN EVALUATION ON THE PRINCIPLES OF TRIBOLOGY AND USAGE IN WEAR APPLICATIONS

Ezgi DOĞAN[1], Senai YALÇINKAYA[2], Memduh KURTULMUŞ[3]

Abstract: Energy, raw material and environmental problems are increasing gradually due to technological developments in the industry, increase in production capacities and mechanization; humanity is getting closer to energy, raw material, and environmental crises every day. Therefore, developments in the field of tribology, whose main goals are to control friction on surfaces, reduce wear and improve lubrication systems, are even more important today. In fact, with the technological developments in the industry, depending on the increase in production methods and diversity, the target scope of tribology studies has expanded over time. With new materials and coating technologies,

- Saving energy and materials,
- Efficient use of energy,
- Reducing harmful emissions and waste,
-Development of biological and nature-friendly lubrication systems,
- Providing shock absorption

It has diversified in subjects such as reducing environmental/noise pollution and has led to the emergence of many new branches of tribology. Tribology is the science and engineering field that studies the principles of friction, wear and lubrication of interacting surfaces in relative motion. Complex and microscopic interactions between sur-

1 Marmara Unıversity, Institute of Pure&Applied Sciences, Istanbul / Turkey, e-mail: ezgi.dogan@marun.edu.tr, Orcid No: 0000-0001-9829-8738

2 Marmara Unıversity, Faculty of Technology, Istanbul / Turkey, e-mail: syalcinkaya@marmara.edu.trr, Orcid No: 0000-0001-7076-7766

3 Marmara Unıversity, Faculty of Applied Sciences, Istanbul / Türkiye, e-mail: memduhk@marmara.edu.tr, Orcid No: 0000-0001-6525-232X

faces that are in mechanical contact and slide relative to each other cause wear by friction. These interactions depend on the geometry of the material, the surface topography and the loading condition to which the material is exposed, the environment in which it is located, the temperature, and the type of contact. All mechanical, physical, chemical and geometric aspects of surface contact and the surrounding atmosphere affect the surface interactions and thus the tribological properties of the system. Tribology studies the phenomena of friction, wear and lubrication and their interaction with each other. Tribology provides economic, ecological and functional optimization of surfaces that are in relative motion relative to each other. Friction is defined as the resistance to sliding between surfaces in contact. There are two types of friction, static and dynamic. Static friction is necessary to initiate motion between two contacting surfaces or to break the bonds formed between two surfaces. Dynamic friction, on the other hand, is associated with the sliding, rolling, or turning of one surface over another. The friction that occurs on the moving surfaces that come into contact with each other in the machines is a major obstacle to the effective use of global energy resources. So much so that about a third of the global energy resources are spent on overcoming the friction force between surfaces. Again, the abrasions that occur on these surfaces are shown as the main cause of material waste and loss of mechanical performance. Therefore, developments and technological applications in the field of tribology are of great importance in terms of sustainability as well as energy and material savings. Recently, the components of machines operating at high speeds are exposed to excessive friction, high wear, and stress. As a result, energy consumption increases, the service life of these components is shortened, the maintenance of production standards and production reliability decrease. For this reason, it is necessary to minimize the negative effects of friction and wear in areas where high technologies are used.

Keywords: Technological Applications, Friction, Tribology, Wear, Lubrication, Production

INTRODUCTION

Extensive research on tribology is based on Leonardo da Vinci's work on the laws of friction. However, the term was first used in 1966 by British mechanical engineer Prof. It was put forward in a report prepared by H. Peter Jost for the UK Department of Education and Science.

Jost, who is known as the founder of the discipline of tribology, clearly revealed the damages of friction, wear and oxidation to the UK economy with this report. Since then, many interdisciplinary research have been carried out in the field of tribology, whose technological and economic importance is thus better understood.

Tribology is a constantly changing and evolving field throughout history. Although the emergence of the concept is based on Jost's report in 1966, it is known that some principles of tribology were used even in ancient times. According to some scientists, making a fire by rubbing pieces of wood together in prehistoric times can be considered the first applications of tribology. The period of early civilization shows that between 3500 and 900 BC, lubrication with animal fat and bitumen was used to reduce friction when moving heavy objects and monuments, as well as using cylindrical wooden pieces. It is possible to say that there was a stagnation in the field of tribology during the Middle Ages. Nevertheless, metallic bearings developed in China are considered the most important development of the period.

With the industrial revolutions, the importance of tribology has increased continuously. In the process until today, significant developments have been achieved in the fields of industry and tribology, in harmony with each other. A better understanding of the processes of friction, wear and lubrication is needed to better understand tribology. We can define friction as the resistance to relative motion between two surfaces in contact. There is friction between two functional surfaces that are in contact with each other and perform relative sliding or rolling motion. The magnitude of the friction force depends on the material, geometry, and surface properties of the objects in contact, as well as the ambient conditions. It is often desirable to minimize friction to maximize energy and material efficiency. Frictional force generally increases with load and surface roughness and can be reduced by using a lubricant. Wear is the loss of material, usually caused by the sliding action of surfaces over each other. In general, wear on system components is undesirable as it will lead to increased friction and machine component failure. Therefore, by using a lubricant, it is aimed to minimize wear as well as friction. In the first of the two most common wear patterns, a harder

material causes the softer material to wear, while in the other, material is transferred from one of the two surfaces in contact to the other.

The dramatic change and transformation that took place in the world during the First Industrial Revolution.

- *Mechanization*
- *Hydro-power*
- *Steam power*
- *Steam engine*
- *The first mechanical weaving loom,*

After the use of these technologies, with the finding of technological and industrial use in areas such as studies on friction, technical development of machine elements such as gears and bearings, studies on mineral oils, development of lubricant formulations can be seen as the first step in the development of tribology.

With the Second Industrial Revolution

- *Mass production*
- *Electricity*
- *With the spread of the first production lines,*

Understanding the importance of the relationships between friction, wear, and lubrication, starting studies on the development of hydrodynamic pressure, developing slip bearings, researching and using additives to transform or improve the desired properties in oils, and development of Reynolds lubrication theory is the second important step in the historical development of the field of tribology.

During the Third Industrial Revolution Period,

- *Development of computer and automation systems,*
- *Studies focusing on electronics science,*
- *After the use of the first programmable logic controllers in commercial production,*

The term tribology was officially introduced to the literature, studies were started on elasto-hydrodynamic lubrication, studies were carried out in the field of computational and experimental tribology, there were

no developments on adhesion and wear theories, industrial applications were concentrated on contact mechanics and surface tribology, advanced science sub-fields such as micro and nanotribology were introduced. The development of low friction bearings, the focus on studies on new materials and coatings, the emergence of the fields of rheology and bio-tribology have allowed many topics with different depths to find their place in both the literature and industrial applications.

In the latest innovations today, where we live the Fourth Industrial Revolution,

- *Development of cyber physical systems,*
- *The spread of augmented reality applications,*
- *Deepening of internet and cloud technologies*

and so on, further development has been achieved in all the aforementioned areas exponentially.

If these are

- *Green tribology*
- *Space tribology*
- *Super lubrication*
- *Tribotronics*

led to the emergence of complex fields of science.

Essentials of Tribology Science

A better understanding of the processes of friction, wear and lubrication is needed to better understand tribology. We can define friction as the resistance to relative motion between two surfaces in contact. There is friction between two functional surfaces that are in contact with each other and perform relative sliding or rolling motion. The magnitude of the friction force depends on the material, geometry, and surface properties of the objects in contact, as well as the ambient conditions.

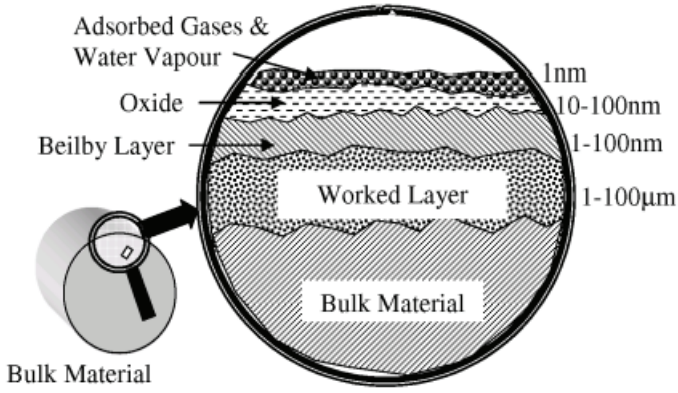

Figure 1. Schematic Representation of a Metal Surface

Depending on external factors such as surface treatment, temperature and oxide formation, the metal can appear clean and shiny despite the presence of different micro-layers that form on the surface. These factors cause disorder deep in the metal, where the physical and mechanical properties of the surface and the crystal structure and thousands of molecular layers are affected.

Depending on the manufacturing process involving material production, the work-hardened zone of the material will form the basis of these additional layers. The upper part of this processed layer is an amorphous or microcrystalline structure called the "Beilby" layer, which is formed as a result of surface flow and melting during the processing of molecular layers. This is the melting of the roughness that causes the formation of the so-called amorphous layer (Beilby layer) on the surfaces, and a change in the surface roughness as a result of oxidation or corrosion on the surface and the effect of wear, as well as a change in the chemical structure of the surfaces due to running-in or possible damage.

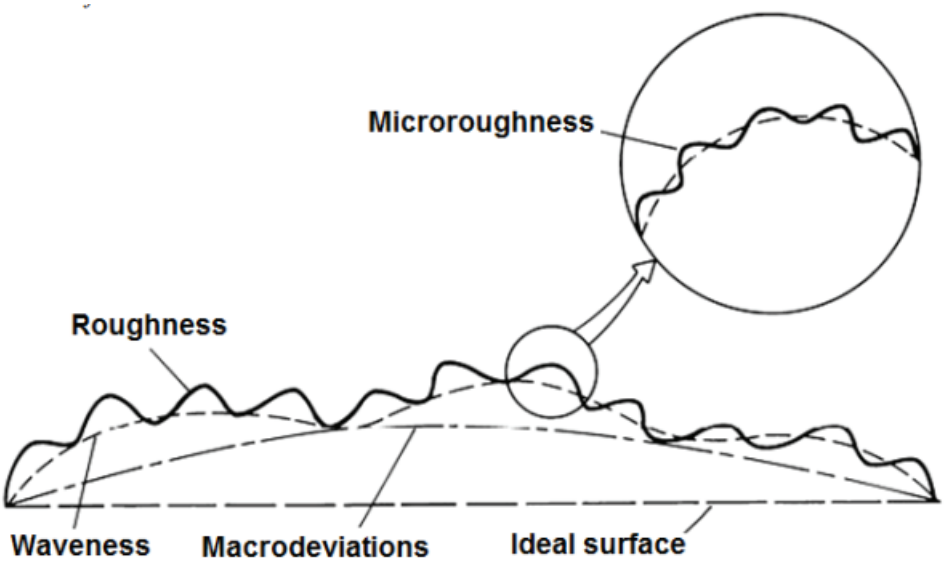

Figure 2. Schematic of Selected Surface Deflection types in Relation to an Ideal Hard Surface

The shape or geometric shape (topology) of the surface used in shaping depends on the formation process; these processes are molding, casting, cutting, sharpening and are often seen microscopically as series of roughness's rather than the flat surface seen macroscopically. Geometric texture can be characterized by the profile of the surface.

The geometric texture of ordinary surfaces is controlled by the characteristic features of the machining process in which they are produced. Close examination of the surfaces, even after very careful processing, shows that they are still rough on a microscopic scale.

- *Macro deviations are errors due to irregular surface deviations in the section design, which are often caused by the precision and lack of rigidity of the machine system.*
- *The waviness is periodic deviations from the geometric surface that are in sinusoidal form and are frequently determined by low-level oscillations of the machine-tool-workpiece system during machining. Typical-*

ly, the wavelength range is between 1-10 mm and the wave height can be up to several hundred micrometers.

- *Roughness is the deviation of the wavy surface itself, caused by the geometry of the cutting tool and its wear, machining conditions, microstructure of the workpiece, vibrations in the system, and similar factors. As a surface undergoes wear, its roughness changes but can be leveled out later.*
- *Micro roughness is fine roughness combined with surface roughness. It can expand at a near-atomic scale and may result from internal defects in the material, corrosion and oxidation that occurs as individual grains on the surface are exposed or exposed to environmental influences.*

It is often desirable to minimize friction to maximize energy and material efficiency. Frictional force generally increases with load and surface roughness and can be reduced by using a lubricant. Wear is the loss of material, usually caused by the sliding action of surfaces over each other. In general, wear on system components is undesirable as it will lead to increased friction and machine component failure. Therefore, by using a lubricant, it is aimed to minimize wear as well as friction.

In the first of the two most common wear patterns, a harder material causes the softer material to wear, while in the other, material is transferred from one of the two surfaces in contact to the other. Another common type of wear in mechanical components is surface fatigue. This type of wear causes cracks in the material with subsurface tensions and these cracks grow towards the surface over time.

As a result, cavities form on the surface and the material wears out. Depending on the different components and conditions in the systems, chemical wear and electric arc wear can be seen as well as impact and erosional wear.

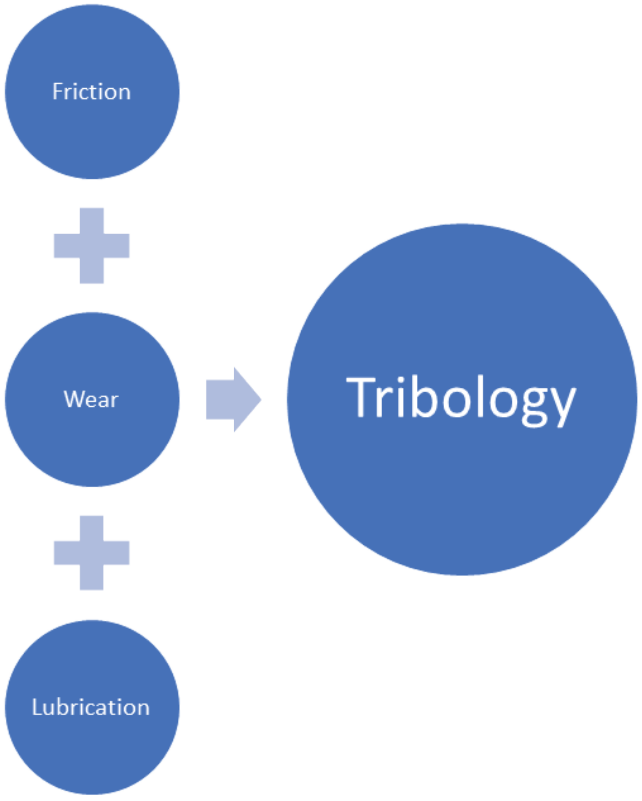

Figure 3. Essentials of Tribology Science

Lubrication attempts to control and minimize friction and wear by forming a film layer that reduces friction between moving surfaces in contact. There are applications where the lubricant film is solid, liquid or even gas. Besides reducing friction and preventing wear, lubricants can perform other important functions such as removing heat and contaminants from the interface and protecting equipment from corrosion. Less friction on lubricated surfaces.

However, it is still possible to talk about the existence of friction. The magnitude of this friction depends on the viscosity of the fluid used, that is, its resistance to flowing and operating conditions.

The friction phenomenon has a more complex structure with the presence of lubricant. One of the most convenient ways to reduce the

friction coefficient is to form an oil film. The main factors affecting the friction in the lubrication condition in Internal Combustion Engines can be listed as follows:

- *Load or pressure,*
- *Way of movement (Sliding, rolling, turning),*
- *The form of contact,*
- *Surface temperature,*
- *Heat flow conditions,*
- *Material type and heat treatments,*
- *Tolerance gaps,*
- *Surface condition or topography,*
- *Environmental condition (dusty, corrosive environment),*
- *The tribological characteristics of the lubricant,*
- *The lubricant is new or used.*

There are different types of lubrication. It is necessary to look at the Stribeck curve that best explains this.

Stribeck curve as seen in the Figure 4; can be used to explain the effects of relative velocity, load, and viscosity on friction. This curve includes boundary, mixed, and hydrodynamic lubrication zones. At low speed, low viscosity or heavy loads, the fluid cannot support the load and direct surface-to-surface contact occurs. Although friction reduction is observed in this region called boundary lubrication, there is still a high friction force.

At high speed, high viscosity or light load, the fluid separates the two surfaces completely and this is called the full film or hydrodynamic lubrication zone. In this region, friction increases due to both the increase in speed and viscosity and the decrease in load. Between the boundary and full film lubrication, parts of the interface are completely separated by liquid, while other areas have a mixed lubrication zone that is not fully separated. Various machine components can operate in one or more lubrication regimes during operation.

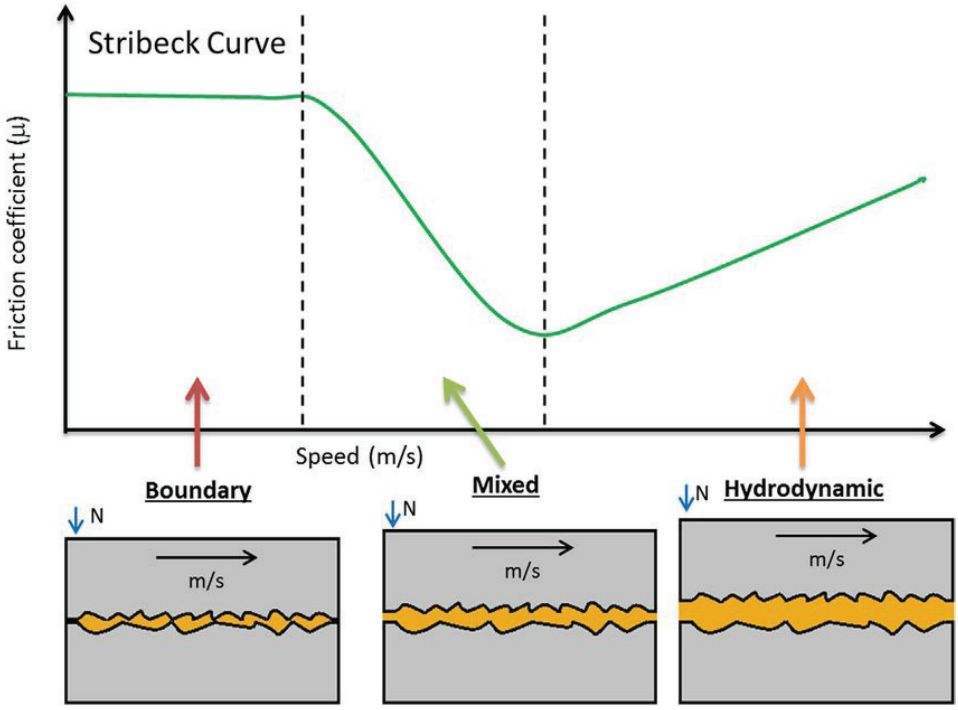

Figure 4. The Stribeck Curve

Tribological data are generally represented by the Stribeck curve, in which the coefficient of friction is shown as a function of sliding speed. This curve basically consists of three regions.

- *In the boundary lubrication zone, the lubricating film is not formed, and the solid/solid contact is dominant. Friction coefficients are high.*
- *In the mixed lubrication zone, a lubricating film begins to form between two surfaces with average sliding speed and the coefficient of friction begins to decrease.*
- *Two surfaces with high shear rate in the hydrodynamic lubrication zone are completely separated from each other by the lubricating film. There is no more solid/solid interaction. The friction coefficient increases with the sliding speed.*

Lubricants can be developed for a wide variety of applications. Generally, one or more mineral or synthetic based oils are used in the devel-

oped formulations. These base oils can be of vegetable or animal origin as well as fossil fuels such as crude oil and natural gas. The performance of these oils is then enhanced by using chemical additives. Additives used to minimize boundary friction, increase chemical stability, and reduce contamination under various operating conditions are usually added at 0.1% to 30% of the total oil volume.

Liquid lubricants are widely used because they are extremely effective. However, in some cases where the use of liquid lubricants is not appropriate and the loads are light, lubrication can be performed using gases. For example, in air bearings, a thin film layer formed with compressed air can provide a low friction interface. Solid lubricants, another type of lubricant, can be preferred due to their layered structure. When choosing the appropriate lubricant, the tribological system must first be fully defined. It is extremely important to analyze a wide variety of parameters such as the type of movement, physical and chemical structures of the surfaces, operating speed, operating temperature, load and operating conditions, and heat or contamination that may occur in the system during the working process, in the development of the most suitable lubricant for the system.

Abrasion is surface damage, or the shearing of material from one or both of two solid surfaces that slide, roll, and bump in relation to each other. In most cases, wear occurs in interactions at the rough edges along the surface. During movement, the material that first comes into contact with the surface can be displaced; thus, the properties of the solid body change at least at or near the surface, but there is little or no material loss. The material may then be lifted from a surface and result in transfer between mating surfaces or may separate as a wear particle. The net volume net mass loss at the interface is zero in the case of transfer from one surface to the other despite abrasion from one of the surfaces (with net mass or net loss of volume). Wear damage is preceded by material loss and can also occur independently. The definition of wear is often based on material loss. However, it should be emphasized that the damage occurs due to the displacement of material in a given body without change in weight or net volume, and also generates wear.

It defines wear types or forms as certain combinations of wear mechanisms with a well-defined canonical process of removing material corresponding to a particular set of contact conditions.

Basic Wear Mechanisms

- *adhesive,*
- *abrasive,*
- *corrosive,*
- *fatigue*

In Addition to the Basic Wear Mechanisms, the Most Well-Known Wear Mechanisms are

- *fretting - spalling*
- *pitting - scoring*
- *scuffing*
- *gouging - cavitation*
- *electrical wear*
- *solution wear*
- *melt wear*
- *impact wear*
- *diffusive wear*
- *light wear*
- *severe wear*

Tribology: It is an interdisciplinary branch of science in which knowledge from many fields such as physics, chemistry, mechanical engineering, material sciences, lubrication technologies, business economics, business management and industrial methods is used. Tribology, which is of great importance in all branches of industry; It finds a wide variety of applications in many industries such as engineering, medicine, textile, optics, and microelectronics, especially in the aerospace and automotive industries. Looking at the historical development of tribology; It is generally seen to be applied to components that roll or slide,

such as bearings, gears, shafts, brakes, and seals. Successes from initiatives focused on increasing the efficiency and extending the lifespan of all these components used in a wide variety of machines, together with new research in the process, pave the way for the development of better tribological applications.

Tribological applications can range from macro scale to nano scale. It has been revealed that tribology studies focusing on the transportation and manufacturing sectors in the traditional sense have a critical importance in different fields recently.

Classical tribology: It focuses on the friction and wear processes and lubrication methods of machine parts such as gears, bearings, plain bearings, clutches, brakes, and wheels, along with other production stages to ensure energy, material and production efficiency.

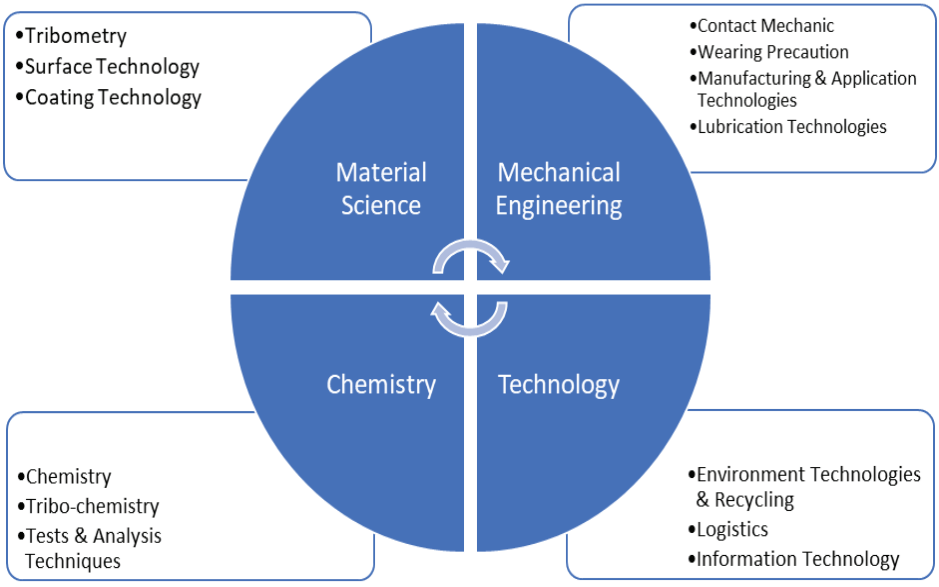

Figure 5. Multidisciplinary Fields Working with Tribology Science

In order to demonstrate the importance of tribology in biological systems, the term bio-tribology was first used in 1970. In general terms, bio-tribology is the field of study that reveals the relationship of tribology with biological systems in various aspects. When the bearing surfaces

of bone and cartilage structures in humans are not sufficiently lubricated, they wear out over time and cause various disorders. The way to prevent these ailments and to apply the necessary treatments is through developments in bio-tribology. Tribology studies in human systems are divided into areas such as oral, ocular, artificial joint applications and cardiovascular tribology.

Components of offshore machinery; exposed to extreme loads, harsh weather conditions and vibration, as well as salty air and water. This branch of tribology also covers the study of friction, wear and lubrication in the marine and ocean environment. Failures in machine components are more common in such environments than in others. The corrosive nature of sea and ocean waters causes roughness on the surfaces of the mechanical parts of the machines. In addition, the effect of lubrication decreases over time, which increases friction and thus energy consumption. On the other hand, due to the corrosive nature of sea water, harmful substances are released to the nature and the ecological balance is adversely affected. For this reason, various tribological studies are being conducted on polymers, metals, alloys and their different combinations for use in ocean and seawater environments. Thanks to these studies, materials that are subject to less friction and wear can be developed even under difficult conditions. Thus, it is aimed to protect machine components and reduce energy consumption.

The field of production tribology, which includes studies on metalworking fluids used in production processes; It focuses on fluids used for cooling and lubrication in operations such as turning, milling, grinding, and drilling. Most metalworking fluids used are mineral oils with good cooling and lubricating properties. The biggest disadvantage of these oils, which increase the efficiency of the production system, is that they are not biodegradable and recyclable. Considering that approximately 320,000 tons of mineral oil is used annually and most of it becomes waste, it becomes necessary to develop more environmentally friendly and effective alternatives instead of mineral oils. Although vegetable oils seem to be a good alternative, their tendency to oxidize at high temperatures limits their use. With a better understanding of

friction and wear mechanisms, research continues to develop lubricants that will perform cooling and lubrication functions with minimal use.

In order to use resources efficiently and to control harmful chemical emissions, governments are enforcing various laws and regulations one after another. These new regulations are forcing the auto industry to develop environmentally friendly vehicles that save energy. For this purpose, researches are continuously carried out to develop motor oils that reduce friction and wear in automobiles. Statistics show that savings to be made by reducing friction and wear in the United States automotive industry can reach $20 billion a year. Tribological parts in automobiles; includes the engine, transmission, traction drive, driveline, and auxiliary. These parts may vary according to different car types.

Tribological studies on auto parts allow the use of more suitable components. In addition, thanks to the development of better-performing and environmentally friendly lubricants, it is possible to reduce friction and wear, as well as save energy and materials. Electric vehicles powered by batteries, fuel cells or hybrid systems are seen as a viable alternative to internal combustion engines in order to reduce greenhouse gas emissions and provide a clean and healthy environment. The technology used not only in passenger cars but also in heavy-duty vehicles offers very important advantages. Although electric vehicles are highly efficient in terms of energy consumption, it is possible to increase this efficiency further. However, there are some difficulties that need to be overcome in order to achieve this. One of these challenges is friction, which causes energy loss.

Hard-facing is the stacking or coating of a type of alloy on the base material to protect a part from corrosion. Hard-facing welding is a low-cost method of creating a wear-resistant surface on metal parts to increase their life. It has advantages such as less replacement of parts, reduced maintenance time, the ability of the main part to be made from cheap materials, and a reduction in overall cost. Many hard-facing welds are performed as part of maintenance or repair operations, but the most effective results cannot be achieved by simply producing a weld metal that takes hardness into account. Hard-facing can be used to prolong and protect the life of new parts that are subject to high wear in service

conditions including metal-to-metal friction, abrasion, impact and impact and wear. Hard-facing can be made with many different types of alloy. Selecting the optimum alloy to resist the combination of wear factors encountered is an easy matter, but for this the behavior and properties of each alloy that determine its contribution to wear resistance must be considered.

The microstructure of the alloy, determined by chemical composition and thermo-mechanical history, is the property that makes the most important and significant contribution to wear resistance. Low stress (force on the abrasive part is not sufficient to break and grind the part), high stress (force on the abrasive part crushes the parts), dry wear, wet wear, high speed part sliding (wet or dry), metal-to-metal wear, (adhesion), impact, etc. There are many types of wear in species. Therefore, when grading hard-facing alloys, it is also necessary to specify the type of wear that it will resist. For this purpose, ASTM standard test methods have been developed to test different types of wear. These are ASTM G65 (low stress wear), ASTM G 99 (high stress wear), ASTM G 105 (wet low stress wear), ASTM G 75 (mixture wear), ASTM G 76 (fluid impingement).

According to a study, about 57% of the energy supplied to the electric vehicle is used to overcome the energy losses due to friction. 1% of these losses occur in the electric motor, 3% in the gearbox, 41% in the rolling resistance, and 12% in the brakes. In electric vehicles, the critical tribological components studied are basically comfort and safety devices (such as air conditioning system, wipers), steering system, electric motor, gearbox, constant velocity joint, suspensions, wheels, wheel bearings, micro-electro-mechanical system (MEMS). and kinematic energy recovery system. Different tribological components in each system lose a significant amount of energy due to friction. Tribology studies on electric vehicles are of great importance in order to make these vehicles more efficient and environmentally friendly.

Cutting-edge technologies in tribology have an important place both during the design phase and during the operation (monitoring, corrective actions based on friction-wear lubrication problems) of industrial components or systems. The efficiency, performance and lifetime of ma-

chine elements can be significantly increased with the right tribological design. The transmission of tribological data in various industrial areas takes place through information and communication technologies such as the internet and wireless connections.

It may be thought that both wear and friction are always disadvantageous, but this is not the case. In many engineering applications, we can use friction to perform the required functions. Thus, despite the stereotype that screw and nut can only work as a result of friction between the two, brakes, clutches, train and car wheels all work in the presence of friction. Likewise, the wear of machines is sometimes advantageous. While component wear provides a strong motivation to replace aging machines, the initial friction that results in better component contact is clearly desirable. In its most extreme form, this leads to "planned obsolescence," in which designers attempt to use the phenomenon of friction to provide machines with a specified lifetime.

Today, the industry's core technologies and tribology also have different interactions. The interaction of tribology with electronics (sensors, smart machines) and informatics (computers, internet, internet of things, wireless data transmission) fields is very strong with today's technologies. With the help of sensors, reliable information about both the wear status of the machines and the lubricants can be easily accessed. This strong connection of tribology with electronic components is also expressed by the term "tribo-tronics".

Detecting problems as soon as possible while a machine is running is very important in terms of reducing downtime and costs. Intelligent tribological systems used today can monitor many data such as wear, friction, lubrication status, vibration, and temperature; According to this data, it can make the necessary changes and adjustments to improve system performance. Thus, the mechanisms for controlling, evaluating, and taking action and making the necessary adjustments operate in a healthy way.

Tribology has an important role in the efficient use of energy and material resources, among which productivity increase, improved reliability and reduced maintenance costs, by leading the production in-

crease in engineering facility and machinery. Before discussing the prevalence and types of tribological problems in industry, we must look at the issue from a universal perspective. We are mainly concerned with the interaction of two hard surfaces within a given environment resulting from two external factors.

1) There is a loss of energy, which is resistance to movement, and this is shown by the coefficient of friction. This loss of energy causes a heat dissipation and a small but sometimes significant amount of noise during contact. It should be emphasized that; Since the two hard surfaces are constantly related to each other, parameters such as the coefficient of friction must correlate well with the two interacting material pairs. It is scientifically wrong and erroneous to talk about the coefficient of friction without mentioning the solids contact. It should also be noted that the idea of frictionless surfaces is scientifically improbable, and the frequently used implication that low friction is associated with smoothness of the surface is fundamentally wrong.

2) During the sliding process, all surfaces undergo a larger or smaller dimensional change in their essential character. They may become softer or harder, have physical properties such as deteriorated hardness, and some substances may be lost in this case, which is called wear processes. Such surface changes are sometimes beneficial, "for example, the surfaces get used to their ideal operating condition", sometimes it is very harmful, "situations where surface defects occur, and components need to be replaced

Based on the foregoing, it may be thought that both wear and friction are always disadvantageous, but this is not the case. In many engineering applications, we can use friction to perform the required functions. Thus, despite the stereotype that screw and nut can only work as a result of friction between the two, brakes, clutches, train and car wheels all work in the presence of friction. Likewise, the wear of machines is sometimes advantageous. While component wear provides a strong motivation to replace aging machines, the initial friction that results in better component contact is clearly desirable. In its most extreme form, this leads to "planned obsolescence," in which designers attempt to use the phenomenon of friction to provide machines with a specified lifetime.

Table 1. Friction Coefficient and Wear Rate of Pin on Ring Test

No	Materials	Coefficient of friciton	Wear rate cm^3/ cm x 10^{-12}
1	Mild steel on mild steel	0,62	157000
2	60/40 leaded brass	0,24	24000
3	Polytetrafluoroethylene	0,18	2000
4	Stellite	0,60	320
5	Ferritic stainless steel	0,53	270
6	Polyethylene	0,65	30
7	Tungsten carbide on itseld	0,35	2

An entirely common misconception that friction and wear are somehow related, on the ground that the surfaces are interacting, exists with the high friction high wear simple coupling. As Table 1 clearly shows, the lowest friction was not associated with the lowest wear. The results on this issue also show quite large wear rates of materials whose coefficients of friction vary quite reasonably. The complexity of the relationship between friction and wear has also been demonstrated by distinctive results; The reduction in friction that can occur as a result of the impression process, sometimes using the same materials, is associated with an increase in wear rate. In almost all industrial situations, more emphasis is placed on the effects of wear than losses due to friction, as they have greater economic consequences. High friction can often be tolerated, with partly higher operating costs, provided the machine provides the harmonious savings associated with increased wear time. Some of the industrial situations where friction and wear are important are illustrated by the next categories.

CONCLUSION

In developed societies, a wide variety of industrial activities need to be made sustainable as energy efficient and environmentally friendly.

Friction and wear; important factors that increase energy consumption, costs and greenhouse gas emissions in sectors such as transportation, manufacturing, power generation and housing. According to the data obtained in the latest research, approximately 23% of the world's total energy consumption, i.e. 119 exajoules (1 exajoule = 1x1018 J), is due to tribological contacts. 87% of this energy is used to overcome friction, and 13% is used to regenerate worn parts and spare equipment. It is predicted that energy losses can be reduced by 18% in 8 years and 40% in 15 years with the surface, material and lubrication technologies developed to reduce friction and prevent wear in vehicles, machinery and other equipment used throughout the world.

The largest energy savings are foreseen in the transportation sector, followed by the energy production, manufacturing and housing sectors, respectively. The global application of advanced tribology technologies is also expected to lead to significant reductions in greenhouse gas emissions. It is predicted that carbon dioxide gas emissions can be reduced by 1.5 million tons per year in the short term and 3 million tons in the long term. With all this, it means that the savings to be made in the long term will reach approximately 970 billion Euros. The problem-free, reliable and long-lasting of all components in advanced and complex machines and production technologies, where many moving and contacting surfaces come together, depends on how well the friction and wear on the contact surfaces are controlled. For this reason, tribology research is of great importance for the development of environmentally friendly materials and technologies and the efficient use of energy and raw material resources. As a result, new technologies developed in the field of tribology and their integration into industry continue to be important for energy efficiency and a sustainable society.

REFERENCES

Dašić, P., Franek, F., Assenova, E., Radovanović, M. (2003) International standardization and organizations in the field of tribology, Industrial Lubrication and Technology, 55(6), 287-291.

Findik, F. (2014) Latest progress on tribological properties of industrial materials, *Materials and Design*, 57, 218-244.

Anand, A., Haq, M.I.U., Vohra, K., Raina, A., Wani, M.F. (2017) Role of Green Tribology in Sustainability of Mechanical Systems: A State of the Art Surve, *Materials Today: Proceedings*, 4, 3659-3665.

Robinson, J., Zhou, Y., Bhattacharya, P., Erck, R., Qu, J., Bays, J., Cosimbescu, L.. (2016). Probing the molecular design of hyper-branched aryl polyesters towards lubricant applications, *Scientific Reports*, 6, 1-10.

Kotecki, D.J., Ogborn, J.S. (1995)Abrasion Resistance of Iron-Based Hardfacing Alloy, *Welding Journal,* 74(8), 269-278.

Farfan-Cabrera, L.I. (2019) Tribology of electric vehicles: A review of critical components, current state and future improvement trends, *Tribology International*, 138, 473-486.

Holmberg, K., Erdemir, A. (2017) Influence of tribology on global energy consumption, costs and emission, *Friction*, 5(3), 263-284.

Shah, R., Woydt, M., Huq, N., Rosenkranz, A. (2021) Tribology meets sustainability, *Industrial Lubrication and Tribology*, 73(3), 430-435.

Kaleli, H. (2018). *Triboloji Prensipleri ve Uygulama* Örnekleri *(Ders Notu)*. İstanbul.

García, A., Varela, A., Montero, J., Mier, J. L., *Zaragoza, S., & Barbadillo, F. (2008). Tribological Behaviour of an A355 Steel Pipe Welding, In Materials Science Forum Trans Tech Publications*, 587, 360–364.

Baydemir, T. (2021) Triboloji: Enerji ve Doğal Kaynakalrı Daha Verimli Kullanmanın Yolu mu? *TÜBİTAK Bilim ve Teknik Dergisi,* 12, 36-49.

REACHING THE HIGHEST INFORMATION TRANSFER RATE VALUE IN EMOTIV EPOC-BASED BRAIN-COMPUTER INTERFACE SYSTEMS

Mesut MELEK[1], Negin MELEK[2], Temel KAYIKÇIOĞLU[3]

Abstract: The brain-computer interface (BCI) is considered as an important link between the brain and device. Since it is non-invasive and easily recorded, electroencephalography (EEG) signals are generally used in these systems. These signals appear as a result of the neural functioning of the brain. Consequent to the processing of EEG signals, thanks to the cooperation of BCI technology and EEG, great convenience is provided. The great advantages of EEG-based BCI applications include communication speed, small signal-to-noise ratio, and user-friendliness. The type of headset used in the proposed study, the Emotiv Epoc, plays an important role in the comfort of the individual under test. Minimizing the problems of recording models commonly used in BCI technology was the main goal of our previous study. In this way, users' EEG signals were successfully classified during looking at four vanes rotating in different directions and speeds. In this study, the probability of the user choice was increased to five by adding one more fixed vane to four previous rotating vanes. The number of the probability of the user choice was inverse to the accuracy rate of the classification and directly proportional to the information transfer rate (ITR). These two metrics were the most common metrics used to compare BCI systems. With the introduction of a new paradigm, the

1 Gumushane University, Department of Electronics and Automation, Gumushane / Turkey, e-mail: mesutmelek@gumushane.edu.tr, Orcid No: 0000-0002-7152-7788

2 Giresun University, Faculty of Engineering, Department of Computer Engineering, Giresun / Turkey, e-mail: negin.melek@giresun.edu.tr, Orcid No: 0000-0001-5297-5545

3 Karadeniz Technical University, Faculty of Engineering, Department of Electrical and Electronics Engineering, Trabzon / Turkey, e-mail: tkayikci@ktu.edu.tr, Orcid No: 0000-0002-6787-2415

highest ITR was achieved with the Emotiv Epoc device. In addition, fewer electrodes were utilized to provide more comfort for the user in the user-friendly Emotiv Epoc device. When 5, 10, and all channels were used, ~29, 32, and 34 bits/min were calculated for ITR, respectively. The results were compared in detail with the literature and the ITR of the present study appeared to be higher than that of the other studies.

Keywords: Brain-Computer Interface, Emotiv Epoc, Classification, Information Transfer Rate, EEG

INTRODUCTION

Neurological disorders are the types of diseases caused by the brain and nervous system, neuromuscular functions, and even the muscles. Individuals with such diseases may experience some serious problems in terms of interaction. BCI systems are the computer systems based on the physical interaction between such patients with disabilities and the people and electronic devices around them (Lang, 2012a). These systems simultaneously record neuronal activities with electroencephalograms and perform the desired control in the outside world by enabling the processing of signals on the computer.

BCI systems consist of three main components:

- The first stage is the signal recording section.
- In the second stage, the recorded signals are preprocessed to perform the effective feature extraction.
- An action stage generates signals to control any equipment or application and explains the situation by giving feedback to the user.

BCIs have two categories as invasive and non-invasive. The non-invasive type attracts great attention because it requires no surgery. Among the non-invasive methods, the BCI systems by using EEG are more popular. Although EEG-based BCI applications are numerous and harmless, they have been limited to research laboratories as they require large and expensive EEG systems and qualified human resources (Lang,

2012b). In addition, the use of EEG devices requires a long preparation time. For quality recording, the subjects are asked to pay attention to the cleanliness of their scalps. Moreover, EEG gel is used to obtain an acceptable impedance between the scalp and the electrodes placed on the skin. In addition, the participants should wear an electrode cap, which may make them feel uncomfortable.

On the other hand, with the advancement in technology, much smaller and more affordable equipment and tools have been introduced, such as the Emotiv Epoc, which was originally intended for the gaming market. Due to its easy use, it has been adopted by many researchers in various applications, even if it does not fall into the category of medical tools such as simple puzzle game, recording the state of the eyes, detecting mental activity, robot control, robot navigation, wheelchair navigation, and auditory event-related potential capturing. Emotiv Epoc is a low-priced ground-breaking wireless EEG device and its preparation time is short. This EEG cap provides great convenience for users because it is not sensitive in cleaning the skin before and is easy to clean after the experiment.

Another advantage is that the working logic of the cap is easily solved. Emotiv Epoc, which has high flexibility and uses wireless technology, has the total of 14 sensors adjusted according to the international 10-10 electrode placement system. Emotiv Epoc is more inexpensive than professional EEG devices and can capture true EEG, although not as well as professional or clinical EEG systems (Research Use of Emotiv EPOC, n.d.). Signals are sampled at the frequency of 128 Hz.

Comparing the working principle of the Emotiv Epoc headset with other devices is the main target of many works. A p300-based BCI system was investigated by researchers to examine the working principle of the Emotiv Epoc headset (X. Liu et al., 2018). As the result of the examinations made in this study, which consisted of 6 subjects, it was observed that P300 was successfully detected from brain signals. In (Martinez-Leon et al., 2016), the evaluation of Emotiv Epoc in motor imagery-based BCI systems was presented. A different BCI base was created using a professional EEG headset to establish a benchmarking base.

Looking at the results, it has been shown that the performance of the headset is good and comparable to that of the professional devices. In another study (Tello et al., 2014a), a detailed review and comparison of BrainNet36 and Emotiv Epoc was made in BCI system modeling based on steady-state visual evoked potential (SSVEP). The results indicated that the Emotiv Epoc had acceptable performance for SSVEP-based BCI systems. Based on the research on Emotiv Epoc headsets in BCI systems modeling in the age of technology, an increase in the number of uses of these headsets was observed (Masood & Farooq, 2017).

The important aims of the current study are to increase the quality of life of individuals with physical disabilities and to provide easy interaction with the environment. Different paradigms are defined in research on BCI technology. These paradigms generally have some disadvantages which can be classified as follows: In the P300 and SSVEP studies, it may lead to some negativities such as eye discomfort due to the point that individuals look at the blinking light page uninterruptedly.

Individuals participating in the motor imagery paradigm need to constantly think about limb movements by developing their imaginations. In order to eliminate these disadvantages, in our previous study, a wired and gel-based BBA system based on rotating hands was modeled (Maleki et al., 2018). Also, in (Melek et al., 2020b), for the convenience of the users, this paradigm was tested by using Emotiv Epoch. In the present study, by adding a fixed vane to the system, the user's choice chances became five. In addition, steps were taken to use less electrodes in the Emotiv Epoc device, which was user-friendly, easy-to-use, inexpensive, but recorded a lower quality signal.

EXPERIMENTAL SETUP

Dataset

Gelecekte The interface designed with Matlab 2014a is displayed in Figure 1. In the designed model, the "A" alphabet written with five capital letters is placed on a black background.

The Working Principle of These Vanes is Described Below

- The vane located at the top left is known as vane 1 and rotates counter-clockwise once every five seconds.
- The vane located at the top right is known as vane 2 and rotates counter-clockwise once every second.
- Vane 3 (center) is fixed with no rotation.
- The vane located at the bottom left is known as vane 4 and rotates clockwise once every five seconds.
- The vane located at the bottom right is known as vane 5 and rotates clockwise once every second.

Vane speed and direction, which are considered as important factors in the study, can be controlled by the written Matlab code. In addition, in previous studies, an investigation has been carried out to determine these factors. As a result, were clarified as mentioned above by using the trial-and-error method.

Five participants aging between 27 and 32 years participated in this experimental set consisting of 4 men and 1 woman. The experiments were carried out according to the rules with registration number 24237859-640 in Ethics Committee, Faculty of Medicine, Karadeniz Technical University. Before starting the recording, vision problems, headaches, and a family history of epilepsy were discussed with the participants. All the participants reported that they had no problems with these issues. The 5-vane model was presented to the participant sitting on a chair at the distance of approximately 1 m on a 32-inch screen. In this experiment, the start and end of which were determined by a beep, it was deemed appropriate for the participants 125 seconds for each vane. After the second beep sound, after about 1 minute of resting, the other vane was followed. In this direction, a data set was prepared as a result of EEG signals from 5 participants. The obtained and processed EEG signals were separated into 2 and 3 second (2 and 3-sec) epochs. As a result of this epoch segmentation, 50% and 75% overlaps were applied for 2-sec and 3-sec fragmentation, respectively, thereby obtaining 120 epochs for both time windows.

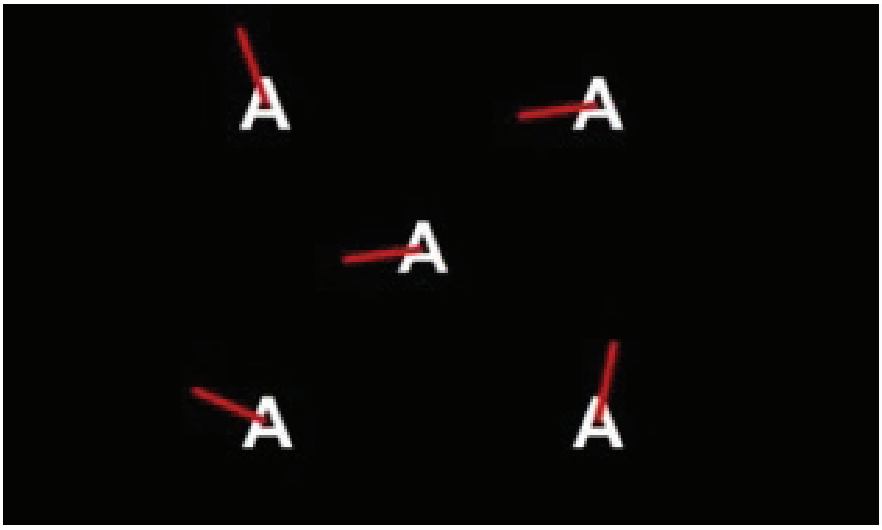

(a)

(b)

Figure. 1. (a) Four Rotating Vanes and a Fixed Vane Designed by Matlab 2014a (b) Emotiv Headset

SIGNAL PROCESSING

Normalization which is considered the first step of EEG signal processing can directly affect classification performance. The normalization process plays a major role in minimizing the effect of amplitudes of EEG signals. In the proposed study, the normalization process was performed by applying the Z-score method to each epoch. During signal recording, very sensitive EEG signals can be easily affected by different types of noise. Therefore, the filtering step is indispensable in the signal processing stage. A 4th order Butterworth filter was selected for each epoch with the passband of 0.1-45 Hz.

In the EEG Signal pre-analysis stage, the Welch method was applied to obtain information about the power distribution and to calculate the power spectral density (PSD) (Welch, 1967). The Welch method is defined as a windowed fast Fourier transform (FFT). In this method, for the periodogram calculation, each epoch divided into appropriate lengths with certain overlaps is multiplied by a determined window and the density is calculated by taking the average of the periodograms. As a result of the calculated spectrum estimates, scaling is performed for the PSD analysis. To obtain the features from the scaled PSD, the PSD was divided into the band ranges given in Table 1 and the area formed by each band interval with the x-axis was calculated with Matlab's trapz command. In this way, 11 features were obtained from each epoch.

To perform the classification process, classification learner app was used. This Matlab application contains various classifiers (Melek et al., 2020a). All classifiers were tested with their default parameters and the best four classifiers were selected based on the accuracy rate. These are the support vector machine (linear, quadratic, cubic) and ensemble subspace discriminant.

Table 1. Frequency Bands Used in the Feature Extraction Process

Bands	frequency (Hz)
Delta band	0-4
Teta band	4-8

Alfa band	8-12
Beta band 1	12-16
Beta band 2	16-20
Beta band 3	20-24
Beta band 4	24-28
Beta band 5	28-32
Gamma band 1	32-36
Gamma band 2	36-40
Gamma band 3	40-44

RESULTS

EEG signals obtained from 14 channels of Emotiv Epoc headphones were analyzed separately. 2-sec epochs for each channel were included in the analysis with 50% overlap. After normalization and filtering processes were performed over epochs, the PSD of each epoch was calculated by the Welch method and, in total, 11 features were obtained. It is envisaged that one of the important goals of this study, user comfort, would be realized with an effort to reduce the number of channels. To determine the effective channels, the classification accuracy rate in each channel was taken into account. The accuracy (ACC) rate, which is one of the important factors in the performance evaluation of the classification method, has been used in many studies. Different combinations of training and testing sets were considered to demonstrate the stability of the designed model. Then, the total accuracy of the model was calculated as taking the mean of all steps. Considering this issue, 75% and 25% were found suitable for training and testing, respectively, in this study. Against unlucky splitting, the training and data sets were mixed 10 times, and average rate of accuracy was calculated. The average accuracy rate of each channel for five participants is given in Table 2.

Table 2. The Results of Five Participants for Each Channel and Ranking of the Best Channels for Each Classifier; Common Channels are Bold-Face

Channel No.	Channel Name	Linear SVM	Quadratic SVM	Cubic SVM	Ensemble Subspace Discriminant
Ch. 1	AF3	0.3287	0.3043	0.2850	0.3240
Ch. 2	F7	0.3767	0.3527	0.3330	0.3623
Ch. 3	F3	0.3310	0.3067	0.2870	0.3303
Ch. 4	FC5	0.3837	0.3487	0.3163	0.3777
Ch. 5	T7	0.4733	0.4577	0.4357	0.4317
Ch. 6	P7	0.3613	0.3217	0.3267	0.3490
Ch. 7	O1	0.3443	0.3330	0.3027	0.3403
Ch. 8	**O2**	0.3980	0.3687	0.3290	0.3760
Ch. 9	P8	0.3740	0.3470	0.3230	0.3610
Ch. 10	T8	0.4423	0.4143	0.3823	0.4197
Ch. 11	FC6	0.4457	0.4243	0.4010	0.4303
Ch. 12	F4	0.4053	0.3743	0.3380	0.3940
Ch. 13	F8	0.3670	0.3357	0.3290	0.3643
Ch. 14	AF4	0.3430	0.3200	0.3100	0.3317
Top five channels according to ACC		**8, 12, 10, 11, 5**	2, **12, 10, 11, 5**	**8, 12, 10, 11, 5**	4, **12, 10, 11, 5**
Next five channels		6, **13**, 9, 2, 4	4, 9, 6, 8, **13**	7, **13**, 9, 4, 2	6, 9, 2, **13**, 8
The last four channels		1, 3, 14, 7	1, 3, 7, 14	**1, 3, 14**, 6	1, 3, 14, 7

Evidently, T7, T8, FC6, and F4 (channels 12, 10, 11, and 5) were among the top five channels in all the four classifiers. Except for these four channels, the O2 channel (Channel 8) entered the top five in two classifiers. For this, the five best channels of the system were T7, T8, FC6, F4, and O2. By looking at the last four channels, it was found that AF3, F3, and AF4 (channels 1, 3, 14) appeared in all the classifiers. Except for

these three channels, channel 7 (O1) appeared in the last four of the three classifiers. In this way, F7, FC5, P7, P8, and F8 were added to the top five channels, and the top 10 channels were detected.

After the effective channels were determined, the classification was performed using the top five channels. In order to achieve an efficient feature extraction process, 55 features from the total of five channels were prepared for each epoch and presented to the classifiers. In this step, again, 75% of the dataset for the training set and 25% for the testing set was used; the process was repeated 10 times against unlucky splitting. The information transfer rate (ITR) provides information about three important parameters that it contains, known as the accuracy rate, recognition time of a selection, and number of tasks for each selection. ITR is mathematically expressed by the following equation (Wolpaw et al., 1998):

$$ITR = \frac{60}{T}\left(log_2 K + p log_2 p + (1-p) log_2\left(\frac{1-p}{K-1}\right)\right) \quad (1)$$

In this formula, T determines the time spent in selection recognition, K determines the number of selections, and p determines the accuracy of the model. The results are given in Table 3.

It is clear that the quadratic SVM performed better than other classifiers. In addition, although the ITR of the system looked good, the accuracy rate of the system for five people was limited to 0.6916. In the next step, the same procedure was followed by using the top 10 channels determined and, finally, all the channels were included in the classification procedure. The results obtained by using 10 channels and all the channels were presented in Table 4 and Table 5.

Table 3. The Results of 2-Sec Epochs by Using Five Channels

Classifier/ subjects	Linear SVM		Quadratic SVM		Cubic SVM		Ensemble Subspace Discriminant	
	Accuracy	ITR	Accuracy	ITR	Accuracy	ITR	Accuracy	ITR
S1	0.6413	19.8907	0.6660	22.0490	0.6693	22.3497	0.6193	18.0625
S2	0.6693	22.3497	0.6527	20.8679	0.6533	20.9262	0.6380	19.6079
S3	0.7053	25.7376	0.7333	28.5586	0.7173	26.9261	0.7220	27.3965
S4	0.7080	25.9991	0.7240	27.5995	0.6993	25.1547	0.7080	25.9991
S5	0.6927	24.5157	0.6820	23.5120	0.6800	23.3264	0.6453	20.2328
AVG.	0.6833	23.6986	0.6916	24.5174	0.6838	23.7366	0.6665	22.2598

Table 4. The Results of 2-Sec Epochs by Using 10 Channels

Classifier/ subjects	Linear SVM		Quadratic SVM		Cubic SVM		Ensemble Subspace Discriminant	
	Accuracy	ITR	Accuracy	ITR	Accuracy	ITR	Accuracy	ITR
S1	0.7293	28.1453	0.7627	31.7042	0.7600	31.4066	0.7167	26.8593
S2	0.6967	24.8980	0.6727	22.6525	0.6793	23.2647	0.6760	22.9575
S3	0.7947	35.3638	0.8060	36.7249	0.8100	37.2137	0.8180	38.2049
S4	0.7567	31.0417	0.7853	34.2686	0.7687	32.3680	0.7847	34.1912
S5	0.6840	23.6985	0.7033	25.5425	0.7027	25.4776	0.6820	23.5120
AVG.	0.7322	28.6294	0.7460	30.1785	0.7441	29.9461	0.7354	29.1450

Table 5. The Results of 2-Sec Epochs by Using All Channels

Classifier/ subjects	Linear SVM		Quadratic SVM		Cubic SVM		Ensemble Subspace Discriminant	
	Accuracy	ITR	Accuracy	ITR	Accuracy	ITR	Accuracy	ITR
S1	0.7347	28.6972	0.7587	31.2603	0.7593	31.3334	0.7300	28.2139
S2	0.6587	21.3952	0.6593	21.4542	0.6913	24.3890	0.6507	20.6937
S3	0.7740	32.9687	0.7933	35.2060	0.7933	35.2060	0.7920	35.0486

S4	0.7667	32.1445	0.7707	32.5924	0.7753	33.1199	0.7953	35.4429
S5	0.6440	20.1185	0.7007	25.2836	0.7227	27.4641	0.7067	25.8682
AVG.	0.7156	27.0648	0.7365	29.1593	0.7484	30.3025	0.7349	29.0535

Table 6. The Results of 3-Sec Epochs by Using Five Channels

Classifier/ subjects	Linear SVM		Quadratic SVM		Cubic SVM		Ensemble Subspace Discriminant	
	Accuracy	ITR	Accuracy	ITR	Accuracy	ITR	Accuracy	ITR
S1	0.7693	21.6285	0.8253	26.0865	0.8567	28.8472	0.6993	16.7698
S2	0.7780	22.2825	0.7667	21.4297	0.7913	23.3134	0.7027	16.9851
S3	0.8707	30.1531	0.8987	32.9211	0.9060	33.6849	0.8400	27.3524
S4	0.8473	28.0024	0.8840	31.4435	0.8800	31.0513	0.8120	24.9732
S5	0.7540	20.5010	0.7400	19.5036	0.8107	24.8637	0.6867	15.9656
AVG.	0.8038	24.5135	0.8229	26.2769	0.8489	28.3521	0.7481	20.4092

Table 7. The Results of 3-Sec Epochs by Using 10 Channels

Classifier/ subjects	Linear SVM		Quadratic SVM		Cubic SVM		Ensemble Subspace Discriminant	
	Accuracy	ITR	Accuracy	ITR	Accuracy	ITR	Accuracy	ITR
S1	0.8467	27.9428	0.8807	31.1164	0.8907	32.1072	0.8073	24.5916
S2	0.8160	25.3036	0.7987	23.8935	0.8133	25.0830	0.7553	20.5976
S3	0.9393	37.4102	0.9453	38.1339	0.9413	37.6493	0.9227	35.4910
S4	0.9407	37.5694	0.9573	39.6441	0.9553	39.3860	0.9253	35.7899
S5	0.7933	23.4706	0.7920	23.3657	0.8440	27.7055	0.7453	19.8801
AVG.	0.8672	30.3393	0.8748	31.2307	0.8890	32.3862	0.8312	27.2700

Table 8. The Results of 3-Sec Epochs by Using All Channels

Classifier/ subjects	Linear SVM		Quadratic SVM		Cubic SVM		Ensemble Subspace Discriminant	
	Accuracy	ITR	Accuracy	ITR	Accuracy	ITR	Accuracy	ITR
S1	0.8305	26.5274	0.8848	31.5225	0.9067	33.7588	0.8457	27.8566
S2	0.8029	24.2328	0.8105	24.8501	0.8495	28.1968	0.8048	24.3861
S3	0.9410	37.6093	0.9648	40.6339	0.9657	40.7562	0.9533	39.1264
S4	0.9029	33.3599	0.9495	38.6482	0.9543	39.2537	0.9162	34.7780
S5	0.7457	19.9061	0.8048	24.3861	0.8505	28.2868	0.7914	23.3186
AVG.	0.8446	28.3271	0.8829	32.0081	0.9053	34.0505	0.8623	29.8931

Based on the results of the 3-sec epochs, there was a large increase in the accuracy rate compared to the results of the 2-sec epochs. By using all the channels, the accuracy rate increased to 0.9053 from 0.7484 for the average of 5 subjects.

As stated earlier, one of the aims of this study was to use fewer electrodes in the Emotiv Epoc device. The best result appeared to be in the cubic SVM classifier using all channels, albeit with very little difference. The accuracy rate obtained by using all the channels with the cubic SVM classifier in 3-sec epochs appeared to be above the accuracy rate obtained with 10 channels, i.e., ~2%. This was reflected in the ITR of the system, causing the system to run faster at 2 bits/min. Therefore, it seemed more beneficial to use all channels in our study based on the Emotiv Epoc headset. In summary, considering ITR as an important metric in BCI systems, it was observed that the highest ITR value was obtained in 3-sec epochs using all channels in the cubic SVM classifier.

To demonstrate the sensitivity of the proposed system to classes, in 3-sec epochs, confusion matrices obtained using the leave-one-out (LOO-CV) strategy were calculated. In LOO-CV strategy, the samples in the dataset were utilized as testing sets one by one and the remain-

ing samples each time constituted the training set. The classifier used in this stage was performed with cubic SVM, which showed the best performance in 3-sec epochs. The confusion matrices for five people are depicted in Figure 2. Classes were defined as V1, V2, V3, V4, and V5. It turned out that the system had no extreme insensitivity or sensitivity for any class.

Confusion matrix for Participant 1 (ACC=0.945)

	V1	V2	V3	V4	V5	Sen.
V1	116	1	2	0	1	%97
V2	1	115	1	1	2	%96
V3	2	2	108	1	7	%90
V4	0	0	3	111	6	%93
V5	1	0	1	1	117	%98

Confusion matrix for Participant 2 (ACC=0.880)

	V1	V2	V3	V4	V5	Sen.
V1	109	4	0	3	4	%91
V2	7	111	0	2	0	%93
V3	0	0	110	2	8	%92
V4	4	1	0	99	16	%83
V5	4	4	1	12	99	%83

Confusion matrix for Participant 3 (ACC=0.8116)

	V1	V2	V3	V4	V5	Sen.
V1	120	0	0	0	0	%100
V2	3	117	0	0	0	%98
V3	0	0	113	5	2	%94
V4	0	0	0	120	0	%100
V5	0	0	0	3	117	%98

Confusion matrix for Participant 4 (ACC=0.977)

	V1	V2	V3	V4	V5	Sen.
V1	119	1	0	0	0	%99
V2	0	116	1	0	3	%97
V3	0	2	115	2	1	%96
V4	1	0	0	117	2	%98
V5	0	0	0	1	119	%99

Confusion matrix for Participant 5 (ACC=0.870)

	V1	V2	V3	V4	V5	Sen.
V1	117	0	1	2	0	%98
V2	7	102	9	1	1	%85
V3	3	1	100	9	7	%83
V4	3	0	3	106	8	%88
V5	2	0	6	15	97	%81

Figure 2. Confusion Matrices Obtained by the Cubic SVM Classifier Based on the LOO-CV Strategy in 3-Sec Epochs

DISCUSSIONS

As a result of the literature review, many studies conducted with the cooperation of BCI technology and Emotiv have not focused on system accuracy and ITR calculation (Alrajhi et al., 2017). For this, In this study, a comprehensive review was performed using the IEEEXplore digital library and the Web of Science (WOS) database to compare the proposed system with the existing ones. These systems were examined in six aspects that are important in BCI systems, and the methods used in

signal processing procedures were taken into account, as summarized in Table 9. Based on Table 9, the highest ITR was achieved by Pedram et al. in 2018 (Soroush & Shamsollahi, 2019b). ITR was not calculated in bits/min, but since the duration of each trial was determined as 3-sec, the ITR of this system can be calculated as 33 bits/min. Another comprehensive study in this area was conducted in 2012. In this successful study based on the SSVEP paradigm, the accuracy rate and ITR were determined as 82.99% and 28.06 bits/min, in offline mode. This study, tested on four participants, provided 16 options for the users (Y. Liu et al., 2012a).

Here, we put forward a comprehensive study aimed at designing a comfortable, suitable for long time use, inexpensive and fast BCI system. By considering the design result quantity, we computed the accuracy rate of the system by about 90.53% with the proposed machine learning techniques and raised the speed of the BCI system to 34.05 bits/min. As seen in Table 9, the values reported in the other studies were below our values. When the similar paradigm and the proposed study were compared, the system's ease of use and eye-catching ITR drew attention. As seen in Table 9, the values reported in the other studies were below our values.

Table 9. Summary of Emotiv Epoc-Based BCI Systems in the Literature

Studies	Paradigm	Classes	ITR	Subjects	Acc.
(Zhang et al., 2019)	Motor imagery	thinking of moving	----	7	93.6
(Brennan et al., 2015)	SSVEP	4 directions (up, down, right, left)	15.23	6	79.2
(Soroush & Shamsollahi, 2019b)	SSVEP	4 cases	1.5 bits/trial	10	94.85

(Mijani et al., 2019)	P300	single, dual and triple rapid serial visual presentation	3.65 7.72 11.5	3	78 63 64
(Li et al., 2019)	SSVEP	two directions (right left)	8	5	90
(Melek et al., 2020c)	Gazing	4 rotating vanes	26	5	77
(Tong et al., 2015)	P300	4× 3 dialling system	7.17	20	88.75
(Y. Liu et al., 2012b)	SSVEP	Numbers 1 to 16	28.06	4	82.99
(Chiuzbaian et al., 2019)	SSVEP	four directions	10.06	10	92.5
(Tello et al., 2014b)	SSVEP	Two squares	8.07	5	66
Proposed method	Gazing	5 rotating vanes	34.05	5	0.9053

CONCLUSIONS

The inconvenience for the user (i.e., cap, gel, etc.) to use BCI systems and the low interaction speed caused these systems to remain in research laboratories. To fill this gap, the Emotiv Epoc headset offers facilities to alleviate the problems of EEG-based BCI technology. This device minimizes user discomfort thanks to its moist electrodes. In addition, this low-cost headset has a short preparation process because it is wireless. Also, steps were taken to use fewer channels, but the results were observed to be better when using all the channels. In general, when looking at the results of this study, two important points appeared; BCI systems based on rotating vanes had sufficient potential to overcome the problems of systems operating with the existing paradigms. The second point was that more cost-effective devices can be used, instead of

expensive EEG devices, in real applications. This offline work can be developed online by considering other feature extraction and classification techniques. In addition, with EEGLAB, analysis can be made in a more flexible environment by transferring brain information to a graphical interface.

REFERENCES

Alrajhi, W., Alaloola, D., & Albarqawi, A. (2017). Smart home: toward daily use of BCI-based systems. 2017 International Conference on Informatics, Health & Technology (ICIHT), 1–5. https://doi.org/10.1109/ICIHT.2017.7899002

Brennan, C., McCullagh, P., Lightbody, G., Galway, L., Feuser, D., González, J. L., & Martin, S. (2015). Accessing Tele-Services Using a Hybrid BCI Approach (pp. 110–123). Springer, Cham. https://doi.org/10.1007/978-3-319-19258-1_10

Chiuzbaian, A., Jakobsen, J., & Puthusserypady, S. (2019, February). Mind Controlled Drone: An Innovative Multiclass SSVEP based Brain Computer Interface. 7th International Winter Conference on Brain-Computer Interface, BCI 2019. https://doi.org/10.1109/IWW-BCI.2019.8737327

Lang, M. (2012a). Investigating the Emotiv EPOC for cognitive control in limited training time Honours Report by. University of Canterbury.

Lang, M. (2012b). Investigating the Emotiv EPOC for cognitive control in limited training time Honours Report by. University of Canterbury.

Liu, X., Chao, F., Jiang, M., Zhou, C., Ren, W., & Shi, M. (2018). Towards Low-Cost P300-Based BCI Using Emotiv Epoc Headset. Advances in Intelligent Systems and Computing, 650, 239–244. https://doi.org/10.1007/978-3-319-66939-7_20

Liu, Y., Jiang, X., Cao, T., Wan, F., Mak, P. U., Mak, P. I., & Vai, M. I. (2012a). Implementation of SSVEP based BCI with Emotiv EPOC. Proceedings of IEEE International Conference on Virtual Environments, Human-Computer Interfaces, and Measurement Systems,VECIMS, 34–37. https://doi.org/10.1109/VECIMS.2012.6273184

Liu, Y., Jiang, X., Cao, T., Wan, F., Mak, P. U., Mak, P. I., & Vai, M. I. (2012b). Implementation of SSVEP based BCI with Emotiv EPOC. Proceedings of IEEE International Conference on Virtual Environments, Human-Computer Interfaces, and Measurement Systems,VECIMS, 34–37. https://doi.org/10.1109/VECIMS.2012.6273184

Maleki, M., Manshouri, N., & Kayikcioglu, T. (2018). Fast and accurate classifier-based brain-computer interface system using single channel EEG data.

26th IEEE Signal Processing and Communications Applications Conference, SIU 2018, 1–4. https://doi.org/10.1109/SIU.2018.8404376

Martinez-Leon, J. A., Cano-Izquierdo, J. M., & Ibarrola, J. (2016). Are low cost Brain Computer Interface headsets ready for motor imagery applications? Expert Systems with Applications, 49, 136–144. https://doi.org/10.1016/j.eswa.2015.11.015

Masood, N., & Farooq, H. (2017). Emotiv-based low-cost brain computer interfaces: A survey. Advances in Intelligent Systems and Computing, 488, 133–142. https://doi.org/10.1007/978-3-319-41691-5_12

Melek, M., Manshouri, N., & Kayikcioglu, T. (2020a). An automatic EEG-based sleep staging system with introducing NAoSP and NAoGP as new metrics for sleep staging systems. Cognitive Neurodynamics, 1–19. https://doi.org/10.1007/s11571-020-09641-2

Melek, M., Manshouri, N., & Kayikcioglu, T. (2020b). Low-Cost Brain-Computer Interface Using the Emotiv Epoc Headset Based on Rotating Vanes. Traitement Du Signal, 37(5), 831–837. https://doi.org/10.18280/ts.370516

Melek, M., Manshouri, N., & Kayikcioglu, T. (2020c). Low-Cost Brain-Computer Interface Using the Emotiv Epoc Headset Based on Rotating Vanes. Traitement Du Signal, 37(5), 831–837. https://doi.org/10.18280/ts.370516

Mijani, A. M., Shamsollahi, M. B., Hassani, M. S., & Jalilpour, S. (2019). Comparison between Single, Dual and Triple Rapid Serial Visual Presentation Paradigms for P300 Speller. Proceedings - 2018 IEEE International Conference on Bioinformatics and Biomedicine, BIBM 2018, 2635–2638. https://doi.org/10.1109/BIBM.2018.8621505 Research Use of Emotiv EPOC. (n.d.).

Sadeghi, S., & Maleki, A. (2019). Accurate estimation of information transfer rate based on symbol occurrence probability in brain-computer interfaces. Biomedical Signal Processing and Control, 54, 101607. https://doi.org/10.1016/j.bspc.2019.101607

Shi, M., Liu, X., Zhou, C., Chao, F., Liu, C., Jiao, X., An, Y., Nwachukwu, S. E., & Jiang, M. (2018). Towards portable SSVEP-based brain-computer interface using Emotiv EPOC and mobile phone. Proceedings - 2018 10th International Conference on Advanced Computational Intelligence, ICACI 2018, 249–253. https://doi.org/10.1109/ICACI.2018.8377615

Soroush, P. Z., & Shamsollahi, M. B. (2019a). A non-user-based BCI application for robot control. 2018 IEEE EMBS Conference on Biomedical Engineering and Sciences, IECBES 2018 - Proceedings, 36–41. https://doi.org/10.1109/IECBES.2018.8626701

Soroush, P. Z., & Shamsollahi, M. B. (2019b). A non-user-based BCI application for robot control. 2018 IEEE EMBS Conference on Biomedical Engineering and Sciences, IECBES 2018 - Proceedings, 36–41. https://doi.org/10.1109/IECBES.2018.8626701

Tello, R. M. G., Müller, S. M. T., Bastos-Filho, T., & Ferreira, A. (2014a). Comparison between wire and wireless EEG acquisition systems based on SSVEP in an Independent-BCI. 2014 36th Annual International Conference of the IEEE Engineering in Medicine and Biology Society, EMBC 2014, 22–25. https://doi.org/10.1109/EMBC.2014.6943519

Tello, R. M. G., Müller, S. M. T., Bastos-Filho, T., & Ferreira, A. (2014b). Comparison between wire and wireless EEG acquisition systems based on SSVEP in an Independent-BCI. 2014 36th Annual International Conference of the IEEE Engineering in Medicine and Biology Society, EMBC 2014, 22–25. https://doi.org/10.1109/EMBC.2014.6943519

Tong, J., Peng, Z., Ran, X., & Lei, D. (2015). The portable P300 dialing system based on tablet and Emotiv Epoc headset. Proceedings of the Annual International Conference of the IEEE Engineering in Medicine and Biology Society, EMBS, 2015-November, 566–569. https://doi.org/10.1109/EMBC.2015.7318425

Welch, P. D. (1967). The Use of Fast Fourier Transform for the Estimation of Power Spectra: A Method Based on Time Averaging Over Short, Modified Periodograms. IEEE Transactions on Audio and Electroacoustics, 15(2), 70–73. https://doi.org/10.1109/TAU.1967.1161901

Wolpaw, J. R., Ramoser, H., McFarland, D. J., & Pfurtscheller, G. (1998). EEG-based communication: improved accuracy by response verification. IEEE Transactions on Rehabilitation Engineering, 6(3), 326–333. https://doi.org/10.1109/86.712231

Zhang, X., Yao, L., Zhang, S., Kanhere, S., Sheng, M., & Liu, Y. (2019). Internet of Things Meets Brain–Computer Interface: A Unified Deep Learning Framework for Enabling Human-Thing Cognitive Interactivity. IEEE Internet of Things Journal, 6(2), 2084–2092. https://doi.org/10.1109/JIOT.2018.2877786

INVESTIGATION OF THE EFFECTS OF COATED AND UNCOATED DRILLS ON HOLE QUALITY IN DRILLING OF STEEL USED IN MOLDING

Senai YALÇINKAYA[1], Alper ÖNER[2], Buğra BAŞIHOŞ[3]

Absract: In the operations of machining drilling has a considerable status. Nowadays the necessity of working with much narrower tolerances and precision has further increased the importance of drilling processes. Changing cutting forces, temperature values, and runout deflection that may occur in the drill during the drilling process significantly have affects the hole quality and measurement accuracy. In this study, surface quality, change in hole diameter and deviation from circularity, which have an important place in the drilling operation of DIN 2738 steel, which is used in manufacturing and especially in molding, were investigated experimentally. Nine types of HSS drills as uncoated, TiN and TiAlN coated with a diameter of 10, 12 and 14 mm has been used. The experiments were carried out at 10, 15 and 20 m/min cutting speeds in a CNC vertical machining center under dry drilling conditions as holes with a depth of 20 mm. The results were obtained by measuring the three parameters for each drilled holes: a) Surface roughness b) Deviation from diameter c) Deviation from circularity and interpreted by comparing them separately for each feature. As a result of the experiments, coated drills compared to uncoated drills; have shown positive results for all evaluation criteria.

1 Marmara University, Faculty of Technology Mechanical Engineering, Istanbul / Turkey, e-mail: syalcinkaya@marmara.edu.tr, Orcid No: 0000-0001-7076-7766

2 Marmara University, Institute of Pure and Applied Science, Istanbul / Turkey, e-mail: muratalper308@hotmail.com, Orcid No: 0000-0003-3381-7474

3 Bilen A.Ş. company R&D Engineer, Düzce / Turkey

Keywords: Drilling, TiN Coated Drill, TiAlN Coated Drill, Circularity in Drilling, Diameter Deviation in Drilling, Surface Roughness in Drilling

INTRODUCTION and THEORETICAL FRAMEWORK

Drilling, which is one of the machining methods, is used to obtain many industrial products. Drilling with drills is common and well known metal removal operations, accounting for nearly one-third of all metal machining. In Figure 1, the ratios of the processes according to the number of processes in the machining processes are given as percentages (Tonshoff et al., 1994).

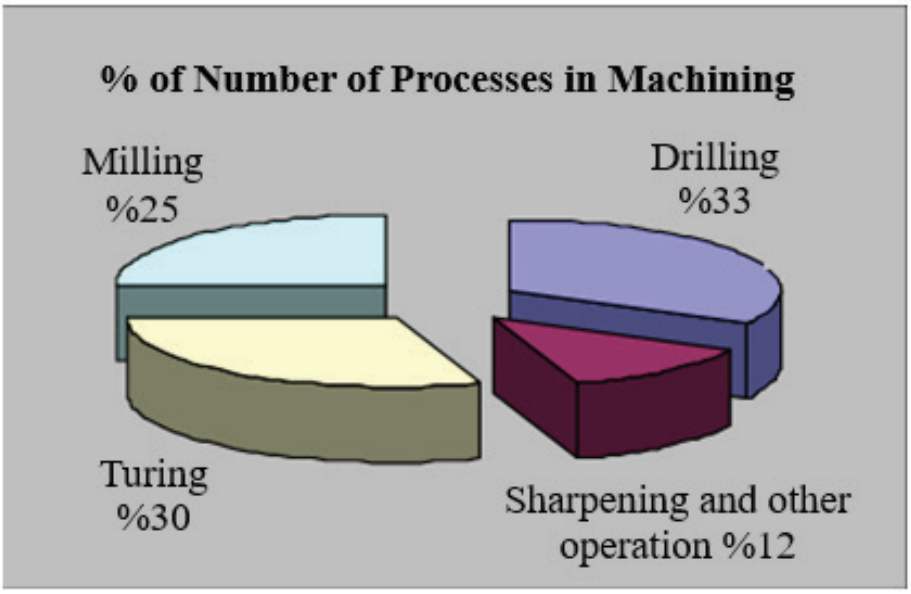

Figure 1. The Percentages of the Processes in the Machining According to the Number of Processes

When viewed in terms of consumed time in machining operations with metal removal, as shown in Figure 2, drilling constitutes a quarter of these operations (Tonshoff et al., 1994).

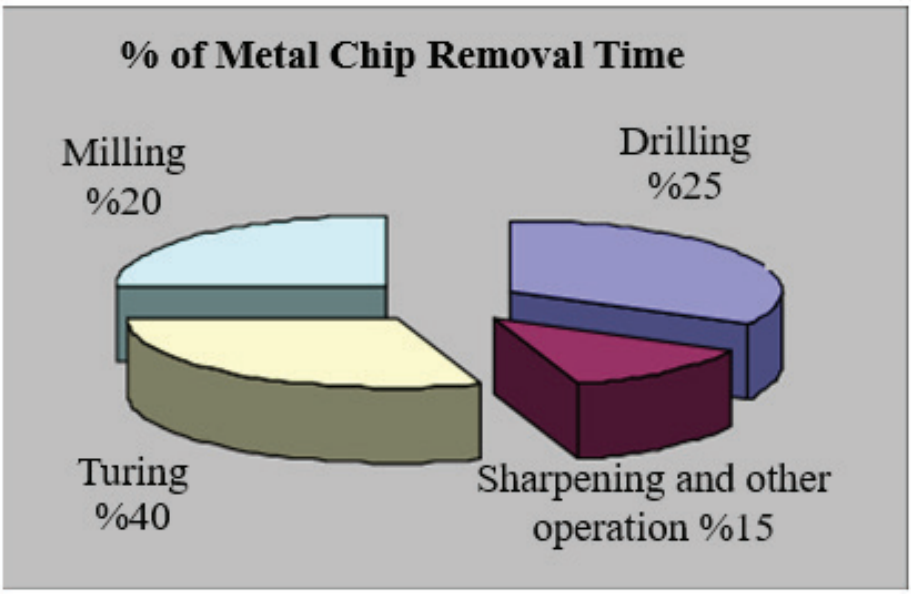

Figure 2. The Percentages of the Processes in the Machining According to the Time Spent

Drilling is carried out by removing chips from a workpiece in conventional drill benches and advanced CNC machines with the appropriate drill. Cutting tool and workpiece costs are the most important cost items in machining. Therefore, it is necessary to consider these factors in order to reduce production costs and make the product cheaper. For this reason, improvements made in drilling, which is a part of machining, are important in terms of reducing manufacturing costs and creating a competitive opportunity (Arafat, 2009). As in the research on all types of machining, in the research on the parts drilled with a drill, facts such as material properties, type and material properties of the cutting tool, coating properties of the cutting tool, depth of cut, feed rate, number of revolutions have been of great importance (Karasoy, 2009). The target of hole drilling production is to perform the processing task with the least technical and economic cost and the highest safety for the worker (Seker, 2006). In hole drilling applications in the manufacturing sector, there are some problems such as changes in cutting forces, tool wear, temperature

changes, deviation from circularity, axial misalignment and deterioration of surface quality. Such problems in machining high-quality holes require secondary operations such as reaming. Ensuring that the hole quality and dimensional accuracy remain within the desired tolerance limits without the need for secondary operations helps to reduce the machining cost by preventing time and production loss. Various types of research have been carried out in literature in order to prevent such negativities encountered in hole drilling operations, to produce solutions and to provide better processing conditions.

Using AI 7075 and AISI 1050 steal materials and inclination angles 60 and 80, have been analysed the heat-affected zones during machining in vertical machining at different cutting and table feed speeds by infrared imaging methods. It has been observed that ascending cutting speed and feed rate caused to the increasing of temperature at the tool and chip interfaces. However it has been determined, the relationship with the tool tilt angle is not distinctive (Dinç et al, 2008).

Testing of coating performance of DLC (Diamond-like carbon) coated on aluminium, brass and 7% Si included drills in the drilling operations were performed on by using uncoated and DLC coated drills. Shear forces of drills have been determined by using the dynamometer. It has been seen the mean of the axial forces of the coated one was 2.5 times lower on mean than the uncoated one (Zaquini, 2006).

On three different composite materials (CYCOM 7701, CYCOM 7714 and ISOVAL11), with 5 mm, 10 mm and 15 mm diameters, uncoated HSS, TiN and Carbide coated drills at three different cutting speeds (125, 250, 315 rpm), feeds values as 0.056, 0.112 and 0.16 (mm / rev) experiments were carried out. Scanning Electron Microscope has been used to determine the surface roughness. Surface roughness of the machined surface ascended when increasing rotation and feed rate.

Better outcomes were obtained in terms of surface roughness in small diameter drills, it was determined that the surface roughness ascended in HSS drills, but descended in TiN coated and carbide drills. Better machined surface was obtained when carbide drills were used (Canpolat, 2008).

The drillability of Inconel 718 was investigated in dry cutting conditions with three different feeds (0.05, 0.075 and 0.1 mm/dev.), four cutting speeds (10, 12.5, 15 and 17.5 m/min) by using three types of 5 mm diameters carbide drills (Uncoated, TiN coated and TiAlN coated). Drilling quality data have been collected and in the light of these measured data, the best performance was obtained from uncoated carbide drills, while TiAlN coated carbide drills were the worst one. It has been found out the hole quality and performance of drills decrease at high cutting speed and feed combinations (Kıvak, 2007).

Hole enlargement was performed using uncoated and TiN coated HSS drills on C45 steel material using bench speed (550 rpm), cutting speed (22.4 m / min) and tool feed (0.13 mm / rev). The macro structures of the wear in the drill cutting edges were examined by taking photographs with the help of SEM. It was observed that the wear of TiN-coated drills is less than that of uncoated drills (Inçal, 2007).

HSS, TiN-coated HSS and solid carbide drills with a diameter of 5 mm and three different tip angles (900, 1180, 1300) were used in the drilling of a 17% SiC particle-reinforced Al 2124 alloy plate. Drilling processes were carried out with 0.08 and 0.16 mm/rev feed rates (and two different revolutions (260, 1330 rpm) to the alloy plate. As a result of the experiments, as the tip angles of HSS and TiN-coated HSS drills increased, the subsurface damage area also increased. However, as the tip angle of the solid carbide drill increases, the damaged area decreases (Tosun and Muratoğlu, 2004).

In High Speed Steel tools, cutting egde effect on tool wear and tool life were investigated by using Böhler mold steel material (M236). For the moment and resultant force measurement, Kistler 9124A dynamometer was connected to CNC vertical machining center and measurements were made. Experimental processes were carried out using 1200 rpm and different feed rates (120, 140, 150, 160, 170, 180 mm/min). Observations from SEM and poly-meters have shown that it can produce various size radius of cutting-edge for coated High Speed Steel drills. As a result of the experiments, the best drills life obtained by using between 24 and 27 μm edge radius for the cutting conditions (Cheung et al, 2008).

Coating of drill bits makes them harder, lubricated, sharp and high temperature resistant than uncoated drill bits. The drill bits after coating have become long-lasting, the higher quality cutting ability, and more durable.

The life of the coated and uncoated drill bits is theoretically calculated using the Taylor tool life equation and compared with the experimental work, given in figure 3 (Puneeth and Smitha, 2017).

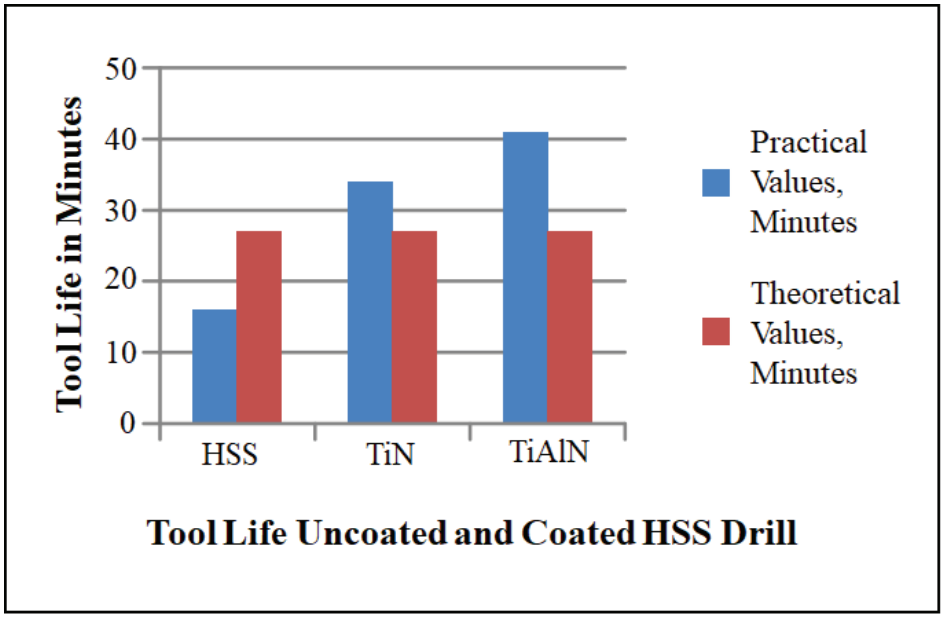

Figure 3. Comparison Between Practical and Theoretical Tool Life in Minutes

By machining uncoated HSS and Titanium Nitride, Titanium Aluminum Nitride coated HSS drill bits EN8 material under dry machining conditions, parameters such as tool life and cutting forces were found experimentally. The number of holes drilled by Uncoated, TiN-coated and TiAlN-coated drill bits is given in figure 4 (Puneeth and Smitha, 2017).

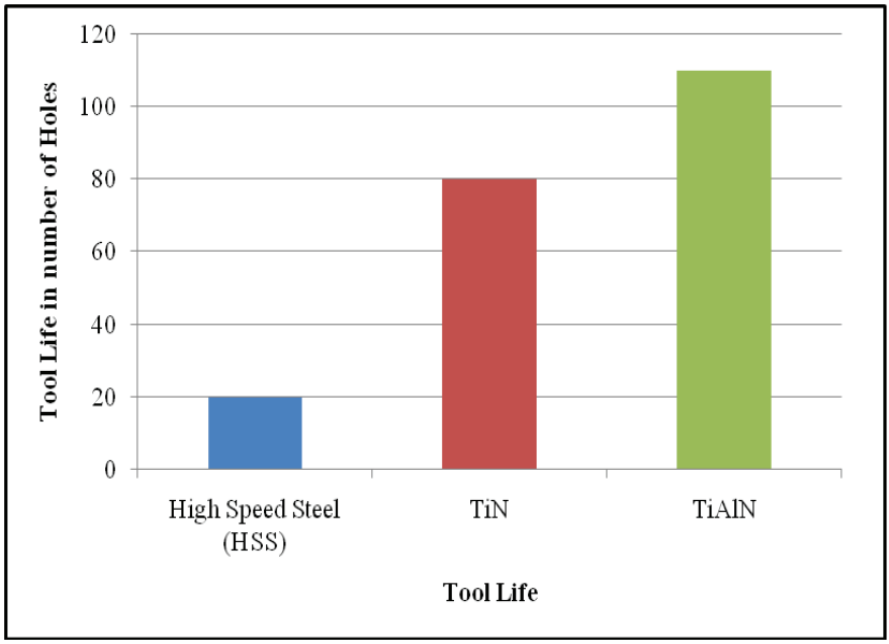

Figure 4. Tool Life for Uncoated and Coated HSS drills in Number of Holes

The deviations from the diameter and surface qualities of the holes produced by the application of the drills made of three types of coated and uncoated HSS materials, TiN, AlCrN, TiAlN, on the plate made of AA5052 material under dry drilling conditions were investigated. Field Emission Scanning Electron Microscopy (FESEM) and Energy Dispersive Spectroscopy (EDS) were used for this work.

As a result of the evaluation of the data obtained from these devices, the TiAlN coated HSS drill showed less tool wear and excellent surface quality on the workpiece. The TiN coated HSS drill ranked second and also showed worse surface quality characteristics than the TiAlN coating. AlCrN coatings ranked third after TiAlN and TiN coatings.

For diameter deviation (cylindricality), experiments were carried out using three different diameter drills and uncoated and TiN, TiAlN and AlCrN coated drills under three different feed rates. Errors accord-

ing to the holes were handled and it was observed that the best drill with less cylindrical error was the TiAlN coated drill.

As a result, it has been determined that the use of TiAlN coating is more suitable for machining AA5052 material than other drills used in the experiments, since it creates good surface quality and shows less wear (Haja Syeddu Masooth and Jayakumar, 2020).

Drilling operations were carried out using 11 different revolutions and feed rates with high-wear resistance and toughness AISI D2 (DIN 2379) steel material by using three different drill bits with Ø8 mm diameter as HSS, TiN and TiAlN coating drill bits on the CNC vertical machining machine. The effects on drill bit wear have determined by increasing the rotation and feed rate regularly during drilling and at the same time feed rate, rotation and cutting speed were recorded. The wear results of the tooltips have been also examined with an optical microscope and compared. The surface roughness of the holes have been measured using a surface measuring device. It has been observed that the TiAlN coating drill bits are more durable than the HSS and TiN-coated drill bits and much smoother surface roughness is obtained. It has been proven that the most wear-resistant bit is the HSS drill bit (Kocabıçak and Yalçınkaya, 2020).

MATERIAL, TOOLS and METHOD

This study, it is aimed to find the optimum drilling conditions required for the drilling of the plate which made DIN 2738 material by using un-coated, TiN-coated and TiAlN-coated HSS drills depending on different cutting parameters and to improve the hole quality. Materials, equipment, machining parameters, machine tools, etc. used in the experiments have een discussed below.

Materials Used in the Experiment

Steel Plate: The chemical composition of DIN 2738 steel material, which is the material of the steel plate used in the experiment, is shown in Table 1

Table 1. DIN 2738 Steel Material Contents

Element	C	Mn	Cr	Ni	Mo
%	0.42	1.5	1.95	1.1	0.2

Drills: Coated and uncoated HSS (DIN 338) drills have used which made by Makina Takım Endüstri A.Ş. The coatings were made with PVD (Physical Evaporation Method) on DIN 338 HSS RN 118° had grinded drills using TiAlN and TiN materials. The DIN 338 HSS RN 118° had grinded drill have chosen as it was produced by grinding completely, providing completeness to the extent thanks to its geometric balances and precision tip sharpening. One of the drill used in experiment shown in figure 5.

Figure 5. Makina Takım Endüstri A.Ş. DIN 338 HSS RN 118° Grinded Drill

Experimental plan

Due to experienced rule which was hole diameter is three times or less than three times from drilling length of hole, drilling length has defined as 20mm. (Michael et al, 1989). 27 experiments have conducted using a separate drill in every experiment. 9 of these experiments were done with ø10, ø12 and ø14 uncoated drills, 9 with ø10, ø12 and ø14 Tin coated drills and 9 with ø10, ø12 and ø14 TiAlN coated drills. All these hole position and plan have shown in Figure 6.

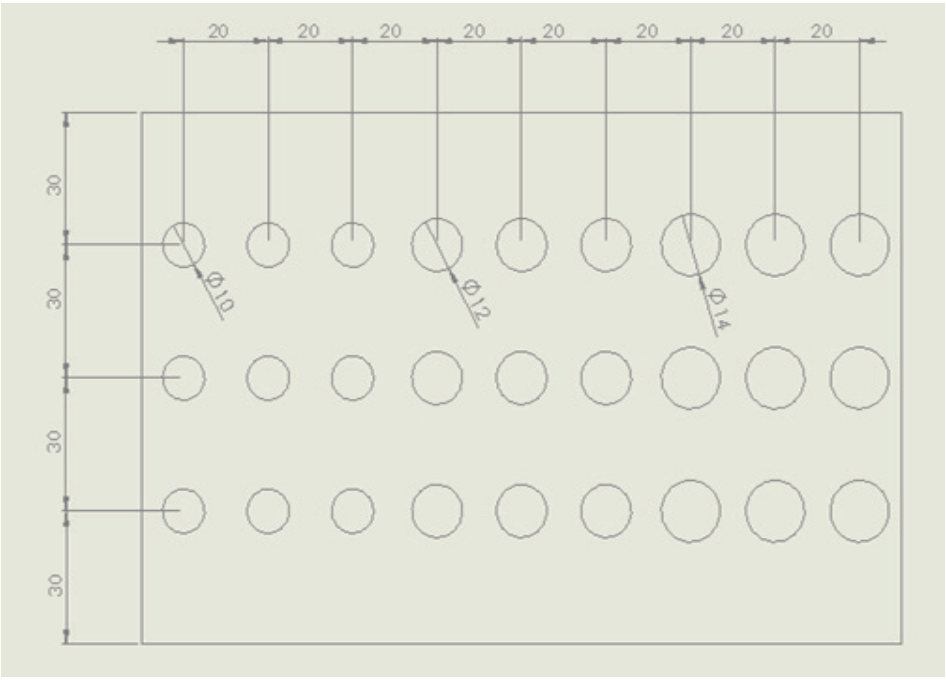

Figure 6. Plan of Hole Positions on Steel Plate for Experiment

Machine, Tool Used in the Experiment

Tool properties and cutting parameters used in operations are shown in Table 2

Table 2. Tool Properties and Cutting Parameters used in Drilling Operations

Drill Type	HSS high-speed steel, N, tip angle 118°, diameter tolerance h8, right-hand cutting
Standard	DIN 338
Drill Geometry	Ø10-12-14 mm, tip angle 118°, helix angle 30
Cutting Speeds	20, 30, 40 m/min
Feed Rate	0.1 mm/rev

For the determination of the drilling parameters, the values recommended in the drilling tool catalogue were taken into consideration as a result of the preliminary experiments.

The JOHNFORD VMC–550 CNC milling machine available at Marmara University, Faculty of Technology, and CNC Workshop was used in experiment.

CNC machine; It is a Vertical Machining Center with a programmable FANUC control unit capable of linear and circular interpolation in three axes. The technical specifications of this machine are shown in Table 3

Table 3. Johnford VMC–550 CNC Vertical Machining Center Features

Bench Power	5 KW
Maximum Speed	8000 rpm/min
Dimensions (x, y, z axes)	600,500,600 mm
Measure precision	0.001 mm
Operation System	Fanuc

Machine Used in Measurement

Today, in parallel with the developing technology, high precision expectations from production have increased. The same high precision expectations are in question for elements containing holes on a product to be produced. The most important features that determine the hole quality are;

- Measurement accuracy,
- Circularity,
- Deviation from the axis (cylindricality) and
- Drilled surface quality.

It is common for holes to be "reamed" as a secondary operation to achieve these properties. However, today, with modern machine tools and modern drilling tools, it is possible to obtain the desired hole quality without an additional process and this application, which brings a significant cost. Correctly selected cutting parameters are majority factors in obtaining the desired hole quality.

Determination of appropriate parameters are important for hole quality. For this purpose,

- Hole diameter measurements

- Deviation from circularity (ovality and cylindricality) measurements and
- Average surface roughness (Ra) measurements of the machined surfaces were made.

If larger or smaller diameter holes are produced than the required diameter, it is usually because the drill is off-centre. Other reasons; the machine spindle is not suitable, the feed rate is too high or the clamping rigidity is insufficient. If the hole is not symmetrical, the source of the problem is often insufficient rigidity in the machine or clamping. It is also possible that the cutting values are incorrect for the material being machined. Poor surface quality is often the result of vibrations due to poor rigidity in the clamping of the machine. The drill may be too long, attached to a poor quality tool holder, or have poor tool position. Cutting values may not be correct for the application or initial input may be made on poor quality surfaces. The coolant supply may be insufficient or chip control may not be good enough when chip evacuation is irregular.

A coordinate measuring device (CMM) was used to measure the hole diameter and deviation from circularity in the holes obtained after the experiments to be carried out by taking measures to eliminate all these negativities.

For determination of surface quality, the Mahr Perthometer M1 device was used to measure the average surface roughness (Ra). The technical specifications of Mahr Perthometer M1 device this are shown in Table 4.

Table 4. Technical Specifications of the Mahr Perthometer M1 Surface Roughness Meter

Model	M1
Scan Speed	0.5 m/sn
Scan	0.75mN
Needle tip half	2μm
Measurement	100-150 μm
Profile	12mm

Filter	Gaussian
Sampling	0.25 – 0.8 – 2.5 mm
Measuring	1.75 – 5.6 – 17.5 mm
Measurable	Ra, Rz ,Rmax

The data obtained in the experimental studies will be presented and discussed in the findings and discussion section.

FINDINGS and DISCUSSION

Data Obtained from Experiments

Twenty-seven experiments were carried out according to the parameters and experiment plan specified in the previous sections. As an "output" as a result of experimental studies in which drill type, diameter and cutting parameters were evaluated as "input"; To determine the hole quality, the completeness of the hole size (deviation from the diameter), the circularity of the resulting hole (ovality or deviation from circularity) and the surface quality of the drilled hole (average surface roughness, Ra) have evaluated. All these data and the results obtained are shown in Table 4.

Table 5. Results from Drilling Experiments with Various Drills

Test No	Cutting Tool	Feed (mm/rev)	Cutting Speed (m/min)	Average Surface Roughness Ra(μm)	Deviation from Diameter (mm/m)	Deviation from Circularity (mm))
1	Uncoated Ø 10	0,1	10	2,307	0,122	0,052
2	Uncoated Ø 10	0,1	15	2,262	0,126	0,071
3	Uncoated Ø 10	0,1	20	2,227	0,131	0,086
4	TiN Coated Ø 10	0,1	10	2,148	0,063	0,061

5	TiN Coated Ø 10	0,1	15	2,093	0,074	0,079
6	TiN Coated Ø 10	0,1	20	2,013	0,078	0,095
7	TiAlN Coated Ø10	0,1	10	2,062	0,049	0,069
8	TiAlN Coated Ø 10	0,1	15	2,024	0,051	0,082
9	TiAlN Coated Ø 10	0,1	20	1,938	0,084	0,113
10	Uncoated Ø 12	0,1	10	2,503	0,125	0,067
11	Uncoated Ø 12	0,1	15	2,445	0,151	0,084
12	Uncoated Ø 12	0,1	20	2,355	0,191	0,106
13	TiN Coated Ø 12	0,1	10	2,214	0,063	0,059
14	TiN Coated Ø 12	0,1	15	2,188	0,077	0,078
15	TiN Coated Ø 12	0,1	20	2,055	0,092	0,099
16	TiAlN Coated Ø 12	0,1	10	2,124	0,058	0,056
17	TiAlN Coated Ø 12	0,1	15	2,072	0,063	0,073
18	TiAlN Coated Ø 12	0,1	20	2,026	0,087	0,098

19	Uncoated Ø 14	0,1	10	2,624	0,118	0,082
20	Uncoated Ø 14	0,1	15	2,531	0,158	0,091
21	Uncoated Ø 14	0,1	20	2,404	0,181	0,118
22	TiN Coated Ø 14	0,1	10	2,475	0,074	0,074
23	TiN Coated Ø 14	0,1	15	2,351	0,086	0,089
24	TiN Coated Ø 14	0,1	20	2,227	0,095	0,098
25	TiAlN Coated Ø 14	0,1	10	2,418	0,061	0,062
26	TiAlN Coated Ø 14	0,1	15	2,356	0,077	0,092
27	TiAlN Coated Ø 14	0,1	20	2,163	0,085	0,114

Surface Quality

Experimental data have been used to obtain graphs with parameters for cutting speed vs. average surface roughness values (Ra) for 3 different drills. First graph is for uncoated drills, the second graph is for TiN-coated drills and the last graph is for TiAlN-coated drills.

The first surface roughness graph is given in graph 1 for uncoated drills. When the graph 1 is examined, Surface roughness decreases depending on the increasing cutting speed. As the diameters increased, the surface roughness also increased.

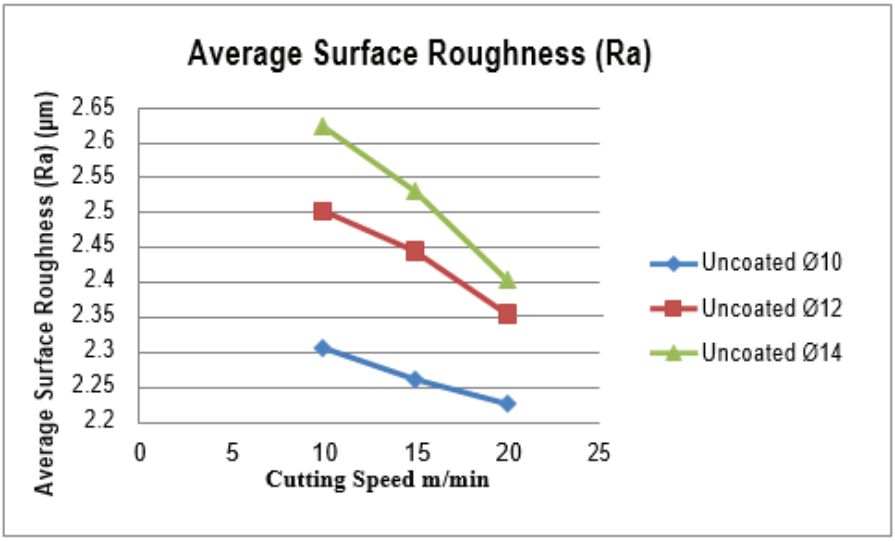

Graph 1. Surface Roughness Graph (Ra) for Uncoated Drills

The second surface roughness graph is given in graph 2 for TiN coated drills. When the graph 2 is examined, surface roughness decreases depending on the increasing cutting speed. As the diameters increased, the surface roughness also increased.

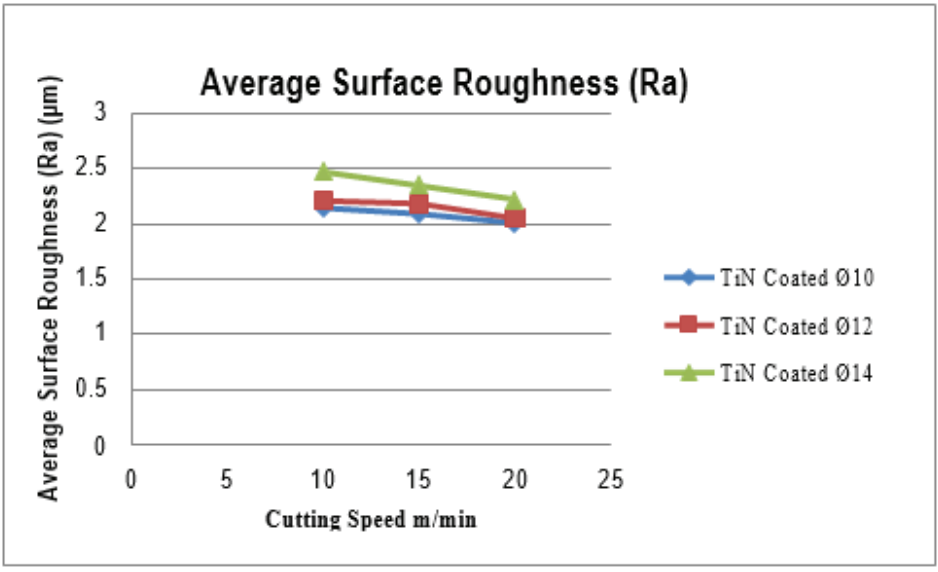

 Graph 2. Surface Roughness Graph (Ra) for TiN Coated Drills

The third surface roughness graph is given in graph 3 for TiAlN coated drills. When the graph 3 is examined, surface roughness decreases depending on the increasing cutting speed. As the diameters increased, the surface roughness also increased.

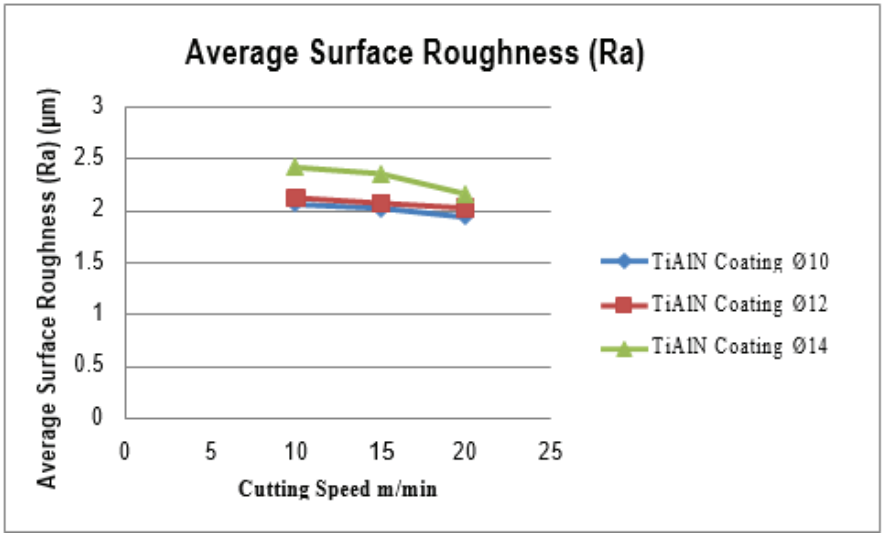

Graph 3. Surface Roughness Graph (Ra) for TiAlN Coated Drills

From graphs 1, 2 and 3, a higher surface roughness was seen in uncoated Ø 14 (2.624 µm), and a lower surface roughness was seen in TiAlN coated Ø 10 (1.938 µm).

The most important result that can be said for coated tools is that better surface qualities are obtained when compared to uncoated tools. This shows that the coating material not only contributes to the wear resistance of the tool, but also improves the surface quality. This is because the coating material also facilitates the flow of chips, as it has a low coefficient of friction.

It has been determined experimentally that the surface roughness values that can be obtained in drilling with a drill should be between 1.6 (N7) and 3.2 (N8). The surface roughness values of 1.938 µm and 2.624 µm, which were determined in 27 experiments with three types of drills, remained within the limits given above and also confirmed experimental studies.

Deviation from Diameter

The main objective is to obtain a hole of the desired diameter within certain tolerances in drilling operations with a drill. The diameter obtained in drilled holes often occurs larger than nominal diameter. The resulting difference must be within the tolerance limits. In the drilling process; the type of application in which the drill is rotating, workpiece is fixed or vice versa, the stability of the clamping tools used, the rigidity of the machine tool, the correct tool geometry of the cutting edges of the drill affect the accuracy of the hole to be obtained. Moreover; it is also important that parameters are selected correctly. In this study, it was investigated how the parameters such as feed, presence of coating, cutting speed and drill diameter impact the exactness of measurement of the holes acquired since the experiments were carried out on the condition that the first external factors remained the same in all experiments. Depending on these parameters, the changes in the diameters of the holes obtained from the experimental studies are shown in graphs in 4, 5 and 6. Deviation from diameter for uncoated drills is shown in graph 4.

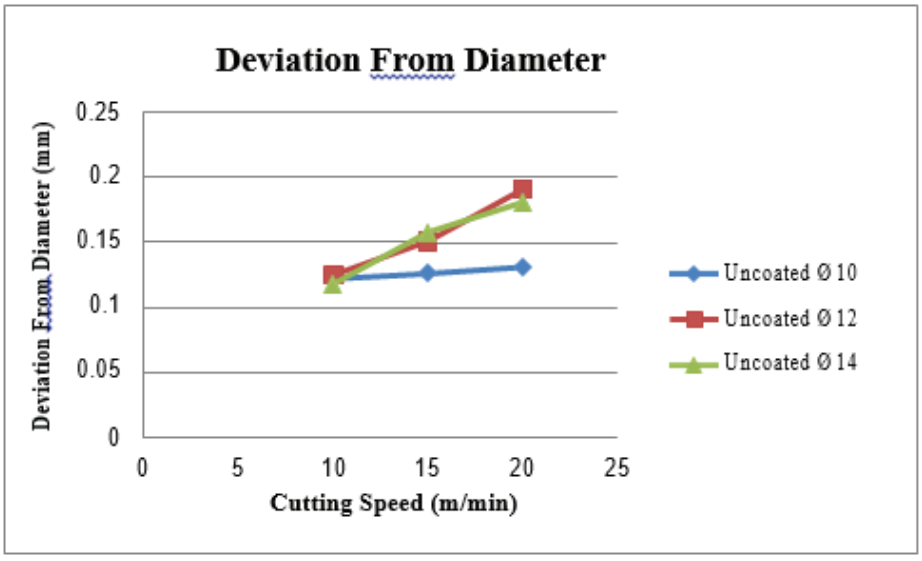

Graph 4. Deviation from Diameter (mm) for Uncoated Drills

When the graph 4 is examined, achieved bore diameter is greater than the nominal diameter in all states. In addition, as the drill diameter increases or the cutting speed increases, the hole diameter increases more than the nominal diameter. In the holes obtained under the same conditions, the deviations from the diameter in the holes drilled with coated drills are less than the holes drilled with uncoated drills.

Second deviations from the diameter's graph is TiN coated drills graph and shown in graph 5.

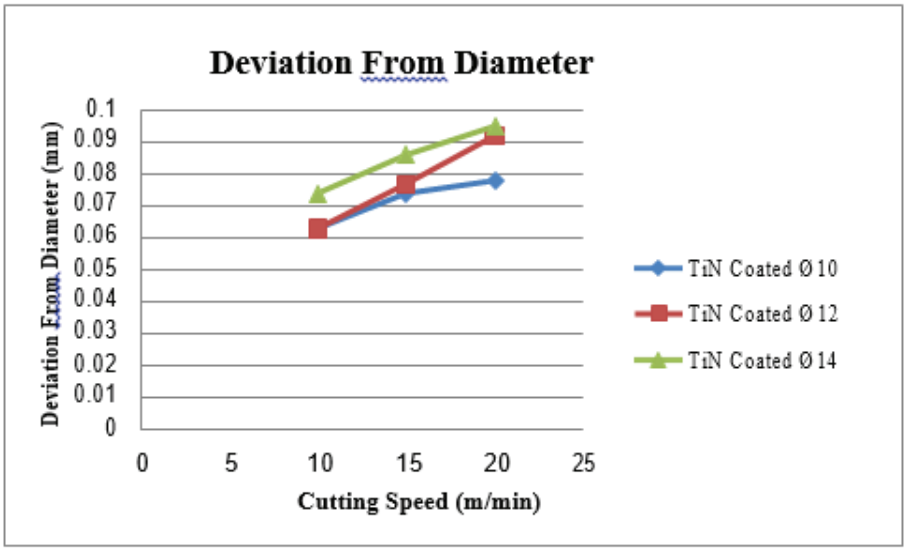

Graph 5. Deviation from Diameter (mm) for TiN Coated Drills

Hole diameter is obtained in graph 5 greater than the nominal diameter in all conditions. As the drill diameter increases or the cutting speed increases, the hole diameter increases more than the nominal diameter. In the holes obtained under the same conditions, the deviations from the diameter in the holes drilled with coated drills are less than the holes drilled with uncoated drills.

Third deviations from the diameter's graph is TiAlN coated drill graph and shown in graph 6.

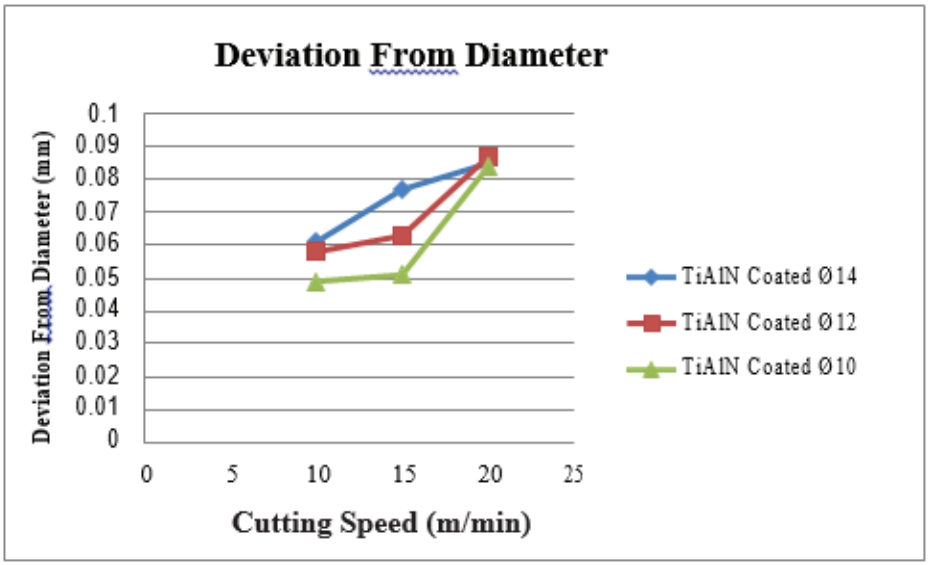

Graph 6. Deviation from Diameter (mm) for TiAlN Coated Drills

Hole diameter is obtained in graph 6 greater than the nominal diameter in all conditions. As the drill diameter increases or the cutting speed increases, the hole diameter increases more than the nominal diameter. In the holes obtained under the same conditions, the deviations from the diameter in the holes drilled with coated drills are less than the holes drilled with uncoated drills.

Deviation from Circularity (Ovality)

In order to determine the parameters that affect the deviation of the drilled holes from circularity (ovality), graph 7 shows the change of ovality as drill diameter and cutting speed in the light of ovality measurements made in the holes obtained from uncoated drills.

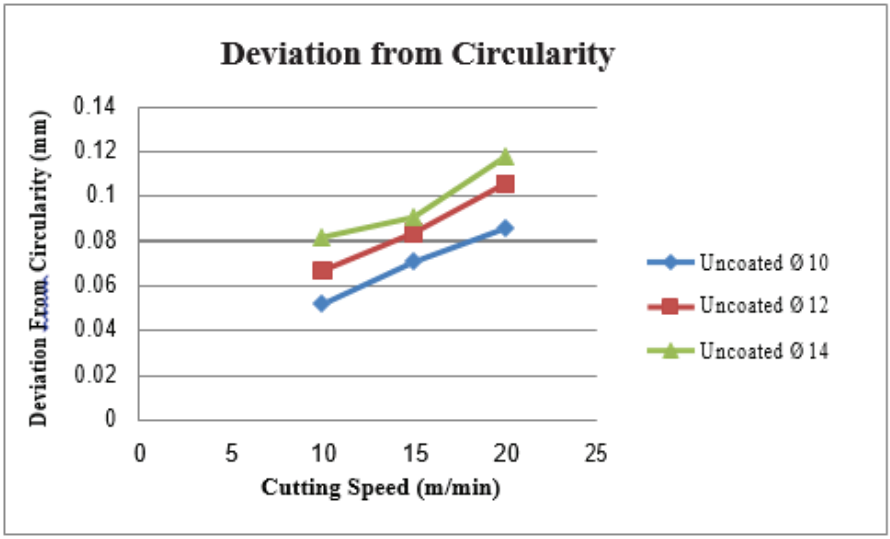

Graph 7. Deviation from Circularity (mm) for Uncoated Drills

The second deviation from circularity graph is given in graph 8 for TiN coated drills. When the graph 2 is examined, deviation from circularity increases depending on the increasing cutting speed. As the diameters increased, the deviation from circularity also increased.

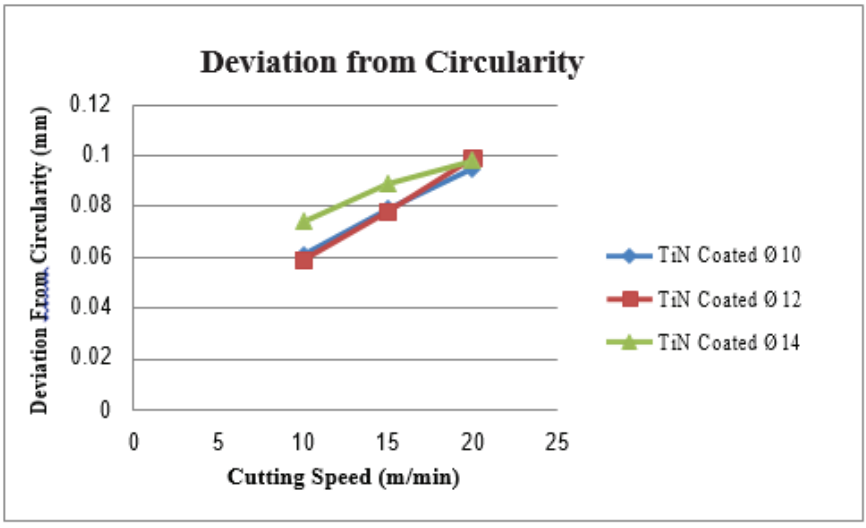

Graph 8. Deviation from Circularity (mm) for TiN Coated Drills

The third deviation from circularity graph is given in graph 9 for TiAlN coated drills. When the graph 2 is examined, deviation from circularity increases depending on the increasing cutting speed. As the diameters increased, the deviation from circularity also increased

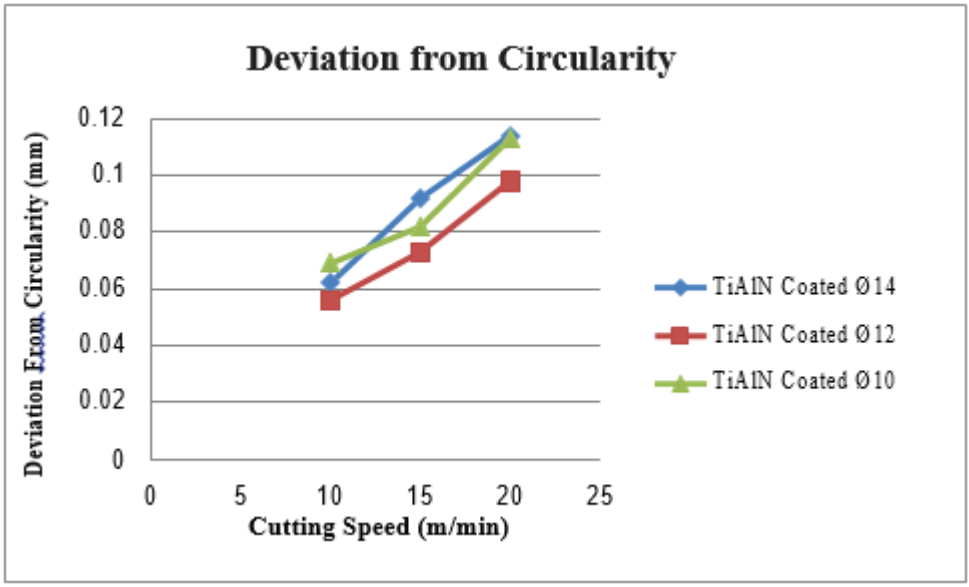

Graph 9. Deviation from Circularity (mm) for TiAlN Coated Drills

When the 7, 8 and 9 graphs are examined, it is observed that the effectiveness of cutting speed is more active on the ovality than the diameter and coating. The ovality values vary between 0.052 mm and 0.118 mm were obtained. In terms of uncoated, TiN coated and TiAlN coatings, the ovality values were close to each other for each diameter. In all three, it was observed that deviation from circularity increased only with cutting speed. Therefore, it may be recommended to choose lower values of cutting speed within the recommended range of cutting speed.

RESULT and RECOMMENDATION

The conclusions reached by the evaluation of the findings obtained as a result of the experiments;

- Due to increasing cutting speed the average surface roughness values obtained decreased within also three diameters.
- In terms of surface quality, TiAlN and TiN coated drills gave better results than uncoated drills. If the aim is to obtain a good surface quality, a coated drill should be used.
- As the drill diameters increase, the surface roughness increases.
- Considering the deviation values from the dimension, achieved bore diameter is greater than the nominal diameter in all states and the deviation from the nominal diameter is generally; It is seen that it increases as the drill diameter increases and the cutting speed increases, and vice versa, with the application of coating, it decreases compared to the holes obtained under the same conditions with uncoated tools.
- It has been observed that the amount of deviation from the diameter obtained with the coated tools is lower than the amount of deviation from the diameter obtained from the uncoated tools, and the TiAlN coating gives a lower diameter deviation than the TiN coating.
- As the drill diameters increased, diameter deviation also increased.
- Increasing cutting speed negatively affected the diameter deviation. Also for all other parameters the amount of deviation from the diameter increased
- It is recommended to use lower cutting speeds and coated tooling, within the recommended limits, for dimensional accuracy depending on the nominal diameter in the resulting hole diameters.
- It has been determined that increasing speeds of cutting parameters have increased the deviation from circularity (ovality) and they are more effective on ovality than diameter and coating.
- The cutting speed is more effective on the geometric integrity of the drilled holes than the coating application and diameter. For this reason, it is suggested to select the cutting speed from low value within the recommended range in applications where circularity is important.

Prospective recommendations based on the results of this study;

- A study can be performed using different workpiece materials under the same conditions for the verification of this study.
- Since it is observed that the coating has a positive effect on the outputs, the effects of different coating applications can be investigated comparatively. The work can be enriched by increasing the number of selected drill diameters.
- Studies including temperature measurement can be done to measure the temperature generated during drilling and to determine its effect on the outputs.
- In the above-mentioned styles, similar studies can be investigated comparatively in terms of performance between unused (new) drills and sharpened drills (taking into account the number and quality of sharpening).

REFERENCES

Arafat, M. (2009). CNC Delme İşleminde Delme Parametrelerinin Yüzey Pürüzlülüğü Açısından Optimizasyonu, *Yüksek Lisans Tezi*, Erciyes Üniversitesi Fen Bilimleri Enstitüsü, Kayseri, Türkiye.

Canpolat, N. (2008). Değişik Takviyeli Kompozit Malzemenin Matkapla Delinebilirliğinin ve Yüzey Pürüzlülüğünün Araştırılması", *Yüksek Lisans Tezi,* Fırat Üniversitesi Fen Bilimleri Enstitüsü, Elazığ, Türkiye.

Cheung, F.Y., Zhou, Z.F., Gedam, A., Li, K.Y. (2008). Cutting Edge Preparation Using Magnetic Polishing and Its Influence on The Performance of High Speed Steel Drills, *Journal of Materials Processing Technology, 208*: 196204.

Dinç, C., Lazoglu, I., Serpenguzel, A. (2008). Analysis of Thermal Fields in Orthogonal Machining with Infrared Imaging, *Journal of Materials Processing Technology, 198*: 147-154

Haja Syeddu Masooth, P., Jayakumar, V. (2020). Experimental investigation on surface finish of drilled hole by TiAlN, TiN, AlCrN coated HSS drill under dry conditions, *Materials Today: Proceedings,* Volume 22, Part 3,

Inçal, E. (2007). PVD Yöntemi İle Kaplanan HSS Takım Çeliklerinin Karakterizasyonu ve Aşınma Dayanımının İncelenmesi", *Yüksek Lisans Tezi*, Yıldız Teknik Üniversitesi Fen Bilimleri Enstitüsü, İstanbul, Türkiye.

Karasoy, T. (2009). Matkapla Delmedeki Sıcaklık Dağılımının Tahmini, Yüksek *Lisans Tezi*, Gebze Yüksek Teknoloji Enstitüsü Mühendislik ve Fen Bilimleri Enstitüsü, Gebze,

Kıvak, T. (2007). Inconel 718'in Delinebilirliğinin Araştırılması, *Yüksek Lisans Tezi*, Gazi Üniversitesi Fen Bilimleri Enstitüsü, Ankara, Türkiye.

Kocabıcak, A. C., Yalçınkaya, S. (2020). HSS, TiN ve TiAlN Kaplamali Matkap Takimlari Kullanilarak AISI D2 Çeliği Üzerine Delik Delme İşlemleri Uygulamasi. Mühendislik Alaninda Teknolojik Gelişmeler, İstanbul: *Güven Plus Grup A.Ş. Yayınları*: 45/2020, 2020, pp.384-407

Michael, F., Kahles, J.F., Koster W.P. (1989). ASM Handbook: Surface Finish and Surface Integrity, *American Society for Metals, 3*: 468-475.

Puneeth, H. V., Smitha, B. S. (2017). Studies on Tool Life and Cutting forces for drilling operation using Uncoated and coated HSS tool. *International Research Journal of Engineering and Technology (IRJET)* 0056 Volume: 04 Issue: 06:1949-1954, 2017.

Seker, U. (2006). Talaş Kaldırma Prensipleri Ders Notları, Ankara, Türkiye.

Tonshoff, H.L., Spintig, W., Konig, W., Neises, A. (1994). Machining of Holes Developments in Drilling Technology, *Annals of the CIRP, 43* (2): 551-560

Tosun, G., Muratoğlu, M. (2004). The Drilling of an Al/SiCp Metal-Matrix Composites. Part I: Microstructure, *Composites Science and Technology, 64*: 299–308 DOI:10.1016/S0266-3538(03)00290-2

Zaquini, L. (2006). Expert System for the Definition of the Cutting Parameters and Machining Strategies, *CaravelCut*, Switzerland.

THE REVIEW OF LASER CLADDING METHOD AND PARAMETERS

İbrahim KARAAĞAÇ[1], Mehmet Okan KABAKÇI[2], Mehmet Yasin DEMİREL[3]

Abstract: Nowadays, significant improvements have been made in the field of engineering with laser technology, and innovative processes have begun to be used and are still be develop and apply in different fields. Manufacturing methods such as cutting and marking using laser technology are widely used in various industrial areas such as defense, space, aviation, and automotive. One of these manufacturing methods is laser cladding. The laser cladding method, which is an additive manufacturing method; is becoming increasingly common in industrial applications because it provides significant benefits such as complex geometries and difficult and time-consuming parts to be produced in a short time, rapid production of prototype products, and repair of features that have lost volume due to damage. In this study, laser technology, laser cladding method, process parameters, application types of the process, problems encountered during the application, and solution suggestions were compiled.

Keywords: Laser Cladding, Laser, Additive Manufacturing

INTRODUCTION

The laser cladding method; is an interdisciplinary technology that uses laser technology, powder metallurgy, computer-aided design and manufacturing (CAD/CAM), robotics technology, sensors, and control

1 Gazi University, Faculty of Technology, Ankara / Turkey, e-mail:ibrahimkaraagac@gazi.edu.tr, Orcid No: 0000-0001-6727-3650

2 Gazi University, Faculty of Technology, Ankara / Turkey, e-mail:mokabakci@gazi.edu.tr, Orcid No: 0000-0003-0086-9294

3 TUSAŞ Turk Aerospace Industries, Ankara / Turkey, e-mail: mehmetyasin.demirel@tai.com.tr, Orcid No: 0000-0002-4244-8562

engineering. L The laser cladding process is a surface improvement process in which a laser beam is used as a heat source and a metal layer is formed on the surface of a fixed or moving part. The process is generally; used to create a protective coating layer to increase the functionality of the product or part, as well as to repair damaged or worn surfaces. The mechanical properties of the parts such as corrosion resistance, wear resistance, and impact resistance can be increased using the laser cladding method. In addition to producing geometries that are difficult to obtain with traditional methods, it also provides the opportunity to continue using by repairing parts that are damaged during operation (Brandt, 2016; Cavaliere, 2021; Dindar et al., 2021; Mahamood, 2018; Majumdar & Manna, 2015; Song et al., 2016; Toyserkani et al., 2005).

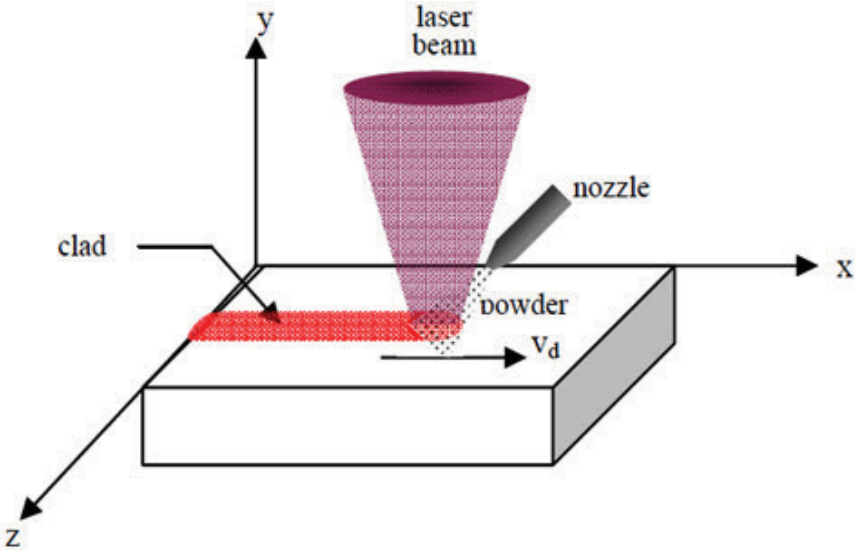

Figure 1. Schematic Illustration of Laser Cladding Process [4]

4 Total materia " Laser Cladding Technology" https://www.totalmateria.com/page.aspx?ID=CheckArticle&site=ktn&NM=377 (E.T. 11.11.2022)

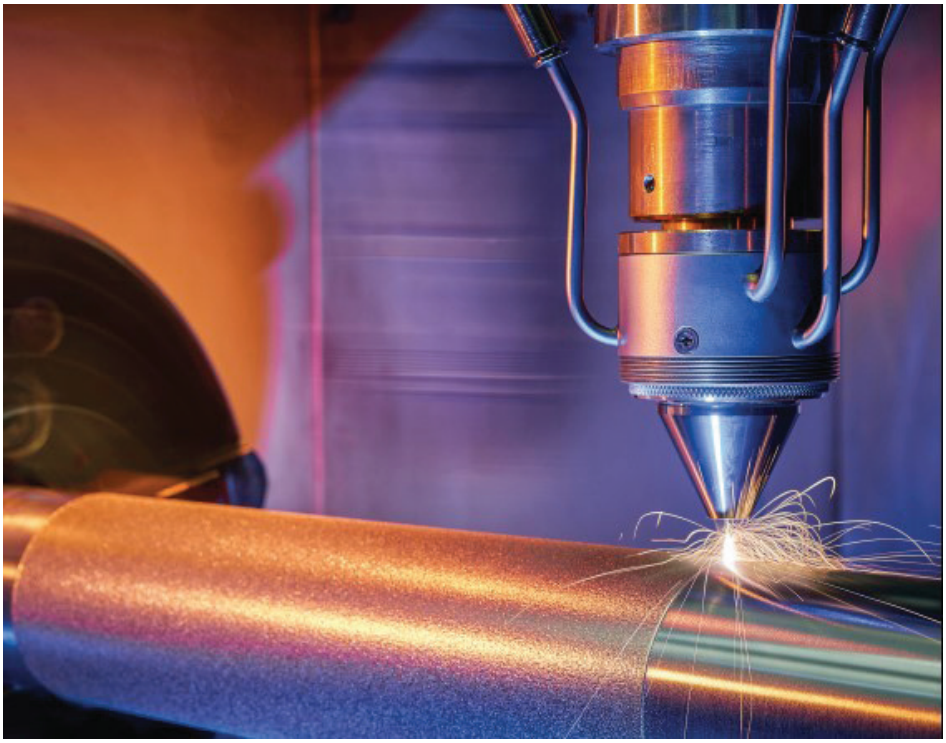

Figure 2. Laser Cladding Process on the Cylindrical Part [5]

In the laser cladding method, the material on which the process is applied is called "*base metal*" or "*substrate*". The laser cladding process is applied on the substrate; it consists of the stages of sending the powder material used as the clad onto the substrate, producing a melt by the laser beam acting on the substrate and the powder, and creating a clad layer by solidifying the melt.

Laser Technology

The invention of laser technology in the early 1960s revolutionized engineering practices, making many things unachievable with traditio-

5 Metalmecanica "Ehla: fast and environmentally friendly coating" https://www.metalmecanica.com/es/noticias/ehla-recubrimiento-rapido-y-amigable-con-el-medio-ambiente (E.T. 11.11.2022)

nal manufacturing methods in the past possible. The word "laser" stands for Light Amplification by the Stimulated Emission of Radiation. (Kovacs, 2018). Laser technology is a light-based processing method. The laser beam is produced from the amplified light source, similar to how a microphone is used to amplify sound.

The laser beam is characterized by a single wavelength, monochromaticity, the same phase position known as coherence, and low divergence and beam propagating in parallel lines. All these features of the laser concentrate the intensity of the produced laser beam so that a high-intensity laser beam can be produced. With these unique features, laser technology finds wide application in industrial applications and many different fields. In addition, one of the most important reasons why laser technology is preferred is that the laser beam can only be directed to the desired point and can be used in small processing areas (Mahamood, 2018; Toyserkani et al., 2005).

Laser types can be classified according to the physical properties and operating parameters used in laser beam production. The most common way is to classify according to the physical state of the active material while there are several ways to classify laser types. According to this criterion, lasers that can be used in laser cladding processes can be classified as follows;

- **Solid-State Lasers:** Solid-state lasers are the general nomenclature given to the laser generation method in which the active medium consists of a solid rather than a liquid or gas.[6] These solid materials usually consist of glasses or crystals doped with rare earth elements such as Neodymium (neodymium), Erbium (erbium), or Ytterbium (ytterbium). Solid state lasers operating in continuous wave (CW) mode can perform operations in many different application areas, from cell research to mechanical production, because of their wide range of wavelengths from ultraviolet (UV) wavelengths to far infrared (far IR) wavelengths. Today's, Ruby, Nd-YAG, Tm-YAG, Yb-YAG, Nd: glass, sapphire, titani-

6 İnnova-teknoloji "CW Solid State Lazerler" http://www.innova-teknoloji.com/lazer/cw-solid-state-lazerler (E.T. 11.11.2022)

um-sapphire, fiber, and many more different types of solid-state lasers are in use.

- **Gas Lasers:** Gas lasers can be created by passing electricity through the environment where the active media is gas as a discharge[7]. For the first time, continuous laser light could be produced with gas lasers. They are also the first lasers in which power can be obtained by converting electrical energy into a laser beam. In the method, stimulated emission is produced from low-energy transitions between the vibrational and rotational states of the molecular bonds of gases. The most important advantage of gas lasers is that they are relatively cheaper than other types of lasers. Also, gas lasers can be produced from vaporized metal ions such as helium-silver (HeAg) and neon-copper (NeCu) to create deep ultraviolet wavelengths. Various gas lasers such as CO_2, CO, nitrogen, argon, xenon, and krypton can be used for different applications.
- **Chemical Lasers:** In chemical lasers, laser beams are produced by chemical reactions that allow the rapid release of large amounts of energy in the laser environment. Chemical lasers can produce powers reaching megawatt levels[8]. It has very important functionality in industrial applications and military activities. There are chemical laser types such as oxygen-iodine laser, all gas-phase iodine laser, hydrogen fluoride (HF) and deuterium fluoride (DF) lasers.
- **Semiconductor Lasers:** It is a type of laser in which the laser medium consists of semiconductor materials. These types of lasers are generally excited by electrical pumping of the laser medium and interband transition under conditions of a high carrier density in the conduction band. Semiconductor lasers are also known as diode lasers in industrial applications. The lasers that have low to medium power are used in laser pointers, laser printers, and CD/DVD players are all made from semiconductor lasers. In addition, it is possible to make industrial semiconductor lasers with high power output as large as desired.

7 Physics-and-radio-electronics "Gas laser" https://www.physics-and-radio-electronics.com/physics/laser/differenttypesoflasers.html (E.T. 11.11.2022)

8 Wikipedia "Chemical laser" https://en.wikipedia.org/wiki/Chemical_laser (E.T. 11.11.2022)

LASER CLADDING METHODS

Laser Cladding with Pre-placed Powder

A thin coating layer is prepared in powder form by laying on the base material to be subjected to a surface improvement process. Afterward, the laser beam is programmed in the direction of the desired geometry, and movement is provided. Depending on the feed rate of the laser beam on the coating material, heating, melting, mixing and solidification processes take place. The laser cladding process is completed by melting the powder material with the base metal and then solidifying it (Toyserkani et al., 2005). This method is an effective option for laser cladding of planar geometries. The schematic representation of a laser cladding process made by the pre-placed powder method is given in Figure 3.

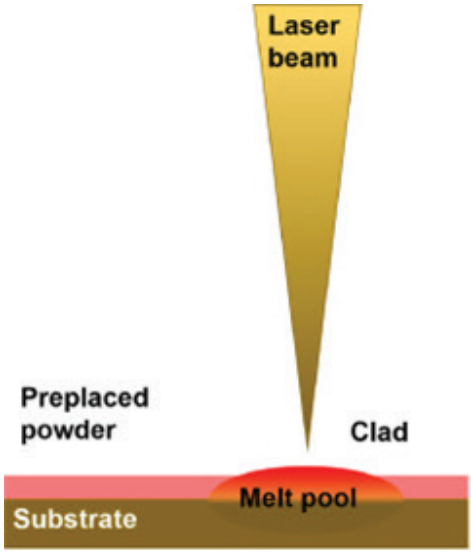

Figure 3. A Laser Coating Process with a Pre-Placed Powder Method (Dindar et al., 2021)

Laser Cladding with Wire Feeding Method

In the laser cladding method, when it is necessary to process non-planar geometries, the pre-placed powder method loses its functionality. In

such cases, the feeding process is carried out on the base metal with the use of wires containing powder materials. The feedstock wire used in the method; it is obtained by mixing the powder particles with a binder, passing the mixture through extrusion molds, cooling the extrudate, giving strength, and packaging as a product. In the laser cladding process, the wire feeding process is carried out by means of a nozzle. The wire material entering the focal point of the laser beam begins to melt with heat. The melt spreads on the base metal, cools, and solidifies, forming the clad layer. In this process, two important parameters are the wire feed rate and the speed of the laser on the tool path. The wire feed rate and the laser beam feed rate should be supporting the process simultaneously. If the wire feed rate is not sufficient, a porous structure is formed on the cladding and a sufficient quality cladding process cannot be performed. If the wire feeding rate is higher than required, then the melting of the wire becomes difficult, and an irregular cladding surface occurs. At the same time, if the feed rate of the laser beam is higher than it should be, the metallurgical bonding takes place at a low rate because sufficient heat cannot be provided, and this may cause the cladding to be of low strength (Toyserkani et al., 2005). Laser cladding with the wire feeding method is schematically illustrated in Figure 4.

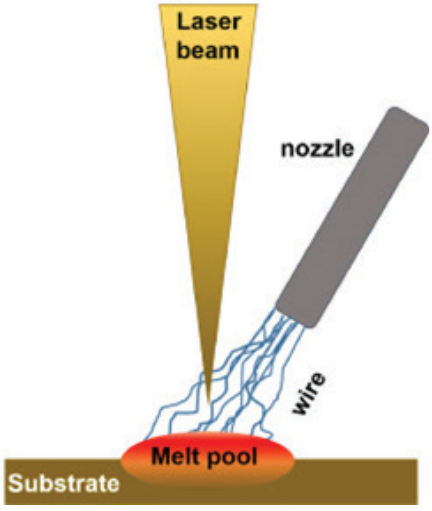

Figure 4. Laser cladding with wire feeding method (Dindar et al., 2021)

Laser Cladding with Powder Feeding Method

In some laser cladding applications, the pre-placed powder cladding method may not show sufficient performance. However, in order for the process to continue, the substrate surface to be treated with the laser cladding method must be brought together with the powder material using a different method. In such cases, powder particles are sent to the substrate surface using a nozzle. The laser cladding process is performed by the powder particles coming out of the nozzle entering the focus of the laser beam on the substrate surface, melting, and cooling. The powder materials used in the method are generally preferred in a spherical form in order to make the powder flow more ease. In addition, the size of powder particles should be considered an important parameter for the process. Because if the powder particles are lower than a certain size, all the particles start to move at the same time. Due to this situation, the nozzle tip may be clogged, and the process may result in failure before the cladding process begins. In addition, the contact of some materials with air during the spraying of powder particles on the substrate through a nozzle creates a negative effect and defect for the cladding process. Applications, where inert gases such as helium (He) and argon (Ar) are used as carrier gases, are commonly encountered in laser cladding processes where contact with air is not desired (Toyserkani et al., 2005). The laser cladding process with the powder feeding method is divided into two groups as lateral powder feeding and coaxial powder feeding according to powder feeding type.

Lateral Feeding

In the laser cladding process, the powder delivery process applied to the substrate surface is carried out with the help of a nozzle. The nozzle, which allows powder particles to be sprayed with a certain carrier gas and sent onto the substrate, also ensures that the powder particles are transmitted to the laser beam focus in the most efficient way possible. It is important for the quality of the cladding that the blasted powder particles enter the laser beam focus, and the melt material settles and solidifies efficiently on the substrate. For this reason, the spraying posi-

tion of the powder particles is important for the process when applying the lateral powder feeding process (Toyserkani et al., 2005). In addition to this difficulty of adjustment in the process, the application of lateral powder feeding on parts with complex geometries and variable angles, where the laser cladding process is difficult to perform, simplifies the process. The schematic representation of the lateral powder feeding method in the laser cladding process is given in Figure 5.

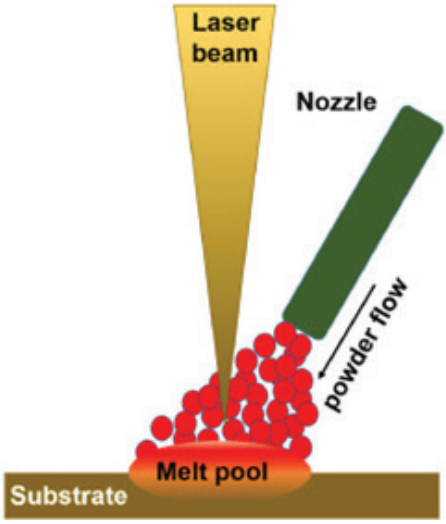

Figure 5. Lateral powder feeding method (Dindar et al., 2021)

Coaxial Feeding

In some applications of the laser cladding process, powder sending to the substrate surface can be performed coaxially with the laser beam. In this method, as in the lateral powder feeding method, the powder particles sent on the substrate are sprayed with the help of a nozzle. The spraying process here is carried out from several powder exit points surrounding the laser beam at equal angular intervals to the focal point of the laser beam. The spraying process can be carried out with the help of air used as the carrier gas, or it can be sprayed with the help of inert gases. By using inert gases as a carrier gas in the spraying process, it is possible to form a protective layer that will cut off the contact of the molten

material with the air. The effect area of shielding gases used in the co-axial powder feeding method is wider than other methods. In addition, this method can be used effectively in the creation of three-dimensional geometries. The schematic representation of the coaxial powder feeding method is given in Figure 6.

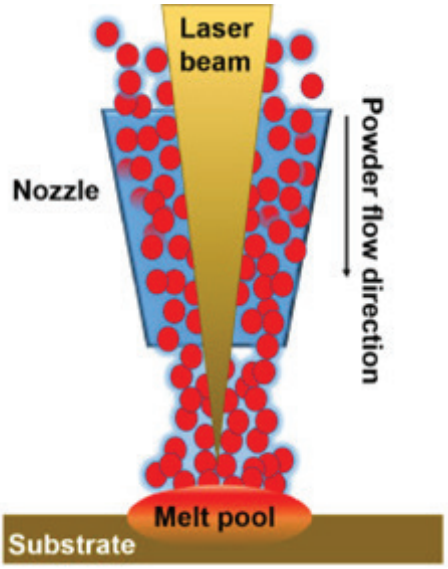

Figure 6. Coaxial powder feeding method (Dindar et al., 2021)

Advantages of Laser Cladding

It is possible to work on complex geometries without being affected by the limitations of traditional production technologies owing to the additive method-based design of the laser coating process. In addition, the use of a laser beam as a heat source during processing in the laser cladding method brings many advantages compared to arc welding or thermal spray methods. The advantages of the laser cladding method are given below.

- **Low Heat Affected Zone (HAZ):** In the laser cladding method, the laser beam is used as a heat source. Due to the nature of the laser beam processing, the temperature is constantly under control (Y. Du et al., 2022). Rapid heating and cooling occur in the process with the cre-

ation of the heat source using the laser beam. In this way, the material properties of the substrate are only slightly affected (Y. Liu et al., 2016; Norhafzan et al., 2021). A controlled heat-affected zone (HAZ) can be obtained on the substrate surface by preventing high heat input and slow cooling thanks to these benefits of lasers. Moreover, with the innovative systems reached, the heat-affected zone can be monitored and optimized during the process and the quality of the process can be improved significantly. The schematic representation of the heat-affected zone in the laser cladding process is given in Figure 7.

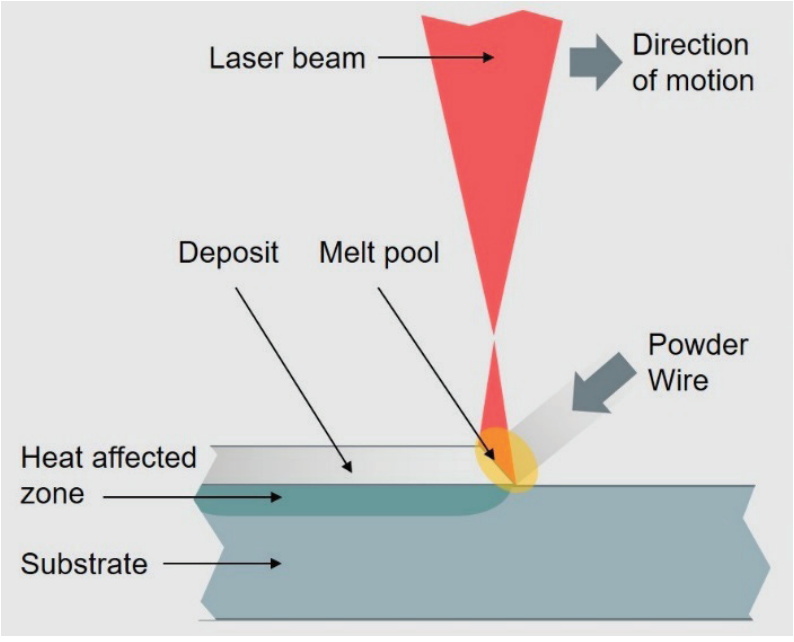

Figure 7. Laser cladding method and heat affected zone [9]

- **Low Distortion:** Since the laser beam is used as the heat source in the laser cladding process, a very low amount of heat input occurs on the substrate surface. For this reason, a very low amount of thermal defor-

9 Zikin, A. (2020, 18 Mayıs) Article 1: Introduction to Laser Cladding Technology https://www.linkedin.com/pulse/article-1-introduction-laser-cladding-technology-arkadi-zikin/ (E.T. 11.11.2022)

mation occurs on the substrate surface[10] and a negligible microstructure change is observed on the base material surface.

- **Low Dilution:** In the laser cladding method, which is a derivative of the processing mechanism welding process, the feedstock sent to the substrate surface with the heat generated by the laser beam is rapidly melted and cooled to form a coating surface in layers. As a result of this heat input, some molten zone is formed on the substrate surface together with the powder particles. As a result of the mixing of two different molten materials formed on the surface of the part, a small dilution zone is formed between the substrate and the cladding layer. Therefore, the composition of the cladding formed on the substrate differs. However, low dilution is required for laser cladding to take place in order to achieve good metallurgical bonding. In the literature, it has been observed that keeping the dilution rate of 5~8% is beneficial for the process's health since the mixing elements from the substrate adversely affect the cladding quality. In addition, it has been observed that in processes with a high dilution rate, losses in cladding properties occur and sufficient surface improvement cannot be achieved (Norhafzan et al., 2021; Song et al., 2016; Zanzarin et al., 2016; Zhang et al., 2020; Zhu et al., 2020)"author":[{"dropping-particle":"","family":"Song","given":"-B.","non-dropping-particle":"","parse-names":false,"suffix":""},{"dropping-particle":"","family":"Hussain","given":"T.","non-dropping-particle":"","parse-names":false,"suffix":""},{"dropping-particle":"","family":"Voisey","given":"K. T.","non-dropping-particle":"","parse-names":false,"suffix":""}],"container-title":"Physics Procedia","id":"ITEM-1","issued":{"date-parts":[["2016"]]},"page":"706-715","title":"Laser cladding of Ni50Cr: A parametric and dilution study","type":"article-journal","volume":"83"},"uris":["http://www.mendeley.com/documents/?uuid=ec9a6459-b400-4d52-9140-243a68e-7abd2"]},{"id":"ITEM-2","itemData":{"DOI":"10.1088/1757-899x/1078/1/012037","ISSN":"1757-8981","abstract":"Laser cladding is one of the advance processes in laser surface treatments. The process involved a

10 Nittanylasertech "Laser Claddıng Advantages" https://www.nittanylasertech.com/about-laser-cladding/page.aspx?id=1099 (E.T. 11.11.2022)

laser beam to combines another material that has different metallurgical properties on a substrate, whereby a very thin layer of the substrate has to be melted for it to achieve metallurgical bonding with minimal dilution of added material and substrate. The resulted properties were characterized by surface topography, subsurface microstructure, hardness, and residual stresses. The objective of this paper is to review the factors that affected of cladding process to get the best cladding, suitable to enhance hot press forming die surface and subsurface. The parameter control, metallurgical bonding between coating and substrate, and effect of powder size were discussed.","author":[{"dropping-particle":"","family":"Norhafzan","given":"B","non-dropping-particle":"","parse-names":false,"suffix":""},{"dropping-particle":"","family":"Khairil","given":"CM","non-dropping-particle":"","parse-names":false,"suffix":""},{"dropping-particle":"","family":"Aqida","given":"SN","non-dropping-particle":"","parse-names":false,"suffix":""}],"container-title":"IOP Conference Series: Materials Science and Engineering","id":"ITEM-2","issue":"1","issued":{"date-parts":[["2021","2","1"]]},"page":"012037","publisher":"IOP Publishing","title":"Laser cladding process to enhanced surface properties of hot press forming die: A review","type":"article-journal","volume":"1078"},"uris":["http://www.mendeley.com/documents/?uuid=9f76fa88-0c4e-40c8-b4df-db6bf4ea1c5b"]},{"id":"ITEM-3","itemData":{"DOI":"10.1080/00325899.2015.1118842","ISSN":"17432901","abstract":"High power diode laser with coaxial powder injection was used to deposit single tracks of cobalt alloy on to a carbon steel plate in order to study dilution. Two different methods to evaluate dilution are proposed and validated: dilution results to be proportional to the average percent or iron present in the clad. To study the correlations between dilution and processing parameters, clads were produced in different processing conditions. Dilution is correlated with the specific energy, and equation to estimate the average iron contamination of the clads was found. 'Trial and error' method was applied to improve this estimation. A statistically better prediction of the iron contamination is obtained when the combined parameter P2.5/F4 is used. Dilution influences clad microstructure and thus hardness of the final

coating, which decreases on increasing dilution. Phase distribution is also affected by dilution, Fe and C contamination stabilises α-fcc phase.","author":[{"dropping-particle":"","family":"Zanzarin","given":"S.","non-dropping-particle":"","parse-names":false,"suffix":""},{"dropping-particle":"","family":"Bengtsson","given":"S.","non-dropping-particle":"","parse-names":false,"suffix":""},{"dropping-particle":"","family":"Molinari","given":"A.","non-dropping-particle":"","parse-names":false,"suffix":""}],"container-title":"Powder Metallurgy","id":"ITEM-3","issue":"1","issued":{"date-parts":[["2016"]]},"page": "85-94","publisher":"Taylor & Francis","title":"Study of dilution in laser cladding of a carbon steel substrate with Co alloy powders","type":"article-journal","volume":"59"},"uris":["http://www.mendeley.com/documents/?uuid=-2d6585a6-1503-4d5f-b950-60b013bc0d3e"]},{"id":"ITEM-4","itemData":{"DOI":"10.1007/s12206-020-0315-0","ISSN":"19763824","abstract":"The change of angle θ between laser cladding powder plane and substrate plane will lead to changes in cladding layer's geometric morphology. Therefore, we established a quantitative numerical prediction model for cladding layer geometry. In this model, we consider the variation of θ, the laser energy attenuation rate and the temperature rise of the powder particles. At the same time, the simulation results were verified by experiments. The results show that when θ is in the range of 50°~90°, the initial temperature is 298 K, the scanning speed is 3.75 mm/s, and the laser spot diameter is 4.5 mm, the Fe#1 powder cladding can achieve better forming effect on Q235. In general, with the decrease of θ, the height of the cladding layer decreases and the width of the layer increases. However, when θ is less than 50°, the quality of the formed morphology significantly deteriorated. The experimental results are in good agreement with the simulation results, which verifies the validity and reliability of the model. This work provides a theoretical reference for further understanding the relationship between the laser cladding morphology and the incident angle.","author":[{"dropping-particle":"","family":"Zhang","given":"Guan","non-dropping-particle":"","parse-names":false,"suffix":""},{"dropping-particle":"","family":"-

Sun","given":"Wenlei","non-dropping-particle":"","parse-names":false,"suffix":""},{"dropping-particle":"","family":"Zhao","given":"Dongmei","non-dropping-particle":"","parse-names":false,"suffix":""},{"dropping-particle":"","family":"Fan","given":"Pengfei","non-dropping-particle":"","parse-names":false,"suffix":""},{"dropping-particle":"","family":"Guo","given":"Feng","non-dropping-particle":"","parse-names":false,"suffix":""},{"dropping-particle":"","family":"Huang","given":"Yong","non-dropping-particle":"","parse-names":false,"suffix":""},{"dropping-particle":"","family":"Li","given":"Pengfei","non-dropping-particle":"","parse-names":false,"suffix":""}],"container-title":"Journal of Mechanical Science and Technology","id":"ITEM-4","issue":"4","issued":{"date-parts":[["2020"]]},"page":"1531-1537","title":"Effect of laser beam incidence angle on cladding morphology in laser cladding process","type":"article-journal","volume":"34"},"uris":["http://www.mendeley.com/documents/?uuid=1c30a5d0-b896-4de0-93ed-72fc0ed0d150"]},{"id":"ITEM-5","itemData":{"DOI":"10.1007/s00170-020-05969-5","ISSN":"14333015","abstract":"During the laser cladding repair, the heat accumulation effect is produced due to the continuous input of energy, which leads to the increase of dilution rate under the same process parameters. In order to get the appropriate dilution rate, an accurate finite element model was established based on the experiment, and the variation of dilution rates under different power functions was analyzed. According to the results of finite element analysis, different power functions and dilution rates at different times were collected, and the dilution rate was optimized through deep learning, and the ideal power function was obtained. The results show that the dilution rate of the whole cladding layer fluctuates around the ideal value all the time by adjusting the laser power in real time, and the results are satisfactory. The maximum error of dilution rate is 21.75%, the minimum error is 0, and the average error is 5.79%.","author":[{"dropping-particle":"","family":"Zhu","given":"Shichao","non-dropping-particle":"","parse-names":false,"suffix":""},{"dropping-particle":"","family":"Chen","given":"Wenliang","non-dropping-particle":"","parse-names":false,"suffix":""},{"dropping-particle":"","famil-

y":"Zhan","given":"Xiaohong","non-dropping-particle":"","parse-names":false,"suffix":""},{"dropping-particle":"","family":"Ding","given":"Liping","non-dropping-particle":"","parse-names":false,"suffix":""},{"dropping-particle":"","family":"Wang","given":"Erhua","non-dropping-particle":"","parse-names":false,"suffix":""}],"container-title":"International Journal of Advanced Manufacturing Technology","id":"ITEM-5","issue":"5-6","issued":{"date-parts":[["2020"]]},"page":"1471-1484","publisher":"The International Journal of Advanced Manufacturing Technology","title":"Optimization of dilution rate of laser cladding repair based on deep learning","type":"article-journal","volume":"110"},"uris":["http://www.mendeley.com/documents/?uuid=3e7d16c1-866b-4f38-834f-5b839d2d6cb5"]}],"mendeley":{"formattedCitation":"(Norhafzan et al., 2021; Song et al., 2016; Zanzarin et al., 2016; Zhang et al., 2020; Zhu et al., 2020.

- **Low Porosity:** In the laser cladding method, in addition to the heating and cooling processes, the feeding of the feedstock to the substrate is carried out in a controlled and adjustable method. Almost all of the powder particles sent on the substrate can be melted, as the method offers high control. In this way, it can be ensured that the obtained coating layer is at full density or has a negligible porosity (>99.9% density) and cracks are prevented.

- **Production of Functionally Graded Parts:** It is very challenging and in some cases impossible to manufacture a part with a layered structure and consisting of different materials using traditional manufacturing methods. However, functionally graded components can be produced quite easily as the laser cladding process is suitable for additive manufacturing and can be used with various material pairs. It also enables the production of desired alloys by mixing different powder particles during the process (Li et al., 2020).

- **Reducing Prototyping Time:** It takes a long time to develop innovative products in industrial applications. One of the important reasons for this situation is that traditional manufacturing methods cause slow production of prototype products. However, with the laser cladding method's fast and flexible structure of layered production, prototype products can be produced more quickly. In addition, with the laser

cladding method, monolithic "intelligent structures" in which components such as sensors and magnets, etc. are embedded can be created. With these intelligent structures, the occurrence of malfunctions and damages caused by environmental conditions in electronic equipment can be reduced. On the other hand, it is possible to use biocompatible ceramic powder particles as well as products using metal powder particles by laser cladding method (Ahmed, 2019)especially those involving the use of laser as a source of energy, are being widely used to fabricate net-shaped parts required for various application sectors including automotive, aerospace and biomedical industries. Such widely used techniques include selective laser sintering (SLS.

- **Parts Repair:** In general, all products, components, and parts that are produced and put into use have a certain working life. When this period is completed, it is inevitable that malfunctions and deteriorations will occur. However, it can take a very long time to produce and assemble a new one instead of each defective part or component. In addition, situations such as production errors or design changes can cause processes to slow down further and waste extra time. In such cases, repairing the defective or damaged part and putting it back into use is the shortest solution that does not disrupt the work. Welding methods are widely used in such short-term repair processes, but since the welding method has a very high heat input, it negatively affects the functionality of the part.

It has been ensured that the damaged parts can be reused with the use of the laser cladding method in such repair processes. The cladding layers filled on the damaged surfaces provide machinable and grindable surfaces because of their high-density structure. In this way, the desired dimensional accuracy in the part geometries can be easily obtained and the loss of functionality of the part can be prevented. Such applications are frequently applied to the wearing surfaces of parts such as piston-cylinder pairs where sealing is important. In addition, it is possible to return the geometries that have lost a large volume to their full dimensions with the laser cladding method. The repair of a turbine blade with a large volume loss and a damaged blisk structure by the laser cladding method is given in Figures 13 – 14. In addition, the representation of the

laser cladding process and the process steps of remanufacturing are given in Figure 15 (Mahamood, 2018; Wilson et al., 2014).

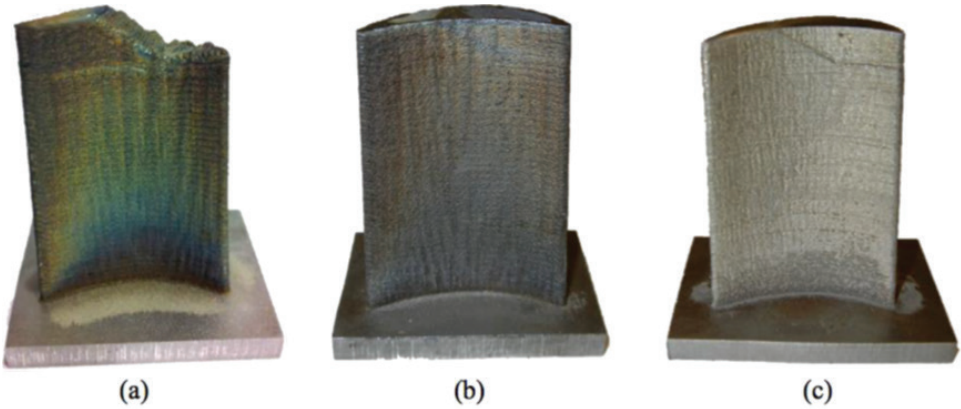

Figure 13. Turbine blade repaired by laser coating method; (a) damaged blade, (b) original blade geometry, (c) repaired turbine blade (S. Liu & Shin, 2019)

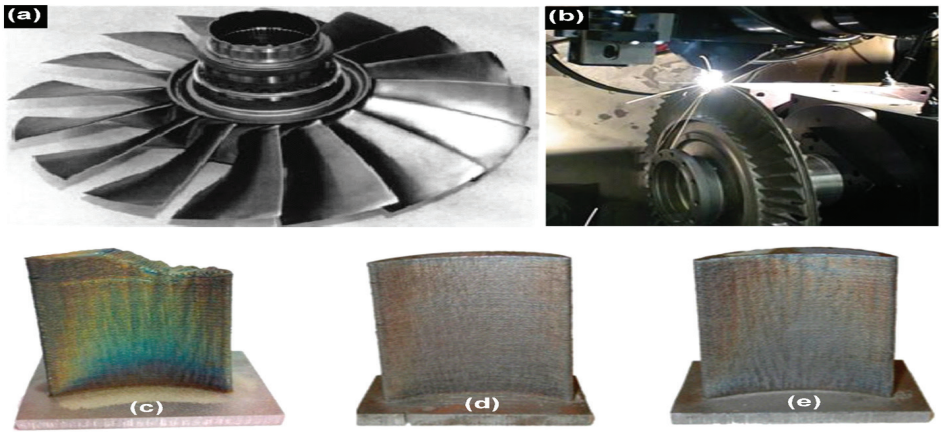

Figure 14. Repair of damaged blisk structure by laser cladding method (S. Liu & Shin, 2019)

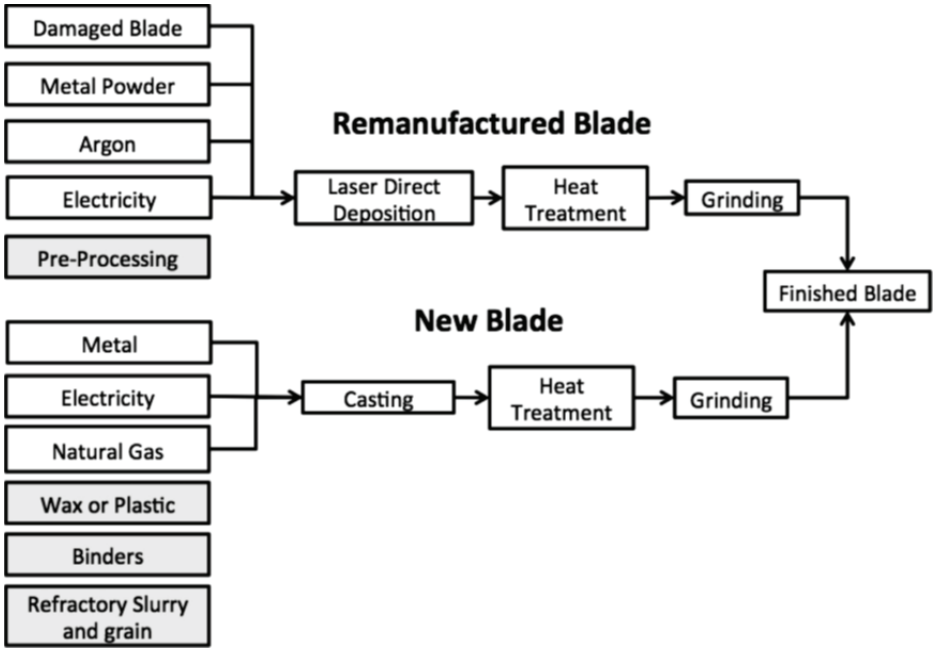

Figure 15. Comparison of Laser Cladding Method and New Production (Wilson et al., 2014)

- **Automation:** The laser cladding method consists of important parameters that directly affect the process, such as laser beam control, feedstock control, and progress control. The control of these challenging parameters can be programmed with sensitive computer-controlled devices (CNC-controlled) to provide a reliable and repeatable process.

Although the laser cladding method has very important advantages, it also has some processing difficulties and limitations. The disadvantages of the method are also given below;

- The machinery and equipment costs required for the initial setup of the laser cladding system are high.
- The operating and maintenance costs of the system are high.
- The system is not portable due to its large dimensions. For this reason, moving the products to be applied to the location of the system may cause problems in some cases.

- The optimization of the method depends on the knowledge based on various experimental studies.
- When there is no knowledge about the material pair consisting of powder and substrate to be laser clad, metallurgical and experimental studies can be a waste of time.
- It is difficult to find qualified operators who can operate the system and informed personnel to provide management.

Although it is widely used today, it is a new technology. Therefore, its applicability and capabilities are limited.

FACTORS AFFECTING the LASER CLADDING PROCESS

Laser Power

In laser cladding processes, laser power directly affects the process as an important parameter and requires some experience. Because insufficient laser power causes insufficient melting of the coating material, while excessive application of laser power causes excessive melting of the substrate and an increase in dilution rate. In both cases, the cladding quality is adversely affected and cannot give a sufficient performance. Continuous wave is used to increase the coverage area of the laser beam focus as much as possible. However, pulsed laser beam application can also be used in some applications to minimize substrate degradation by reducing the energy input.

Beam Distribution

In laser cladding processes, some of the powder particles that reach very high temperatures make splashes. It may cause the process to stop or the device to malfunction if these splashing particles come into contact with the lens transmitting the laser beam. For this reason, it is observed that it is preferred to use mirrors instead of lenses in laser beam transmission.

Heating

The most suitable heating method to obtain homogeneous thickness and wide cladding surfaces is the use of a large heat source with a uni-

form energy distribution. The laser beam can be sent perpendicular or parallel to the direction of the tool path, with a frequency of around 1 – 3 kHz to achieve a good quality cladding surface. The cladding surface roughness can be reduced by re-melting a small upper portion of the cladding using a second laser beam pass (Ion, 2005).

Traverse Rate

The traverse rate used in laser cladding processes is chosen higher than required for melting the substrate surface. Because powder materials can be melted more easily than a solid substrate surface. The traverse rate can be determined by the power effect at which the powders can be sufficiently melted, and minimum melting occurs on the substrate surface. The traverse rate directly affects the obtained coating thickness. There is an inverse relationship between the traverse rate and the cladding thickness, and a decrease in the cladding thickness occurs with the increase in the speed (Emamian et al., 2010; Ion, 2005).

Laser Cladding Process Parameters

In laser cladding processes, there are various parameters that affect the cladding quality.

Pre-Heating

The pre-heating process is used in the laser cladding process to prevent cracking by reducing the cooling rate in the clad layer and increasing the dilution rate to regulate the composition of the cladding layer by balancing the insufficient laser power at high deposition rates. The metallurgical bonding of the cladding can be increased significantly by pre-heating (Norhafzan et al., 2021).

Post Heat Treatment

In laser cladding processes where high energy input occurs, such as the creation of thick coating layers or the coating of large areas, the formation of residual stresses can be triggered due to the increased thermal effect. As a result of the formation of residual stresses, deterioration of

the part may occur. For this reason, applying a heat treatment after the cladding process in order to relieve stress is beneficial for the health of the process.

Mechanical Post-Processing

The coated surfaces can be machined or ground to obtain dimensional tolerances and surface quality after the laser cladding process. In addition, it is observed that shot peening is used in some applications to remove residual stresses that increase mechanical fatigue.

Process Errors Encountered in Laser Cladding

Various process errors may occur in laser cladding processes depending on the processing parameters. Common errors encountered during the process and solutions that can be applied to prevent these errors are given in this section.

Lack of Adhesion

Sufficient adhesion may not be achieved at the ends of the cladding geometry if the aspect ratio (thickness/width) of the coating is high. In this case, it is necessary to increase the heat input applied in the process or to use the heat effect more effectively. Therefore, it may be advisable to reduce the powder feed rate or reduce the traverse rate to achieve better adhesion (Lee, 2008).

Cracking

The formation of cracks in the coating layer is a common process error in the laser cladding process. Different thermal expansion of the substrate and the clad surface leads to crack formation. In addition, hard particles used as cladding material also increase residual stresses on the substrate, causing cracks to occur. Therefore, it may be advisable to pre-heat the substrate.

Distortion

Residual stresses occur on the substrate during the laser cladding process. These stresses cause substrate degradation, pass over the dimensional tolerances, and various problems that increase the amount of post-processing required. Distortions occur when there is a high energy input to the process and can be reduced by lowering the energy input. Therefore, it can be reduced or avoided by reducing the power of the continuous beam or using a pulsed laser beam. If there is a very high distortion formation, the substrate can be bent in the opposite direction of distortion to compensate for the distortion introduced during cladding.

Porosity

One of the important factors that determine the cladding quality created on the substrate surface in laser cladding processes is the number of porous structures (Lu et al., 2021). The number of porous structures affects the cladding density and reduces the desired surface improvement performance. Porous structures arise as a result of the rapid cooling of the outer wall of the coating layer and the slow cooling of the particles remaining in the interior. In addition, insufficient cleanliness of the substrate surface can affect the composition of the cladding and cause the formation of a porous structure. Therefore, thorough cleaning of the substrate surface prior to processing and exposing it to vibration while the cladding layer cools and solidifies may be beneficial to reduce the formation of porosity.

Dilution

The heat source used in laser cladding processes melts the entire coating material sent on the substrate and a part of the substrate surface. Two different melted materials mix into each other and form metallurgical bonding. This situation has to occur at a certain rate (4~8%) for the cladding to adhere well to the surface and is called dilution in the process. This situation can be regulated by feed rate and controlled melting (Zanzarin et al., 2016)clads were produced in different processing conditions. Dilution is correlated with the specific energy, and

equation to estimate the average iron contamination of the clads was found. 'Trial and error' method was applied to improve this estimation. A statistically better prediction of the iron contamination is obtained when the combined parameter P2.5/F4 is used. Dilution influences clad microstructure and thus hardness of the final coating, which decreases on increasing dilution. Phase distribution is also affected by dilution, Fe and C contamination stabilises α-fcc phase.","author":[{"dropping-particle":"","family":"Zanzarin","given":"S.","non-dropping-particle":"","parse-names":false,"suffix":""},{"dropping-particle":"","family":"Bengtsson","given":"S.","non-dropping-particle":"","parse-names":false,"suffix":""},{"dropping-particle":"","family":"Molinari","given":"A.","non-dropping-particle":"","parse-names":false,"suffix":""}],"container-title":"Powder Metallurgy","id":"ITEM-1","issue":"1","issued":{"date-parts":[["2016"]]},"page":"85-94","publisher":"Taylor & Francis","title":"Study of dilution in laser cladding of a carbon steel substrate with Co alloy powders","type":"article-journal","volume":"59"},"uris":["http://www.mendeley.com/documents/?uuid=2d6585a6-1503-4d5f-b950-60b013bc0d3e"]}],"mendeley":{"formattedCitation":"(Zanzarin et al., 2016.

RESULTS

Parts with complex geometries that are difficult to produce have become more accessible with the rapid development of laser technology and additive manufacturing methods. The laser cladding process is frequently used in industrial applications as an effective manufacturing method that combines the advantages of laser technology and additive manufacturing. The advantages of the laser cladding method developed in the face of the difficulties experienced in the field of manufacturing are briefly given below.

- Parts with complex geometries, which are difficult and time-consuming to produce, can be produced in a short time with the laser cladding process.

- Prototype products, which are in the initial design stage, can be obtained with additive manufacturing methods faster and with lower costs compared to traditional manufacturing methods.
- In some cases where it may require a long process, such as remanufacturing and putting into use parts that have lost volume due to damage, the part can be repaired and reused by using laser cladding methods.
- A low amount of heat-affected zone (HAZ) occurred on the laser cladding applied material. Very little thermal deformation occurs on the material because of a low amount of thermal input affects the process. In this way, the mechanical properties are affected very little due to no general change observed in the microstructure of the material.
- In the laser cladding process, where laser beam and powder metals are used together, strong metallurgical bonds can be obtained, and high-strength coatings can be obtained.
- A cladding with full density or negligible porosity (>99.9% density) can be achieved by carrying out the process in a controlled system.
- The fact that the laser cladding process, which has an additive manufacturing method-based, can be used with various material pairs, allows the production of functionally graded components quite easily.
- Parameters such as laser beam, feedstock, and feed can be programmed with computer-controlled machines (CNC-controlled) to ensure a reliable and repeatable process.

The laser cladding method has some disadvantages as well as very important advantages. The disadvantages of the method are also given below.

- The machinery and equipment costs required for the initial setup of the laser cladding system are high. In addition, the operating and maintenance costs of the system are high.

- The system is not portable due to its large dimensions. For this reason, moving the products to be applied to the location of the system may cause problems in some cases.
- Optimization of the method depended on knowledge based on various experimental studies.
- Metallurgical and experimental studies can be a waste of time when there is no knowledge about the material pair consisting of powder and substrate to be laser cladding.

REFERENCES

Ahmed, N. (2019). Direct metal fabrication in rapid prototyping: A review. *Journal of Manufacturing Processes*, *42*, 167–191. https://doi.org/10.1016/j.jmapro.2019.05.001

Brandt, M. (2016). *Laser Additive Manufacturing: Materials, Design, Technologies, and Applications* (M. Brandt (ed.); 1st ed.). Woodhead Publishing. https://doi.org/10.1016/B978-0-08-100433-3.12001-9

Cavaliere, P. (2021). Laser Cladding of Metals. In P. Cavaliere (Ed.), *Laser Cladding of Metals* (1st ed.). Springer Cham. https://doi.org/10.1007/978-3-030-53195-9

Dindar, Ç., Altay, M., & Aydın, H. (2021). Lazer Kaplama Prosesi ve Proses Parametreleri: Derleme Çalışması. *Uludağ University Journal of The Faculty of Engineering*, *26*(2), 723–736. https://doi.org/10.17482/uumfd.798666

Du, Y., Zhou, Z., He, G. Xu, L. (2022). Multi-parameter Optimization of Laser Cladding 15-5PH Using TOPSIS-GRA Based on Combined Weighting Method. *Journal of Materials Engineering and Performance 31*, 1934–1948. https://doi.org/10.1007/s11665-021-06369-w

Emamian, A., Corbin, S. F., & Khajepour, A. (2010). Effect of laser cladding process parameters on clad quality and in-situ formed microstructure of Fe-TiC composite coatings. *Surface and Coatings Technology*, *205*(7), 2007–2015. https://doi.org/10.1016/j.surfcoat.2010.08.087

Ion J. C. (2005). *Laser Processing of Engineering Materials* (Ion J. C. (ed.); 1st ed.). Butterworth-Heinemann. https://doi.org/10.1016/B978-075066079-2/50015-5

Kovacs, T. (2018). Laser welding process specification base on welding theories. *Procedia Manufacturing*, *22*, 147–153. https://doi.org/10.1016/j.promfg.2018.03.023

Lee, H. K. (2008). Effects of the cladding parameters on the deposition efficiency in pulsed Nd:YAG laser cladding. *Journal of Materials Processing Technology*, *202*(1–3), 321–327. https://doi.org/10.1016/j.jmatprotec.2007.09.024

Li, Y., Feng, Z., Hao, L., Huang, L., Xin, C., Wang, Y., Bilotti, E., Essa, K., Zhang, H., Li, Z., Yan, F., & Peijs, T. (2020). A Review on Functionally Graded Materials and Structures via Additive Manufacturing: From Multi-Scale Design to Versatile Functional Properties. *Advanced Materials Technologies*, *5*(6). https://doi.org/10.1002/admt.201900981

Liu, S., & Shin, Y. C. (2019). Additive manufacturing of Ti6Al4V alloy: A review. *Materials and Design*, *164*, 107552. https://doi.org/10.1016/j.matdes.2018.107552

Liu, Y., Qu, W., & Su, Y. (2016). TiC Reinforcement Composite Coating Produced Using Graphite of The Cast Iron by Laser Cladding. *Materials*, *9*(10). https://doi.org/10.3390/ma9100815

Lu, Y., Sun, G., Xiao, X., Ren, W., Sprague, E., Ni, Z., & Mazumder, J. (2021). In suit monitoring of solidification mode, porosity and clad height during laser metal deposition of AISI 316 stainless steel. Journal of Manufacturing Processes, 68(June), 1705–1713. https://doi.org/10.1016/j.jmapro.2021.06.078

Mahamood, R. M. (2018). *Laser Metal Deposition Process of Metals, Alloys, and Composite Materials* (R. M. Mahamood (ed.); 1st ed.). Springer Cham. https://doi.org/10.1007/978-3-319-64985-6

Majumdar, J. D., & Manna, I. (2015). Laser surface engineering. In A. Y. C. Nee (Ed.), *HandBook of Manufacturing Engineering and Technology* (1st ed., pp. 2639–2676). Springer London. https://doi.org/10.1007/978-1-4471-4670-4_27

Norhafzan, B., Khairil, C. M., & Aqida, S. N. (2021). Laser cladding process to enhanced surface properties of hot press forming die: A review. *IOP Conference Series: Materials Science and Engineering*, *1078*(1), 012037. https://doi.org/10.1088/1757-899x/1078/1/012037

Song, B., Hussain, T., & Voisey, K. T. (2016). Laser cladding of Ni50Cr: A parametric and dilution study. *Physics Procedia*, *83*, 706–715. https://doi.org/10.1016/j.phpro.2016.08.072

Toyserkani, E., Khajepour, A., & Corbin, S. (2005). *Laser cladding*. CRC Press.

Wilson, J. M., Piya, C., Shin, Y. C., Zhao, F., & Ramani, K. (2014). Remanufacturing of turbine blades by laser direct deposition with its energy and environmental impact analysis. *Journal of Cleaner Production*, *80*, 170–178. https://doi.org/10.1016/j.jclepro.2014.05.084

Zanzarin, S., Bengtsson, S., & Molinari, A. (2016). Study of dilution in laser cladding of a carbon steel substrate with Co alloy powders. *Powder Metallurgy*, *59*(1), 85–94. https://doi.org/10.1080/00325899.2015.1118842

Zhang, G., Sun, W., Zhao, D., Fan, P., Guo, F., Huang, Y., & Li, P. (2020). Effect of laser beam incidence angle on cladding morphology in laser cladding process. *Journal of Mechanical Science and Technology*, *34*(4), 1531–1537. https://doi.org/10.1007/s12206-020-0315-0

Zhu, S., Chen, W., Zhan, X., Ding, L., & Wang, E. (2020). Optimization of dilution rate of laser cladding repair based on deep learning. *International Journal of Advanced Manufacturing Technology*, *110*(5–6), 1471–1484. https://doi.org/10.1007/s00170-020-05969-5

INTERNET REFERENCES

Metalmecanica "Ehla: fast and environmentally friendly coating" https://www.metalmecanica.com/es/noticias/ehla-recubrimiento-rapido-y-amigable-con-el-medio-ambiente (E.T. 11.11.2022)

Nittanylasertech "Laser Claddıng Advantages" https://www.nittanylasertech.com/about-laser-cladding/page.aspx?id=1099 (E.T. 11.11.2022)

Physics-and-radio-electronics "Gas laser" https://www.physics-and-radio-electronics.com/physics/laser/differenttypesoflasers.html (E.T. 11.11.2022)

Total materia " Laser Cladding Technology" https://www.totalmateria.com/page.aspx?ID=CheckArticle&site=ktn&NM=377 (E.T. 11.11.2022)

Zikin, A. (2020, 18 Mayıs) Article 1: Introduction to Laser Cladding Technology https://www.linkedin.com/pulse/article-1-introduction-laser-cladding-technology-arkadi-zikin/ (E.T. 11.11.2022)

Wikipedia "Chemical laser" https://en.wikipedia.org/wiki/Chemical_laser (E.T. 11.11.2022)

EVALUATION OF FLAME RETARDANTS FOR VARIOUS ENGINEERING MATERIALS

Zafer KAHRAMAN[1]

Abstract: Efforts to improve the strength properties specific to the place of use of materials are constantly increasing. Studies on the effects of flame retardant materials on various engineering materials in different usage areas have gained importance. Flame retardant additives, especially wood, textile, polymer, cable, etc. products and areas with critical importance (hospital, security facility, data processing, etc.), in case of possible fire, both to prevent negative situations for living things (reducing the risks of suffocation and death due to toxic gases caused by combustion in indoor environments, etc.). It provides the opportunity to reduce possible material losses by protection or removal. In addition, flame retardants also contribute to the fire teams in terms of saving time to respond effectively to the fire. In determining the flame retardant additives according to the conditions of ambient, the material structure (polymer, wood, metal, textile, etc.), surface properties (surface geometry, cleanliness, etc.), usage conditions (indoor or outdoor environment, living condition, temperature, time etc.) stand out as the main factors. After determining the place of use of flame retardant materials in accordance with their properties, it should be evaluated according to other flame retardant materials at the application stage and its relationship with various flame retardants (mixing ratio, application amount, application method, etc.) should be known very well. Otherwise, the expected positive effects will not be achieved with the flame retardant to be chosen, and moreover, the probability of encountering negative results may increase. The effective use of environmentally friendly flame retardants (especially halogen-free flame

1 Öztiryakiler Madeni Eşya San. ve Tic. A.Ş, R&D Center, İstanbul / Türkiye, e-mail: zkahraman@oztiryakiler.com.tr, Orcid No: 0000-0002-2008-0533

retardants) in wider areas has become widespread. Scientific studies on the changes in the properties of the material with which flame retardants in different compositions are added or coated in various proportions continue to increase. In this study, the evolution process of flame retardant additives, the tests related to the combustion performance of the materials, the effects of different flame retardants used in various fields and evaluations were made.

Keywords: Flame Retardants, Restrict the Spread of Flame, Effects of Flame Retardants on Polymer Materials

INTRODUCTION

Flame retardant materials, depending on their structural properties, are used in household products (furniture, television frame, etc.) (Rodgers at el., 2021), transportation (vehicle seats, cables, etc.) to resist the spread of flame (Flambard et al., 2005) , textile (curtains, carpets, clothing, etc.) (Tokumura et al., 2019), electronic equipment (control cards, etc.) (Brandsma et al., 2014) and the building industry (wood products, insulation materials, cables, etc .) (Huang et al., 2022), their use is increasing in many areas today.

Flame retardants can have very different effects on materials depending on their content and additive ratios.

The historical development of flame retardants is shown in Figure 1 (Wahabi et al., 2021a).

Figure 1. Historical Development of Flame Retardants (Vahabi et al., 2021a)

The application processes of flame retardant is given in Figure 2 (Vahabi et al., 2021a).

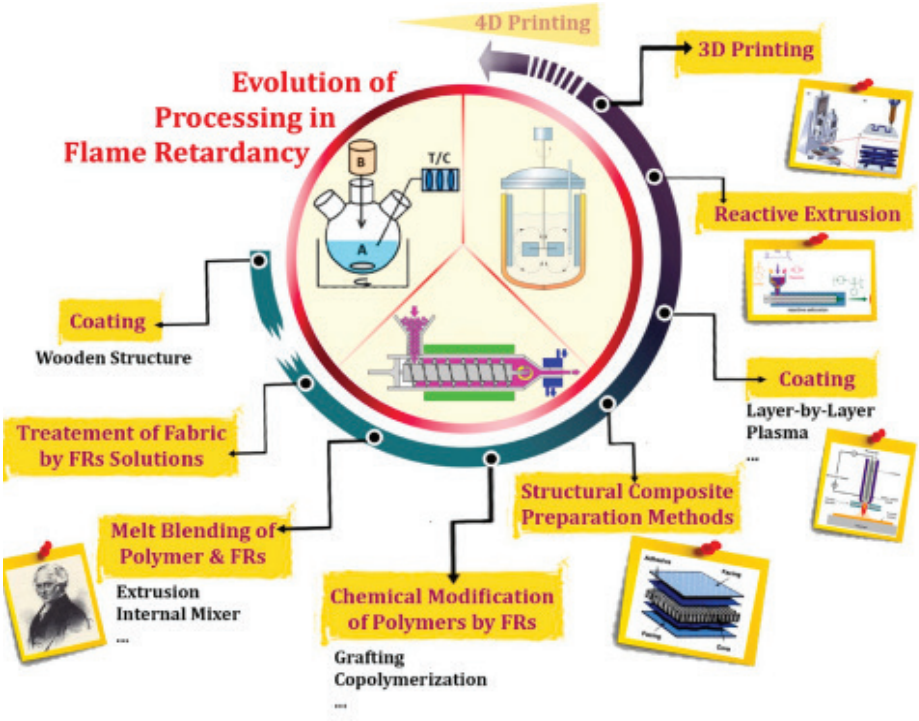

Figure 2. Development of Application Processes of Flame Retardants (Vahabi et al., 2021a)

Wahhabi and his working group reported that flame retardant materials are developing rapidly, especially in polymer materials, with many uses, and that they will appear in various applications in the field of high-tech. A schematic representation of potential application areas of flame retardant materials is given in Figure 3 (Wahabi et al., 2021b).

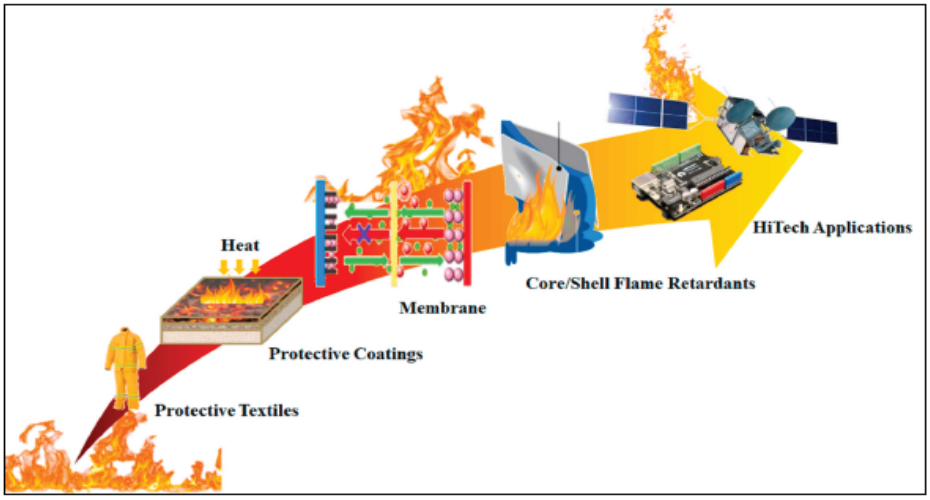

Figure 3. Schematic Representation of Potential Application Areas of Flame Retardant Materials (Vahabi et al., 2021b)

In recent years, ultraviolet curing technology, plasma technology, physical and chemical vapor depositions (PVD and CVD), sol–gel process, layer-by-layer assembly approach have come to the fore among flame retardant application technologies (Liang et al, 2013).

Explanations on the comparison of surface treatment methods in the application processes of flame retardants are given in Table 1 (Wen at el., 2023).

Table 1. Comparison of Various Surface Finishing Methods (Wen at el., 2023)

Details	Advantages	Disadvantages	Room for improvements
Layer-by-layer deposition	• Low temperature deposition • Simple and straightforward • Utilize an environmentally friendly solvent (e.g., water) • Tunable thickness (control of number of BL) • Multifunctionality (high)	• Surface treatment is sometimes required • Requires a proper selection of opposite charged polyelectrolytes • Limited pairs (usually organic) • Scalability (low to moderate) – not straightforward to develop continuous roll-to-roll plants	• Explore potential of organic-inorganic pairs • Search for high performing pairs to reduce required number of BL
Dip coating or dip-pad-dry-cure	• Low temperature deposition • Suitable for deposition of sol gel-based or organosilicon-based flame retardants • Amenable to scale up (continuous mode) • Multifunctionality (high)	• Chemical based processes (impact of chemical precursors) • Inorganic materials layer cannot be deposited as thin film • Inorganic particles need to be prepared separately	• Explore method to in-situ form the particles as one dip the substrates into the formulation (eliminate the need to synthesize the particles separately)
In-situ solution-based synthesis	• More generic approach than that of dip-coating (able to deposit organic, inorganic, or hybrid coating) • Able to handle a wider range of substrates (types, shapes, etc.) • Ability to form fully inorganic flame-retardant coating	• Chemical based processes (impact of chemical precursors) • Poor interaction between inorganic layer and substrates (low coating durability) • High temperature solvothermal/ hydrothermal synthesis (batch mode)	• Improve adherence of inorganic nanoparticles to substrates
Brushing/spray coating	• Low temperature deposition • Simple and straightforward • Excellent for deposition on rigid substrates • Allow for large area coating (amenable to scale up)	• Multifunctionality (low) • Narrow viscosity range to create fine droplets for spray coating • Amount of binder used is unnecessarily high (potentially undermining the flame retardancy effects)	• Prevent potential demulsification of waterborne coatings after addition of flame-retardant components • Develop flame-retardant formulation with lower binder content • Explore possibility of coating on non-rigid substrates

Ahmed and his working group divided the mechanisms of flame retardant materials under two main headings are given in Figure 4 (Ahmed et al., 2018).

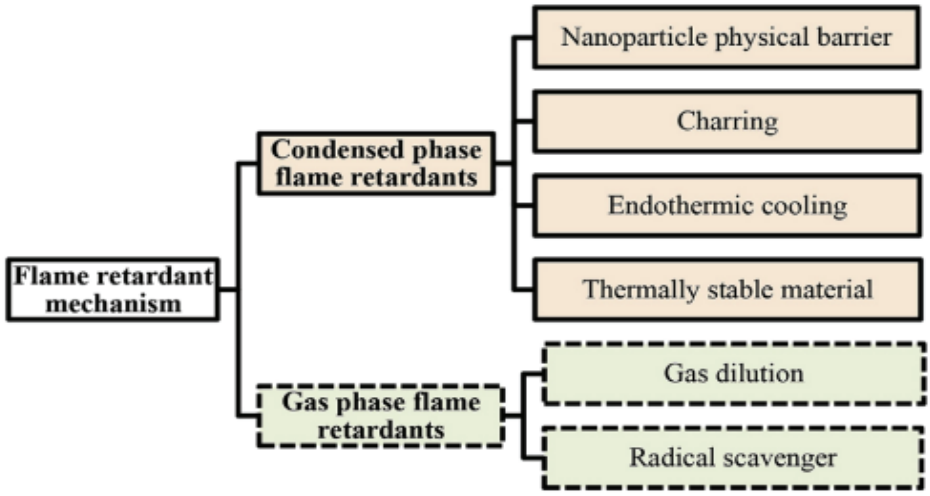

Figure 4. Mechanism of Flame Retardant Additives (Ahmed et al., 2018)

The mechanisms of action of flame retardant materials in two different phases (gas and condensed) are given in Figure 5 (Wahabi et al., 2021a).

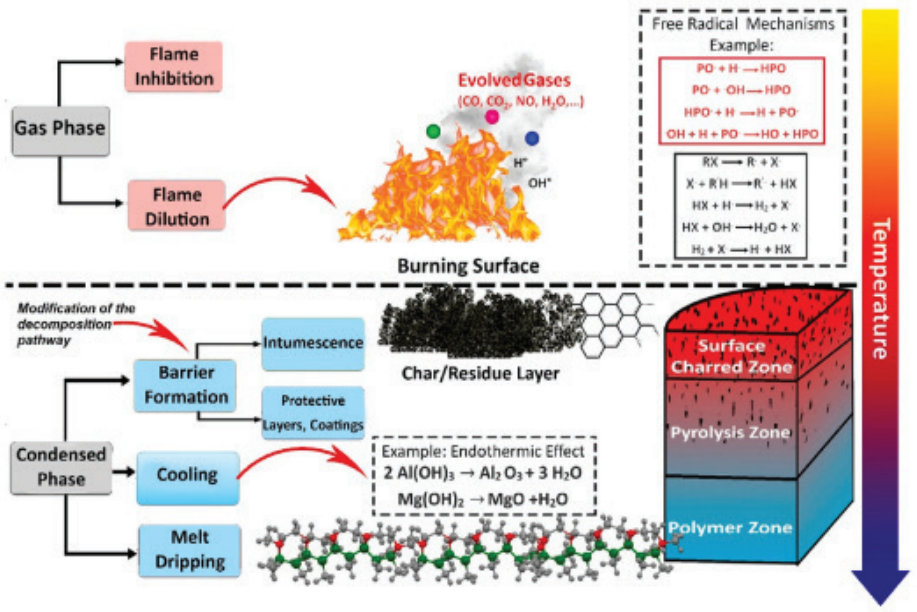

Figure 5. Demonstration of Potential Mechanisms of Action of Flame Retardant Materials in Two Different Phases (Gas and Condensed) (Vahabi et al., 2021a)

The combustion mechanism of polymers is given in Figure 6. (Malucelli et al., 2014).

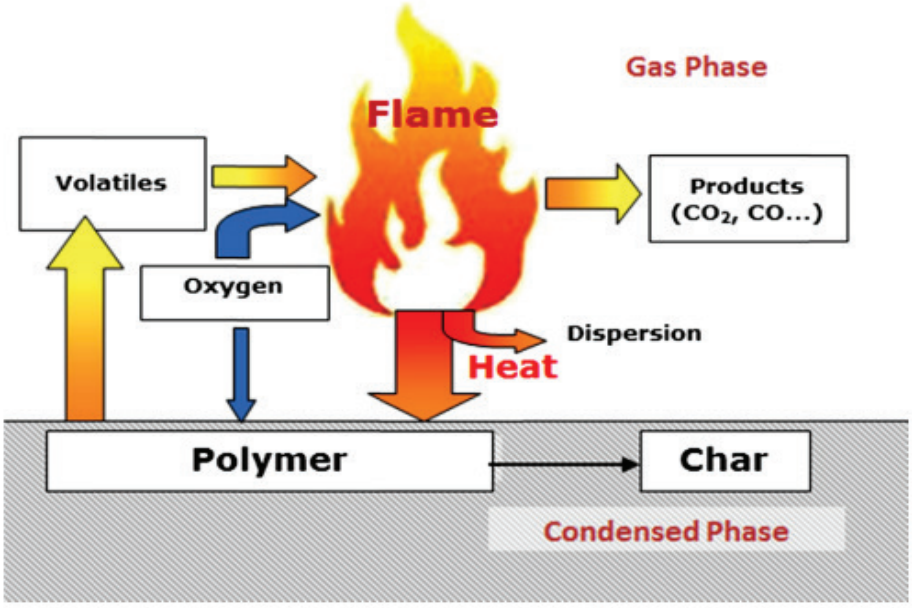

Figure 6. The Combustion Mechanism of Polymers (Malucelli et al., 2014)

The combustion process of materials containing flame retardants is given in Figure 7. (Mensah et al., 2022).

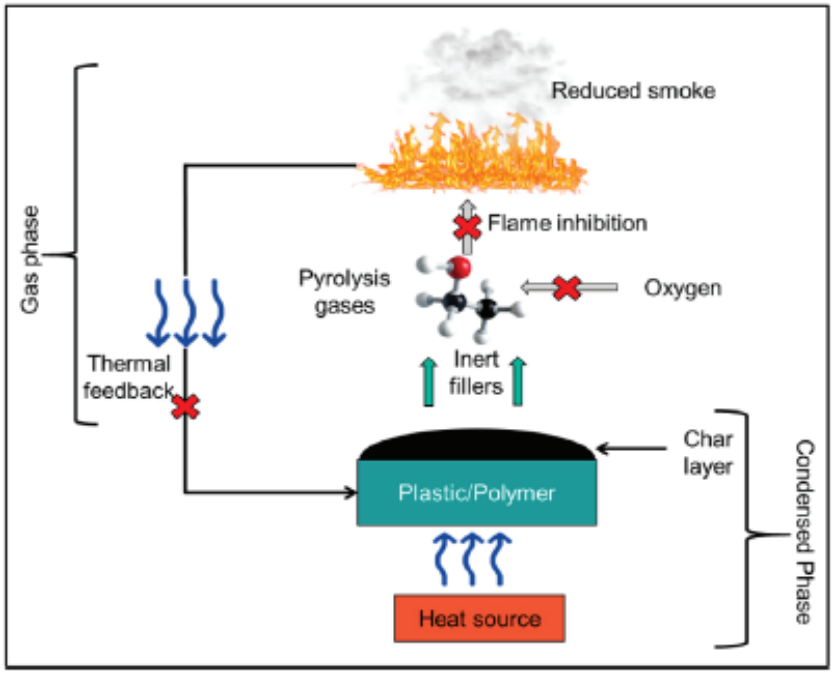

Figure 7. Demonstration of the Combustion Process of the Material Containing Flame Retardant (Mensah et al., 2022)

Ahmed and his working group evaluated the initiation and development process of combustion (char layer formation and non-formation on the surface) in polymer materials.

The situation regarding the absence of a char layer on the surface is shown in Figure 8 (a). Figure 8 (b) shows schematically that it functions as a protective layer by slowing down the oxygen transfer and the rate of heat release required for the continuation of the combustion in the lower layer with the formation of a carbonization layer on the surface (Ahmed et al., 2018).

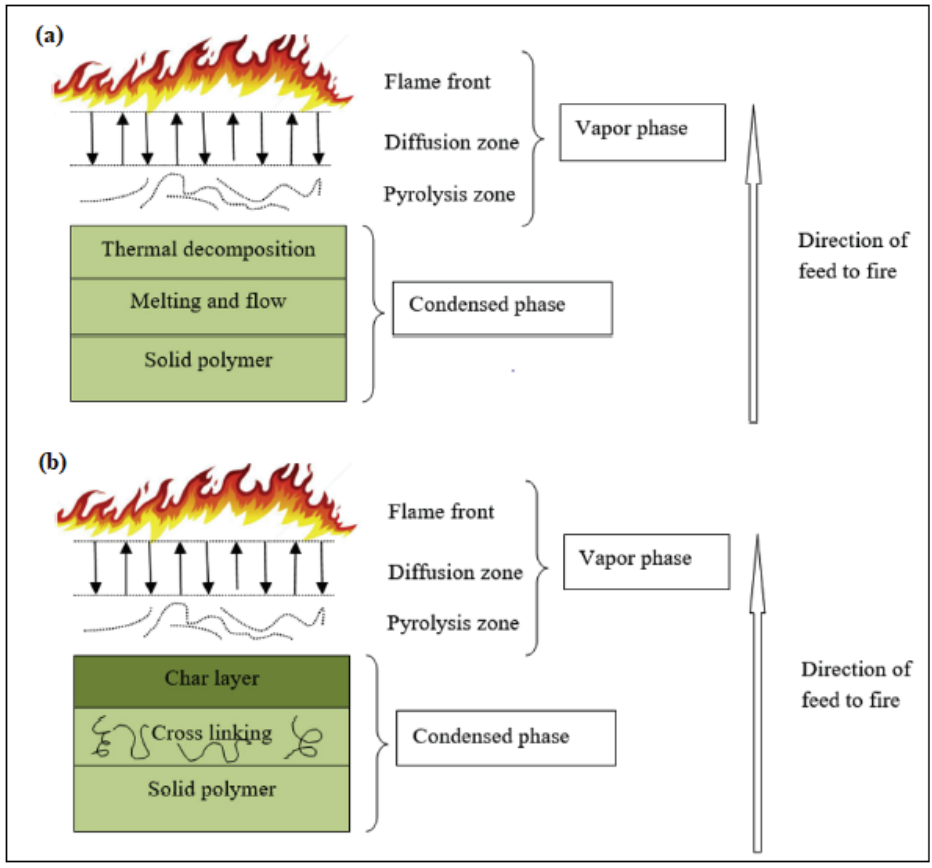

Figure 8. The Degradation of Polymer Materials by Heat Source (a) Non-C-harring, (b) with Char Layer (Ahmed et al., 2018)

Evaluations for the improvement of flame retardancy in polymer composite materials are shown in Figure 9 (Bar et al., 2015).

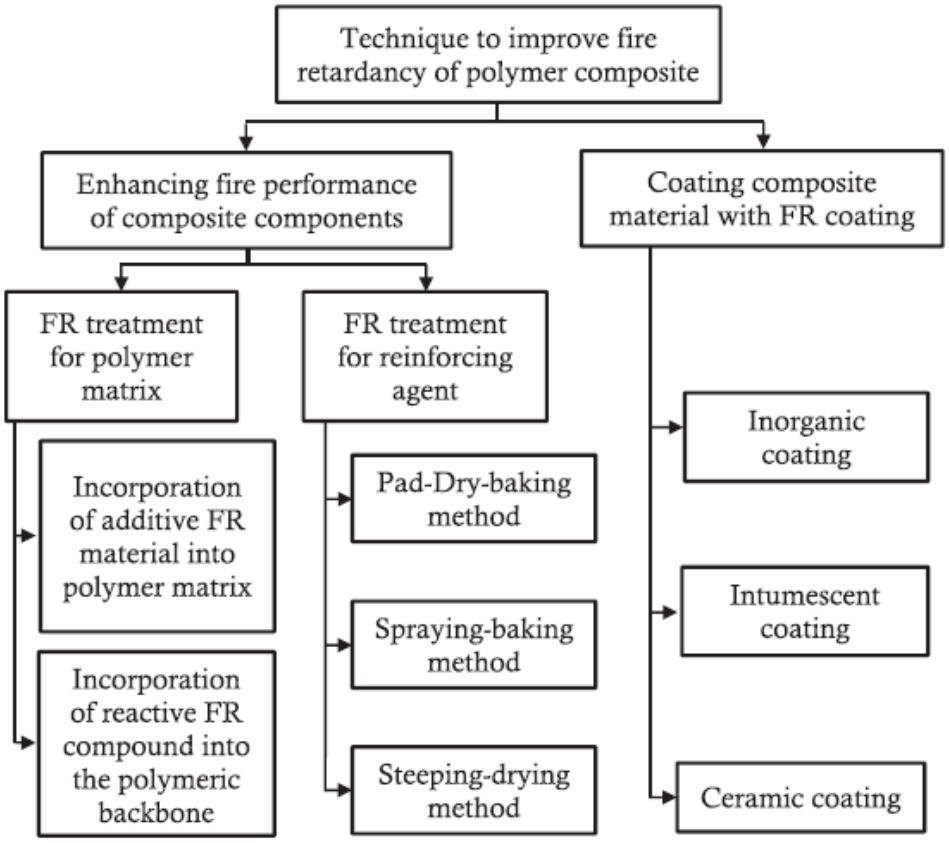

Figure 9. The Process of Improving Flame Retardancy in Polymer Composite Materials (Bar et al., 2015)

Research and development activities on flame retardant materials increased after the Second World War. In the 1960s, while cheap polymer products became widespread, serious fire risks emerged and demands for reducing flammability in polymer materials increased. As of the 1970s, the demands for reducing the smoke generated in the combustion process have increased.

The development of halogen-free flame retardants against halogen-containing flame retardants in the 2000s, the demands for sustainable flame retardants have increased in the 2010s, along with climatic changes and environmental concerns (Table 2).

Table 2. R&D Studies on Flame Retardant Additives by Years (Zope, 2018)

Decade	Event	Demand
1960s	Widespread availability of cheap polymer product—more serious fires	Reduced ignitability
1970s	Smoke much worse	Reduced smoke
1980–1990s	Development of Cone Calorimeter (and emphasis on peak heat release rate, rather than ignitability)	Reduced peak heat release
	Increase in deaths from smoke inhalation	Reduced Fire Toxicity
2000s	Halogen FRs found across the ecosystem	Halogen-free FRs
2010s	Climate change and other environmental concerns become mainstream	Sustainable FRs

Tests for Evaluation of Combustion Performance of Flame Retardants

Test methods and test setups for the combustion process of flame retardant additives in various materials are grouped under three main headings: small, medium and large. The illustration of the test method and test setups is given in Figure 10 (Vahabi et al., 2021a).

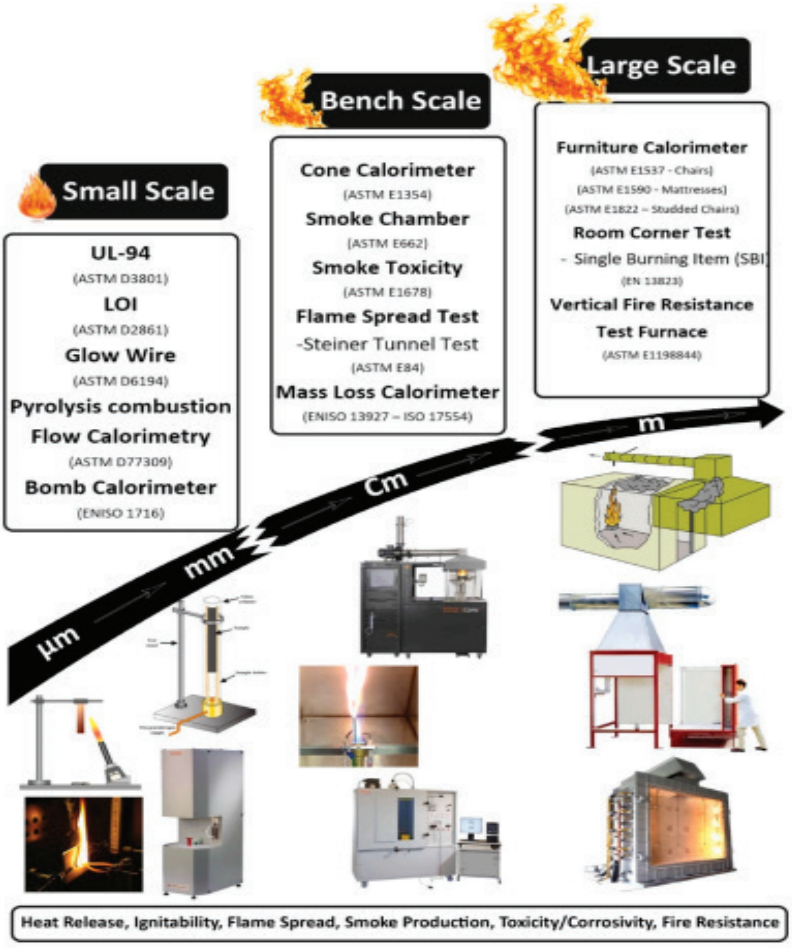

Figure 10. Various Test Methods and Setups Associated with Flame Retardants in Polymer Materials (Vahabi et al., 2021a)

Flammability (UL-94), Limit Oxygen Index (LOI) and Cone Calorimetry tests are used to evaluate the effectiveness of flame retardants against various materials with international standards (McCoy, C.G. and Stoliarov, 2021).

Flammability Test (UL-94)

The setup of this test method is small in scale and provides easy applicability with the use of small samples in practice. Therefore, the UL-94 test is widely used. Underwriters' Laboratory (UL-94) test applications are carried out under two headings, horizontal and vertical. The UL-94 Vertical Flammability Test setup is shown in Figure 11 (Wang and Zhang, 2013).

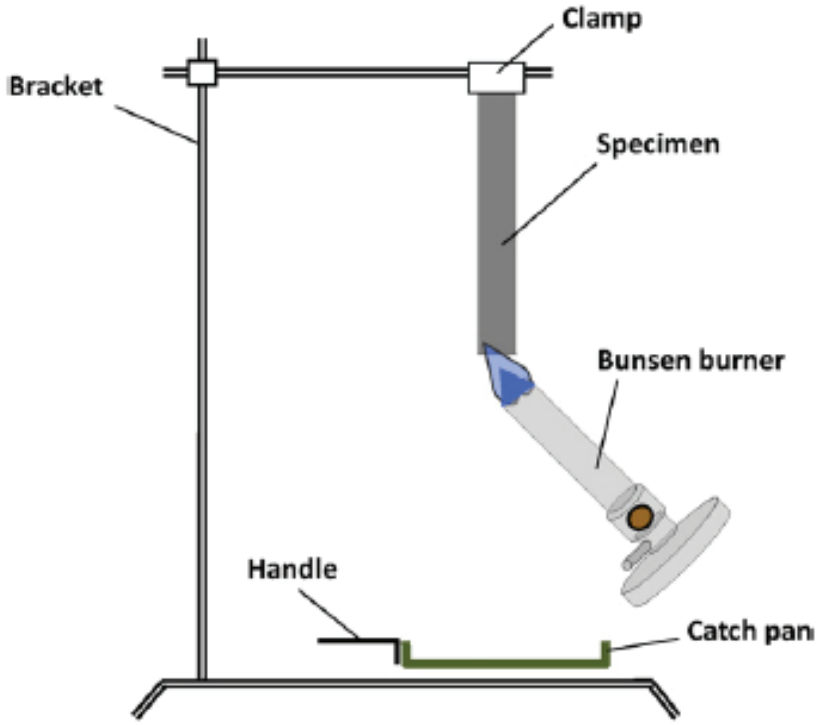

Figure 11. The Test Setup Used for UL-94 Vertical Flammability (Wang and Zhang, 2013)

Classifications within the scope of UL-94 Vertical Flammability Test are given in Table 3 (Laoutid et al., 2009).

Table 3. Classification of UL-94 Vertical Flammability Test (Laoutid et al., 2009)

Fire classification	
UL94 V_0	t_1 and t_2 less than 10 s for each specimen $t_1 + t_2$ less than 50 s for the five specimens $t_2 + t_3$ less than 30 s for each specimen No afterflame or afterglow up to the holding clamp No burning drops
UL94 V_1	t_1 and t_2 less than 30 s for each specimen $t_1 + t_2$ less than 250 s for the five specimens $t_2 + t_3$ less than 60 s for each specimen No afterflame or afterglow up to the holding clamp No burning drops
UL94 V_2	t_1 and t_2 less than 30 s for each specimen $t_1 + t_2$ less than 250 s for the five specimens $t_2 + t_3$ less than 60 s for each specimen No afterflame or afterglow up to the holding clamp Burning drops allowed

Limit Oxygen Index Test (LOI)

Limit Oxygen Index (LOI) test applications are generally evaluated according to ASTM D 2863 (Liu et., 2022) and ISO 4589-2 (Filippi et al., 2020) standards. The Limit Oxygen Index test value is briefly stated as "the higher the LOI value, the higher the inflammability". LOI test setup is given in Figure 12 (Laoutid et al., 2009).

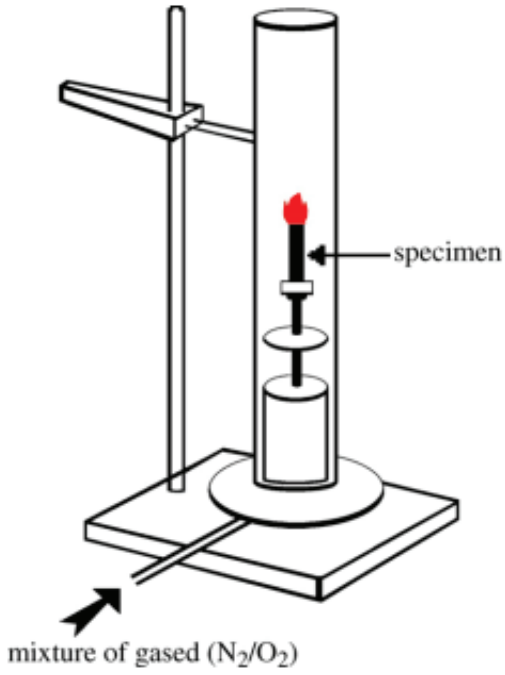

Figure 12. Experimental Setup for Limit Oxygen Index (LOI) (Laoutid et al., 2009)

Cone Calorimeter Test

Cone Calorimeter test is at the mid-range test level compared to the low scale UL-94 and Limit Oxygen Index (LOI) tests. Cone calorimeter tests can be performed with ISO 5660-1 and ASTM E 1354 standards (Laoutid et al., 2009). Cone Calorimeter test, evaluations are made regarding the data specified in Table 4. (Chen et al, 2022; Shahari et al., 2021);

Table 4. Data Evaluated by Cone Calorimetry Test

• The Time to Ignition (TTI),	• Smoke Production Rate (SPR),
• Heat Release Rate (HRR)	• Total Smoke Production (TSP),
• The Peak Heat Release Rates (PHRR),	• Fire Growth Rate (FIGRA)
• Total Heat Released (THR)	• Fire Performance Index (FPI)

The placement locations of thermocouples for temperature measurements on the samples used in the Cone Calorimetry test are given in Figure 13 (Tsai, 2009).

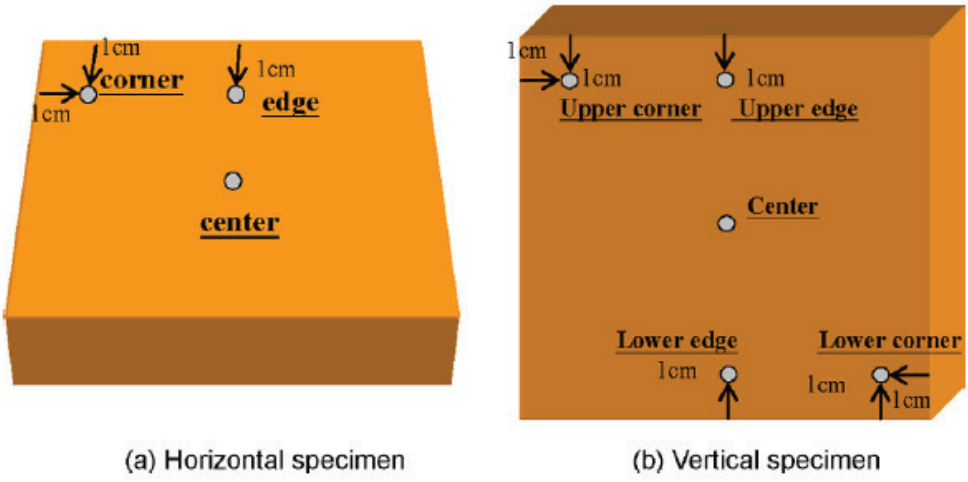

Figure 13. The Placement of Thermocouples on Samples Used in Cone Calorimetry Testing (Tsai, 2009)

The distribution of heat transfers according to horizontal and vertical sample placement positions in the Cone Calorimetry test is shown in Figure 14 (Tsai, 2009).

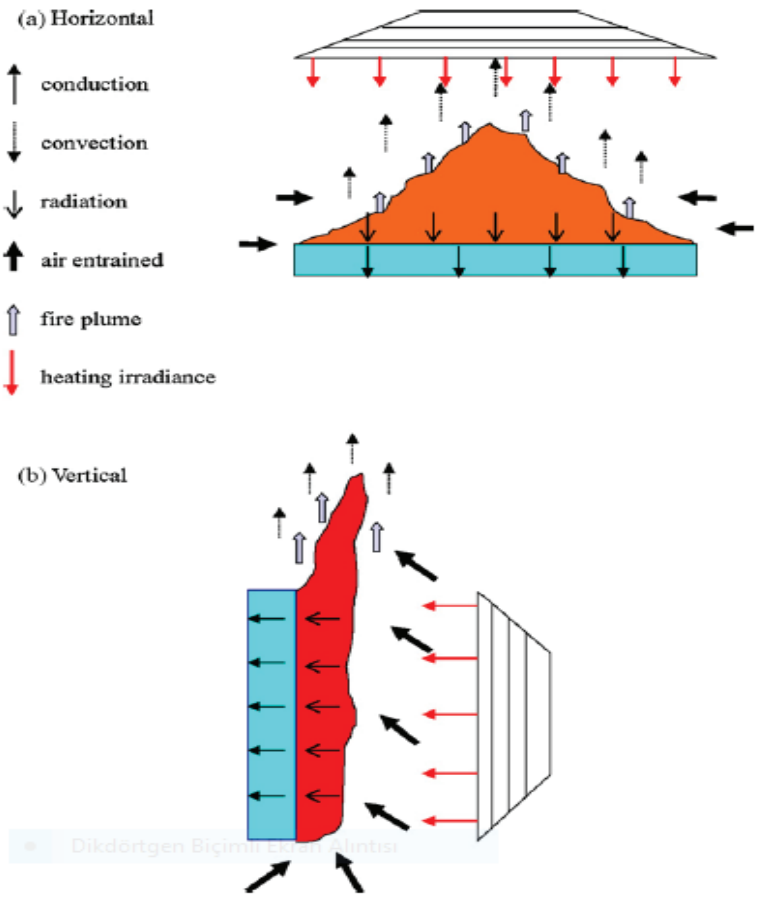

Figure 14. Heat Transfer in Cone Calorimetry Test According to Different Sample Placement Positions (Tsai, 2009)

Cone Calorimeter test setup is given in Figure 15 (Laoutid et al., 2009).

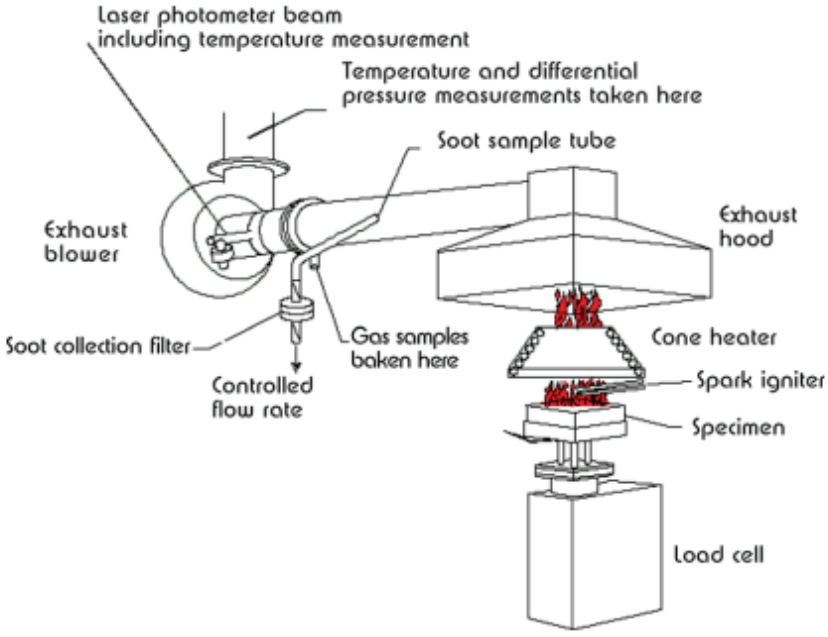

Figure 15. Cone Calorimeter Test Setup (Laoutid et al., 2009)

The illustration of the Cone Calorimeter test setup under a protective atmosphere is also given in Figure 16 (Hermouet et al., 2021).

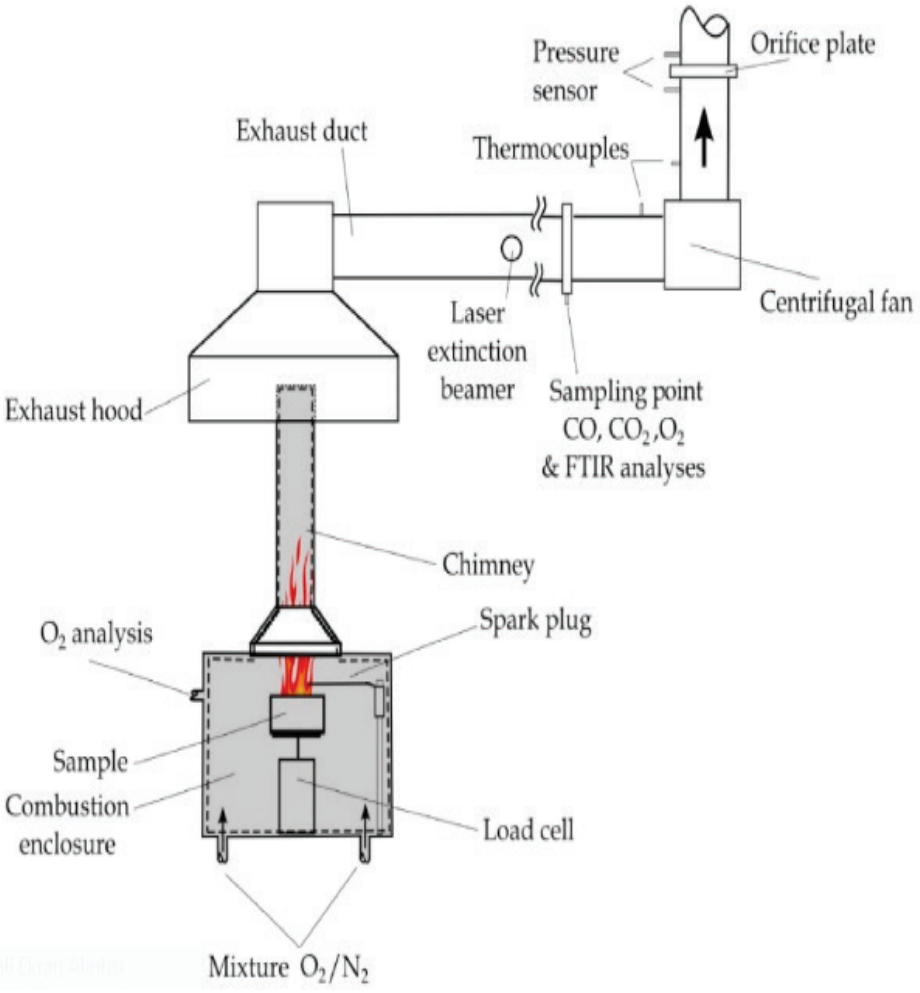

Figure 16. Conical Calorimeter Test Setup with Controlled Atmosphere Application (O_2/N_2 Mixture) (Hermouet et al., 2021)

The biggest disadvantage of halogen-containing flame retardant materials is that they create toxic fumes and pose a great danger to living things, especially in indoor applications. For this reason, halogen-free flame retardant materials do not have adverse effects on human health in terms of use. Therefore, the usage areas of these flame retardants are expanding as environmentally friendly. The general properties of

flame retardant materials (halogen and halogen-free) are given in Table 5 (Jeong et al., 2022).

Table 5. Properties of Halogen and Non-halogen Flame Retardant Materials (Jeong et al., 2022)

Category	Type	Reaction process	Advantage	Limitation
Halogen	Brominated Chlorinated	Releases gaseous hydrogen halide (i.e., active bromine atoms) into the air, isolating oxygen and interacting with active free-radicals OH• and H•	High thermal stability, high flame retardancy, and low filler content	Accelerates toxic smoke production, corrosion, and bioaccumulation
Non-halogen	Phosphorus-based	Active phosphorus-containing radicals such as PO• and PO_2• act in the gaseous phase, reacting with free-radical OH•	Enhanced char production and non-toxicity	High loading
	Nitrogen-based	Mostly melamine based. Condensed-phase melamine transforms into cross-linked structures, producing solid-phase char layers	Low toxicity and low smoke release	Dependent on acid source
	Metallic hydroxide	Acts as a catalyst to produce carbonized residues during combustion	Environmentally friendly	Low efficiency and high loading

Bio-based flame retardant materials are grouped under two main groups as biomass and animal origin (Figure 17) (Taib et al., 2022).

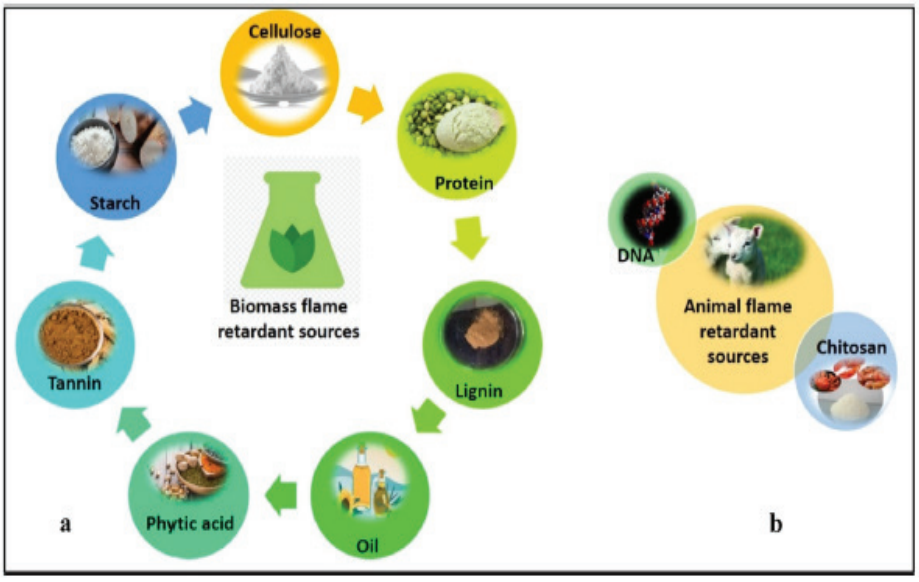

Figure 17. Source of Bio-based Flame Retardants (a. Biomass and b. Animal Origin) (Taib et al., 2022)

The process for gaining flame retardant properties as a composite of Polypropylene (PP), which is widely used among polymer materials, is given in Figure 18 (Chen, et.al., 2023).

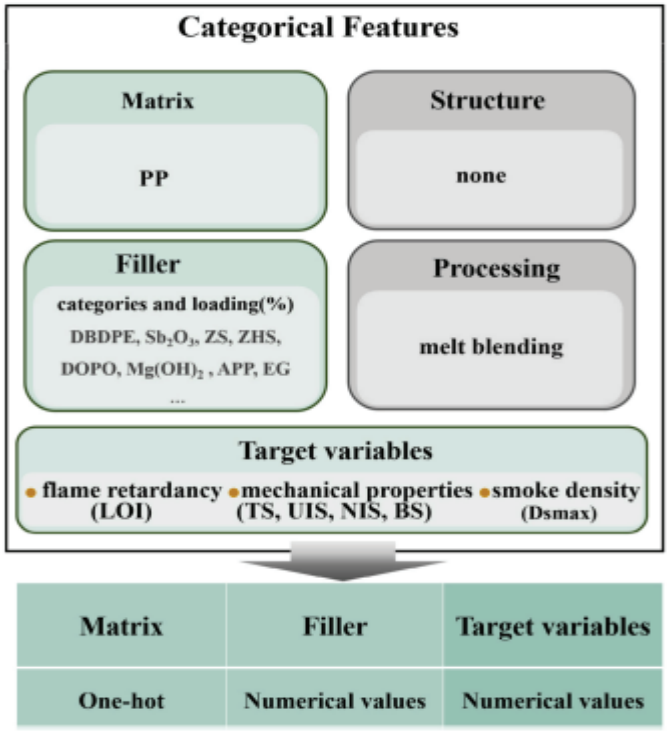

Figure 18. Demonstration of Various Properties of Flame Retardant Polymer Based Composites (Chen, et.al., 2023)

The development process of bio-based flame retardant materials has increasingly continued. Classification of bio-based flame retardant materials is given schematically in Figure 19. (Jeong et al., 2022).

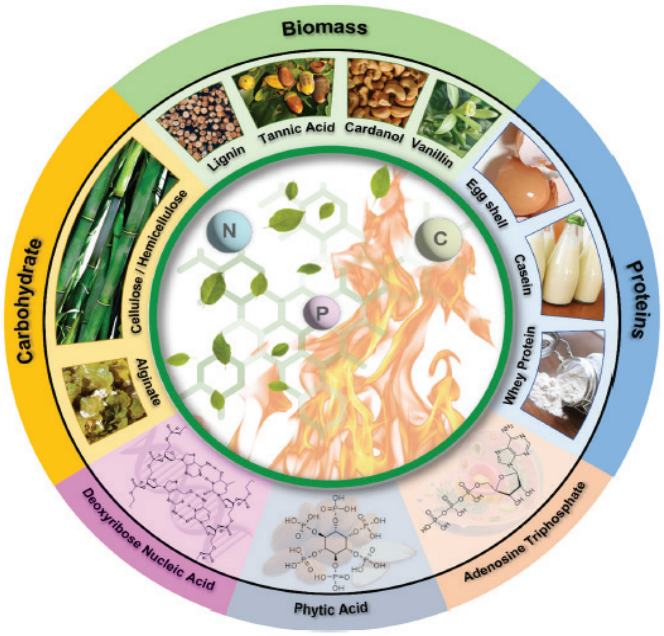

Figure 19. Clasification of Bio-based Flame Retardants (Jeonh et al., 2022)

Various usage areas of rigid polyurethane foam materials containing flame retardant are given in Figure 20. (Zhu et al., 2022).

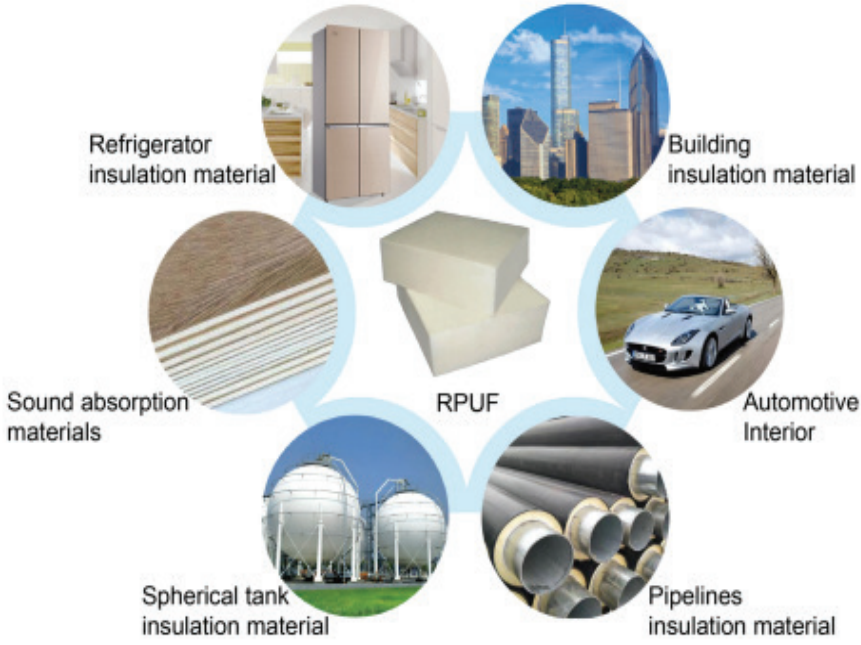

Figure 20. Various Application Areas of Flame Retardant Rigid Polyurethane Foam (RPUF) (Zhu et at., 2022)

The addition of flame retardants to polycarbonate materials and their evaluation in terms of fire safety are given schematically in Figure 21 (Mu et al., 2022).

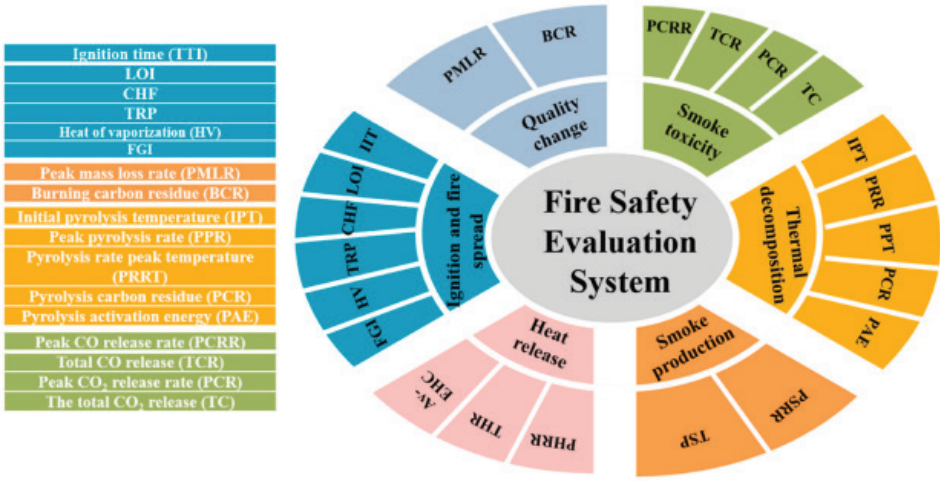

Figure 21. Safety Assessment for Flame Retardant Polycarbonate (PC) Materials (Mu et at., 2022)

The general evaluation of flame retardant materials has been conveyed in the various studies cited above. The differentiation of the usage areas of flame retardants and the increase in the amount of use, scientific researches on the evaluation of various flame retardants in different materials at different rates and by forming mixtures with different flame retardant types in various proportions are also increasing.

UL-94, LOI and cone calorimeter test setups and international standards related to these tests are also prominent in studies conducted at the research laboratory scale. In obtaining technological application methods of flame retardant materials, nanocomposite and intumescent flame retardant mechanisms have come to the fore among the subjects studied in recent years.

CONCLUSION

Flame retardants have positive effects when applied with appropriate parameters to improve the restrict flame spread properties of various materials (polymer, textile, wood, etc.) to which they are coated or added to their compositions. The conditions of use (indoor and outdoor en-

vironment, etc.) and the targeted strength properties of the materials to which the flame retardants will be applied must be accurately known. In case of not choosing the appropriate flame retardant composition during the use of the materials and not applying it with an effective method, it may be possible to encounter negativities in a possible fire. Therefore, in the selection process of flame retardants before use, their chemical structures and technical properties should be well known.

Restrictions have been made in the use of halogen-containing flame retardants due to the negative risks such as suffocation and death on living things, especially in closed areas, resulting from the contact of toxic gases with the heat source. The widespread use of environmentally friendly halogen-free flame retardants (halogen elements such as fluorine, chlorine, bromine and iodine are not found in the structure) and the use of chemical compounds, the obstacles to the preference of these flame retardant materials have been removed. Thus, the importance of flame retardants in the development of restrict flame spread to materials is constantly increasing in line with their intended use.

In addition to improving the restrict flame spread properties of materials with flame retardant additives, it is desired that the mechanical properties of the materials are not adversely affected. However, while some flame retardants provide positive effects in terms of restrict flame spread, they can cause negative effects in terms of the mechanical properties of the material (tensile strength, elongation at break, etc.). The necessity of determining the flame retardant in accordance with the intended use of the material gains importance in this regard.

The widespread use of flame retardant additives in increasing the restrict flame spread properties on various material surfaces (furniture, automobile seat, carpet, etc.), scientific studies on halogen-free flame retardants are increasing in order to prevent environmental problems. The use of suitable flame retardant additives in the development processes of restrict flame spread materials will provide significant advantages for users along with technological developments. While flame retardant materials are especially encountered in the fields of electronics, automotive, construction, textiles etc., they have a strategic importance in

increasing the restrict flame spread properties of many critical parts and hardware for the defense and aerospace sectors.

Evaluations can be made effectively in accordance with international standards with UL-94, LOI and cone calorimeter tests in order to determine the flame spread properties of additives with new ingredients obtained by mixing flame retardants in different proportions. In addition to these test setups, the properties for flame spread are evaluated with test setups specific to various products (cable, furniture, etc.). With large-sized room corner and furniture calorimeter test setups, effective product-specific examinations are carried out.

The technological developments, the usage areas of flame retardant additives are increasing. In many engineering fields (metallurgy and materials, machinery, chemistry, polymer engineering, etc.), gains are achieved in the direction of obtaining flame retardant additives according to different surface properties through interdisciplinary studies. It is anticipated that R&D activities and studies on flame retardant materials will increasingly continue.

REFERENCES

Ahmed, L., Zhang, B., Hatanaka, L.C., and Mannan, M.S. (2018). Application of polymer nanocomposites in the flame retardancy study. *Journal of Loss Prevention in the Process Industries*. 55, 381-391. https://doi.org/10.1016/j.jlp.2018.07.005

Bar, M., Alagirusamy, R., and Das, A. (2015). Flame retardant polymer composites. *Fibers and Polymers*, 16, 705–717. https://doi.org/10.1007/s12221-015-0705-6

Brandsma, S.H., Boer, J.D., Velzen, J.M. and Leonards, P.E.G. (2014). Organophosphorus flame retardants (PFRs) and plasticizers in house and car dust and the influence of electronic equipment. *Chemosphere*, 116, 3-9. https://doi.org/10.1016/j.chemosphere.2014.02.036

Chen, F., Weng, L., Wang, J., Wu, P., Ma, D., Pan, F., and Ding, P. (2023). An adaptive framework to accelerate optimization of high flame retardant composites using machine learning. *Composites Science and Technology*, 231, 109818. https://doi.org/10.1016/j.compscitech.2022.109818

Chen, Q., Zhang, J., Li, J., Sun, J., Xu, B., Li, H., Gu, X., and Zhang, S. (2022). Synthesis of a novel triazine-based intumescent flame retardant and its effects

on the fire performance of expanded polystyrene foams. *Polymer Degradation and Stability*, 203, 110079. https://doi.org/10.1016/j.polymdegradstab.2022.110079

Flambarda, X., Bourbigot, S., Kozlowski, R., Muzyczek, M., Mieleniak, B., Ferreira, M., Vermeulen, B., and Poutch, F. (2005). Progress in safety, flame retardant textiles and flexible fire barriers for seats in transportation. *Polymer Degradation and Stability*, 88, 98-105. https://doi.org/10.1016/j.polymdegradstab.2004.02.024

Filippi, S., Cappello, M., and Polacco, G. (2020). Limiting oxygen index reduction in bitumen modified with nanoclays. *Fire Safety Journal*, 111, 102929. https://doi.org/10.1016/j.firesaf.2019.102929

Hermouet, F., Rogaume, T., Guillaume, E., Richard, F., Marquis, D., and Ponticq, X. (2021). Experimental characterization of the reaction-to-fire of an Acrylonitrile-Butadiene-Styrene (ABS) material using controlled atmosphere cone calorimeter. *Fire Safety Journal*, 121, 103291. https://doi.org/10.1016/j.firesaf.2021.103291

Huang, Y., Ma, T., Li, L., Wang, Q., and Guo, C. (2022). Facile synthesis and construction of renewable, waterborne and flame-retardant UV-curable coatings in wood surface. *Progress in Organic Coatings*, 172, 107104. https://doi.org/10.1016/j.porgcoat.2022.107104

Jeong, S.H., Park, C.H., Song, H., Heo, J.H., and Lee, J.H. (2022). Biomolecules as green flame retardants: Recent progress, challenges, and opportunities. *Journal of Cleaner Production*, 368, 133241. https://doi.org/10.1016/j.jclepro.2022.133241

Laoutid, F., Bonnaud, L., Alexandre, M., Lopez-Cuesta, J-M., and Dubois, P. (2009). New prospects in flame retardant polymer materials: From fundamentals to nanocomposites. *Materials Science and Engineering*, R 63(3), 100–125. https://doi.org/10.1016/j.mser.2008.09.002

Liang, S., Neisius, N.M., and Gaan, S. (2013). Recent developments in flame retardant polymeric coatings. *Progress in Organic Coatings*, 76, 1642–1665. https://doi.org/10.1016/j.porgcoat.2013.07.014

Liu, Y., Ding, D., Lu, Y., Chen, Y., Liao, Y., Zhang, G., and Zhang, F. (2022). Efficient and durable cotton fabric surface modification via flame retardant treatment. *Colloids and Surfaces A: Physicochemical and Engineering Aspects*, 648, 129005. https://doi.org/10.1016/j.colsurfa.2022.129005

Malucelli, G., Carosio, F., Alongi, J., Fina, A., Frache, A., and Camino, G. (2014). Materials engineering for surface-confined flame retardancy. *Materials Science and Engineering R*, 84, 120. https://doi.org/10.1016/j.mser.2014.08.001

McCoy, C.G. and Stoliarov, S.I. (2021). Experimental characterization and modeling of boundary conditions and flame spread dynamics observed in the UL-94V test. *Combustion and Flame*, 225, 214-227. https://doi.org/10.1016/j.combustflame.2020.10.054

Mensah, R.A., Shanmugam, V., Narayanan, S., Renner, J.S., Babu, K., Neisiany, R.E., Forsth, M., Sas, G., and Das, O. (2022). A review of sustainable and environment-friendly flame retardants used in plastics. *Polymer Testing*, 108, 107511. https://doi.org/10.1016/j.polymertesting.2022.107511

Mu, X., Jin, Z., Chu, F., Cai, W., Zhu, Y., Yu, B., Song, L., and Hu, Y. (2022). High-performance flame-retardant polycarbonate composites: Mechanisms investigation and fire-safety evaluation systems establishment. *Composites*, Part B 238, 109873. https://doi.org/10.1016/j.compositesb.2022.109873

Rodgers, K.M., Bennett, D., Moran, R., Knox, K., Stoiber, T., Gill, R., Young, T.M., Blum, A., and Dodson. R.E. (2021). Do flame retardant concentrations change in dust after older upholstered furniture is replaced?. *Environment International*, 153, 106513. https://doi.org/10.1016/j.envint.2021.106513

Shahari, S., Fathullah, M., Abdullah, M.M.A.B., Z. Shayfull, Z., Mia, M., and Darmawan, V.E.B. (2021). Recent developments in fire retardant glass fibre reinforced epoxy composite and geopolymer as a potential fire-retardant material: A review. *Construction and Building Materials*, 277, 122246. https://doi.org/10.1016/j.conbuildmat.2021.122246

Taib, M.N.A.M., Antov, P., Savov, V., Fatriasari, W., Madyaratri, E.W., Wirawan, R., … and Hussin, M.H. (2022). Current progress of biopolymer-based flame retardant. *Polymer Degradation and Stability*, 205, 110153. https://doi.org/10.1016/j.polymdegradstab.2022.110153

Tokumura, M., Ogo, S., Kume, K., Muramatsu, K., Wang, Q., Miyake, Y., Amagai, T., Makino, M. (2019). Comparison of rates of direct and indirect migration of phosphorus flame retardants from flame-retardant-treated polyester curtains to indoor dust. *Ecotoxicology and Environmental Safety*, 169, 464-469. https://doi.org/10.1016/j.ecoenv.2018.11.052

Tsai, K-C. (2009). Orientation effect on cone calorimeter test results to assess fire hazard of materials. *Journal of Hazardous Materials*, 172, 763–772. https://doi.org/10.1016/j.jhazmat.2009.07.061

Vahabi, H., Laoutid, F., Mehrpouya, M., Saeb, M.R., and Dubois, P. (2021). Flame retardant polymer materials: An update and the future for 3D printing developments. *Materials Science & Engineering R*, 144, 100604. https://doi.org/10.1016/j.mser.2020.100604

Vahabi, H., Wu, H., Saeb, M.R., Koo, J.H., and Ramakrishna, S. (2021). Electrospinning for developing flame retardant polymer materials: Current status

and future perspectives. *Polymer*, 217, 123466. https://doi.org/10.1016/j.polymer.2021.123466

Wang, Y., and Zhang, J. (2013). Thermal stabilities of drops of burning thermoplastics under the UL 94 vertical test conditions. *Journal of Hazardous Materials*, 246–247, 103–109. https://doi.org/10.1016/j.jhazmat.2012.12.020

Wen, O.Y., Tohir, M.Z.M., Yeaw, T.C.S., Razak, M.A., Zainuddin, H.S., and Hami, M.R.A. (2023). Fire-resistant and flame-retardant surface finishing of polymers and textiles: A state-of-the-art review. *Progress in Organic Coatings*, 175, 107330. https://doi.org/10.1016/j.porgcoat.2022.107330

Zhua, M., Maa, Z., Liua, L., Zhanga, J., Huoc, S., and Song, P. (2022). Recent advances in fire-retardant rigid polyurethane foam. *Journal of Materials Science & Technology*, 112, 315–328. https://doi.org/10.1016/j.jmst.2021.09.062

Zope, I.S. (2018). *Fire Retardancy Behavior of Polymer/Clay Nanocomposites*. Singapore, Springer Nature.

ENERGETIC INVESTIGATION OF A REFRIGERATOR WORK WITH DIFFUSION ABSORPTION REFRIGERATION CYCLE

Mustafa ELEGELMEZ[1], *Anıl BASARAN*[2]

Abstract: Today, as energy becomes more valuable, cooling systems attract attention due to their energy consumption. The energy efficiency of cooling systems becomes important in terms of contributing to the sustainability goals of the United Nations and reducing the carbon footprint. In this context, several regulatory regulations are put into effect by international authorities. At the beginning of these regulations is the new energy regulation published by the European Union (EU) in 2021. EU's new energy regulation encourages manufacturers to make improvements in terms of energy efficiency and forces them to produce efficient and ecological devices. Refrigerators working with an absorption refrigeration cycle (also called absorbe refrigerators) are preferred devices due to their advantages. The main advantages of absorption refrigerators are that the number of moving parts is less compared to products with compressors so they work silently and operate with environmentally friendly fluids. In addition to being environmentally friendly systems, the use of different sources such as renewable energy brings absorption cooling systems to the fore. On the other hand, the energy consumption of absorption refrigerators is not low. This situation necessitates energy analysis of absorption refrigerators in terms of increasing energy efficiency and efficiency. In this context, methods of thermodynamic analysis of a single-stage diffusion-absorption minibar refrigerator are presented. The determi-

1 ISM Minibar Machinery Electric Industry and Trade Inc., Manisa / Turkey, e-mail: m.elegelmez@hotmail.com, Orcid No: 0000-0003-1716-1778

2 Manisa Celal Bayar University, Faculty of Engineering, Department of Mechanical Engineering, Manisa / Turkey, e-mail: anil.basaran@cbu.edu.tr, Orcid No: 0000-0003-0651-1453

nation of energy efficiency with energy analysis is shown in this study. For a better understanding of the subject, a sample situation analysis is included. In the case analysis, a refrigerator with diffusion absorption is considered. In the refrigerator under consideration, ammonia was used as the refrigerant, water as the absorbent fluid, helium gas as the pressure stabilizer, and electrical resistance as the power source. In the study, the refrigerator was arranged as an experimental setup for thermodynamic analysis, and temperature measurements were made from different points of the refrigerator. Experimental measurements were carried out both in the cooling cabinet of the refrigerator and in the absorption refrigeration cycle. The obtained data were used to calculate the Coefficient of Performance (COP) of the system. As a result, the evaporator heat gain of 7,764 W was calculated by considering the 0,375 ammonia concentration ratio in the absorption system operating with 62 W resistance power. Accordingly, the COP value of the system was found to be 0,1252.

Keywords: Absorption Cooling System, Energy Efficiency, Efficiency Effectiveness Coefficient (COP), Energy Analysis

INTRODUCTION

Cooling devices are among the indispensable devices of daily and industrial life. The high energy consumption of these widely used devices is one of the issues that need to be taken care of today, where energy is precious. 6% of the world's total energy consumption takes place in refrigerators and freezers (Basaran, 2022; Dizaji et al., 2015). To reduce this high rate, it is necessary to design refrigeration cycles with low energy consumption, in other words, with high energy efficiency (Basaran, 2020).

Considering today's conditions, it is thought to leave it to absorption cooling systems (ACS), which are seen as an alternative to vapor compression cooling systems with compressors and high operating costs. However, absorption systems, which were first produced in America and Japan in the 1950s, started to lose their former popularity with the decrease in the initial investment cost of vapor compression systems. Although the heat energy required in ACSs is high, the mechanical energy required for the cycle to work is very low. For this reason, providing

the heat energy needed in this type of cooling system from cheap energy sources such as geothermal or solar energy reduces the operating costs of the system (Yagcıoglu, 2018). Absorption refrigerators, which are defined as refrigerators working with ACS, provide an advantage with their silent operation, although their energy efficiency is not very high compared to other cooling systems. The compressor, which should be found in vapor compression cooling systems, is not found in absorption refrigerators. The absence of noisy components such as compressors makes absorption refrigerators quiet and vibration-free. This feature offers absorption refrigerators in various applications. For example, in hotel rooms and in-car applications, absorption refrigerators are one step ahead. The rapidly changing environmental factors in the world and the diversity of energy needs have led human beings to new quests. The working fluids used in ACS are natural refrigerants and therefore are important in terms of protecting the ozone layer and the environment. Many working fluids can be used when designing a cooling system or cycle. In one cycle; working fluids that carry heat from one environment to another are called refrigerants (also called secondary or working fluids). The refrigerant takes the heat from the low-temperature region and carries it to the high-temperature region, and this process is usually accomplished with the help of condensation-evaporation phase change. Choosing the right refrigerant varies by application and is of great importance. The design of the equipment of a system is largely determined by the characteristics of the selected refrigerant. In addition, the initial investment and operating costs of the system are highly dependent on the characteristics of the refrigerant (Basaran, 2013; Radermacher, et al., 2005). Looking at the historical development of refrigerants, it is seen that chemical refrigerants have been developed and used in refrigerators in addition to natural fluids. Later, it was determined that these refrigerants have negative effects on the environment. The ozone crisis and climate change on top of these environmental issues have caused ripples in the refrigeration and air conditioning and refrigeration industry and have led to a scrutiny of refrigerants (Cengel and Bole, 1996). After these environmental problems, many international negotiations and agreements have been made to reduce and terminate the production and

use of environmentally harmful refrigerants (Bolaji and Huan, 2013). The Montreal Protocol is the most important protocol signed to protect the ozone layer, and the Kyoto Protocol is the most important protocol to prevent global warming and climate change. The environmental effects of refrigerants, which are used in almost every area of modern life, have become important for human beings to lead a better quality and healthy life. Refrigerants are, after all, chemicals. Like most chemicals, it is inevitable to examine nature positively or negatively in refrigerants. When a refrigerant is desired to be used, it is important to consider the environmental impact of the refrigerant as well as its thermodynamic performance. The working fluids used in ACS are natural refrigerants and do not harm global warming and the ozone layer. In this context, refrigerators with ACS can be qualified as ecological devices.

On the other hand, coolers such as absorption refrigerators indirectly cause greenhouse gas emissions due to their energy consumption (Basaran, 2022; Xue et al., 2017). For this reason, the energy efficiency of absorption refrigerators is one of the issues that should be emphasized in terms of both energy resources and global warming. Globally, refrigeration has become a highly regulated industry, after refrigerators were identified as products with the potential to reduce energy consumption. Through legislation, governing bodies set minimum energy performance standards so that new products introduced to the market increasingly offer green certification. While these standards vary between countries and regions, they share common goals such as energy efficiency and reducing indirect carbon footprints[3]. At the beginning of these regulations is the European Union Energy Label Regulations. The Energy Labelling Regulation is a European Union (EU) legislation that establishes a framework for the labeling and labeling of energy-related products in the EU. The regulation aims to provide consumers with information about the energy efficiency of products, so they can make informed choices when purchasing household appliances, lighting, and other products that use energy. It also aims to reduce energy consumption and greenhouse gas

3 https://truerefrigeration.eu/be-ready/

emissions by encouraging the use of energy-efficient products[4]. In addition to all these, the use of different energy sources such as renewable energy makes ACSs the reason for preference.

It requires thermodynamic analysis to describe the efficiency of systems involving heat transfer steps such as heating-cooling. In other words, thermal systems are generally evaluated using energy analysis (Basaran et. al., 2020; Basaran and Ozgener, 2013). The basic approach is to apply the first law of thermodynamics to evaluate the conversion of energy [JLP publication]. The first law of thermodynamics is also known as the conservation of energy. The first law considers the quantity of energy. According to the first law, the sum of the amount of energy entering, leaving, stored, and produced in a system in a steady state should be zero. In other words, according to the first law, during the interaction of the system with the environment, the energy gained by the system must be equal to the energy lost by the environment (Olcayer, 2005). Energy efficiency is used in the analysis of thermal systems to better examine and understand the system and to evaluate it correctly and effectively. In a common approach, efficiency is defined as the desired ratio of output and input for an engineering system. Energy efficiency only considers the amount of input and output energy forms in the system (Basaran et. al., 2020) The most reliable way to compare the efficiencies of thermodynamic systems is to determine the maximum amount of useful output. Therefore, energy efficiency is used to determine the performance of the system under consideration.

Previous studies on the energy efficiency of ACSs.

One of the basic parameters in cooling systems is the efficient use of energy. In recent years, interest in studies on improving the performance of absorption cooling systems has increased and scientific studies have focused on performance evaluation with a focus on efficiency.

It is aimed to increase the system performance by detecting the heat losses on the absorber system. Especially in the studies on minibars, am-

4 https://commission.europa.eu/energy-climate-change-environment/standards-tools-and-labels/products-labelling-rules-and-requirements/energy-label-and-ecodesign/rules-and-requirements_en

monia was used as a refrigerant, water as an absorbent fluid, and helium to balance the pressure. The thermal values found by the first law of thermodynamics were evaluated with the help of a computer program and the performance effects on the system were discussed (Arslan and Egrican, 2004).

The airflow conditions in the freezer section placed on top of the domestic refrigerator were examined. Velocity investigations of particle images due to the effect of different temperature conditions were applied with Particle Imaging and Velocity Measurement System (PIV). The places where the flow rate was maximum were observed in the lower sections. It has been observed that the temperature values in the system have a significant effect. The stopping and running effects of the compressor are indicated (Lacerda et. al., 2005).

Air flows with natural convection were investigated in a domestic refrigerator. The effects of cold wall surface area and temperature values were investigated. The situations where the interior volume is full and empty were evaluated and it was found that the filled volume reduces the air flow rate. The highest air velocity was seen at the bottom of the cold surface and was found to be 0.2 m/s. Particle image examinations were observed experimentally with the PIV system (Laguerre et. al., 2008).

Ammonia water was used in the system and helium gas was preferred as the diffuser. After the investigations on LPG and solar energy for the heat source, theoretical calculations were made. The contribution of the use of ejectors to the system performance has been investigated. In LPG experiments, the most efficient results were obtained in terms of both cooling time and cooling. (Ozbas, 2009).

The effects of He gas at different pressures on the NH_3-H_2O fluid double absorber system were investigated. Experiments were carried out at pressures of 5 bar, 10 bar, and 15 bar, keeping 25% and 410 grams constant. As a result, it has been observed that the most efficient pressure value is 15 bar. In addition, the first law analyzes of thermodynamics were made for system components (Ucar, 2009).

Thermodynamic analyzes were carried out on a single-effect absorber system using the H_20-LiBr mixture. Exergy calculations were made using the first and second law analyzes of thermodynamics. The effects of the heat exchanger on the system efficiency were investigated. It has been observed that the molten heat exchanger contributes more to the system. The entropies obtained on the components of the system were compared and as a result, the highest production was observed in the boiler (Saka, 2010).

Exergy analysis and finite time thermodynamics methods are aimed to be applied to a single-effect absorber system. Investigations were made for H_2O-LiBr and NH_3-H_2O fluids and the results were discussed. With the help of the Engineering Equation Solver and Mathematica program, the irreversibilities in the system were calculated and the effects of the components on the overall performance were discussed (Kaya, 2011).

Diffuse absorption systems with and without precooling have been studied in large volumes. These systems were compared with vapor compression systems. Ammonia was used as the refrigerant, water as the absorbent, and helium for pressure balancing. The thermal loads were calculated by taking measurements from certain points of the system (Memisoglu, 2013).

Analyzed the system performance of different types of absorbent fluids in mini-absorption refrigerators. Basically, NH_3-H_2O and H_2O-LiBr fluids are emphasized. Different ratios of absorbent fluids were used and it was aimed to determine the optimum values. The results are indicated by increasing 5%, 7%, and 9% for both fluids. It was concluded that LiBr's compatibility with the refrigerant is more efficient than H_2O (Oztas, 2015).

The effects of different generator powers on system performance for ammonia-water absorption refrigerators are discussed. Generators with 46,56 and 67 W power were used in the tests. The most efficient generator was obtained in the 46 W system, which corresponds to a temperature of 167 °C and a Coefficient of Performance (COP) value of 0.159. System analyzes were calculated numerically with the Aspen-Plus program and

compared with the measured experimental values. A 1% difference was observed between the program and the experimental values (Mansouri et. al., 2017).

Investigations have been made for different fluid types in absorber systems. Exergy analyzes were performed on different components for LiBr-H_2O, NH_3-H_2O, NH_3-$LiNO_3$, and NH_3-NaSCN fluid couples, and the results were observed. Flow analyzes were made with the MATLAB program. It has been determined that the performance values of the LiBr-H_2O couple are more efficient than the other couples. NaSCN observed that the cooling effect coefficient was higher (Yağcıoğlu, 2018).

The working status of renewable energy sources on absorber systems has been examined. Solar energy was used as a source and it was aimed to reduce the damage to nature and the ozone layer. Irreversibility in the system is solved over NH_3-H_2O, LiBr-H_2O, and LiCl-H_2O fluid pairs. COP values are calculated for different fluids. Calculations were made on the first and second laws of thermodynamics. Month-based solar energy values for Antalya and Kocaeli were calculated and comparisons were made (Gunduz, 2020).

Absorption Cooling Cycle

Ammonia is a substance that dissolves very quickly in water. Also, when the mixture of water and ammonia is heated to 140 ^oC, ammonia is completely separated from the water. By taking advantage of these properties of ammonia, absorption cooling systems have been made[5]. The schematic representation of the ammonia-water mixed absorption refrigeration cycle is given in Figure 1. It can be used as a heat pump or resistance energy source. After the ammonia-water couple mixed in a certain chamber receives sufficient heat with the energy source, water and ammonia are separated from each other. The ammonia-rich melt passes through the absorber to the condenser, and the poor melt returns to the climbing pipe. Ammonia, which comes out as liquid by condensing in the condenser, passes to the evaporator, absorbs heat from the environment, and performs cooling. The system is pressed with ammo-

5 https://sogutmasistemi.com/mesleki-bilgi/absorbsiyonlu-sogutma-calisma-prensibi.html

nia and water and helium. Using the pressure difference of helium and liquid ammonia, the system passes from the evaporator to the absorber, where it combines with the weak melt that initially went to the climb pipe and returns to the mixing chamber, and the cycle is repeated.

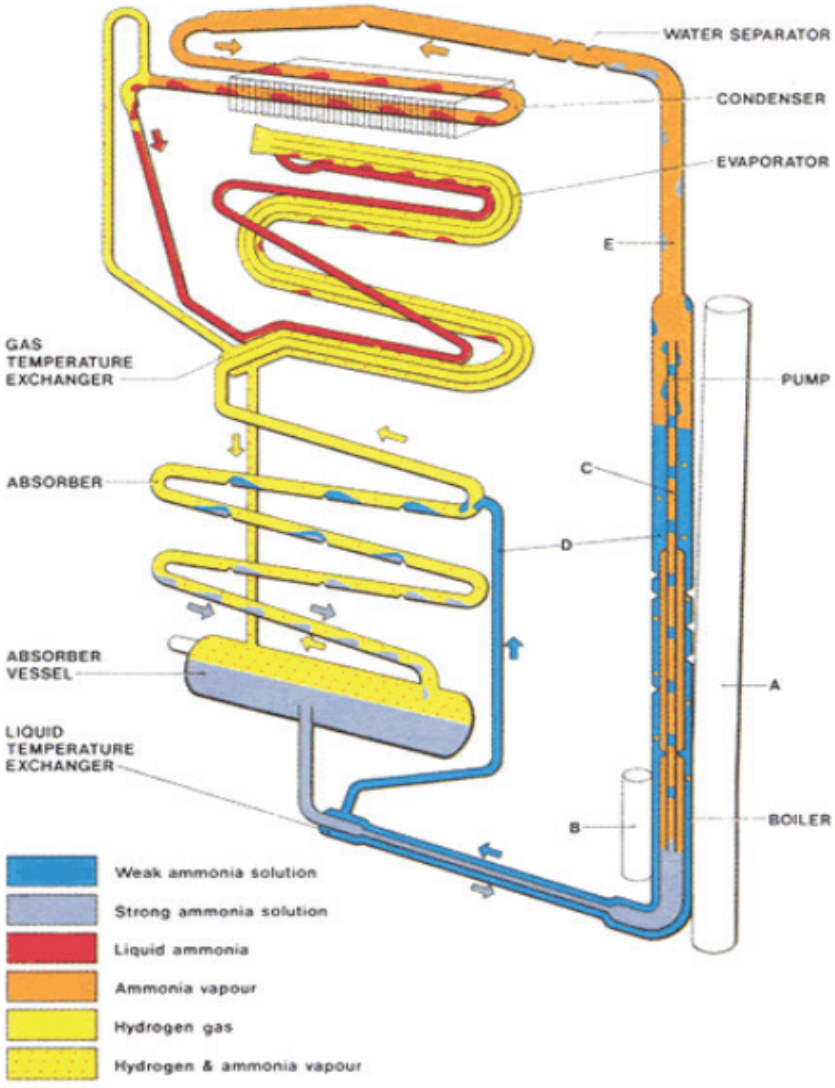

Figure 1. Ammonia-Water Mixed Absorption Cooling Cycle[6]

6 https://www.daviddarling.info/encyclopedia/A/AE_absorption_cooling.html

The main differences between the absorption refrigeration cycle and the mechanical vapor compression refrigeration system can be listed as follows:

- Due to the high number of stationary parts in ACS, they can work without noise.
- ACS is advantageous at low evaporator temperatures. The reason for this is that there are power losses due to friction in the compressor in the vapor compression system and overheating problems are not in question in these systems.
- Controls of ACS can be done easily and can be used for a long time.
- ACS can provide cooling loads ranging from 0-100%.
- When there is a decrease in evaporator pressure and temperature in ACS, the loss in cooling capacity is less.
- A rapid cooling load is provided in ACS.
- 2-9% of the electrical energy used in vapor compression systems is used in ACS.
- Despite the high initial investment costs in ACS, the fact that it does not require maintenance and that it has fewer malfunctions makes the system advantageous.
- While a single fluid is used in the vapor compression mechanical cooling system, there must be a refrigerant and an absorber fluid in the ACS.
- While there is a possibility of crystallization in ACS, there is no such possibility in a vapor compression mechanical cooling system (Memisoglu, 2013; Oztas, 2015).

European Union New Energy Label Regulation

The regulations determined by the European Union have created a new era in our lives as of March 2021. Energy regulation has been implemented to increase energy efficiency. In this context, if the standards set as of March 2021 are not complied with, product sales to Europe are not possible.

Under the New Energy Label Regulation, energy-related products must be labeled with a standard label that provides information about the energy efficiency of the product. The label includes a scale from A+++ (most efficient) to G (least efficient) and a host of other information such as the product's energy consumption, annual energy costs, and other technical specifications. The label must be prominently displayed on the product and in any advertising material.

Energy Label Regulation, household appliances such as refrigerators, washing machines, and dishwashers; lighting products such as light bulbs and LED lamps; and office equipment such as computers and printers. It is also valid for products used in the construction and building industry such as boilers, windows, and insulation materials.

The Energy Labeling Regulation is part of the EU's broader efforts to improve energy efficiency and reduce energy consumption and greenhouse gas emissions. It is designed to help consumers make informed choices about the products they buy and to encourage the use of more energy-efficient products. The maximum EEI values of the cooling devices for 2021 are given in Table 1 as a percentage.

Table 1. Maximum EEI Values of Cooling Devices (%) 2021

	EEI
Dedicated low-noise refrigerating appliances with fresh food compartment(s)	375
Low-noise refrigerating appliances with transparent doors	380
Other low-noise refrigerating appliances, except for low-noise combi appliances with a frozen compartment	300
Wine storage appliances with transparent doors	190
Other wine storage appliances	155
All other refrigerating appliances, except for low-noise combi appliances with a frozen compartment	125

After 2021, the 2024 energy regulation has been published by going one step further. In this context, it has become more difficult to catch annual consumption amounts. Due to the potential to limit product sales,

manufacturers have a very serious sensitivity in this regard. The maximum EEI values of the cooling devices for the year 2024 are given in Table 2 as a percentage.

Table 2. Maximum EEI for Refrigerating Appliances, Expressed in %

	EEI
Dedicated low-noise refrigerating appliances with fresh food compartment(s)	312
Low-noise refrigerating appliances with transparent doors	300
Other low-noise refrigerating appliances, except for low-noise combi appliances with a frozen compartment	250
Wine storage appliances with transparent doors	172
Other wine storage appliances	140
All other refrigerating appliances, except for low-noise combi appliances with a frozen compartment	100

Energy analysis of diffusion absorption cooling system (ACS)

As stated earlier, energy analysis is a rational way to evaluate performance. In this section, the energy analysis of the diffusion absorption refrigeration system based on the first law of thermodynamics is shown. The energy interactions of the system and the Coefficient of Performance (COP) calculation methods are given.

For the thermodynamic analysis of the diffusion absorption cooling system, firstly, the control volumes approach is applied. Each component of the system was determined as the control volume and the control volumes were analyzed separately as a system. Mass and energy balance equations were applied to the systems created with the control volume approach. The heat transfer rates between the system and the environment and the energy transfers between the mass and the system were determined. The analyzed systems and energy interactions are shown in Figure 2:

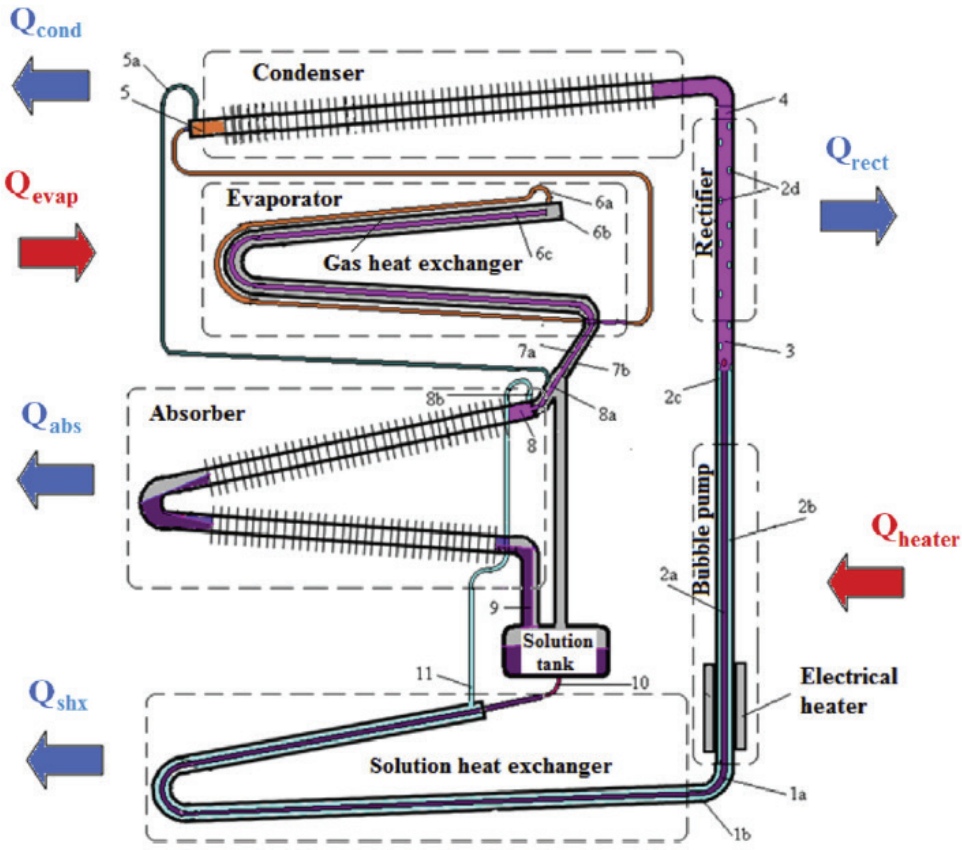

Figure 2. Schematic View of Diffusion Absorption Cooling System (Yıldız, 2013)

Conservation equations of mass and energy have been applied for the thermodynamic analysis of this system, which is presented in Figure 2. The following assumptions were made during the analysis:

- Pressure drops along the pipes are negligible;
- Hydrostatic pressures are negligible;
- Liquid solution (case 2c) and vapor bubbles (case 3) exit the capillary, leaving the generator at the same temperature (T2c = T3);
- The generator is thermally insulated, so heat losses to the environment are negligible;

- The mixture of refrigerant and inert gas at the inlet of the evaporator is assumed to be adiabatic;
- No flow occurs at point 5'a;

The subscripts in the mass and energy balance equations given below are given in Figure 3.1. Accordingly, from the principle of conservation of mass;

$$\sum m_g = \sum m_ç \tag{1}$$

From the principle of conservation of energy;

$$\sum m_g h_g = \sum m_ç h_ç \tag{2}$$

In the applied solutions, the mass flow rate of the working substance is ṁ (kgs^{-1}), h is the specific enthalpy (kJ kg^{-1}), Q is the heat loss and boiler values (W), and X is the mass ratio of the NH_3-H_2O mixture.

Generator and Bubble Pump

The rich solution ($\dot{m}_{1a}$) enters the generator-bubble pump. Ammonia vapor is separated from the rich solution by being heated by electrical resistance ($Q_{jeneratör}$). The ammonia vapor

() rising by the bubble pump and then reaching the purifier. The weak solution (), at the outlet of the bubble pump, returns to the solution heat exchanger via the generator. According to this cycle, the mass and energy equations for the generator-bubble pump are given below;

$$\dot{m}_{1a} = \dot{m}_3 + \dot{m}_{2c} \tag{3}$$

$$\dot{m}_{1a} x_{1a} = \dot{m}_3 x_3 + \dot{m}_{2c} x_{2c} \tag{4}$$

$$\dot{m}_{1a} h_{1a} + Q_{jeneratör} = \dot{m}_3 h_3 + \dot{m}_{2c} h_{2c} \tag{5}$$

Separator

After the steam leaves the boiler, it is not pure refrigerant. This means that there is still a small amount of absorbent. Because it is important to send ammonia to the condenser as much as possible separated from the

water after the boiler, in terms of increasing the efficiency of the system. As a result of the relationship between ammonia and water, which have different boiling points, water vapor accumulates by condensation and returns to the boiler with the effect of gravity. As a result of this process, near-purity ammonia vapor is obtained at the condenser inlet. According to this cycle, the mass and energy equations for the separator are given below;

$$\dot{m}_3 = \dot{m}_4 + \dot{m}_{2d} \quad (6)$$

$$\dot{m}_3 x_3 = \dot{m}_4 x_4 + \dot{m}_{2d} x_{2d} \quad (7)$$

$$\dot{m}_3 h_3 = \dot{m}_4 h_4 + \dot{m}_{2d} h_{2d} + \dot{Q}_{\text{ayırıcı}} \quad (8)$$

Solution Heat Exchanger

In the solution heat exchanger, the weak solution (4) exiting the generator energizes the rich solution coming from the absorber at a lower temperature. According to this cycle, the mass and energy equations for the solution heat exchanger are given below;

$$\dot{m}_{10} = \dot{m}_{1a} \quad (9)$$

$$\dot{m}_{1b} = \dot{m}_{11} \quad (10)$$

$$\dot{m}_{1b} = \dot{m}_{2c} + \dot{m}_{2d} \quad (11)$$

$$\dot{m}_{1b} x_{1b} = \dot{m}_{2c} x_{2c} + \dot{m}_{2d} x_{2d} \quad (12)$$

$$\dot{m}_{1b} h_{1b} = \dot{m}_{2c} h_{2c} + \dot{m}_{2d} h_{2d} \quad (13)$$

$$\dot{m}_{1b} h_{1b} + \dot{m}_{10} h_{10} = \dot{m}_{11} h_{11} + \dot{m}_{1a} h_{1a} + \dot{Q}_{\text{ısı değiştirici}} \quad (14)$$

Condenser

Condensation of ammonia vapor is provided in the condenser. Thanks to the operating pressure, the refrigerant vapor reaches the condenser, in which the liquid condenses, with the same high pressure. According to this cycle, the mass and energy equations for the condenser are given below;

$$\dot{m}_4 = \dot{m}_5 \quad (15)$$

$$\dot{m}_4 h_4 = \dot{m}_5 h_5 + \dot{Q}_{\text{kondenser}} \quad (16)$$

Evaporator

Leaving the condenser at operating pressure, the liquid refrigerant reaches the evaporator inlet. Here it mixes with the inert gas from the absorber in the gas heat exchanger. As a result, the partial pressure of the liquid refrigerant drops and evaporation occurs at low temperatures.

According to this cycle, the mass and energy equations for the evaporator are given below;

$$\dot{m}_{6a} + \dot{m}_{ig} = \dot{m}_{7b} \quad (17)$$

$$\dot{m}_{6a} h_{6a} + \dot{m}_{ig} h_{ig} + Q_{\text{evaporatör}} = \dot{m}_{7b} h_{7b} \quad (18)$$

Absorber

Water absorbs ammonia vapor, forming a melt. As the temperature drops, the ability of water to absorb ammonia increases. However, it cannot go below the freezing point of the water. The formation of solidification is not the desired situation. With this in mind, 0°C is the absolute value. In the system, the refrigerant vapor is absorbed by the weak solution returning from the generator and the rich solution flows into the solution tank. Helium and ammonia waste flow toward the evaporator. According to this cycle, the mass and energy equations for the absorber are given below;

$$\dot{m}_{9} + \dot{m}_{ig} = \dot{m}_{7b} + \dot{m}_{8b} \quad (19)$$

$$\dot{m}_{9} h_{9} + \dot{m}_{ig} h_{ig} + Q_{\text{soğurucu}} = \dot{m}_{7b} h_{7b} + \dot{m}_{8b} h_{8b} \quad (20)$$

Coefficient of Performance (COP)

The COP is defined as the ratio of the heat gained by the evaporator to the heat given off by the resistor in the bubble pump;

$$\text{COP} = \frac{\dot{Q}_{evaporatör}}{\dot{Q}_{jeneratör}} \quad (21)$$

Case Study: Experimental energy analysis of a refrigerator with a diffusion absorption cooling system (absorption refrigerator)

The experimental method in research is a method that helps to obtain information most objectively. There are many parameters (arguments) that affect a result. The most reliable way to reveal the effect of these parameters on the desired result (dependent variable) is through experimental studies. With experimental studies, variable parameters can be controlled, cause-effect relationships can be easily observed and reliable results can be obtained.

A minibar refrigerator working with a single-stage diffusion-absorption cooling system was arranged as an experimental setup and its thermodynamic analysis was carried out. The experiments were carried out at the ISM Minibar factory in Manisa. The fluids used in the system as the working fluid are important. In the system, ammonia (NH_3) is used as a refrigerant, water (H_2O) as an absorber, and helium (He) as a pressure stabilizer. The measurements obtained from the experimental setup are included in the energy analysis carried out in the light of the 1st law of thermodynamics. Temperature measurements were made on the absorber minibar used as a test setup. After the measurements were taken on the components of the absorption cooling system, they were used for energy analysis.

Experimental Setup

Electrical resistance was used in the considered ACS and the absorption device was mounted. Heat input is provided in the generator with the help of the resistance using electrical energy. Figure 3 shows the temperature measurement points and manometer connection of the diffusion absorption cooling device.

Figure 3. Temperature Measurement Points and Manometer Connection of the Absorption Cooling Device

The temperature measurements were made with the measurement points indicated in Figure 2 and Figure 3. After the temperature mea-

surement points were prepared, an electrical resistance was connected to the generator part of the device, and the insulation of the area was ensured. Figure 4 shows the installation of the ACS system in the refrigerator, the insulation of the generator area, and the measurement points.

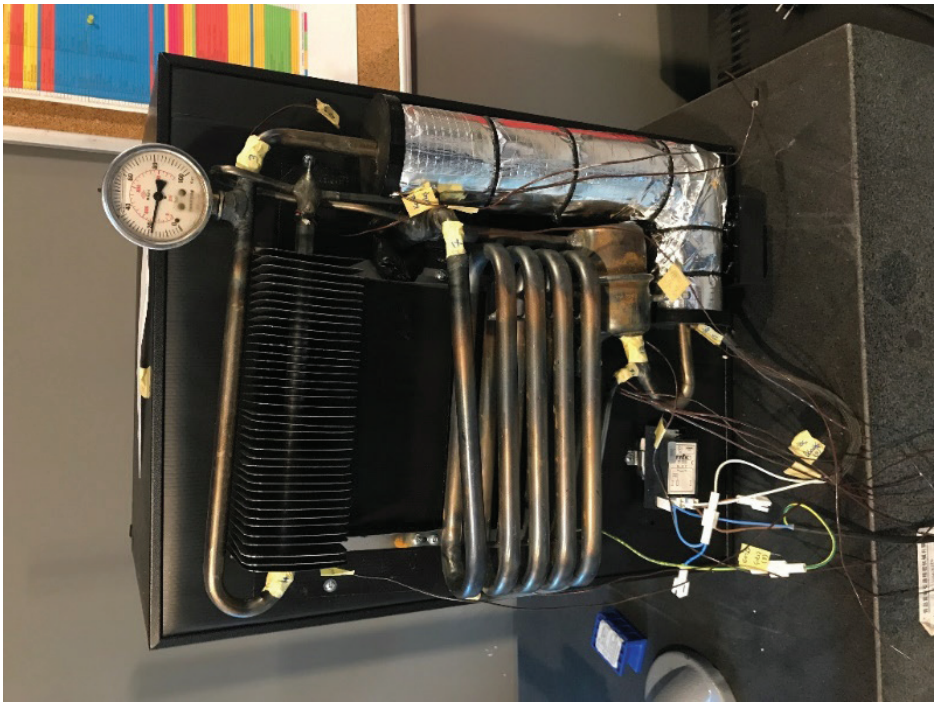

Figure 4. Isolation of the Generator Zone of the Absorption Cooling Device

After the device is prepared, it is connected to the polyurethane body. Temperature measurement points are determined in the connected body. Figure 5 shows the temperature measurement points of the polyurethane body.

Figure 5. Temperature Measurement Points of the Polyurethane Body

RESULTS and DISCUSSION

In the case study, the thermodynamic analysis of a single-stage diffusion absorption refrigerator was experimentally carried out. Analyzes were made according to the first law of thermodynamics based on experimental measurements. Experimental measurement data are presented in Table 3. These data were used in the energy analysis.

Table 3. Experimental Measurement Data

Parameter	Value
Generator heat input (W)	
System pressure (bar)	
Ammonia-water concentration (%)	
Generator temperature (°C)	
Heat exchanger temperature (°C)	
Separator temperature (°C)	
Condenser temperature (°C)	
Evaporator temperature (°C)	
Absorber temperature (°C)	
Ambient temperature (°C)	

Mass flow rate, mass concentration values, and enthalpies calculated for each point according to the values in Table 3 are given in Table 4. Measurement points are named as shown in Figure 2. As seen in Table 4, the fluid concentration leaving the separator was determined as 0.992. This indicates that almost only ammonia is delivered to the condenser.

Table 4. Experimentally Calculated Mass Flow Rates, Mass Concentration Ratios, and Enthalpy Values

Point	X (%)	)	h ()
1a			
1b			
2c			
2d			
3			
4			
5			

6a
7b
8b
9
10
11

The heat transfer rates calculated by Equation (1-19) are given in Graph 1. The heat input of 62W in the generator is provided by an electric heater. This heat input is the required input to run the cycle. Apart from the evaporator and generator, heat is transferred from the system to the environment in other components. In the evaporator, heat is transferred from the cooled environment (minibar interior) to the system. Accordingly, the highest heat transfer rate from the system to the environment occurs in the separator with 27.2 W (Graph 1). The separator is followed by the heat exchanger with 24.5 W and the absorber with 10.4 W, respectively. As can be seen in Figure 2, the lowest heat transfer rate from the system to the environment with 6.6 W occurred in the condenser. On the other hand, 7.8 W of heat was drawn from the environment cooled in the evaporator. In this case, the efficiency impact coefficient (COP) of the system was determined as 0.125.

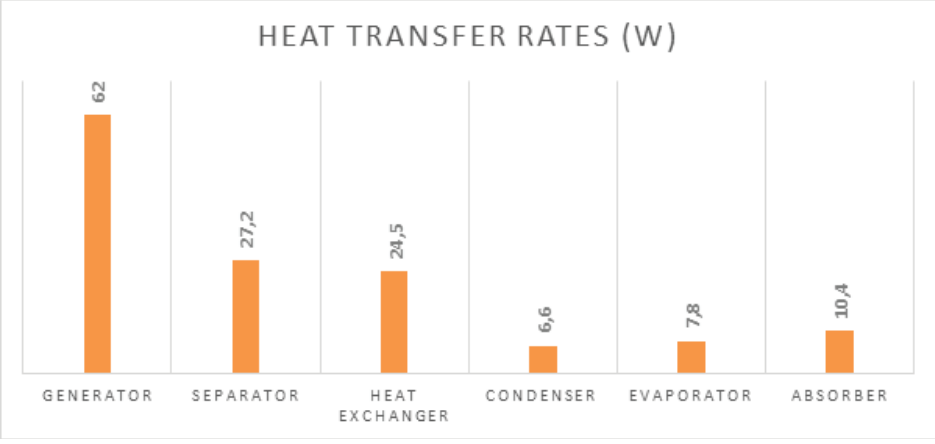

Graph 1. Heat Transfer Rates of Control Volumes

CONCLUSION

In this study, the performance of ACS using fluid NH_3-H_2O-He was experimentally examined and thermodynamic analysis was made.

The results of the study are given below:

- The average energy consumption of the electrical resistance used is 62 W.
- It has been determined that the highest heat transfer rate from the system to the environment occurs in the separator and the lowest heat transfer rate in the condenser.
- System pressure was measured at 22 bar with a manometer.
- Due to the high rate of heat transfer in the heat exchanger, it can be aimed to increase the COP by increasing the insulation length of the region.

ABBREVIATIONS

EU: European Union

COP: Performance Efficiency Coefficient

ACS: Absorption Cooling System

CFC: Chlorofluorocarbon

W: Watt

EEI: Energy Efficiency Index.

REFERENCES

Adewusi, S.A., Zubair, S.M. (2003). Second Law Based Thermodynamic Analysis of Amonia-Water Absorption Systems, Department of Mechanical Engineering, King Fahd University of Petrolium and Minerals, Saudi Arabia.

Arslan, M.E., Egrican, A.N. (2004) Thermodynamic Analysis of Absorption Cooling System Used in Refrigerator Application, *Journal of Plumbing Engineering*, 83, 53-63.

Basaran, A., Ozgener, L. (2013). Investigation of the effect of different refrigerants on performances of binary geothermal power plants, *Energy Conversion and Management*, 76, 483-498.

Basaran, A., Ozgener, L. (2013). Environmental effects of halocarbon refrigerants harmful to nature and precautions taken, *Engineer and Machinery*, 45-53.

Basaran, A. (2020). Microchannel condenser design for refrigerators, Ph. D. Thesis.

Basaran, A., Yilmaz, T., Civi, C. (2020). Energy and exergy analysis of induction-assisted batch processing in food production: a case study—strawberry jam production, *Journal of Thermal Analysis and Calorimetry*, 140(4), 1871-1882.

Basaran, A., Yılmaz, T., Azgın, Ş. T., & Civi, C. (2021). Comparison of drinking milk production with conventional and novel inductive heating in pasteurization in terms of energetic, exergetic, economic and environmental aspects, *Journal of Cleaner Production*, 317, 128280.

Basaran, A. (2022). Experimental investigation of R600a as a low GWP substitute to R134a in the closed-loop two-phase thermosyphon of the mini thermoelectric refrigerator, *Applied Thermal Engineering,* 211, 118501.

Bolaji, B.O., Huan, Z. (2013). Ozone Depletion and Global Warming:Case for the Use of Natural Refrigerant a Review, *Renewable and Sustainable Energy Reviews*, 18, p. 49-54.

Cengel, Y.A., Boles, M. A. 1996. Thermodynamics with an Engineering Approach, (T. Derbentli, Trans.), Istanbul:Literatür Publishing.(Original study published: 1994).

Dizaji, H. S., Jafarmadar, S., Khalilarya, S., Moosavi, A. (2016). An exhaustive experimental study of a novel air-water based thermoelectric cooling unit, *Applied Energy*, 181, 357-366.

Gunduz, A.H., (2020). Thermodynamic Analysis Of Solar Sourced Absorption Cooling Systems. Msc. Thesis, Kocaeli University, Institute Of Natural Sciences, Mechanical Engineering, Kocaeli,109p.

Kaya, A. (2011). Performance Analysis And Optimization Of Absorption Cooling Systems. Msc. Thesis, Yıldız Technical University, Graduate School Of Natural And Applied Sciences, Naval Architecture and Marine Engineering, Istanbul, 103p.

Lacerda, V. T., Melo, C., Barbosa, J. R., Duarte P. O. O. (2005), Measurements Of The Air Flow Field In The Freezer Compartment Of A Top-Mount No-Frost Refrigerator: The Effect Of Temperature, *International Journal of Refrigeration,* 28, 774–783

Laguerre, O., Amara, S.B., Charrier-Mojtabi, M.C., Lartigue, B., Flick, D. (2008), Experimental Study Of Air Flow By Natural Convection In A Closed Cavity: Application İn A Domestic Refrigerator, *Journal of Food Engineering*, 85, 547–560

Mansouri, R., Bourouis, M., Bellagi, A. (2017). Steady State İnvestigations Of A Commercial Diffusion-Absorption Refrigerator: Experimental Study And Numerical Simulations, *Applied Thermal Engineering*, 129, 725-734.

Memisoglu, A., (2013). Experimental Investigation Of The Availability Of Unpre-Cooling Distribution Administration Cooling Systems In Large Volumes. Msc. Thesis, Karabuk University, Institute of Science and Technology, Energy Systems Engineering, Karabuk, 74p.

Olcayer, A., (2005). Performance and Exergy Analysis in Two-Stage NH_3-H_2O Absorption Cooling Systems.Msc. Thesis, Yıldız Technical University, Institute of Science and Technology, Heat Process, Istanbul,110p.

Ozbas, E., (2009). Diffusion Absorption Cooling System Design Manufacturing, Experimental and Theoretical Analysis and Performance Improvement. PhD thesis, Gazi University, Institute of Science and Technology, Machine Education, Ankara, 158p.

Oztas, S., (2015). The Effect Of Absorbent Fluids On Cooling Performance In Diffusion Absorption Mini Cooling Systems. Msc. Thesis, Gazi University, Department Of Chemical Engineering, Ankara, 140p.

Radermacher, R., Hwang, Y. (2005). Vapor Compression Heat Pumps with Refrigerant Mixtures, CRC Press,Taylor & Francis Group, LLC, Boca Raton.

Saka, K., (2010). Thermodynamic Analysis of Single Stage Absorption Cooling System. Msc. Thesis, Uludağ University, Institute of Science and Technology, Mechanical Engineering, Bursa, 54p.

Ucar, R., (2009). H_2O– NH_3 Fluid Double Absorption Cooling Effect Of Pressure On System Performance. Msc. Thesis, Karabuk University, Graduate School of Natural and Applied Sciences, Mechanical Education, Karabuk,117p.

Yagcıoglu, K.C., (2018). Thermodynamic and Exergy Analysis for Different Refrigerants in an Absorption Refrigeration System. Msc. Thesis, Necmettin Erbakan University, Institute of Science and Technology, Mechanical Engineering, Konya,137p.

Yıldız, A., (2013). Energy And Exergy Analyses Of The Diffusion Absorption Refrigeration System, *Energy* : 407-415

Xue, M., Kojima, N., Zhou, L., Machimura, T., Tokai, A. (2017). Dynamic analysis of global warming impact of the household refrigerator sector in Japan from 1952 to 2030, *Journal of Cleaner Production*, 145, 172-179.

INTERNET REFERENCES

https://www.termodinamik.info/katkilar/absorpsiyonlu-sogutma-sistemlerinin-rolu-ve-etkinligi (Date of access 20.12.2022)

https://truerefrigeration.eu/be-ready/ (Date of access 20.12.2022)

https://commission.europa.eu/energy-climate-change-environment/standards-tools-and-labels/products-labelling-rules-and-requirements/energy-label-and-ecodesign/rules-and-requirements_en (Date of access 20.12.2022)

https://sogutmasistemi.com/mesleki-bilgi/absorbsiyonlu-sogutma-calisma-prensibi.html (Date of access 20.12.2022)

https://www.daviddarling.info/encyclopedia/A/AE_absorption_cooling.html (Date of access 20.12.2022)

AN OVERVIEW OF PALM FIBER REINFORCED COMPOSITES

Yalçın BOZTOPRAK[1], Belma GJERGJJZI[2]

Abstract: With the increasing awareness of the importance of renewable green resources around the world, efforts to develop environmentally friendly and biodegradable materials are gaining momentum. Natural fiber reinforced composites stand out with their properties such as biodegradability, low weight, low cost and good strength. Its use in various sectors such as automotive, construction and energy is increasing day by day in order to reduce polluting greenhouse gas emissions, carbon footprint and dependence on fossil fuels. Despite its environmentally friendly features, it has disadvantages such as moisture absorption and low adhesion with the matrix, but methods are being applied to strengthen the interfacial bond with surface treatments and to reduce moisture absorption. Natural fiber reinforced composites are composites in which various plant, animal or mineral origin fibers are used as reinforcement material. Plant-based fibers are the most commonly used. The most popular ones are linen, hemp, sisal and jute. Their chemical contents consist of cellulose, hemicellulose, lignin. The mechanical properties of these fibers vary according to their different chemical contents. Mechanical properties also depend on fiber length, distribution, and ratio. Matrix materials can be from biopolymers, as well as synthetic thermosets or thermoplastics. In this study, a research was conducted on the properties of palm fibers, the surface treatments applied to these fibers, palm fiber reinforced composites and their areas of use.

1 Marmara University, Technology Faculty, Istanbul / Turkey, e-mail: yboztoprak@marmara.edu.tr, Orcid No: 0000-0003-1714-7394

2 Marmara University, Institute of Science, Istanbul / Turkey, e-mail:belmagjergjizi@gmail.com, Orcid No: 0000-0002-3651-0163

Keywords: Palm Fiber, Palm Fiber Composites, Natural Fiber Reinforced Composites

INTRODUCTION

The popularity of natural fiber research is fueled by the demand for environmentally friendly goods. Natural fibers made from plants are meant to lessen reliance on non-renewable resources. All elements of the palm tree, including the sap, trunk, fruits, and leaves, are useful, making it a tree with many uses. Fiber is yet another crucial component of the palm tree. The palm tree's fibers can be found in a variety of tree sections, including the black palm fibers (ijuk), palm frond, palm bunch, and palm trunk. Previous research on palm fibers found that they are excellent as reinforcing agents for composite materials and have good tensile qualities (Bachtiar et al. 2009).

Polymer composite materials are one of the materials that offer ease of processing, increased productivity and lower costs. Due of their abundance, accessibility and affordability, natural fibers have many benefits over synthetic fibers. To make the composites lighter, natural fibers are used in place of synthetic fibers. Natural fibers have a density between 1.2 and 1.6 g/cm^3, which is lower than glass fiber's density (2.4 g/cm^3) and allows for the creation of lightweight composites (Thyavihalli et al. 2019).

Most natural fiber composites offer a healthier working environment in contrast to glass fiber composites. Humans are exposed to dust from the trimming, cutting and mounting of glass fiber components, which might irritate their skin and lead to respiratory ailments. In addition, natural fibers have a lower abrasive character than glass fibers. This provides a nicer processing environment since tool wear may be greatly decreased. Additionally, natural fibers are readily recyclable and biodegradable, and they have outstanding thermal and insulating characteristics (Misri et al. 2010).

Palm Leaf Fibers

Because they are mostly consisting of waxy substances, as well as lignin, cellulose, hemicellulose and pectin, plant fibers are known as lig-

nocellulosic fibers. Cellulose is regarded as the primary structural component (Kabir et al. 2012).

A family of perennial flowering plants known as Arecaceae. These plants referred to as palms, can grow as climbers, shrubs, tree-like plants or stemless plants. The date palm tree and its fibers that encircle the stems are depicted (Figure 1). Due to its sustainability, environmental friendliness, biodegradability and cost-effectiveness as a filler, palm fiber has gained popularity. In the production of natural fiber composites, extracts from the sugar palm-Arenga pinnata, date palm-Phoenix, oil palm-Elaeis and peach palm-Bactris gasipaes have been used (Alhijazi et al. 2020).

(a) (b)

Figure 1. (a) Tree Of Date Palm and (b) Fibers From The Date Palm Tree That Around The Stems

Palm Fiber's Chemical Composition

Cellulose, hemicellulose and lignin are many natural fibers' most crucial structural elements. (Al-Oqla et al. 2014). The structure of natural fiber is shown in Figure 2.

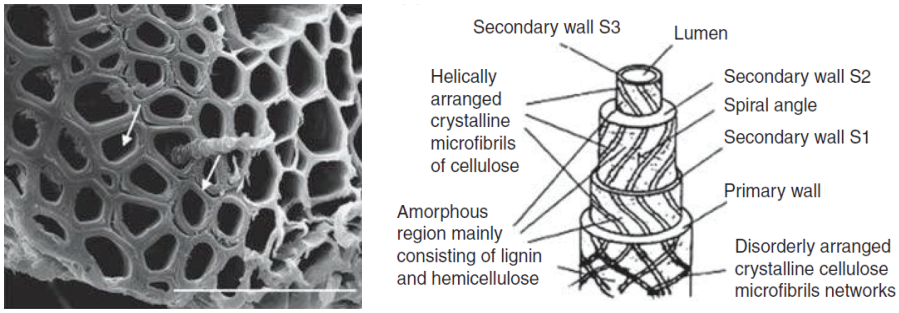

Figure 2. Structure of Bio-Fiber (a) Fiber Cell and Lumen (Ernestina *et al.*, 2013); b) Natural Fiber Structure (John and Thomas, 2008)

Plant cellulose is arranged into micro fibrils, which serve as the primary structural support for plants. Cellulose is durable to oxidizing agents, hydrolysis and strong alkalis, but it can degrade to some amount when subjected to chemical modifications (Azwa et al. 2013). The hemicellulose-cellulose linkage, which contributes to the primary structural element of the fiber cells, is made up of hydrogen-bonded hemicellulose molecules that act as a cementing matrix between each cellulose microfibril. An sophisticated hydrocarbon polymer, lignin, typically offers rigidity to plants and aids water movement (Huzaifah et al. 2017). Because of its hydrophobic nature, lignin is completely soluble in most solvents. Hemicellulose is very hydrophilic, quickly hydrolyzed in acids, and soluble in alkalis. (John and Thomas, 2008). Table 1 refers to the chemical composition of plant fibers.

Table 1. Palm Fiber's Chemical Composition

Fibers	Cellulose (%)	Hemicellulose (%)	Lignin (%)	References
Oil palm fibers	49.8	83.5	20.5	Khalil et al. (2006)
Oil palm trunk	46.58	72.1	23.0	Ahmad Z et al. (2010)

Sugar palm bunch	61.8	71.8	23.5	Sahari J et al. (2012)
Sugar palm fibers	66.5	81.2	18.9	Sahari J et al. (2012)
Sugar palm trunk	40.6	61.1	46.4	Sahari J et al. (2012)
Date palm fibers	46	18	20	Alhijazi M et al. (2020)

Surface Treatments

The natural fiber composition depends on fiber and matrix constituents and their interfacial bonding (Ghori et al. 2017). Interfacial shear strength between the polymer matrix and reinforcing natural fibers has a significant impact on the composite's final mechanical properties. (Alhijazi et al. 2020). Natural fibers are hydrophilic chemicals and polar, whereas the majority of thermoplastic polymers are hydrophobic substances and nonpolar. Because of this distinction, natural fiber composites are typically incompatible and exhibit poor interfacial adhesion. (AL-Oqla et al. 2014).

Belgacem and Gandini (2005) reported on many methods of improving the qualities of cellulosic fibers, including physical, physicochemical, chemical grafting, etc. In their study of recent advances in the chemical characterization and modification of natural polymeric-fiber composites, John and Anandjiwala (2008) came to the conclusion that sodium hydroxide (alkaline) has been used as a chemical treatment for all types of palms most frequently.

Oil Palm Fiber Treatment

The choice of the matrix is based on the intended final attributes of the composites because the matrix properties have a significant impact on composite properties.

Oil palm fiber has been used in a variety of matrices; in mercerization, natural rubber and alkali treatment on the fibers lowered the water

uptake by oil palm fiber-natural rubber composites. (Jacob et al., 2005). Additionally, the treatment with NaOH solution encourages activation of the cellulose's hydroxyl groups by rupturing hydrogen bonds. Treatment with vinyl silane and flurosilane showed the most water uptake among the three treatments (amino silane, fluro silane and vinyl silane) with silane applied to the fibers (Sreekala and Thomas, 2003).

Hexamethylene diisocyanate (HMDI) and toluene diisocyanate (TDI) treatments enhanced the tensile strength of composites oil palm fiber with polyvinyl chloride (Rozman et al. 2007). Tensile strengths of 26 MPa, 30 MPa, and 28 MPa, respectively, were shown by untreated fiber composites, TDI-treated fiber composites, and HMDI-treated fiber composites with a fiber loading of 40% and an NCO/OH ratio of 1.1. OPF and PU matrix interaction has improved with the addition of isocyanates from TDI or HMDI.

Date Palm Fiber Treatment

In order to alter the fiber surface, several alkali treatments with concentrations ranging from 0.5 to 5% were utilized as well as acid treatments with concentrations of 0.3, 0.9, and 1.6 N that were carried out at 100 °C for one hour (Alawar et al. 2009). The tensile strength of the fibers exposed to NaOH increased and the surface morphology improved significantly. Because hydrochloric acid treatment has a detrimental effect on tensile strength and surface morphology, it has been determined to be adverse for fibers.

When hydrogen bonds are broken by liquid ammonia, it can enter the inside of cellulose fibers and produce a complex molecule. The liquid ammonia treatment has the ability to transform cellulose X's initial crystal structure into cellulose Y's. Then, after being treated with hot water, cellulose Y turns back into cellulose X (Pickering 2008, Rachini et al. 2012). The natural fibers' surface is smoothed after this kind of treatment. The fiber cross-section also changes to a round shape, and the lumens get smaller (Kozlowski and Przybylak 2004, Rowell et al. 1997).

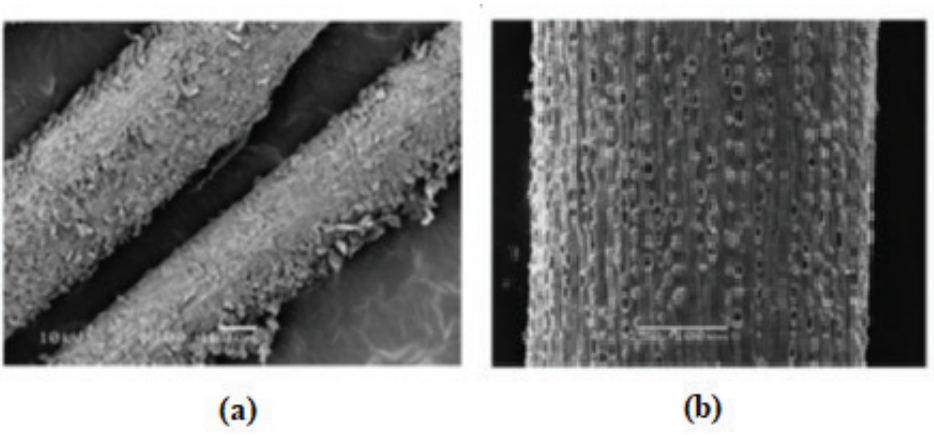

Figure 3. Scanning Electron Microscope (SEM) Image of (a) Date Palm Fiber Not Treated, (b) Treated Date Palm Fiber with 1.5 % NaOH (Alawar et al. 2009)

Sugar Palm Fiber Treatment

Owing to the fact that the impurities and waxy materials were eliminated, the treatment with alkaline had the effect of removing the hemicellulose and lignin content from the sugar palm fiber, giving it a rougher surface than the not treated sugar palm fiber. This improved the interface quality and increased mechanical interlocking (Bachtiar et al. 2008).

Three distinct soaking periods and two different sodium hydroxide (NaOH) solution concentrations (0.25 and 0.5 M) were used for the alkaline treatment (one, four and eight hours). Tensile strength data demonstrates the various reactions at various NaOH concentrations. The tensile strength at 0.5 M NaOH concentration improved significantly before declining after 1 hour of soaking. After soaking in 0.25 M of NaOH for an hour, the tensile strength rises to 49.88 MPa; however, after four hours, the tensile strength considerably decreased. The researcher anticipates that increasing the alkali concentration will have a positive impact on the composites' tensile strength. However, tensile strength is not increased by utilizing the 0.5 M alkali concentration for an hour compared to the untreated and 0.25 M NaOH samples. Furthermore,

because it might damage the fiber and lower its tensile strength, high concentrations of alkaline solution will have a detrimental impact on the treatment of sugar palm fibre and epoxy (Bachtiar et al. 2008).

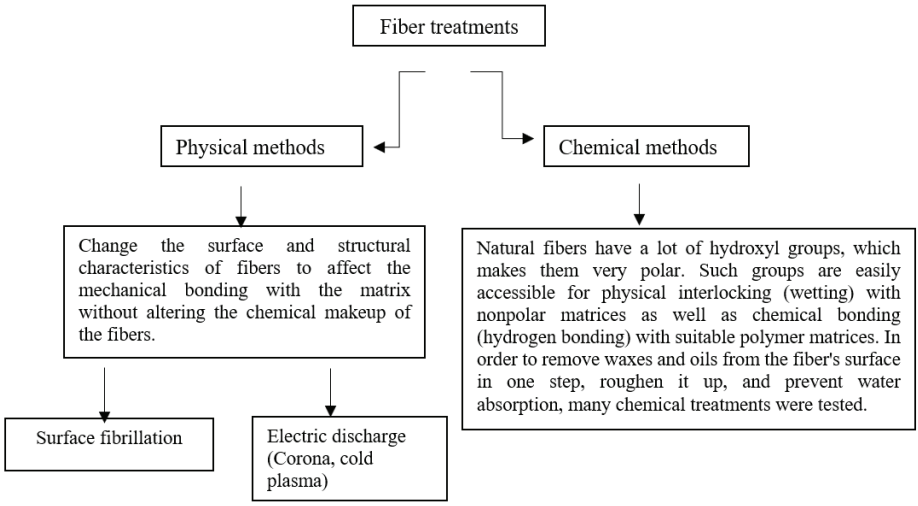

Scheme 1. Shchematic Presentation on Treatment Methods of Fibers

Table 2. Chemical Modifications Made on Palm Fibers

Chemical methods	Oil palm fiber	Date palm fiber	Sugar palm fiber
Alkaline treatment	Shinoj S et al. (2011)	Alawar A et al. (2009)	Bachtiar et al. (2008)
Silane treatment	Sreekala, M S & Thomas, S (2003)	AL-Oqla F M et al. (2014)	Huzaifah M R M et al. (2017)
Hydrochloric acid	-	Ghori W et al. (2017)	-
Acetylation treatment	Khalil H P S A et al. (2000)	-	-
Peroxide treatment	Shinoj S et al. (2011)	-	-

Acrylation treatment	Shinoj S et al. (2011)	Ghori W et al. (2017)	-
Maleated coupling enzyme treatment	-	Ghori W et al. (2017)	-
Liquid ammonia treatment	-	AL-Oqla F M et al. (2014)	-
Graft coopolimerizaation	-	AL-Oqla F M et al. (2014)	-

Mechanical Properties of Different Palm Fiber Composites

The mechanical characteristics of composite materials play a major role in determining how they will be used. By measuring the tensile strength of the material, the Young's modulus may be calculated to pinpoint the point at which the material starts to deform plastically. Young's modulus is a gauge of a material's stiffness (Mohammed et al 2018).

The majority of the time, date palm fiber composites with various matrices, fiber treatments, and fiber contents have been used to determine tensile strength. Epoxy composites had the highest tensile testing value, 41 MPa (Bachtiar et al. 2008), while the lowest is obtained in polyester composites, 14.34 MPa (Misri et al. 2010).

The polyester/oil palm fiber composites had the least strength, 21.88 MPa, according to a fewer group of scientists who assessed the tensile strength of oil palm fiber composites (Anggawan AD et al. 2020) while HDPE matrix/clay/oil palm fiber composite material showed the value 28.7 MPa and the highest value was obtained from epoxy/oil palm fiber composites, 64.7 MPa (Hanan et al. 2020).

In order to evaluate tensile tests, Essabir et al. reported the manufacture of five specimens from oil palm fiber/clay HDPE composites in accordance with ISO 527-1:2012. Therefore, it was evident that adding more filler had a propensity to make the composite stiffer. All hybrid composites with 25% weight of fibers have Young's moduli that are in-

flated than pure HDPE (650 MPa), whereas composites supported with 25% weights of palm oil have Young's moduli of respectively, 910 MPa and 885 MPa. This is a common result that were disclosed by Jawaid et al. (2011), Kakou et al. (2015), and Parparita et al. (2014). Since inorganic particles typically have more rigidity than organic fibers or polymers, these authors studied if adding hard fillers like clay particles to a polymer could increase the rigidity of composite materials. Qaiss et al. (2015) released that as polymer chain mobility decreases in the presence of fillers, composites become more rigid.

Peak strength for sugar palm fiber composites was also attained using a 50 MPa epoxy matrix and a NaOH chemical treatment. In PP composites, polyester resin was taken into consideration, and the strengths that were obtained ranged from 28 to 44.88 MPa.

Additionally, the enhanced moisten of alkali treated fiber with the matrix is responsible for the increase in tensile modulus in alkali treated fiber composites (with 1 h soaking period for 0.25 M alkali concentration). The tensile strength of composite should increase with increasing alkali concentration, but this experiment shows that the alkali concentration of 0.5 M for 1 h does not produce any excess value compared to the untreated and 0.25 M alkali concentration's samples. A very concentrated alkali solution, as claimed by Mwaikambo and Ansell, will undoubtedly damage the fiber and thus lower the tensile strength of fiber and their compositions.

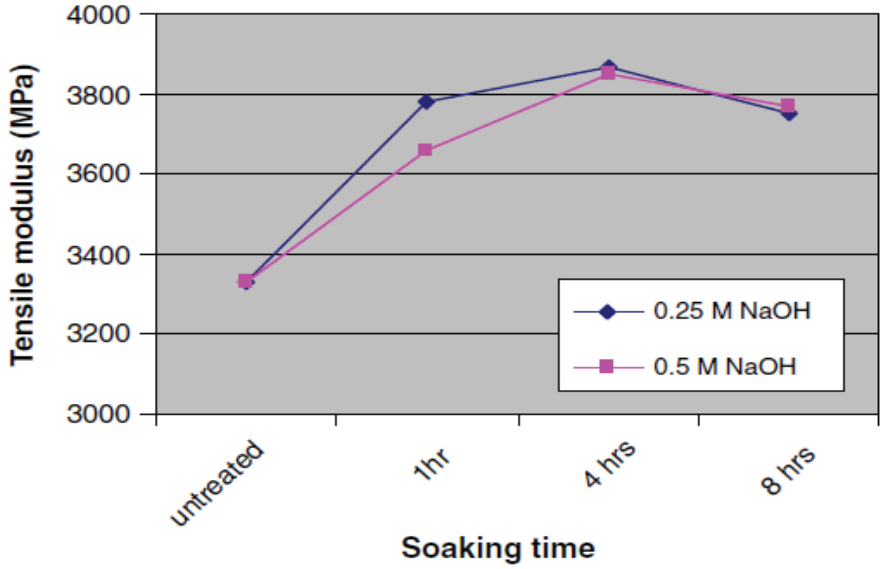

Figure 4. Sugar Palm Fiber Reinforced Epoxy Composite's Average Tensile Modulus in Relation to Soaking Time

Figure 4. demonstrates that for the various soaking times, alkali concentrations of 0.25 M yielded the highest tensile modulus. The analysis has shown that alkali treatment of the palm fiber significantly increased the tensile modulus of composites made of sugar palm fiber.

Table 3. Mechanical Properties of Different Palm Fibers and Resins Used

Palm fiber type	Mechanical properties	Resin	Result	Testing standard	References
Oil palm fiber	Tensile	Epoxy	64.7 MPa	ASTM D3039	Hanan F et al. (2020)
		Polyester	21.88 MPa	ASTM D638	Anggawan AD et al. (2020)
		HDPE	15 MPa	ISO 527–1	Essabir H et al. (2016)

	Young's modulus	Epoxy	3640 MPa	ASTM D3039	Hanan F et al. (2020)
		Polyes-ter	3.95 GPa	ASTM D638	Anggawan AD et al. (2020)
		HDPE	885 MPa	ISO 527–1	Essabir H et al. (2016)
Date palm fiber	Tensile	Epoxy	41 MPa		D. Bachtiar et al. (2008)
		Polyes-ter	14.34 MPa		Misri S et al. (2010)
		HDPE	20 MPa	ISO 527–1	Abdal-hay A et al. (2012)
	Young's modulus	Epoxy	2.5 GPa		D. Bachtiar et al. (2008)
		HDPE	1.5 GPa	ISO 527–1	Mohammed AA et al. (2018)
Sugar palm fiber	Tensile	Epoxy	50 MPa		Abdal-hay A et al. (2012)
		Polyes-ter	43 MPa	ASTM D5083-10	Sadik T et al. (2017)
		Polyu-rethane	18.42 MPa	ASTM D638	Mahdavi S et al. (2010)
	Young's modulus	Epoxy	3.89 GPa		Abdal-hay A et al. (2012)
		Polyes-ter	1.841 GPa	ASTM D5083-10	Sadik T et al. (2017)
		Polyu-rethane	1.3 GPa	ASTM D638	Mahdavi S et al. (2010)

Resins-Matrices Used for Palm Leaf Fibers

Because of their improved mechanical, thermal, and electrical qualities, modified resins are currently widely employed in the creation of natural fiber supported composites and in the production of its various industrial products (Saba et al. 2015).

In the evaluation of numerous thermoplastic, thermosetting, natural, and ceramic matrices, a variety of characteristics were discovered. The ultimate properties of the composite are based on how well the selected matrix performs and how it interacts with the fibers. Numerous polymeric matrices, including high density polyethylene (HDPE), polyester, epoxy, polypropylene (PP), and others, have been used to study palm fibers. Epoxy was frequently chosen as the matrix for OPF, SPF, and DPF as shown in Table, and its strong performance led to high characteristics. Mustapha et al. (2020) considered Polyester Composite in blended palm oil fibers. While Momoh & Osofero (2020) et al. focused on the application of oil palm fibers in cement composites. To assess mechanical and thermal qualities, several studies have suggested date palm seed/vinyl ester composites. Finally, sugar palm starch (SPS) has been the subject of recent research as a polymer. According to Sahari et al. (2013), when a plasticizer is present and the temperature is high, starch can behave as a thermoplastic. The physical characteristics of plasticized syndiotactic polystyrene (SPS), such as water absorption, density, thickness and moisture content decreased with increasing glycerol content, according to research by Sahari et al. (2012) on SPS with the use of glycerol as a plasticizer.

Table 4. Types Of Resins Used for Palm Fiber Composites

	Oil Palm Fiber	Date Palm Fiber	Sugar Palm Fiber
Polyester	Mustapha N H et al. (2020)	Raghavendra & Lokesh (2019)	Leman Z et al. (2008)
Epoxy	Jawaid M et al. (2013)	-	Atiqah A et al. (2018)
Cement	Momoh & Osofero (2020)	Lahouioui M et al. (2020)	-
Vinyl ester	-	Nagaprasad N et al. (2020)	Alhijazi M et al. (2020)
Bitumen	-	-	-

Glycerol	-	Ibrahim A et al. (2011)	Alhijazi M et al. (2020)
HDPE	Essabir H et al. (2016)	-	-
Polypropylene	Suradi SS et al. (2010)	-	-
Polyurethane	-	Oushabi A et al. (2017)	Alhijazi M et al. (2020)
Polyvinyl alcohol	-	-	-
Poly lactic acid	-	Kharrat F et al. (2020)	-

Recent Applications on Palm Fiber Composites

Date palm fibers are among other natural fibers the cheapest, the most widely distributed in tropical areas, and the easiest to separate from the leaves. The fundamental benefit of this fiber is that it gives sturdy compositions with various polymer matrices and meets the necessary cost-to-young's-modulus requirements.

Additionally, date palm fibers have prompted the automotive industry to use them in order to solve and manage an environmental waste problem as well as for their mechanical performance, environmental friendliness, cost effectiveness, and societal side. Date palm fibers are generally recognized in the textile industry and are already employed in items for our daily lives. (Ghori et al. 2018). Many scientists in most developing nations work to reduce environmental pollution by using waste materials and renewable resources. Concrete was created in the building industry by Wahyuni and Elhusna (2016) by mixing sugar palm fibers. This study aims to increase the tensile strength and mechanical characteristics of concrete. As a result, tensile strength for concrete with 10% sugar palm fiber addition was up to 24% greater than for unaltered concrete (2.15 MPa).

A small boat was created by Misri et al. (2010) utilizing the hand-lay-up approach and a composite made of sugar palm fiber and fiber glass

supported unsaturated polyester. With a tensile modulus of 1840.6 MPa and an impact strength of 2.471 kJ/m2, it demonstrates that mechanical characteristics greatly improved. Sanyang et al. (2016) demonstrated that sugar palm fiber had a lower density than commercial E-glass fiber. The densities of the two fibers were 2.55 kg/m3 for commercial E-glass fiber and 1.22-1.26 kg/m3 for sugar palm fiber. As a result, the weight of a boat made from a hybrid of a sugar palm and a fiber-glass composite has been lowered by 50%. Figure 5 illustrates the boat's production process.

Figure 5. Boat construction process (Misri et al., 2010)

Imran (2015) redesigned a zinc roof using sugar palm fiber to reduce vibration and insulate sound derived from the heating, ventilation, and air conditioning system. The samples were tested on straight and bend ducting in accordance with ASTM E477.

According to the findings, all materials exhibited the same performance trends: at frequencies below 500 Hz, insertion loss was substantial and constant until 6,300 Hz, and it remained there until 10,000 Hz at a level of about 6–40 dB.

Sajid et al. explore three novel nonwoven composites that have been needle-punched in 2020 by combining raw palm fiber in a 70:30 weight ratio with cotton, wool, and polyester fibers. SEM images supported a weak adhesion between palm fiber and polyester fibers, cotton, wool, and polyester fibers. The great diameter of the palm fibers caused the nonwoven materials to have a high porosity. The thermal resistance is improved as a result. In comparison to other nonwovens, nonwoven Palm/Wool (89.51%) exhibits the highest level of porosity. Then, at 25 °C, the least the heat conductivity is noted (36.84 mW/mK). Nonwoven Palm/Polyester had the best tensile strength (162.30 N) and the maximum thermal conductivity (38.76 mW/mK at 25 °C). After the climatic ageing test, the tensile modulus of nonwovens did not considerably alter.

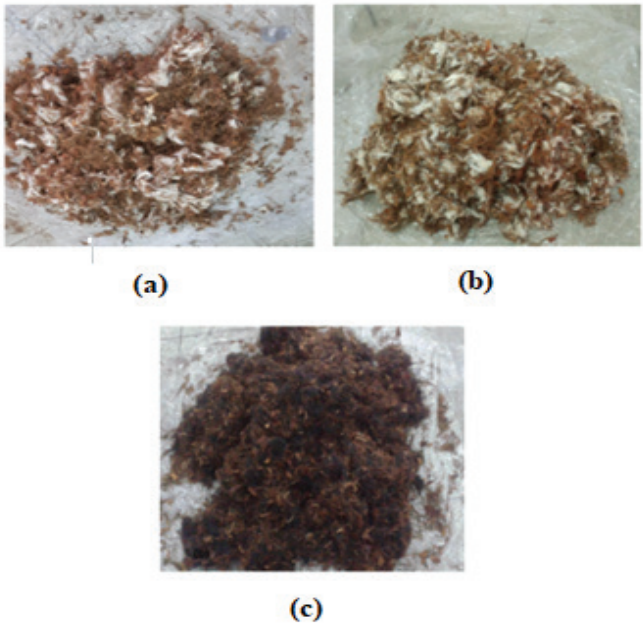

Figure 6. Prepared Fillings for Sandwiches: (a) Palm and Wool; (b) Palm and Cotton and (c) Palm and Polyester

In 2020, editors Midani et al. published the findings of experimental studies on the mechanical and thermal characterisation of date palm reinforced adobe clay bricks with sand dunes. It is common practice in brick manufacture to incorporate additional sand dunes to reduce brick fluidity, improve mechanical characteristics, and reduce shrinkage. Dune sand's weight percentage ranged from 0 to 40%, while MDPSF's ranged from 0 to 3%.

In addition, they discussed the findings of tests performed on samples of gypsum and cement mortar, highlighting the significant differences between their physical characteristics, particularly in the area of thermal conductivity, when compared to gypsum, cement mortar has a heat conductivity that is three times greater, which is estimated to be 0.58 W/m°C. Additionally, it was discovered from the experiments' findings that employing multi-layer networks made of palm fibers and gypsum reduced the material's thermal conductivity more effectively than using separated fibers in a mixture, where the ratio for gypsum samples plus cut fibers (PF) was concerned. 13.33% is the estimated reduction. The proportion reached 23.33% in the samples of gypsum plus multi-layer fibers (PFM). As the fiber networks divide the gypsum layers from one another, thermal bridges inside the samples are reduced, which accounts for this.

Figure 7. Date Palm Supported Adobe Bricks Failing Flexurally and Demoulding

(a) With lone-paired fibers **(b) Fiber with multi-layer mesh**

Figure 8. Reinforced Gypsum Date Palm Fibers

Table 5. Gypsum That Has Been Reinforced with Date Palm Fiber Mixture Portions

Weight % fibers	0	1	2	3	4	5
Gypsum (kg)	4.175	4.133	4.091	4.050	4.008	3.966
Fibers (kg)	0	0.042	0.083	0.125	0.167	0.209
Water (kg)	2.505	2.505	2.505	2.505	2.505	2.505

Using date palm fiber biomass, a research team led by the University of Portsmouth in the UK has created a biocomposite material that may utilized in nonstructural components, such as automobile bumpers and door linings. Unlike synthetic composites bonded with glass and carbon fibers, the date palm fibre polycaprolactone (PCL) biocomposite is 100 percent biodegradable, renewable, sustainable, and recyclable. Investigations have been done into how processing variables, for instance, screw rotation speed, affect the features of tensile and low-velocity impact damage. With a 28 wt % of supported of date palm fibers, the tensile strength of pure PCL rose from 19 MPa to 25 MPa. Similar to this, after reinforcement, the tensile modulus of neat PCL rose from 140 - 282 MPa. The morphologies of palm fibers and the tensile properties of the biocomposites were both slightly and moderately affected by the screw rotation speed. Specimens with incident energies of 25 J or less demonstrated greater impact resistance than those of 50 J. Scanning electron microscopy (SEM) analysis of the impact damage to biocomposites on the cracked surfaces revealed several damage modes (Dhakal et al., 2018).

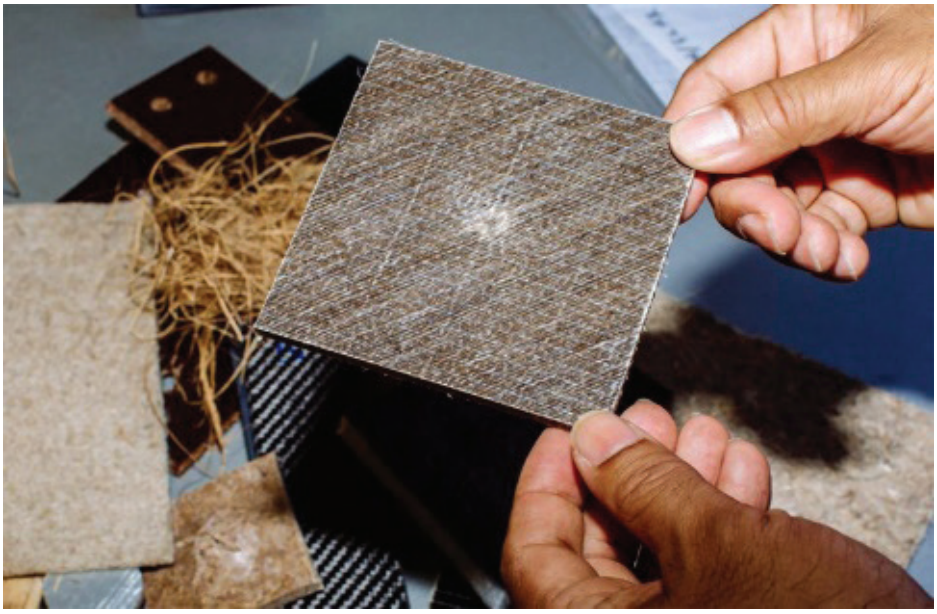

Figure 9. Composite Made of Leaf Sheath Date Palm Fiber Waste and Polycaprolactone

The possibilities and difficulties of using oil palm biomasses from agro resources, such as the palm reinforced fiber biocomposites, empty fruit bunch, trunk and frond for furniture applications are also taken into account by Suhaily et al. in 2012. A recent multi-layered biocomposite product comprised of wood veneer and bamboo strips and bound with palm fiber resin is also an valuable issue. Combining bamboo particles and strips, wood veneer creates a symmetrical structure with a smooth and flat surface that is utilized as a novel material for concrete formwork and truck side boards. To generate high-performance composites, for instance, bamboo rod was stacked with OPF fibers as illustrated in Figure 10, giving versatility in design and applications. In addition to this, the parquet boards that were made using three palm midrib boards (mats) with dimensions of 700 x 60 mm and a thickness of 8 mm for each piece. The parquet pieces were delivered to a facility for finishing and assembling the groove and tongue after being removed from the press. In the laboratories of the Egyptian Organization for Standardization and

Quality (ESO), parquet samples were tested to determine how dimensions changed as a result of changes in temperature ranged from 30-35 °C and humidity 55, 60, and 80%. The findings show that longitudinal dimensions alter with temperature and relative humidity levels.

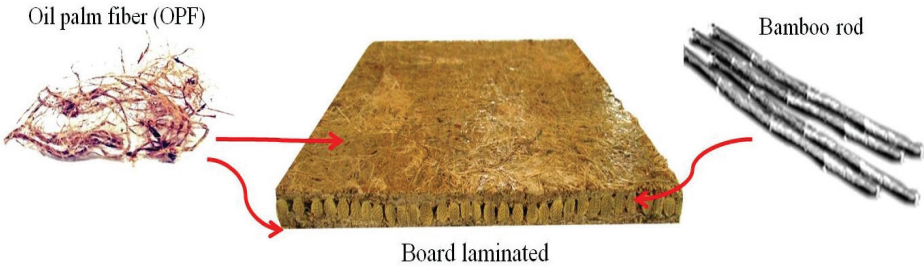

Figure 10. Hybrid Biocomposite Sheet; Used Palm Fiber Laminated with Bamboo Stick

RESULTS

Natural fiber reinforced composite materials stand out with their environmental friendliness, strength and lightness. Although there is a decrease in strength due to moisture sorption and low adhesion with the matrix, this situation can be improved by improving the interfacial bond and the studies on this subject are increasing day by day. The use of natural fiber reinforced composites in the commercial field is increasing day by day with the understanding of the importance of turning to environmentally friendly and biodegradable solutions. They show potential to replace many petroleum-based synthetic materials in the future.

Date fibers are the cheapest among other natural fibers. They are the fibers that grow most widely in the tropics and are the easiest to separate from the leaves. The main feature of this fiber is its ability to combine with various polymer matrices.

Date fibers are generally recognized in the textile industry and are already used in products used in our daily lives. Concrete composite works by mixing sugar palm fibers are also made for the construction sector.

Scientists in many countries around the world are working to reduce environmental pollution by using waste materials and renewable

resources. In the automotive industry, it is important to reduce carbon emissions, solve the environmental waste problem, use recycled materials, and produce parts using materials that reduce weight and fuel consumption. Fabrics and composites produced from palm fibers can be used in the automotive industry due to their contribution to these properties.

REFERENCES

Abdal-hay A, Suardana NPG, Jung DY, Choi K-S, Lim JK (2012). Materials Selection for Natural Fiber Composites. *International Journal of Process Engineering* 13, 1199–1206

Alhijazi M, Zeeshan Q, Safaei B, Asmael M, Qin Z (2020). Recent Developments in Palm Fibers Composites: A Review. *Journal of Polymers and the Environment,* https://doi.org/10.1007/s10924-020-01842-4

Al-Oqla F M, Alothman O Y, Jawaid M, Sapuan S M, Es-Saheb M H (2014). Processing and Properties of Date Palm Fibers and Its Composites. *Biomass and Bioenergy: Processing and Properties*, 1, DOI 10.1007/978-3-319-07641-6_1

Alawar A, Hamed AM, Al-Kaabi K (2009). Characterization of treated date palm tree fiber as composite reinforcement. *Composites Part B Engineering* 40, 601–606

Ahmad Z, Saman H M, Tahir P M (2010). Oil palm trunk fiber as a biowaste resource for concrete reinforcement. *International Journal of Mechanical and Materials Engineering* 5,199-207.

"*Arecaceae* Bercht. & J. Presl, nom. cons". Germplasm Resources Information Network. United States Department of Agriculture. 2007-04-13. Archived from the original on 2009-08-11. Retrieved *2009-07-18.*

Agro-Residues: Surface Treatment and Characterization of Date Palm Tree Fiber as Composite Reinforcement

Anggawan AD, Mohamad N (2020). Effect of different fibre treatment of oil palm fibre reinforced polyester composite. 13th International Engineering Research Conference. 2233

Atiqah A, Jawaid M, Sapuan SM, Ishak MR (2018) Polym Compos 40:1329–1334

Alhijazi M, Zeeshan Q, Safaei B, Asmael M, Qin Z (2020). Recent Developments in Palm Fibers Composites: A Review. *Journal of Polymers and the Environment,* https://doi.org/10.1007/s10924-020-01842-4

Azwa Z, Yousif B, Manalo A, Karunasena W (2013). A review on the degradability of polymeric composites based on natural fibers. *Materials and Design* 47, 424–442

Bachtiar D, Sapuan S M, Hamdan M M(2008). The effect of alkaline treatment on tensile properties of sugar palm fiber reinforced epoxy composites. *Materials and Design* 29, 1285–1290

Dhakal H, Bourmaud A, Berzin F, Almansour F, Zhang Zh, Shah U D, Beaugrand J, (2018). Mechanical properties of leaf sheath date palm fibre waste biomass reinforced polycaprolactone (PCL) biocomposites. *Industrial Crops & Products*, 126 (394–402).

Essabir H, Boujmal R, Bensalah MO, Rodrigue D, Bouhfid R, Qaiss A (2016). Mechanical and thermal properties of hybrid composites: Oil-palm fiber/clay reinforced high density polyethylene. *Mechanics of Materials*, doi: 10.1016/j.mechmat.2016.04.008

Ghori W, Saba N, Jawaid M, Asim M (2017). A review on date palm (phoenix dactylifera) fibers and its polymer composites. IOP Conf. Series: Materials Science and Engineering 368, 012009

Huzaifah M R M, Sapuan S M, Leman Z, Ishak M R, Maleque M A (2017). A review of sugar palm (Arenga pinnata): application, fibre characterisation and composites. https://doi.org/10.1108/MMMS-12-2016-0064

Hanan F, Jawaid M, Md Tahir P (2020). Mechanical performance of oil palm/kenaf fiber-reinforced epoxy-based bilayer hybrid composites. *Journal of Natural Fibers* 17, 155-167

Imran, M K M (2015). Sound insulation and vibration of modified Zinc roof using natural fiber

(Arenga Pinnata), Master thesis, Universiti Tun Hussein Onn, Malaysia.

Ibrahim A (2011). Preparation and characterization of natural composite based on plasticized potato starch and date palm fibers. *Materials Science*, Corpus ID: 138026216

Jawaid M, Abdul Khalil H P S, Hassan A, Dungani R, Hadiyane A (2013). Effect of jute fibre loading on tensile and dynamic mechanical properties of oil palm epoxy composites. *Composites Part B: Engineering* 45, 619-624

John M and Thomas S (2008). Biofibres and biocomposites. *Carbohydrate Polymers*, 71, 343-364, http://doi.org/10.1016/j.carbpol.2007.05.040

Kakou CA, Arrakhiz FZ, Trokourey A, Bouhfid R, Qaiss A, Rodrigue D (2014). Influence of coupling agent content on the properties of high density polyethylene composites reinforced with oil palm fibers. *Materials & Design* 63, 641–649

Kharrat F, Khlif M, Haboussi M (2020). Minimally processed date palm (*Phoenix dactylifera* L.) leaves as natural fillers and processing aids in poly (lactic acid) composites designed for the extrusion film blowing of thin packages. *Industrial Crops and Products* 154:112637

Khalil H P S A, Rozman H D, Ahmad M N, Ismail H, (2000). Acetylated plant-fiber-reinforced polyester composites: a study of mechanical, hygrothermal, and aging characteristics. *Polymers Plastics Technology & Engineering* 39, 757–781.

Khalil H P S A, Alwani M S, Omar A K M (2006). Chemical composition, anatomy, lignin distribution, and cell wall structure of Malaysian plant waste fibers. *BioResources* 1, 220-232

Kabir M M, Wang H, Lau K T, and Cardona F 2012 Chemical treatments on plant-based natural fibre reinforced polymer composites: An overview. Composites Part B 43 2883-2892

Lahouioui M, Arfi R B, Fois M, Ibos L, Ghorbal A (2020). Investigation of Fiber Surface Treatment Effect on Thermal, Mechanical and Acoustical Properties of Date Palm Fiber-Reinforced Cementitious Composites. *Waste and Biomass Valorization* 11, 4441–4455

Leman Z, Sapuan SM, Saifol AM, Maleque MA, Ahmad MMHM (2008). Physical and Chemical Properties of Different Morphological Parts of Sugar Palm Fibres. *Materials Design* 29:1666–1670

Midani M, Saba N, Alothman O Y, (2020). Date Palm Fiber Composites; Processing, Properties and Applications. *Composites Science and Technology*, Springer Nature Singapore Pte Ltd.

Misri S, Leman Z, Sapuan S M, Ishak M R (2010), "Mechanical properties and fabrication of small boat using woven glass/sugar palm fibers reinforced unsaturated polyester hybrid composite", IOP Conference Series: Materials Science and Engineering, 11, 1-13, http://doi.org/10.1088/1757-899X/11/1/012015

Misri S, Leman Z, Sapuan SM, Ishak MR (2010). Mechanical properties and fabrication of small boat using woven glass/sugar palm fibres reinforced unsaturated polyester hybrid composite. *IOP Conference Series: Materials Science and Engineering*, 11, 012015

Mohammed AA, Bachtiar D, Rejab MRM, Siregar JP (2018). Effect of microwave treatment on tensile properties of sugar palm fibre reinforced thermoplastic polyurethane composites. *Defence Technology* 14, 287–290

Mahdavi S, Kermanian H, Varshoei A (2010). Comparison of Mechanical Properties of Date Palm Fiber- Polyethylene Composite. *BioResources* 5, 2391–2403

Mustapha N H, Farahaika N, Norizan C W, Roslan R, Mustapha R (2020). Effect of Kenaf/Empty Fruit Bunch (EFB) Hybridization and Weight Fractions in Palm Oil Blend Polyester Composite. *Journal of Natural Fibers*, DOI: 10.1080/15440478.2020.1788686

Momoh E O, Osofero A I (2020). Recent developments in the application of oil palm fibers in cement composites. *Frontiers of Structural and Civil Engineering* 14, 94–108

Nagaprasad N, Stalin B, Vignesh V, Ravichandran M, Rajini N, OluwarotimiIsmail S O (2020). Effectof cellulosic filler loading on mechanical and thermal properties of date palm seed/vinyl ester composites. *International Journal of Biological Macromolecules* 147, 53-66

Oushabi A, Sair S, Abboud Y, Tanane O, El Bouari A (2017). An experimental investigation on morphological, mechanical and thermal properties of date palm particles reinforced polyurethane composites as new ecological insulating materials in building. *Case Studies in Construction Materials 7, 128-137*

Raghavendra S, Lokesh G N (2019). Evaluation of mechanical properties in date palm fronds polymer composites. *AIP Conference Proceedings* 2057, 020021

Sahari J, Sapuan, S M, Zainudin, E S, Maleque M A (2012). A new approach to use Arenga pinnata as sustainable biopolymer: effects of plasticizers on physical properties. *Procedia Chemistry* 4, 254-259

Saba N, Alothman O Y, Jawaid M, Tahir P M (2015). Recent advances in epoxy resin, natural fiber reinforced epoxy composites and its applications. *Journal of Reinforced Plastics and Composites*, DOI: 10.1177/0731684415618459

Sadik T, Sivaram N, Senthil P (2017). Date Palm Fiber Composites. *International Journal of Chemical Technology Resources* 10, 558–564

Sajid L, Azmami O, El Ahmadi Z, Benayada A, Majid S, Gmouh S, (2020). Introduction of raw palm fibers in the textile industry by development of nonwoven composite materials based on Washingtonia palm fibers. *The Journal of the Textile Institute*, DOI: 10.1080/00405000.2020.1840690.

Sanyang M L, Sapuan S M, Jawaid, M, Ishak M R, Sahari J (2015). Recent developments in sugar palm (Arenga pinnata) based biocomposites and their potential industrial applications: a review. *Renewable and Sustainable Energy Reviews*, 54, 533-549

Shinoj S, Visvanathan R, Panigrahi S, Kochubabu M (2011). Oil palm fiber (OPF) and its composites: A review. *Industrial Crops and Products* 33, 7-22

Suhaily S S, Jawaid M, Abdul Khalil H P S, Mohamed A R, Ibrahim F, (2012). A review of oil palm biocomposites. *Bioresources,* 7 (4400-4423).

Suradi SS, Yunus RM, Beg MDH (2010). Oil palm fiber reinforced polypropylene composites: effects of fiber loading and coupling agents on mechanical, thermal, and interfacial properties. Journal of Composite Materials 45, 1853–1861

Sreekala M S, Thomas S, (2003). Effect of fibre surface modification on watersorption characteristics of oil palm fibres. *Composites Science and Technology* 63, 861–869.

Shinoj S, Visvanathan R, Panigrahi S, Kochubabu M (2011). Oil palm fiber (OPF) and its composites: A review. *Industrial Crops and Products* 33, 7-22

Thyavihalli Girijappa YG, Mavinkere Rangappa S, Parameswaranpillai J, Siengchin S. 2019. Natural fibers as sustainable and renewable resource for development of eco-friendly composites: a comprehensive review. *Frontiers in Materials*, 6-226

Wahyuni A S and Elhusna (2016). The tensile behaviour of concrete with natural fiber from sugar palm tree. *International Conference on Engineering and Science for Research and Development*, pp. 15-18.

THE IMPORTANCE OF HYDRAULIC SYSTEMS IN THE MACHINERY MANUFACTURING INDUSTRY

Hayriye Sevil ERGÜR[1]

Abstract: Modern technological machines have in their design hydraulic systems used to control operation. Hydraulic systems are complex systems consisting of many subsystems and separately operating elements. An analysis of the causes that lead to the failure of hydraulic systems shows that their reliability often depends on a large number of interconnected factors. These factors include external influence of the environment, properties of materials and working hydraulic fluid, wear processes, magnitude of loads, operating time, as well as regulations for the maintenance of the hydraulic system as a whole and its individual elements. Evaluation of modern technical methods of operation made it possible to determine a priority condition that would allow the transition from diagnostic to predictive assessment of the state of the elements of the hydraulic systems of technological machines. Almost all mechanical applications in industry today are based on hydraulic technologies. This has led hydraulic services and products to reach new heights. These heavy-duty machines help our economy stay productive. Critical industries such as mining, large machinery transportation and other heavy-duty industries including oil refineries all depend on hydraulic services to keep their doors open.

Keywords: Fluid Power, Hydraulic System, Mobile Hydraulic System, Energy Efficiency, Manufacturing Industry

1 Eskişehir Osmangazi Üniversitesi, Mühendislik Mimarlık Fakültesi, Makine Mühendisliği Bölümü, Eskişehir / Türkiye, e-mail: hsergur@ogu.edu.tr, Orcid No: 0000-0003-1679-1137

INTRODUCTION

Fluid power is as old as our civilization itself. For centuries, water has been used to generate power via waterwheels, and air has been used to turn windmills and move ships. The Chinese used wooden valves to control the flow of water through bamboo pipes in 4000 BC. The ancient Egyptians built a masonry dam along the Nile, 14 miles south of Cairo, to control irrigation water with canals, sluices, brick pipes, and ceramic pipes. During the Roman Empire, extensive water systems were built using aqueducts, reservoirs, and valves to transport water to the cities. However, these early uses of fluid power required the movement of large quantities of fluid due to the relatively low pressures nature provided. Fluid power technology actually started with the discovery of Pascal's law in 1650. Simply put, this law explains that the pressure in a stationary fluid is transmitted equally in all directions within a finite mass of fluid. But for Pascal's law to be valid for practical use, a piston had to be made to fit exactly. But more than 100 years later this has been achieved. The hydraulic press developed by Joseph Brahmah in 1795 consisted of a submersible pump and ram attached to a large cylinder. This new hydraulic press has found wide use in the UK, providing industrial applications with a more efficient and economical means of applying large force (Parr, 2006; Childs, 2019).

The first use of a large hydraulic press was made by Whitworth in 1860. Over the next 20 years, many attempts were made to reduce the waste and excessive maintenance costs of original type hydraulic accumulator. Until these years, electrical energy was not developed to power industrial machinery. Instead, cranes, presses, shearing machines, etc. Fluid power is used to operate hydraulic equipment such as Emerging dominantly in the 19th century, electricity was found to be superior to fluid power for transmitting power over long distances.

The modern era in fluid power began at the turn of the century. In 1906, liquid applications were made to facilities such as the main weapon system. Since then, the shipping industry has applied fluid power to cargo handling systems, controllable pitch controllers, submarine control system, aircraft lifts, aircraft and missile launch system, and radar/

sonar guided systems. With a variety of applications, hydraulic systems are used in all types of large and small industrial environments, as well as in buildings, construction equipment and vehicles. Paper mills, wood cutting, manufacturing, robotics and steel processing are prominent users of hydraulic equipment. The purpose of a particular hydraulic system may vary, but all hydraulic systems operate on the same basic concept. Simply defined, hydraulic systems operate and perform tasks using a pressurized fluid (Ergür, 2017).

The power of the fluid is important in hydraulics and as a result hydraulic regulation is widely used in heavy equipment. In a hydraulic system, the pressure applied to the fluid at any point is transmitted unabated. This pressurized fluid acts on every part of the section of a containing vessel, creating force or force. Depending on how this force is used and how it is applied, operators can lift heavy loads and precise repetitive work can be done with ease. Hydraulic systems use fluid to build pressure. Liquid particles are close together, meaning the liquid is almost incompressible. Since the pressure in the liquid is transferred equally in all directions, the force applied to the liquid at any point passes to the other points of the liquid. In hydraulic systems, a small force over a small cross-sectional area transmits pressure and generates a large force over a larger cross-sectional area (Rabie, 2009).

Fluid power solutions have made the greatest contribution to the modern industrial revolution. It is worth noting that there is a wide variety of applications for fluid power systems. Most heavy-duty equipment operating in industrial sectors depends on the hydraulic or pneumatic principle, where the main power source in these systems comes from oil in hydraulic systems and air in pneumatic solutions. Early control principles were based on the use of mechanical techniques as the main source of power to add force and motion to the required application. Today, most liquid power systems are controlled by electrical and digital control techniques that facilitate their use and application and provide higher performance to power systems (Abu Hanieh, 2021).

Today, due to rising fuel costs and new regulations regarding internal combustion engine emissions, the energy efficiency of hydraulically driven machines has become one of the most important issues in system

design. Components and systems have been developed over the years to meet the increasing requirements for higher efficiency and better functionality. Vehicles, forklifts, manipulators, etc. For cyclically operating machines, energy consumption can be significantly reduced by using special valve concepts or hydrostatic machine control in conjunction with hydraulic accumulators as energy storage devices.

The best example of the hydraulic system that every user uses every day without thinking is the brake system in his vehicle. Other examples include lifting equipment such as hydraulic jacks and wheelchair lifts, lift and digging arms on backhoes and other heavy equipment, hydraulic presses that produce metal components, and some parts of aircraft and boats, including wing blades and rudders. Every hydraulic system uses the same basic principle (Chapple, 2003). Three methods are used in industry to transmit power from one point to another. These are Mechanical, Electrical and Fluid power transfer, respectively. Mechanical transmission shafts, gears, chains, belts etc. through. Electricity transmission wires, transformers etc. through. Fluid power is in a confined space through liquids or gas.

THEORETICAL FRAMEWORK

Fluid Power and Extent

The diverse application and usage versatility of fluid power equipment results in multiple modes of operation. These various operating modes make it difficult to standardize testing as well as to compare and measure the performance of fluid power systems, components, and fluids. The consensus in the industry is that the low volumes of specific equipment type available and the great diversity are proving too costly to allocate resources to characterize entire duty cycles. In addition to the high volumes of variable duty cycles, instrumentation of a fluid power system downstream of the engine requires further development, as most of the parameters that require monitoring are within the operating components (e.g., fluid properties inside the cylinder). While many component and subsystem level design and testing standards exist, there are currently no widely accepted standardized test methods for evalu-

ating equipment level efficiency over a duty cycle. Understanding the statistical significance of the measured differences is also an area of need for performance validation as there is not enough data collected to date to determine their significance. This key issue is often encountered in industry where the overall system is still inefficient despite using optimized components. An example of this is the field of mobile hydraulics. The peak efficiency of a typical diesel engine can reach around 40% and that of the hydraulic system up to 80%. The typical total system efficiency of such machines is approximately ten percent, meaning only ten percent of the chemical energy stored in the fuel is converted into useful mechanical power. As shown in Figure 1, this is partly due to the inefficient operating point of the internal combustion engine, averagely 25% of efficiency, losses in hydraulic pumps, and increased throttling losses in proportional valves, averagely 40% of hydraulic efficiency (Vukovic & Hubertus, 2015).

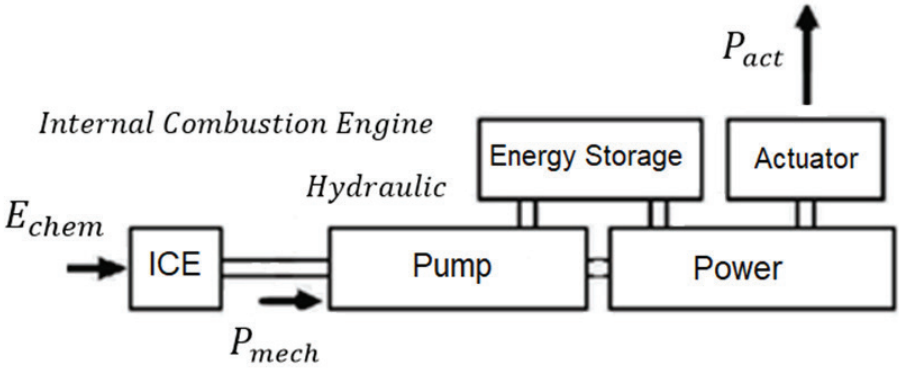

Figure 1. Schematic Representation of the Mobile Hydraulic System (Vukovic & Hubertus, 2015)

Fluid power is technology that deals with the generation, control and transmission and movement of forces of a mechanical element or system using pressurized fluids in a confined system. Both liquids and gases are considered liquids. The fluid power system includes a hydraulic system. Oil hydraulics uses pressurized liquid petroleum oils and synthetic oils, while pneumatics uses compressed air that is released into the atmosphere after completing the work. The term fluid refers to

air or oil because water has been shown to have certain drawbacks in transmitting hydraulic power in machine operation and control. Commercially pure water contains various chemicals as well as impurities and is difficult to keep valves and working surfaces in satisfactory condition unless special precautions are taken when used (Walters, 2001). A hydraulic system is a system of liquids, gases and solids used to transfer, store and distribute energy. There are four main benefits of using a hydraulic system in manufacturing: (a) Hydraulic systems are more efficient than pneumatic systems as they use less energy and emit less heat. (b) Hydraulic systems are more flexible, which is useful during design revisions and for optimizing production lines. (c) The hydraulic system provides more effective control over machine settings, which can help reduce wasted time and errors in production processes. (d) In hydraulic systems, which can be adjusted according to the minimum working requirement, new products are easily and seamlessly integrated into existing production lines.

In fluid power engineering, hydraulics is used for power generation, control, and transmission through the use of pressurized fluids. Fluid mechanics provides the theoretical basis for hydraulics. Hydraulics topics range between some fields of science and most engineering modules and cover concepts such as pipe flow, fluids, fluid power motion control, pumps, valves, actuators, turbines, hydropower, computational fluid dynamics, and flow measurement. The role of the human in the professional environment changes from being deeply integrated into the production process to higher planning and guiding tasks due to smarter production and personalized assistance systems. Technicians who specialize in a single field can become systems engineers, as rapidly changing environments and systems require high flexibility and a readiness for continuous learning. While current developments differ in many ways, they are all matched by significantly increased internal system complexity. Tasks of smart manufacturing systems will be to address complexity and make basic functions much easier to use for operators, customers and everyone who interacts with the systems (George & Victor, 2012).

In addition to power transmission, the common use of hydraulic fluid when the hydraulic system is off provides the benefits of non-water

lubrication as well as increased life and efficiency of packing and valves. In some special cases, soluble oil diluted with water may be used for safety reasons. The application of fluid power is limited only by the creativity of the designer, production engineer or plant engineer. If the application is concerned with lifting, pushing, pulling, clamping, bending, forcing, pressing, or any other linear and multi-rotational movement, it is possible that the power will meet the requirement (Mitchell & Pippenger, 1997). Fluid power applications can be classified into two main parts such as fixed hydraulic systems and mobile hydraulic systems.

SCOPE and METHODS

Fixed and Mobile Hydraulic Systems

Fixed hydraulic systems can stay firmly fixed in one position. The characteristic feature of stationary hydraulics is the use of solenoid and/or manually controlled valves. There are many application circuits in the Machine manufacturing industry. One of the most effective strategies for increasing circuit efficiency is secondary control. The pressure in the control system in these systems is kept at a "semi-constant" level by a pressure compensated pump (Fig.2). The main feature of the pressure compensated pump is that it can give the system the demanded flow rate by changing the pump pressure within a small area adjusted by the pressure compensator, slightly increase the pump flow rate until the pump fails completely. On the other hand, to reduce the pump pressure, the pump can slightly increase the flow rate until the pump is fully stroked. The accumulator is used on the high pressure side to recover energy when lowering or slowing a load. Flow, throttling loss.

The rotational speed of the hydraulic motor in a secondary control system can be controlled by adjusting the motor displacement.

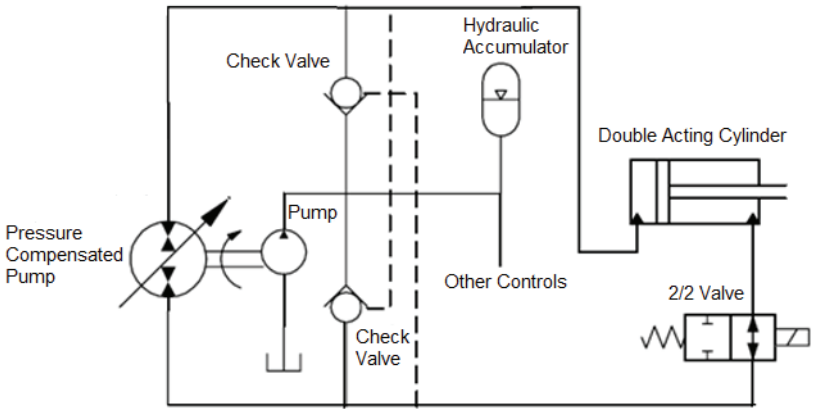

Figure 2. Hydraulic Pump Controlled Double Acting Cylinder (Ergür, 2017)

The basically hydraulic pump controlled clamping circuit in Fig. 3 can be shown as an example of a stationary hydraulic circuit. In addition to leak completion and power saving, when the clamp jaws shown in the figure are in the clamping position, the accumulator added to the circuit will keep the system pressure constant, so the pump outlet pressure will also decrease.

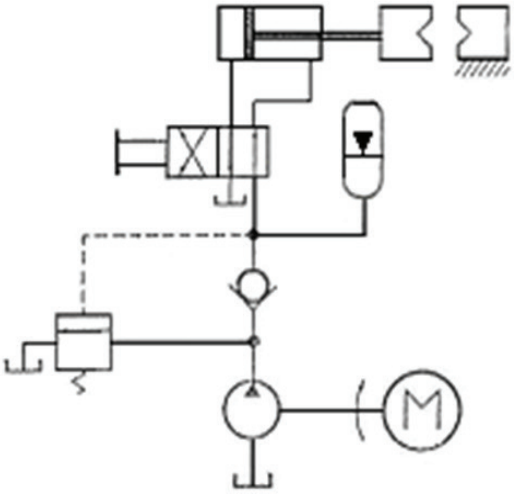

**Figure 3. Hydraulic Pump Controlled Clamping Circuit
(Pancar & Ergür, 2010)**

When the squeezing pressure drops below the load reduction set pressure, the valve will close and the pump's accumulator will be charged. Examples of places where stationary hydraulic circuits are used are Machine tools and transfer lines, plastic processing machinery such as lifting and conveying devices, metal forming presses, injection molding machines, rolling machines, elevators, food processing machinery, automated handling equipment and robots may be shown.

In Figure 4 (a), the weight is lifted with the sequencing valve in the system, since the fluid coming from the pump will return directly to the tank in the open position of the closing valve, the lifting process will be terminated or it will be possible to hold the load at the desired level.

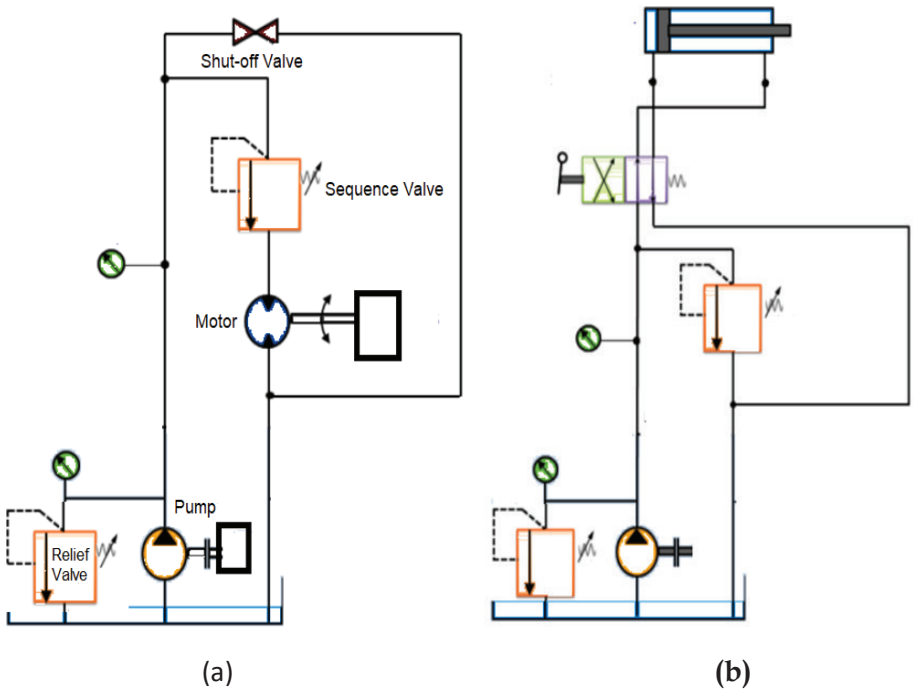

Figures 4. (a) Hydraulic Circuit Designed for Package and (b) Oven Door Lifting

As an example to the fixed hydraulic circuit, another circuit could be the system to be designed for opening and closing the oven door. A double acting cylinder can be used to control the movements of the oven

door. The cylinder will be activated by a spring return 4/2 way valve. This will ensure that the gate will only open as long as the valve is operated. The door closes again when the valve operating lever is released (Konami & Nishiumi, 2016). In Figure 4 (b), the circuit to be used for the furnace and its door to be controlled is shown. As an example to a fixed hydraulic circuit, another circuit can be shown, in which a one-way hydraulic motor controlled by a constant flow hydraulic pump is used

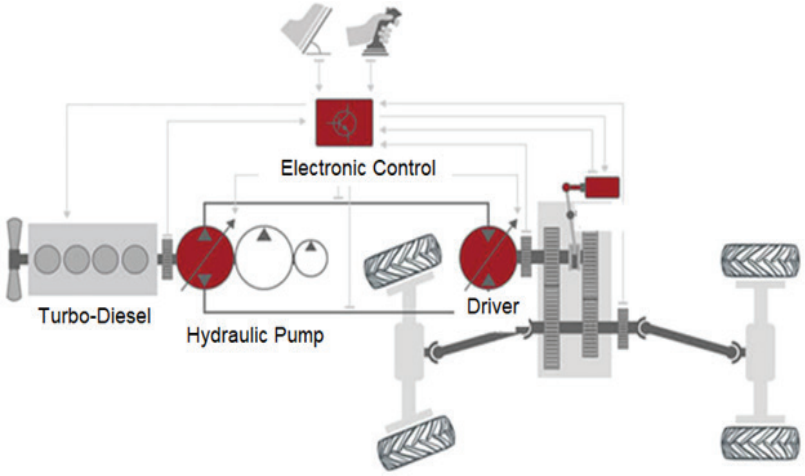

Figures 5. Circuit of a Vehicle Using a Hydraulic Pump-Motor Coupled with a Diesel Engine (Esposito, 2004)

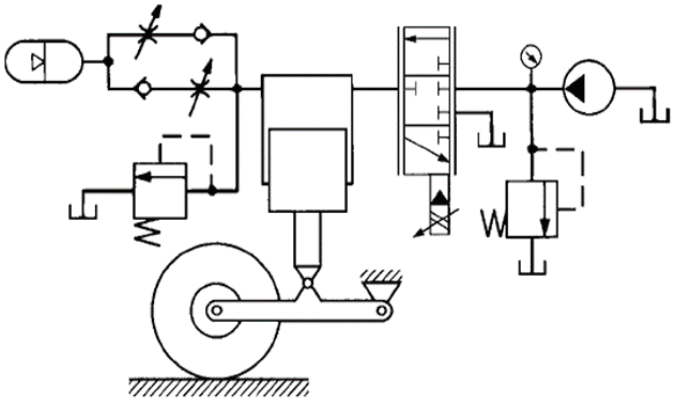

Fig. 6. An Accumulator in the form of a Hydraulic Spring in Vehicle Balancing (Konami & Nishiumi, 2016)

Examples of mobile circuits can be given for many different uses. Figure 5 shows the circuit of a vehicle using a hydraulic pump and a hydraulic motor coupled with a diesel engine. Figure 6 is an example of a mobile circuit application in vehicles. It is possible to use the hydraulic accumulator to dampen the vibration. Mobile hydraulic systems work in many different locations or on the go, by acting on wheels or tracks, such as a tower crane or excavator. A characteristic feature of mobile hydraulics is the frequent manual actuation of valves. Mobile hydraulic applications can be summarized as in Table 1.

Table 1. Fluid Power Sample Applications (Mitchell & Pippenger, 1997)

Agriculture	Tractors, mowers, plows, threshing machines
Automation	Automated lines, robots
Automobiles	Steering, braking system, Hydraulic transmission
Aircraft Industry	Landing wheels, helicopters, trunk loading/ unloading system
Defense	Missile launchers, navigation controls
Amusement	Amusement park
Manufacturing industry	Grinders, drills, riveting machines, nut runners
Food and Beverage	Food manufacturing products, packaging and bottling
Casting	Molding machines, furnaces, casting machine
Glass industry	Vacuum caps for conveying
Molds	Part holding units, vices
Machine Tools	Automatic Machine tools, forklifts, transport system
Medicine	Breathing devices, heart devices, dental devices, etc.
Mining	Drilling and digging equipment, mine carriers, loaders

Newspaper	Edge trimming unit, stapling, printing, packaging
Paper and packaging	Product control systems, roller and packaging system
Pharmaceutical	Product control systems, bottling and packaging.
Plastics industry	Injection machines, raw material feeding

FLUID POWER SYSTEMS

The hydraulic system is one of the best ways to generate a lot of power, as they can provide high pressure with a small amount of hydraulic fluid. A hydraulic system is a system of liquids, gases and solids used to transfer, store and distribute energy at one point. It consists of fluid moving through a closed pipe or tube that can be controlled by valves that allow pressure to be applied or released to the fluid. The hydraulic fluid is then transferred to another location where it can be used for power generation or cooling. These systems are useful because they are simple and very efficient. They generate usable power by using the force created by the liquid flowing through the pipes.

There are four main benefits to using a hydraulic system in production: (a) Hydraulic systems are more efficient than pneumatic systems as they use less energy and emit less heat (b) Hydraulic systems are more flexible and this can be useful during design revisions as well as for optimizing production lines (c) The hydraulic system provides greater control over machine settings, which can help reduce wasted time and errors in production processes (d) Hydraulic system allows for seamless integration of new products into existing production lines as it can be easily adjusted with minimal effort.

The general classification of hydraulic systems can be made as Fluid transport systems and fluid power systems. In fluid transport systems, the sole purpose is to transfer fluid from one location to another in order to achieve some useful purpose. Examples include pumping stations for pumping water into homes, interurban gas lines, etc. Fluid power systems are designed to do work. In fluid power systems, work is achieved

by pressurized fluid acting directly on a fluid cylinder or fluid motor. A cylinder produces a force that results in linear motion, while a fluid motor produces a moment that results in rotational motion. Fluid power systems can also be classified by Open/Closed loop system and Control type based on Control system.

Open and Closed Loop System Based on Control System

There is no feedback in the open system and performance depends on the characteristics of the individual components of the system. Open loop system is not accurate and error can be reduced with proper calibration and control. Closed loop system uses feedback. The output of the system is fed back to a comparator by a measuring element. The comparator compares the actual output with the desired output and signals an error to the control element. The error is used to change the actual output and bring it closer to the desired value. A simple closed-loop system uses servo valves and an advanced system uses digital electronics (Konami & Nishiumi, 2016).

Fluid Logic Control and Electrical Control

This type of system is controlled by hydraulic oil or air. The system can be AND, NAND, OR, NOR etc. It uses fluid logic devices. There are two types of fluid logic systems such as (a) *Moving Part Logic (HPM)* devices are miniature fluid elements that use moving parts such as diaphragms, disks, and poppets to implement various logic gates, and (b) *Fluid* devices have no moving parts and depend only on interacting fluid jets to implement various logic gates.

Electrical type of system is controlled by electrical devices. Four basic electrical devices are used to control fluid power systems, these are switches, relays, timers and solenoids. These devices help control starting, stopping, sequencing, speeds, positioning, timing and reversing of drive rollers and fluid motors. Where remote control is required, electrical control and fluid power are successful together (Bunger, 2013). Each type of power transmission and control system has specific application areas. However, we can make some general comparisons between them.

Fluid power and electricity are good at transmitting power over long distances and can also be better controlled compared to mechanical devices. In terms of cost, electrical appliances are the least expensive, while hydraulic systems have a better power-to-weight ratio. Table 2 gives a relative comparison of hydraulic (H), pneumatic (P) and mechanical/ electromechanical (M) and Electric (E) systems.

Table 2. Relative Comparison of Systems (Sastry, 2011)

Specification	Best	Good	Fair
Moment/inertia	H	P	M
Power/Weight	H,P	-	M
Rigidity	H	M	P
Vulnerability to Dirt	E,M	-	H,P
Response velocity	E	H	M,P
Compactness	E	H	M,P
Working, unfavorable condition	-	P,M,H	E
Relative cost	M,E	H,P	-

The hydraulic system is an efficient transmission for many reasons. First, simple levers and buttons make it easy to start, stop, accelerate and decelerate. This also ensures control accuracy. In addition, as it is a very fluid system without gears, pulleys or levers, a constant force can be maintained regardless of changes in speed while operating easily. Hydraulic systems are often simple, safe, and economical because they use fewer moving parts and are easier to maintain than mechanical and electrical systems. Hydraulic systems can be used safely in chemical plants and mining operations because they do not generate sparks (Pancar & Ergür, 2010).

- *Fluid power systems are simple, easy to operate and can be accurately controlled*: Fluid power provides flexibility to equipment without the need for complex mechanisms. Using fluid power, we can start, stop, accelerate, decelerate, reverse or position large forces/ components with great accuracy using simple levers and push

buttons. For example, on earthmoving equipment, the bucket payload can be lifted or lowered by an operator using a lever.

- *Multiplication and variation of forces*: Linear or rotary force can range from one kilogram to several hundred tons.
- *Multifunctional control*: A single hydraulic pump can provide power and control for multiple machines using valve manifolds and distribution systems. Fluid power controls can be placed at the central station so the operator can always have full control of the entire production line for the multi-process machine or group machine.
- *Low Speed Torque*: Unlike electric motors, hydraulic motors can produce a large amount of torque when operating at low speeds. Some hydraulic motors can also maintain torque at very slow speeds without overheating.
- *Constant force or moment*: Fluid power systems can provide constant torque or force regardless of velocity changes.
- *Economic*: Not only the reduction in required manpower, but also the production or elimination of operator fatigue as a factor of production is an important element in the use of fluid power.
- *Low weight/power ratio*: The hydraulic system has a lower weight/power ratio compared to the electromechanical systems.
- *Fluid power systems can be used where safety is vital*: Safety is vital in air and space travel, the manufacture and operation of motor vehicles, mining and the manufacture of precision products.

RESULTS and DISCUSSION

Disadvantages of Hydraulic Systems

Hydraulic systems also have some drawbacks. Handling hydraulic fluids is complex and completely eliminating leaks in the hydraulic system can be difficult. If hydraulic fluid leaks in hot areas, it can catch fire. If hydraulic lines burst, they can cause serious injury. Care should be taken when using hydraulic fluids because too much contact can cause health problems. Hydraulic fluids are corrosive, but some types are less

corrosive than others. To keep the hydraulic system in good condition, hydraulic systems should be periodically checked for leaks, lubricated, and filters and gaskets replaced.

The field of fluid power control can be expanded to a wider multidisciplinary range, which can include efficiency, component design and optimization, integration and compactness, environmental impact, and user-friendly and energy-efficient applications. It is believed that there is still a very promising future, as the actuators have distinctive and important advantages such as high power/weight ratio, system sensitivity, etc., (Johnston & Plummer, 2008).

Challenges and Suggestions

There are still many challenges in the fields of fluid power and motion control. Major challenges include its efficiency, compactness and environmental impact. Overcoming these problems will significantly increase the acceptability of fluid power and lead to its more widespread use.

Energy efficiency, which is a very important topic in fluid power systems, has attracted the attention of many researchers and engineers. High efficiency fluid power machines or devices can be achieved by using components with less energy loss, intelligent system design approaches and intelligent control. New fluid power control methods are also needed to increase its efficiency. Compactness and integration of fluid power machines or devices, fluid power affect the development of systems. Portable and lightweight human-scale fluid power devices such as personal service robots, lightweight fluid power components are sought after by customers. Modern fluid power-based compact power and drive systems will provide greater energy and user convenience. The integration and compactness of the systems, which will further increase the acceptability of fluid power, facilitates future work. Fluid strength can be plagued by a number of factors that hinder its wider acceptance. Users always demand a clean, quiet, safe and easy to use fluid power device. Effectively interfacing fluid power machines or devices with human, low noise and leakage is required. The future requirement

is to have leaks so quiet that they do not disturb the operator, and so rare that their aesthetic and environmental impact is negligible (Mays, 2000).

For many years, due importance was not given to fluid power training. But about 15 years ago education and training activities related to this branch have been started in a few universities in our country. In some countries the teaching of Hydraulics as a special branch of Technology dates back to the early 1950s of the last century. Most countries in the world are still very heavily involved in transforming their education systems and learning content. Different views and experiences can serve as an incentive for the general public to start intensifying their education, finding appropriate methods and ways to train professionals who can meet today's challenges, including the digitization of industry and society, as well as countries with more and better potential for engineering and technical personnel in the future. It will clearly be helpful. The transition from industry to post-industrial society is a global phenomenon reflecting the Information age, which includes virtualization and Virtual Reality.

In some countries the teaching of hydraulics as a special branch of Technology dates back to the early 1950s of the last century. Most countries in the world are still very heavily involved in transforming their education systems and learning content. Much more progress will be made in the future in countries with large and good potential for engineering and technical personnel, as differing views and experiences will encourage users to start intensifying their education (Raymond, 2004). While the anticipated benefits are very promising, it is necessary to pay close attention to the changing conditions in the Fluid Power space that are driving new requirements for future products and enabling new potential digital business models. Recent research shows that especially small and medium-sized enterprises do not follow any implementation strategy or take part in the development and implementation of their technologies. In high investments there may be other difficulties in tackling the lack of technical expertise and infrastructure on the one hand, and measuring the resulting benefits on the other. Besides the concerns about Cyber Security, another challenge in classical informatics is understanding the correlation between digital business models discussed

abstractly in the machine manufacturing industry and the required design changes in machines (Gramatikov, 2011; Khayal, 2017)

The Future of the Fluid Power Industry in Turkey

It is estimated that the automation market in Turkey is 1/20 of China. If Turkey has to be one of the world's leading economies based on production, it has to reach higher technological standards and a higher level of automation in production. In the last 30 years, fluid power technology has risen as an important industry. Fluid power technology should continue to expand in Turkey, with an increasing emphasis on automation, quality control, safety and more efficient and green energy systems. Fluid power industry is gaining a lot of importance in our country's industry. In Turkey, the growth rate of this industry is typically about twice that of the economy.

The reasons for this can be summarized as follows; (1) As the economy grows, this sector also grows, (2) There is a lot of automation and conversion to complex methods that increase speed. (3) The interesting things that has happened in this industry is that in Turkey, some products are produced and exported become an attractive destination for resource use. These reasons create a situation where the growth of the industry is twice the GDP (gross national product) in Turkey. Fluid power industry in Turkey, Festo, Rexroth, Vickers, Eaton, Parker Hannifin, Norgen, Donfos, Siemens and etc. Its advances consist of partnerships with many global fluid power technology leaders and many advanced Turkish industries. One of the most important segments of the hydraulic industry in India is mobile hydraulics. Due to the large programs in road construction, there is also a large expansion in the construction machinery industry. In addition, we are witnessing a trend towards the use of more sophisticated hydraulics in tractors and agricultural equipment.

The manufacturing industry in Turkey strives for higher automation and output quality. As the Turkish industry moves towards modernization to meet productivity and compete in the global market, excellent potential is also expected for the pneumatic application. Another area of interest for the fluid power industry will be opportunities in the de-

fense industry. Defense is an important market segment in the Turkish fluid power industry. There is also a shift towards products that include miniature pneumatics, process valves, servo drives, hydraulic power steering with new controls, and advanced PLC, microprocessor controls. However, the basic input required for the effective use of fluid power is the education and training of users. Therefore, there is a great need for education and training in the design, application and maintenance of fluid power systems. Some external sources have opened many competence centers to train manpower and raise awareness about the use of fluid power in our country's industry.

CONCLUSIONS

Hydraulic systems are a popular choice in manufacturing. They help reduce costs by allowing materials to be processed without the need for additional power sources. These systems have assumed a wide variety of applications in manufacturing, including the food and beverage, petrochemical, automotive and aerospace industries. They help increase productivity and production rates by reducing the number of parts required for each task. Hydraulic systems have many benefits and uses in different production processes, and as new inventions are made, new and better ways of making things with the help of hydraulic power will be developed.

It has proven to be much more durable than its electrical and mechanical counterparts. They work better, longer, and are less likely to break down or fail due to their much simpler and more robust design. Having fewer moving parts than other systems means they are less likely to cause problems anyway, but there is also the fact that the moving parts they do have are much more durable. They tend to be more economical than electrical or mechanical systems because they use fewer parts and are therefore much easier to maintain. Thus, it becomes easier to find the problems that the system will have, and faster and more practical solutions are provided in case of failure. In addition, hydraulic systems also require much less maintenance. It is possible to understand that these systems work smoothly with simple control elements such as backup filters and liquid samples.

In simple terms, hydraulic systems produce repetitive motion using pressurized fluid (usually oil or water). They are known for their efficiency, cost effectiveness and adaptability. They can be used in several applications. Hydraulic systems are widely used in large industrial applications, including construction, logging, manufacturing, and robotics. As a result, hydraulic systems have many benefits and uses in different manufacturing processes, and as new inventions are made, new and better ways of making things with the help of hydraulic power will certainly continue to be seen.

REFERENCES

Abu Hanieh, A.M. (2021). *Fluid Power Control*. (2nd Ed.,) p.344, Jerusalem: Cambridge International Science Publishing.

Bunger, A.P., McLennan, J. & Jeffrey, R. (2013). *Effective and Sustainable Hydraulic Fracturing*. p.1072, Rijeka, Croatia: Intech Open Publications.

Chapple, P. (2014). *Principles of Hydraulic Systems Design*. (2nd Ed.,) p.200, New York: Momentum Press, LLC.

Ergür, H.S. (2017). Safety with two hand control systems in hydraulic presses. *AKU J. Sci. Eng*. 17(015903), 280-291. https://doi:10.5578/fmbd.53962

Esposito, A. (2008). *Fluid Power with Applications*. New York: Pearson Education Publication.

George, E.T. & Victor, J., DeNegri (2012). *Handbook of Hydraulic Fluid Technology*. (2nd Ed.), p. 212, New York: Taylor & Francis, CRC Press.

Gramatikov, I. (2011). *Design of Hydraulic Systems for Lift Trucks*. (2nd Ed.) p. 264. USA: Courtesy of Balkancar Record, Gramatic Pub.

Johnston, D.N. & Plummer, A.R. (2008) *Fluid Power and Motion Control (FPMC)*. pp. 13-25, Britain: Hadley Ltd.

Khayala, O. (2017). Introduction to hydraulic systems. *NPTEL, Mechanical-Mechatronics and Manufacturing Automation: Lecture Notes*, p.63.

Konami, S. & Nishiumi, T. (2016). *Hydraulic Control Systems: Theory and Practice*. p. 328, Singapore: World Scientific.

Mays, L.W. (2000). *Hydraulic Design Handbook*. New York: McGraw Hill.

Mitchell, R.J. & Pippenger, J.J. (1997). *Fluid Power Maintenance Basics and Troubleshooting*. USA, New York: Taylor & Francis, Marcel Dekker Inc. Press.

Mulley, R. (2004). *Flow of Industrial Fluids: Theory and Equations*. (1st Ed.). Florida, New York: CRC Press.

Pancar, Y. & Ergür, H.S. (2010). Hydraulic circuits I and II: *Eskisehir Osmangazi University, Engineering and Architectural Faculty, Mechanical Eng. Dep.: Lecture Notes*, p.367.

Parr, A. (2011). *Hydraulic and Pneumatics*. (3rd Ed.,) p.249, Butterworth-Heinemann: Elsevier.

Peter, R.N., Childs (2019). *Mechanical Design Engineering Handbook: Pneumatics and Hydraulics*. (2nd Ed.), 849-874, London: Elsevier,. https://doi:10.1016/B978-0-08-097759-1.00018-6

Rabie, M.G. (2009). *Fluid Power Engineering*. p.443, New York: McGraw Hill.

Sastry, P.A. (2011). Notes on hydraulic systems. *Okland University, MVSR Engineering College*, Hyderabad, 1-38.

Vukovic, M. & Hubertus, M. (2015). Dynamics and vibroacoustics of machines (DVM2014): The next generation of fluid power systems. *Procedia Engineering*. 106(2015), 2-7.

Walters, R.B. (2014). *Hydraulic and Electric-Hydraulic Control Systems*. (2nd Ed.), p. 344, UK: Springer.

GÜVEN PLUS GRUP A.Ş.

GPGD

ORP